Cooperative Diversity Relaying Techniques in Wireless Communication Networks

by

Furuzan Atay, B.Sc., M.Sc.

A thesis submitted to
the Faculty of Graduate Studies and Research
in partial fulfilment of
the requirements for the degree of
Doctor of Philosophy

The Ottawa-Carleton Institute for
Electrical and Computer Engineering (OCIECE)

Department of Systems and Computer Engineering
Carleton University
Ottawa, Ontario, Canada
January 2009

Your file Votre référence
ISBN: 978-0-494-47470-9
Our file Notre référence
ISBN: 978-0-494-47470-9

Abstract

In wireless networks, link budget can be relaxed by delivering the data using intermediate relay nodes. Although the immediate purpose of relaying is to obtain gain against path loss, it can also create spatial diversity due to the broadcast nature of the wireless medium. The objective of this work is to design and analyze relaying protocols that induce e2e cooperative diversity for ad hoc and infrastructure based networks.

One of the main limitations of digital multi-hop relaying is the occurrence of detection errors at the relays. If the relaying is not done selectively, these errors cause significant performance degradation at the destination, a problem usually called *error propagation*. The first part of this thesis studies threshold digital relaying techniques to reduce error propagation. A set of optimal thresholds are derived and their performance for a single relay network is evaluated. It is shown that threshold digital relaying achieves full – in this case dual - diversity. A good approximation to the optimal threshold is also derived. For multiple relay scenarios, a relay selection protocol based on threshold is proposed and threshold functions that achieve full diversity are provided.

Most studies on cooperative diversity assume relays at favorable locations, which cannot be justified in random topologies. These studies are not necessarily good indicators of network-wide benefits of cooperative relaying. The second part of this

thesis analyzes the network-wide benefits of cooperative relaying in random topologies. Assuming that the relays are distributed according to Poisson point process, the performance of cooperative relaying is derived as a function of relay density.

The relays can be user terminals serving for each other, as well as dedicated fixed relays that are part of the infrastructure. Due to their less stringent space and cost constraints, infrastructure-based relays can accommodate multiple-antennas. The last part of this thesis is a preliminary study on an uplink scenario, where multiple single-antenna users communicate with a common multi-antenna destination with the help of a multi-antenna relay. It is shown that using multi-stream relaying and practical Multiple Input Multiple Output (MIMO) receivers, e2e diversity benefits can be achieved.

Yol arkadaşım İlker'e,

Yerlerimiz, hep,
yeni yollarımızın başları;
yollarımız da, hep,
yeni yerlerimizin sonları ola...

Oruç Arıoba

Acknowledgments

I would like to express my deep gratitude to my supervisor Prof. Halim Yanıkömeroğlu for his guidance during this thesis. His valuable feedback and enthusiasm for research made my doctoral study a very enjoyable experience. I would also like to thank him for providing me with an ideal research environment.

Parts of the research in this thesis benefited significantly from the collaborations with other researchers. The comments from Dr. Yijia Fan, Dr. Abdulkareem Adinoyi, Prof. John Thompson, Prof. Ian Marsland, and Prof. Vincent Poor on the first part of this thesis are greatly appreciated. I would like to thank Dr. Dan Avidor and Dr. Sayandev Mukherjee for their insights on the second part of this thesis. The last part of this thesis was funded by Wireless Technology Labs of Nortel and improved with the feedback from Dr. Shalini Periyalwar.

I would like to thank all my colleagues in Prof. Yanıkömeroğlu's research group for the friendly research environment they created. The residents of Lab MC 7039, Maryam Sabbaghian, Hamid Saeedi, Nastaran Mobini, Matthew Dorrance, Sina Tolouei, Mahmudur Rahman, and Ahmed Abdelsalam, you made this lab a great place to work. Thank you all for your friendship and company.

The NATO A1 Scholarship awarded by Turkish Scientific and Research Council (TÜBİTAK) was curial to start my graduate studies and made this journey possible.

Thanks to my parents, my brother, and my parents-in-law for their constant love and support.

Table of Contents

List of Figures

List of Symbols and Acronyms

List of Acronyms

Acronym	Explanation
ACK	Acknowledgement
AR	Analog Relaying
ARQ	Automatic Repeat reQuest
BER	Bit Error Rate
BPSK	Binary Phase Shift Keying
CDF	Cumulative Distribution Function
CDR	Conventional Digital Relaying
C-MRC	Cooperative Maximal Ratio Combining
CRC	Cyclic Redundancy Check
CSI	Channel State Information
CTP-SN	Cooperative Transmission Protocol for Sensor Networks

DF	Decode-and-forward
DR	Digital Relaying
e2e	End-to-end
HARBINGER	Hybrid ARq-Based Intra-cluster GEographically-informed Relaying
H-BLAST	Horizontal Bell Laboratories Layered Space-Time architecture
i.i.d.	Independent identically distributed
JZF-DF	Joint Zero Forcing Decision Feedback Detection
LAR	Link Adaptive Relaying
MAC	Medium Access Control
MIMO	Multiple-Input Multiple-Output
MISO	Multiple-Input Single-Output
ML	Maximum Likelihood
MPSK	M-ary Phase Shift Keying
MRC	Maximal Ratio Combining
NDR	Non-Selective Digital Relaying
PMF	Probability Mass Function
PDF	Probability Density Function

PZF-DF	Parallel Zero Forcing Decision Feedback Detection
R-ARQ	Relay-assisted Automatic Repeat reQuest
RRM	Radio Resource Management
RS	Relay Selection
SC	Selection Combining
SDR	Selective Digital Relaying
SER	Symbol Error Rate
SISO	Single-Input Single-Output
SNR	Signal-to-Noise Ratio
TDDT	Time Division Direct Protocol
TDR	Threshold Digital Relaying
TRS	Threshold based Relay Selection
V-BLAST	Vertical Bell Laboratories Layered Space-Time architecture
ZF-DF	Zero Forcing Decision Feedback Detection

List of Symbols

Symbol	Explanation
$\mathbf{a}$	A vector
$\mathbf{A}$	A matrix
$\mathbf{A}^T$	Transpose of matrix $\mathbf{A}$
$\mathbf{A}^H$	Hermitian of matrix $\mathbf{A}$
$diag\{a_1, a_2, \ldots, a_n\}$	$n \times n$ Diagonal matrix with given elements on its diagonal
$\mathbf{I}_n$	$n \times n$ Identity matrix
$\mathbf{0}_{m,n}$	$m \times n$ Zero matrix
$\mathbf{A}(i, j)$	Element at row-i and column j of $\mathbf{A}$
$\mathbf{A}(i_1 : i_2, j_1 : j_2)$	Submatrix of $\mathbf{A}$ composed of rows $i = i_1, i_1 + 1, \ldots, i_2$ and columns $j = j_1, j_1 + 1, \ldots, j_2$
$\mathbb{P}\{\mathcal{A}\}$	Probability of event $\mathcal{A}$
$\mathbb{E}_X$	Expectation with respect to random variable X
S	Source node
D	Destination node
R	Relay node
M_r	(Maximum) number of (transmitting) relays

SNR	Reference SNR
K_{tx}	Number of transmit antennas
K_{rx}	Number of receive antennas
C	Capacity
d	Diversity order
r	Multiplexing gain
α_{ij}	Fading coefficient for the link from node i to node j
$E_{b,i}$	Energy per bit spent by node i
x_i	Symbol transmitted by node i
n_{ij}	Noise component in the link from node i to node j
γ	Instantaneous SNR
$\bar{\gamma}$	Average SNR
$p_X(x)$	PDF of random variable X
I_i	Set of parameters known at the relay in Model i
α_m, β_m	Modulation dependent parameters for BER expressions
erf	Error function
erfc	Complementary error function

P_b	Bit error rate
$\bar{P}_b$	Average bit error rate
$\mathrm{BER}_{e2e}^{(i)}$	End-to-end BER for Model i
$\mathcal{E}_{ij}$	Error event in the link between node i and node j
$\mathcal{E}_{coop}$	Cooperative error event
$\mathcal{E}_{prop}$	Error propagation event
$\pi(I_j)$	Relaying policy based on information I_j
$\gamma_{t,i}$	Threshold value for Model i
$\gamma_{t,i}^{*}$	Optimal threshold value for Model i
$\gamma_t^{*,approx}$	Approximately optimal threshold
κ_{ij}	Relative SNR
N_r	Number of reliable relays
$\mathcal{A}_s$	The event that the destination selects the signal received from the source
$\mathcal{A}_{r,k}$	The event that the destination selects the signal from relay k
λ	Node/relay density
K_c	Constant gains such as antenna gain, processing gain
υ	Path loss exponent

$\mathcal{P}_T$, $\mathcal{P}_N$	Transmit power and noise power
$\mathcal{P}_s$, $\mathcal{P}_r$	Source and relay transmit power
r_N	Transmission range in the absence of fading
r_{Ns}, r_{Nr}	Transmission range of the source and relay in the absence of fading
d_{ij}	Distance between node i and node j
X_{ij}	Rayleigh fading coefficient between node i and node j
Z_{ij}	Lognormal fading coefficient between node i and node j
σ	Lognormal parameter
g_{ij}	Normalized average SNR
μ_r	Average number of reliable relays
Γ	Gamma function
$F_X(x)$	CDF of random variable X
$\Gamma(.)$	Gamma function
$B(a, b; r)$	A disc with radius r centered at point (a, b)
$C(a, b; r)$	A circle with radius r centered at point (a, b)
$g_{(i)}$	i-th largest average SNR
$W(.)$	Lambert's W function

g_{min}	Minimum SNR required for relay transmission
M_s	Number of source nodes
K_d	Number of receive antennas at the destination
K_r	Number of antennas at the relay
$\mathbf{H_{sd}}$	Source-destination channel matrix
$\mathbf{H_{sr}}$	Source-relay channel matrix
$\mathbf{H_{rd}}$	Relay-destination channel matrix
$\mathbf{H_e}$	Equivalent end-to-end channel matrix
$\mathbf{C}$, $\hat{\mathbf{C}}$	Data block transmitted by the users and its estimate at the relay
$\mathbf{Y_{d1}}$, $\mathbf{Y_{d2}}$	Received block at the destination in phase I and II
$\mathbf{N_{d1}}$, $\mathbf{N_{d2}}$	Noise matrix at the destination in phase I and II
$\mathbf{Y_e}$	Equivalent received block at the destination
$\mathbf{N_e}$	Equivalent noise matrix at the destination
L	Number of symbols per block
R_i	Data rate of source-i
$\beta_{i,r}$	Post-processing SNR for user/stream i at the relay
$\beta_{i,d}$	Post-processing SNR for user/stream i at the destination

$\gamma_{tr,i}$ Target SNR for source-i

P_o Outage probability

$\chi^2(n)$ Central chi-square random variable with n degrees of freedom

Chapter 1

Introduction

1.1 Motivation

As wireless communication becomes more prevalent, the demand for higher data rates and uninterrupted connectivity is increasing. Future wireless systems are provisioned to be highly heterogeneous and interconnected. On one side, wireless ad hoc networks are emerging for a wide range of new applications, on the other side, infrastructure based broadband wireless systems are expanding to provide increasing number of services with ubiquitous coverage.

Ad hoc networks have a wide range of applications including peer-to-peer wireless data exchange, home networks, and sensor networks. These networks operate in a new paradigm wherein the network does not rely on any infrastructure. Self-organization feature reduces the cost and effort for their configuration and maintenance. In most applications the network consists of battery-powered nodes. Due to low transmit power, these nodes have limited communication range. Thus, cooperative communication, in which nodes share their resources to facilitate each others' communication, is essential for these networks.

In wireless broadband networks cooperative communication emerged as an upgrade to single hop cellular architecture. As evident from the current and upcoming standards, there is a growing consensus in wireless community on adding multihop capability to these networks [1,2]. In infrastructure based wireless networks, enabling multihop relaying brings many opportunities at different network layers. Replacing long and weaker links with short and stronger links can mitigate the burden on the link budget. Alternative routes between the users and the basestation provide robustness against shadowing and multi-path fading, and introduce new design options for scheduling and routing.

In physical layer an important opportunity arises with cooperation; due to the broadcast nature of wireless medium, as the data is transmitted to its destination in multiple hops, many nodes in the vicinity can hear these transmissions. Transmissions from different nodes are generally affected by different and statistically independent fading. Hence, the final destination of the data can combine all the received signals using traditional combining methods such as Maximal Ratio Combining (MRC) or Selection Combining (SC) and obtain diversity against the harming effects of fading. Diversity obtained through multihop transmissions is usually referred to as *cooperative diversity* [3].

Diversity is a very powerful technique to increase robustness against channel fading. Cooperative diversity is a kind of spatial diversity that can be obtained without multiple transmit or receive antennas. It is especially useful when time, frequency, and spatial diversity through multiple antennas are not feasible. The first examples of practical cooperative diversity protocols were studied by Laneman et al. [4]. It was shown that diversity relaying has the potential to improve end-to-end (e2e) performance in slow fading environments despite the penalty of relaying in terms of bandwidth expansion. The main objective of this thesis is to design and analyze protocols to induce e2e diversity through the cooperation of relay nodes with source and destination.

Depending on the level of signal processing performed at the relay, cooperative relaying schemes can be classified as *analog relaying* or *digital relaying*. In analog relaying, the relay terminal amplifies the received signal and retransmits it. In digital relaying, the relay detects the received signal and retransmits regenerated version of the detected signal. In this thesis, the applications of cooperative digital relaying in several wireless scenarios are investigated. Most of the treatment is centered around two-hop networks, as a two-hop network is the simplest but non-trivial case for the physical layer cooperative diversity relaying problems studied in this thesis. The main contributions are summarized below.

1.2 Contributions

1.2.1 Error Propagation and Threshold Digital Relaying in Cooperative Wireless Networks

In digital relaying, if the relay detection is correct, the destination receives the signal through multiple branches and thus obtains diversity by combining them. However, if the relay makes any errors, post-combining SNR at the destination reduces significantly. This phenomenon is called *error propagation*. Error propagation limits the e2e performance of the protocols in which the relay always retransmits. Selective relaying can be used to reduce the probability of error propagation. The first part of this thesis focuses on relaying schemes that do not rely on the error detection and correction capabilities of the relays. These schemes are particularly useful for relaying among sensor devices that performs detection, but may not afford decoding at every hop due to stringent energy constraints.

A simple way of reducing error propagation is to make forwarding decisions based on the link SNRs in the network. The relay can use a threshold to decide when to retransmit, and retransmits only if the source-relay SNR is above this threshold.

The choice of the threshold has considerable impact on the e2e performance of the cooperative diversity schemes. In the first part of this thesis, we study threshold-based relaying schemes to minimize the e2e Bit Error Rate (BER) in uncoded cooperative digital relaying systems. In the literature, the threshold value has been determined empirically from numerical results. In some asymmetric networks, where the SNRs of the links are not statistically identical, this empirical threshold results in poor performance.

Optimal threshold values that minimize the e2e BER are derived and the importance of choosing the threshold optimally is illustrated. Studying the performance under different models, it is shown that knowledge of the instantaneous source-destination SNR at the relay can be exploited. When the average source-destination SNR is large, there is a gain from the instantaneous source-destination SNR knowledge at the relay. However, knowledge of the instantaneous relay-destination SNR at the relay does not change the performance significantly.

The asymptotic e2e BER of threshold digital relaying is also studied. It is shown that as the average link SNRs are increased simultaneously, directly proportional to a reference value (SNR), the optimal threshold that minimizes the e2e BER increases as $\log(\mathsf{SNR})$. The resulting e2e BER decreases as $\log(\mathsf{SNR})/\mathsf{SNR}^2$. Moreover, any threshold of the form $\log(c\,\mathsf{SNR})$, achieves the same order of e2e BER as the one achieved by the optimal threshold and provides dual diversity. A value of c that performs very close to the optimal threshold is also proposed.

Although multiple relays can offer higher diversity gains, large number of retransmissions is usually prohibitive due to limited radio resources. To this end, a threshold based relay selection algorithm is introduced to limit the retransmissions to one. A threshold function in the form of $\log(c\,\mathsf{SNR}^{M_r/\alpha_m})$, where M_r is the number of the relays, α_m is a modulation dependent parameter, and c is a positive constant, is proposed. It is proven that this protocol achieves full diversity ($M_r + 1$ order) with the proposed threshold.

1.2.2 Cooperative Digital Relaying in Wireless Ad-hoc Networks

Most studies on cooperative relaying consider simple and optimistic scenarios, in which, for example, all the relays are in the midpoint between the source and the destination. In ad hoc networks, the topology will be random due to random node deployment or node mobility. While for some source-destination pairs there might be many relays at favorable locations, there might also exist pairs which can find no relays at all. Although the studies conducted for deterministic topologies provide useful initial understanding of cooperative diversity relaying, the performance obtained in these scenarios is not a good indicator of the network-wide gain from cooperative diversity in random relay deployments. The randomness in node positions is an integral part that must be incorporated into the problem formulation.

In the second part of this thesis, two-hop cooperative diversity relaying in wireless ad hoc networks is studied. The problem is formulated recognizing that node positions, as well as the fading states of the channels among the nodes, are random. A simple protocol which requires minimal a priori knowledge of node positions and channel fading states is proposed. This protocol assumes that each node in the vicinity of the source knows its average link gain to the destination. The source transmits a packet, and then chooses relays among the nodes that can decode the received packet reliably. Assuming that the relay nodes are distributed according to a 2-dimensional Poisson point process, the e2e outage probability of the protocol is studied analytically as a function of node density, fading parameters and node transmit powers. Performances of other relay selection criteria such as instantaneous link gain and distance to the destination are also studied through simulations. Both maximal ratio combining and selection combining are considered at the destination.

1.2.3 Relay-Assisted Spatial Multiplexing in Wireless Fixed Relay Networks

In infrastructure based networks a practical alternative to user cooperation is deploying *fixed relays* that are dedicated nodes for forwarding other nodes' data. Fixed relays can take the burden of cooperation from users. They are provisioned to have direct access to the power line, hence their operation is not limited by battery lifetime [5]. While mounting multiple antennas at mobile user terminals might be impractical due to space and cost constraints, these constraints are less stringent for fixed relays. Therefore, they can easily accommodate multiple antennas.

The last part of this thesis in an initial study on the potential benefits of multi-antenna relays. A system in which multiple users want to communicate with a common multi-antenna receiver, such as a basestation, is considered. Independent data of the users are spatially multiplexed. In particular, end-to-end outage probability with Zero Forcing Decision Feedback (ZF-DF) type receivers is studied. A novel method to combine the signals from the source and the relay is proposed and its performance is analyzed.

1.3 Organization

The rest of this thesis is organized as follows: Chapter 2 provides a background on cooperative communication and cooperative diversity relaying. Chapters 3-5 focus on threshold based digital relaying. In Chapter 3 the optimal threshold values that minimize e2e BER are derived and their performances are evaluated. Chapter 4 investigates the diversity gain achievable through threshold digital relaying. In Chapter 5 multiple relay case is considered and a threshold based relay selection protocol is studied. Chapter 6 studies the performance of cooperative relaying in random topologies. In Chapter 7, cooperative diversity benefits obtained through a multiple antenna relay in a distributed spatial multiplexing system is studied.

The main results in the literature in the general area of cooperative relaying are summarized in Chapter 2. In the beginning of each chapter, the literature that is particularly relevant to that chapter is reviewed. Wherever necessary, the references that are relevant to multiple chapters are reviewed more than once, from each chapter's viewpoint. A list of the papers published, submitted, and in preparation are also given as an appendix.

Chapter 2

Background on Cooperative Communication and Cooperative Diversity Relaying

Cooperative communication refers to the sharing of resources and the realization of distributed protocols among multiple nodes in a network. It is a very active research area with promising developments. Cooperation among peer nodes have been considered in the 1980's under the title of packet radio networks [6–8]. Since the 1990's, proliferation of highly capable mobile devices brought the attention back into peer cooperation and wireless ad hoc networks appeared as an active research area. The main characteristics of ad hoc networks are self-configuration and autonomous operation without relying on any infrastructure. The promise of ad hoc networks has been that – as the term "ad hoc" suggests – their self-organization feature will allow them to adapt to a wide spectrum of applications and network conditions and will reduce the cost for configuration and maintenance. One of the main focuses of research on ad hoc networks has been mobility and dynamic topologies. Besides the uncertainty of link qualities due to wireless fading, nodes can join and leave a network and the topology of the network changes over time. Although the success of ad hoc networks in the commercial domain has been somewhat limited, some new classes of networks emerged, such as community mesh networks and sensor networks, that share some of the characteristics of ad hoc networks. Research on wireless sensor networks is mainly driven by the advances in low-power RF and microelectronics, which enabled large scale deployment of small-size and low-cost sensors. In addition to sensing units, sensors are equipped with transceivers and they can form networks to transmit their measurements. Wireless sensor networks are expected to find a wide range of applications such as security, habitat monitoring, and remote diagnostics and patient care. Typically, a low-cost sensor is constrained to work and last with limited energy resources. This limits the computation and communication capabilities of wireless sensor nodes.

The idea of cooperation has found support also in infrastructure based broadband wireless networks. Conventionally, infrastructure based networks follow a single hop cellular architecture, in which users and the basestations communicate directly. The main challenge in today's wireless broadband networks is to support high rate data communication with continuous coverage at a reduced cost. Despite decades of research in wireless communication, and significant advances in signal processing and multi-antenna architectures, these demands are not fully met. The scarcity of wireless spectrum encouraged the allocation of high frequency bands, where power attenuation with distance is more severe. This factor significantly decreases the coverage of a basestation. Fast decay of power with distance suggests that both the capacity and the coverage of networks can be improved by increasing the density of basestations. However, this trivial solution – sometimes called deploying microcells – adds to the already high infrastructure and deployment costs. As a result, we face a situation in which the wireless systems can achieve any two, but not all three, of high capacity, high coverage and low cost [9]. Integrating cooperative communication to cellular networks and forming hybrid networks emerged as a pragmatic solution to mitigate this problem. Although wireless relays use additional radio resources, they have lower cost compared to basestations since they do not require a high capacity wired connection to the backbone. In the final cost analysis, wireless relays can be a more viable solution than microcells to increase the coverage and to distribute the capacity uniformly with the coverage of a basestation. Multihop relaying is already part of the standards currently being developed for wireless broadband systems such as 802.16j and 802.16m, which is an indication of growing consensus on the effectiveness of cooperative communication.

The conventional and simplest form of cooperation is multihop relaying, in which data is delivered to its destination through relay nodes forming a multihop path. Next, we provide the preliminaries of multihop relaying.

2.1 Preliminaries of Multihop Relaying

Relaying protocols can be classified into two according to the processing at the relay: Analog Relaying (AR) or Digital Relaying (DR). AR can be implemented in a very primitive way in which the relay functions as an active reflector. In DR, the relay performs detection and regenerates a noise-free version of original signal based on its detection. If the resource and performance constraints – such as relay energy and latency – permit, digital relays can also decode and re-encode the received data. This way, some of the errors occurring at the source-relay link can be corrected at the relay. These protocols are also referred as decode-and-forward (DF) relaying protocols in the literature.

AR and DR incur different limitations in practice. In DR, the relay is required to first demodulate and detect the received signal, and then modulate and retransmit the regenerated signal. These operations potentially require more processing and causes more latency than simple AR. In its basic form, AR does not require any of these.

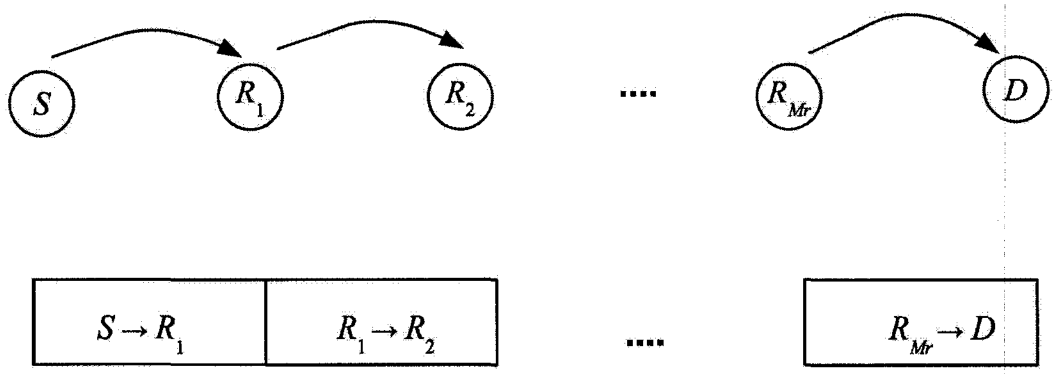

Figure 2.1: Multihop relaying and the corresponding time-division protocol.

However, if implemented blindly, AR can generate constant interference to the rest of the network. Using analog relays as regular network nodes controlled by certain Medium Access Control (MAC) and Radio Resource Management (RRM) protocols requires analog relaying to be implemented digitally. In this case, the relay is required to store analog samples, possibly after quantization.

The relay nodes can operate in full-duplex or half-duplex modes. In full-duplex mode the relay can transmit and receive at the same time on the same frequency band. To implement full-duplex operation, in principle, the relay can cancel its self-interference from the received signal. However, in practice using low cost radios this approach may not be robust. Thus, in the near future relays are expected to operate in half-duplex mode only.

The half-duplexity constraint requires the use of orthogonal channels for transmission and reception. For instance, the relay can use different time slots to receive and transmit as shown in Fig. 2.1. In the first time slot the source node transmits and the next relay node R_1 receives. In the second time slot, R_1 transmits the processed signal to the next relay. With this protocol, relaying can be easily integrated to wireless networks using time-division multiple access. As the number of hops increases, the number of time slots allocated for delivering data from the source to the destination increases. To increase the spectral efficiency, spatial reuse can be allowed among the relay nodes.

BER performance of AR deteriorates at low SNR since analog relays amplify both the noise and the information bearing parts of the received signal. In the presence of distance dependent attenuation only, DR performs significantly better than AR [10, pp. 313-315]. However, under Nakagami fading with different parameters, the BER and outage performance of two-hop AR and DR are very close at high SNR values. DR has a negligible gain over AR at low SNRs [11]. On the other hand, the end-to-end performance gain of DR can become significant as the number of hops increases [12].

In the context of infrastructure based networks, multihop relaying through both fixed relays and user cooperation are being considered [5]. The orthogonal channel requirement mentioned above reduces the end-to-end capacity of multihop networks significantly, which can be prohibitive for broadband networks. Optimal number of hops in broadband networks is analyzed in [13] and it is argued that in cellular networks, as a rule of thumb, the number of hops should be limited to that required for coverage. Capacity of multihop networks with different number of relays and reuse factors has been studied in [14].

In ad hoc networks literature, in addition to a significant research effort put on MAC and network layer aspects of wireless multihop networks [15, 16], some problems closely coupled with physical layer of multihop relaying, such as power control, scheduling [17], directional transmissions using beamforming [18] were also considered. The initial tendency to abstract wireless links as wired-line links with more frequent failures, evolved to better understanding of the effects of physical layer on the rest of the protocols [19]. Furthermore, cross-layer design appeared as a new design philosophy.

2.2 Multiple Antennas and Cooperative Communication

Multihop relaying imposes a chain structure in which each node listens one other node in the chain. It can be seen as the simplest form of cooperative communication. However, introducing relays into the picture brings many more possibilities. For instance, consider the network in Fig. 2.1 with $M_r = 2$ relays and assume that the link from S to R_1 is error-free. Then, R_1 can act as a second transmit antenna for S. Similarly, if R_2 and D has an error free link, R_2 can serve as a receive antenna for D.

Multi-antenna techniques can improve the performance of wireless links in terms of both capacity and reliability without additional bandwidth use. Multiple receive antennas provide the classical spatial receive diversity, whereas multiple transmit antennas can be leveraged through space-time coding to obtain diversity [20]. Availability of multiple antennas both at the transmitter and receiver sides creates a MIMO link. In scattering rich environments, at high SNR, the information theoretic capacity of a MIMO link grows linearly with the number of transmit and receive antennas. In particular, the capacity $C \approx \min\{K_{tx}, K_{rx}\} \log(\mathsf{SNR})$, where K_{tx} and K_{rx} are the number of transmit and receive antennas, as opposed to the capacity of a Single-Input Single-Output (SISO) link $C \approx \log(\mathsf{SNR})$. At asymptotically high SNRs these two kinds of gains, namely multiplexing gain and diversity gain, can be quantified by diversity order d and multiplexing gain r. A scheme attains diversity order d and multiplexing gain r if its transmission rate scales as $\mathrm{R} = r\log(\mathsf{SNR})$ and its error rate scales as $\mathrm{BER} \approx \mathsf{SNR}^{-d}$ [21, pp. 386]. Although these two kinds of gains can be obtained simultaneously in MIMO links, they are coupled. An important result by Zheng and Tse shows that there is a fundamental trade-off between the two gains [22]: for MIMO links, simultaneously achievable diversity gain d and multiplexing gain r

satisfy

$$d(r) = (K_{tx} - r)(K_{rx} - r), \qquad 0 \leq r \leq \min\{K_{tx}, K_{rx}\}.$$

Similar to MIMO systems, through distributed protocols, cooperation can increase the transmission rate (or enlarge the achievable rate region) or improve the reliability for a given rate. Capacity in the presence of relay nodes is a classical problem in information theory [23, 24], which recently received much attention. Some important results on the achievable rates in wireless networks include [25, 26]. As opposed to the work on relay channel capacity, cooperative diversity aims to improve the performance, typically in terms of the outage probability and the error rate, for a given fixed transmission rate. The main focus of this thesis is on cooperative diversity aspects of cooperative communication.

2.3 Cooperative Diversity

Cooperative diversity relies on two principles:

- Due to the broadcast nature of wireless medium, most transmissions can be heard by multiple nodes in the network with no additional transmission power and bandwidth.
- Different nodes have independent channel fading statistics to a given destination node and the destination can listen, store, and then combine signals from different nodes.

One of the first studies that introduced the concept of cooperative diversity is [3] by Sendonaris et al. In this paper, an uplink scenario is considered, in which two users cooperate by relaying data for each other. After showing the potential of cooperation in enlarging the achievable rate region of the two users, the authors demonstrated that cooperation can improve other measures such as outage capacity, error probability

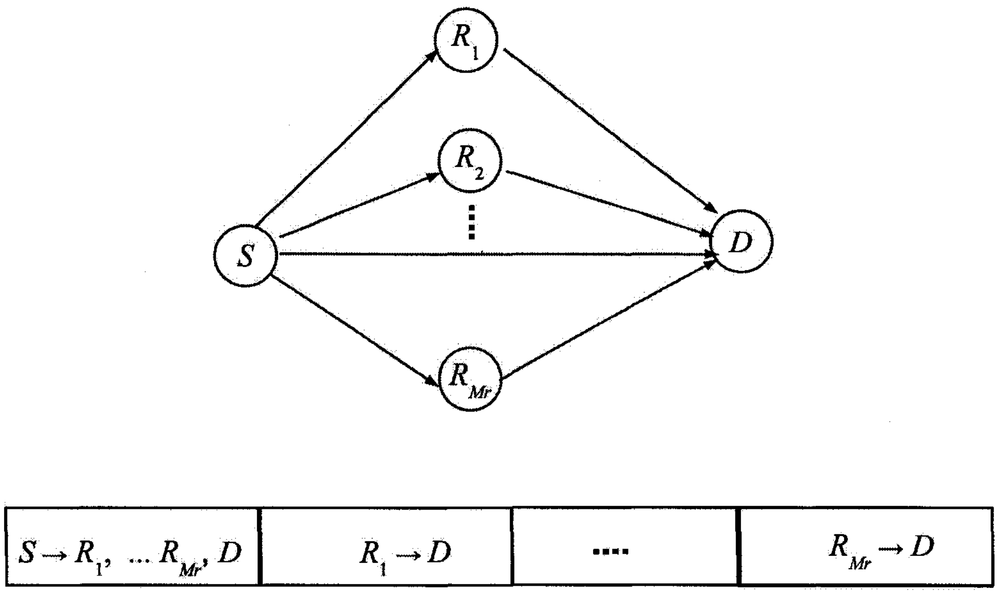

Figure 2.2: Cooperative diversity relaying with parallel relays and the corresponding time-division protocol.

and coverage. The first practical cooperative relaying protocols have been proposed by Laneman et al. in [4]. In this seminal paper, the authors identified different classes of cooperative diversity protocols such as fixed protocols, in which the relay always retransmits, selective protocols, in which the relay retransmits only when it decodes reliably, and incremental protocols, in which the relay retransmits only when the direct transmission fails. Detection aspects and BER performance analysis for cooperative diversity protocols have been conducted in [27–31]. It is observed that while simple analog relaying achieves diversity gain, in order to achieve diversity gain digital relaying requires either error detection mechanisms or more sophisticated combiners. The next three chapters focus on this problem and investigate threshold based relaying as an alternative to error detection at the relay.

In a network exploiting cooperative diversity, every node can potentially be considered to be "connected" to all the other nodes. However, hardware and resource constraints do not allow all the links be used for delivering a given packet and certain "connectivity graphs" can be more viable than the others. Reference [32] derives the maximum e2e diversity orders achievable for any given connectivity graph.

In the earlier decode-and-forward protocols, source and relays use a common codebook, which is equivalent to repetition coding for destination. However, it is possible to obtain coding gain if different nodes use non-identical codebooks [33, 34]. For instance, in [34], source data is encoded in two partitions. In the first time slot, the source transmits the first partition. Then, the relay decodes the data based on the first partition. If its decoding is reliable, it obtains the second partition and transmits it to destination in the second time slot. The destination decodes the data based on both the first partition received from the source and the second partition received from the relay, thereby obtains additional coding gain in addition to the diversity gain.

Cooperative diversity protocols, due to retransmissions, can decrease the effective rate while increasing the reliability. Hence, it is important to evaluate their performance in terms of diversity-multiplexing trade-off. In [4] the outage capacity and diversity-multiplexing trade-off achieved by various protocols are analyzed. When multiple relays are used according to the time division protocol described in Fig. 2.2, the multiplexing loss is especially high. One way of overcoming this loss is through distributed space-time coding [35]. In distributed space-time protocols all the relays that decode the source information transmit different columns of a space-time code matrix simultaneously, i.e., the protocol takes place in two time slots instead of M_r+1. These protocols can potentially achieve a better diversity-multiplexing trade-off than repetition based protocols. In [36], the authors propose a distributed space time coding scheme that does not require decoding at relays. Relays implement distributed linear dispersion codes, which requires only linear operations at each relay. A similar scheme for the specific case of two relays implementing Alamouti coding is studied in [37].

Another method to reduce the multiplexing loss is relay selection. Instead of retransmitting the data from all the relays, only a small number of relays can be selected based on their channel quality to the source and the destination. Such protocols are proposed in [38–40] and will be discussed in more detail in Chapters 5 and 6.

Recently, it has been shown that the multiplexing loss of relaying is mostly due to the fixed time slots allocated for the source and relay transmissions rather than the half-duplex constraint. More sophisticated protocols that reduce the multiplexing loss by allowing dynamic time slots were proposed to improve diversity-multiplexing trade-off [41–43].

Although cooperative diversity is a technique that can induce spatial diversity in the absence of multiple antennas, its benefits can be combined with those of multiple antennas. For instance, fixed relays used in infrastructure based networks can accommodate multiple antennas. Advantageous and performance limits of multi-antenna relaying have been considered in [44, 45]. In Chapter 7 we propose and analyze schemes that combine spatial multiplexing and cooperative diversity.

Chapter 3

SNR-based Threshold Digital Relaying

In this chapter we introduce the concept of SNR-based selective digital relaying. In digital cooperative relaying, if the relay detection is correct, the destination receives the signal through two branches (from the source and the relay) thereby achieving diversity by combining them. However, if the relay has a detection error, the effective SNR at the destination after combining is significantly reduced. This phenomenon is called *error propagation*. The e2e performance of simple digital relaying, in which the relay always retransmits, is limited by error propagation.

To reduce the probability of error propagation, the relays can forward the data selectively. One measure that can be used for forwarding decisions is the link SNR. If the received SNR at the relay is low, the data is likely to have errors and hence the relay discards the data. In many wireless applications, relaying schemes might incorporate channel coding techniques. In this case, other measures of reliability that are extracted from the received signal at the relay can be used in conjunction with SNR [46].

If the reliability information is extracted from the received data, the relay is required to perform channel estimation, demodulation, and then error detection for each data block before making a forwarding decision. These operations cause additional delay and extra power consumption even if the relay eventually decides not to transmit. In cellular systems, the amount of power consumed by the terminals in receive mode is less significant compared to that in transmit mode. However, these two power levels are comparable in low power devices such as battery powered sensor nodes [47]. In SNR-based selective relaying, the relaying decisions are simpler and remain the same for a time duration in the scale of the channel coherence time in the network. Thus, when the source-relay SNR is low, the relay can be put into sleep mode. More importantly, sensor networks can adopt uncoded transmission or avoid decoding at intermediate relay nodes due to resource constraints [48, 49]. Hence, in networks that include nodes with a wide range of computation and communication capabilities, SNR-based relaying can be desirable in order not to isolate the nodes with scarce power and limited computational capability. SNR-based selective relaying is especially suited for applications where either uncoded transmission is used, or the relaying and channel coding are required to be transparent to each other, or the delay and the power consumption incurred for extracting the reliability information from the received data are significant.

In this chapter we address the design of SNR-based relaying policies for cooperative two-hop networks employing uncoded signaling. These polices minimize the e2e BER and lead to threshold rules for the source-relay link. If the source-relay SNR is larger than a threshold, the probability of an error at the relay is small and hence the relay retransmits the signal. Otherwise, the relay remains silent. These kind of schemes are called Threshold Digital Relaying (TDR).

The choice of the threshold has considerable impact on the e2e performance of TDR. For instance, consider a relay detection threshold value of zero. This protocol is akin to simple digital relaying and its diversity order is equal to one [27]. On the other hand, for a very high threshold setting, the system degenerates to one path channel, which is the source-destination channel and dual diversity is not realized.

The trade-off between creating the required diversity branches to the destination and minimizing the risk of error propagation has motivated research on SNR-based threshold relaying [4, 50–52]. Some studies considered a system with ideal coding, where no error occurs at the relay as long as source-relay SNR is larger than a target SNR which depends on a specified target rate [4,35]. This assumption implies that the SNR threshold for relaying must be equal to the target SNR. Herhold et al. studied SNR-based threshold relaying for an uncoded system [50]. In this work, the authors formulate the power allocation and threshold selection jointly. They numerically obtain power allocation fraction and threshold pairs that minimize the e2e BER for a given modulation scheme used by the source and the relay. Based on these numerical results, they also provide empirical rules to approximate the optimal parameters.

In [51], the performance of TDR in a multi-antenna multi-relay architecture is studied. It is shown that threshold relaying is essential in uncoded systems when the relay has a small number of receive antennas. In [50], the threshold – if used jointly with the optimal power fraction – is a function of the average SNRs of the source-relay, relay-destination and source-destination links while in [51] the threshold depends on the average SNR of the source-relay link only. Our analytical formulation shows that for arbitrary network configurations and given fixed transmit powers used by the source and the relay, the optimal threshold is independent of the average source-relay SNR.

In [52], the authors derive the BER of threshold-based relaying for an arbitrary threshold value and obtain the optimal threshold and power allocation by minimizing the BER numerically. However, their assumption that the channel coefficients are real Gaussian random variables does not apply to practical wireless scenarios.

The idea of threshold relaying, or on-off relaying, can be generalized to the adaptation of relay transmit power. In [31] and [53], the authors considered a scheme to control the relay power adaptively based on the link SNRs in order to mitigate error propagation. They propose a scaling factor for relay power that is based on the source-relay and relay-destination SNRs.

An alternative approach to mitigate error propagation is to design the destination receiver by taking error propagation into account. In [29], cooperative demodulation techniques for a two-hop parallel relaying protocol are considered. In this protocol, the relays always retransmit, which would result in a diversity order of 1 under simple MRC at the destination. The authors propose maximum-likelihood (ML) combining and demodulation at the destination assuming that the destination knows the average bit error probability at each relay during the first hop. They derive ML receivers and piecewise linear approximations to ML receivers for different relaying schemes.

Wang et al. [30] propose a novel combining scheme that can be employed at the destination for digital parallel relaying. This scheme, which is called Cooperative-MRC (C-MRC), exploits the instantaneous BER of source-relay links at the destination. The C-MRC can achieve full diversity in uncoded digital relaying systems. However, it requires the relays to send their instantaneous BER values to the destination.

The models used by [29] and [30] both place the computing burden on the destination while keeping the relays relatively simple. In our model, however, the relay implicitly participates in combining the two branches; by remaining silent, the relay effectively assigns weight zero to the relay-destination signal. Then, the destination performs MRC. Avoiding transmissions from branches that make little contribution to the post-processing SNR can reduce interference in the network. Furthermore, in threshold relaying the instantaneous source-relay SNR is exploited at the relay while C-MRC needs the instantaneous source-relay SNR at the destination, which requires additional signaling.

We formulate the selection of the optimal threshold as a simple decision problem from the relay's point of view. Four models that differ in the amount of SNR information available at the relay are considered. In the first model, Model 1, the relay makes decisions based on the instantaneous source-relay SNR, the average relay-destination SNR, and the average source-destination SNR. Model 2 assumes that the instantaneous SNR of source-relay and relay-destination links are available to the relay while Model 3 assumes that the instantaneous SNR of the source-relay and source-destination links are available to the relay. Finally, Model 4 assumes that the relay knows the instantaneous SNRs of all three links. Expressions for the optimal threshold values and the minimum e2e BER are derived for Rayleigh fading.

This chapter is organized as follows: The system model is presented in Section 3.1 and the optimal threshold and the e2e BER for selective relaying schemes are analyzed in Section 3.2. In Section 3.3, performance benchmarks are described and numerical examples on the e2e BER performance are presented. The chapter concludes with a summary of our findings.

3.1 System Model

The network model is shown in Fig. 3.1. It includes a source node S, a destination node D, and a relay node R that assists the communication between S and D. For clarity of exposition, it is assumed that all the links use Binary Phase Shift Keying (BPSK) modulation. Appendix A.4 provides a sketch for the extension of some of the analysis to M-ary Phase Shift Keying (MPSK). In accordance with the half-duplex constraint, S and R work in time division mode as described in Chapter 2. This constraint prohibits most practical relay terminals from transmitting and receiving simultaneously on the same channel. The protocol has two phases: In phase I, S transmits and R and D listen. In phase II, R detects the signal and either retransmits, in which case S is silent, or declares that it will remain silent and S starts phase I with the next data. If R retransmits in phase II, D combines the signals received in phase I and phase II using MRC and performs detection based on the combined

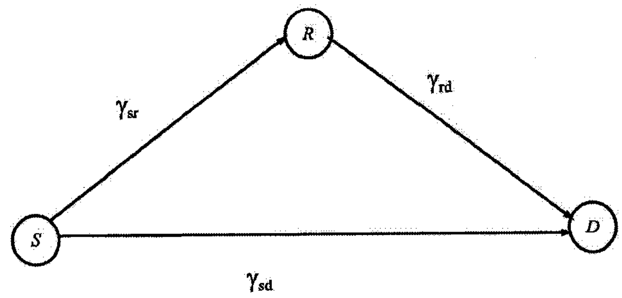

Figure 3.1: The system model.

signal.

Let the signal received at the destination from the source be denoted by y_{sd}.

$$y_{sd} = \alpha_{sd}\sqrt{E_{b,s}}\,x_s + n_{sd}, \tag{3.1}$$

where $x_s \in \{+1, -1\}$, $E_{b,s}$ is the energy per bit spent by the source, α_{sd} is the fading coefficient and n_{sd} is a complex Gaussian random variable with zero mean and a variance of $N_0/2$. Similarly, the signal received at the relay is equal to $y_{sr} = \alpha_{sr}\sqrt{E_{b,s}}\,x_s + n_{sr}$. If the relay transmits, the received signal at the destination as a result of this transmission is given by

$$y_{rd} = \alpha_{rd}\sqrt{E_{b,r}}\,x_r + n_{rd}, \tag{3.2}$$

where $x_r \in \{+1, -1\}$ is the symbol sent by the relay based on its detection of x_s and $E_{b,r}$ is the energy per bit spent by the relay. The noise components n_{sr}, n_{rd}, and n_{sd} are assumed to be i.i.d. random variables. The instantaneous link SNRs are equal to $\gamma_{sr} = |\alpha_{sr}|^2 E_{b,s}/N_0$, $\gamma_{rd} = |\alpha_{rd}|^2 E_{b,r}/N_0$, and $\gamma_{sd} = |\alpha_{sd}|^2 E_{b,s}/N_0$. All the links are assumed to exhibit flat fading with Rayleigh envelope distribution. However, some of the analysis in this chapter is general and not limited to Rayleigh distribution. We assume that both $E_{b,s}$ and $E_{b,r}$ are fixed, predetermined values. Hence, the instantaneous link SNRs can be expressed as $\gamma_{ij} = \bar{\gamma}_{ij}\, X_{ij}^2$, where X_{ij}^2 is an exponential random variable and $\bar{\gamma}_{ij}$ is the average SNR. All X_{ij}^2's are independent and identically distributed with unit mean. The PDF of γ_{ij} is then given by $p_{\gamma_{ij}}(\gamma_{ij}) = (1/\bar{\gamma}_{ij})\exp(-\gamma_{ij}/\bar{\gamma}_{ij})$ for $\gamma_{ij} \geq 0$. The average SNR $\bar{\gamma}_{ij}$, incorporates the energy per bit spent by node i and the path loss between node i and node j. Hence, the average SNR of $S-R$, $R-D$, and $S-D$ links, denoted by $\bar{\gamma}_{sr}$, $\bar{\gamma}_{rd}$, and $\bar{\gamma}_{sd}$, respectively, are known parameters that are not necessarily identical but constant for at least the duration of the two phases.

The channel states remain constant during phase I and phase II. The two phases constitute one *block*. We assume that the channel states are either independent from block to block or their correlation is not exploited. We assume that the CSI is available at the receiver side for all three links and the signal is demodulated coherently. We consider various models with different levels of adaptation in relaying decisions. In these models, the relay makes use of either the mean or the instantaneous SNR for each link. In Model j, the relay uses the set of parameters denoted by I_j, where $j = 1, 2, 3, 4$, to make relaying decisions. The following sets are considered:

$$I_1 = \{\gamma_{sr}, \bar{\gamma}_{rd}, \bar{\gamma}_{sd}\}, \quad I_2 = \{\gamma_{sr}, \gamma_{rd}, \bar{\gamma}_{sd}\}, \quad I_3 = \{\gamma_{sr}, \bar{\gamma}_{rd}, \gamma_{sd}\}, \quad \text{and} \quad I_4 = \{\gamma_{sr}, \gamma_{rd}, \gamma_{sd}\}. \tag{3.3}$$

How well a relaying configuration can adapt to varying channel conditions depends on the information used by the relay. In general, the average SNR values change much more slowly than the instantaneous values. Although a more adaptive scheme is expected to perform better, a system using average channel characteristics is easier to implement since it requires less frequent updates to resource allocations. Another challenge is to acquire the necessary SNR information at the relay. Since the relay is the receiver in the $S-R$ link, it can estimate γ_{sr} and additional overhead of Model 1 is minimal. Model 2 requires the relay to make decisions based on the instantaneous SNR of its forward channel γ_{rd}. Thus, a feedback channel from D to R might be necessary. Similarly, Model 3 requires γ_{sd}, which can be estimated in the first phase at D and can be sent to R through the same feedback channel. Model 4 has the highest complexity since it requires that both γ_{rd} and γ_{sd} are sent to R by D. The analysis in this chapter focuses on the best possible performance under the different models. Therefore, we assume that the SNR information required by each model is available at the relay.

Notation

In the rest of this chapter and in Chapters 4 and 5, we use the following definitions and notation. The error events in the $S-R$ and $S-D$ links are denoted by $\mathcal{E}_{sr}$ and $\mathcal{E}_{sd}$, respectively. The event that an error occurs after the destination combines the source signal and the incorrectly regenerated relay signal is referred to as *error propagation* and is denoted by $\mathcal{E}_{prop}$. We use the term *cooperative error* for the event that an error occurs after the destination combines the source signal and the correctly regenerated relay signal. The cooperative error event is denoted by $\mathcal{E}_{coop}$.

The BER in point-to-point links conditioned on the instantaneous link SNR and average link SNR are denoted by $P_b(\gamma_{ij})$ and $\bar{P}_b(\bar{\gamma}_{ij})$, respectively. Consider a general modulation scheme for which the bit error probability can be expressed as $P_b(\gamma) \approx \beta_m \operatorname{erfc}(\sqrt{\alpha_m \gamma})$, where $\alpha_m, \beta_m > 0$ and the error function (erf) and the complementary error function (erfc) are defined as

$$\operatorname{erf}(z) = \frac{2}{\sqrt{\pi}} \int_0^z e^{-t^2} \mathrm{d}t \quad \text{and} \quad \operatorname{erfc}(z) = 1 - \operatorname{erf}(z).$$

We note that typically α_m depends on the minimum distance in the constellation and β_m depends on the number of neighbors with minimum distance; the bit error probability of most practical modulation schemes can be approximated by selecting

(β_m, α_m). For instance, assuming Gray coding, the nearest neighbor approximation for MPSK is equivalent to $(\beta_m, \alpha_m) = (1/\log_2 M\,, \log_2 M \sin^2(\pi/M))$. Based on this general P_b expression, the average bit error probability under Rayleigh fading is calculated as [54, pg. 185]:

$$\bar{P}_b(\bar{\gamma}) = \mathbb{E}_\gamma[\beta_m \,\mathrm{erfc}(\sqrt{\alpha_m \gamma})] = \beta_m \left[1 - \sqrt{\frac{\alpha_m \bar{\gamma}}{1 + \alpha_m \bar{\gamma}}}\right]. \tag{3.4}$$

For BPSK modulation, which is considered in this chapter, $(\beta_m, \alpha_m) = (0.5, 1)$ and the expression is exact:

$$P_b(\gamma_{ij}) = \mathbb{P}(\mathcal{E}_{ij}|\gamma_{ij}) = \frac{1}{2}\mathrm{erfc}(\sqrt{\gamma_{ij}}), \tag{3.5}$$

$$\bar{P}_b(\bar{\gamma}_{ij}) = \mathbb{P}(\mathcal{E}_{ij}|\bar{\gamma}_{ij}) = \frac{1}{2}\left(1 - \sqrt{\frac{\bar{\gamma}_{ij}}{1 + \bar{\gamma}_{ij}}}\right). \tag{3.6}$$

The optimal threshold for Model j is denoted by $\gamma^*_{t,j}$; the policy used by the relay to make forwarding decisions is denoted by π; and the e2e bit error probability calculated at the relay based on the link SNR observations I_j when the relay follows policy π is denoted by $\mathbb{P}\{\mathcal{E}_{e2e}|I_j, \pi(I_j)\}$. The average e2e BER of the optimal relaying under Model j is denoted by $\mathrm{BER}^{(j)}_{e2e}$.

3.2 Analysis of Threshold Digital Relaying

There are two actions that can be taken by the relay node: a_0, which represents remaining silent and a_1, which represents detecting and retransmitting the source signal. In this chapter, we focus on analyzing the potential of selective relaying to prevent error propagation and to decrease e2e BER. The relay makes decisions to minimize the expected e2e error probability with given SNR observations.[1]

[1]If the relay retransmits in phase II, the overall transmission uses more bandwidth and more power compared to direct transmission. To keep the analysis tractable these factors are not taken into account in relaying decisions. However, any selective relaying scheme compares favorably to simple relaying in terms multiplexing loss and total average power.

Then, the relaying policy that minimizes the e2e BER is given by

$$\pi^*(I_j) = \arg \min_{a_i \in \{a_0, a_1\}} \mathbb{P}\{\mathcal{E}_{e2e}|I_j, a_i\},$$

which can be expressed as

$$\mathbb{P}\{\mathcal{E}_{e2e}|I_j, a_0\} \underset{a_0}{\overset{a_1}{\gtrless}} \mathbb{P}\{\mathcal{E}_{e2e}|I_j, a_1\}. \tag{3.7}$$

If the relay does not forward the signal received in the first hop, the e2e bit error probability for the block depends only on the $S-D$ channel: $\mathbb{P}\{\mathcal{E}_{e2e}|I_j, a_0\} = \mathbb{P}\{\mathcal{E}_{sd}|I_j\}$. If the relay does forward, we can express the e2e bit error probability as

$$\mathbb{P}\{\mathcal{E}_{e2e}|I_j, a_1\} = \mathbb{P}\{\mathcal{E}_{sr}|I_j\}\, \mathbb{P}\{\mathcal{E}_{prop}|I_j\} + (1 - \mathbb{P}\{\mathcal{E}_{sr}|I_j\})\, \mathbb{P}\{\mathcal{E}_{coop}|I_j\}. \tag{3.8}$$

By substituting (3.8) into (3.7), we obtain

$$\mathbb{P}\{\mathcal{E}_{sr}|I_j\} \underset{a_1}{\overset{a_0}{\gtrless}} \frac{\mathbb{P}\{\mathcal{E}_{sd}|I_j\} - \mathbb{P}\{\mathcal{E}_{coop}|I_j\}}{\mathbb{P}\{\mathcal{E}_{prop}|I_j\} - \mathbb{P}\{\mathcal{E}_{coop}|I_j\}}. \tag{3.9}$$

The derivation up to this point is not specific to Rayleigh channels and is valid under any SNR distribution.

3.2.1 Probability of Cooperative Error

Since the destination employs MRC, the SNR after combining the two signals is the sum of the SNRs of the $S-D$ and the $R-D$ channels. If the relay has $I_4 = \{\gamma_{sr}, \gamma_{rd}, \gamma_{sd}\}$, the probability of cooperative error calculated at the relay is equal to

$$\mathbb{P}\{\mathcal{E}_{coop}|I_4\} = \mathbb{P}\{\mathcal{E}_{coop}|\gamma_{rd}, \gamma_{sd}\} = P_b(\gamma_{rd} + \gamma_{sd}) = \frac{1}{2}\text{erfc}\left(\sqrt{\gamma_{rd} + \gamma_{sd}}\right). \tag{3.10}$$

The cooperative error probability given $I_3 = \{\gamma_{sr}, \bar{\gamma}_{rd}, \gamma_{sd}\}$, is equal to

$$\mathbb{P}\{\mathcal{E}_{coop}|I_3\} = \mathbb{P}\{\mathcal{E}_{coop}|\bar{\gamma}_{rd}, \gamma_{sd}\} = \mathbb{E}_{\gamma_{rd}}\left[\frac{1}{2}\text{erfc}\left(\sqrt{\gamma_{sd} + \gamma_{rd}}\right)\right] \tag{3.11}$$

$$= \frac{1}{2}\int_0^\infty \frac{1}{\bar{\gamma}_{rd}} e^{-\gamma_{rd}/\bar{\gamma}_{rd}} \text{erfc}\left(\sqrt{\gamma_{rd} + \gamma_{sd}}\right) \mathrm{d}\gamma_{rd} \tag{3.12}$$

$$= e^{\gamma_{sd}/\bar{\gamma}_{rd}} \int_{\gamma_{sd}}^\infty \frac{1}{2\bar{\gamma}_{rd}} e^{-t/\bar{\gamma}_{rd}} \text{erfc}\left(\sqrt{t}\right) \mathrm{d}t = e^{\gamma_{sd}/\bar{\gamma}_{rd}} h(\gamma_{sd}, \bar{\gamma}_{rd}), \tag{3.13}$$

where we use change of variables to obtain (3.13) from (3.12) and define $h(.,.)$ as $h(x,y) = \int_x^\infty \frac{1}{2y}\mathrm{erfc}(\sqrt{t})e^{-t/y}\mathrm{d}t$. This function can be calculated in terms of erfc function (See Appendix A.1 for the derivation.) :

$$h(x,y)=\frac{1}{2}e^{-x/y}\mathrm{erfc}(\sqrt{x}) - \frac{1}{2}\sqrt{\frac{y}{1+y}}\,\mathrm{erfc}\left(\sqrt{x\left(1+\frac{1}{y}\right)}\right). \tag{3.14}$$

Similarly, the cooperative error for $I_2 = \{\gamma_{sr}, \gamma_{rd}, \bar{\gamma}_{sd}\}$ is equal to

$$\mathbb{P}\{\mathcal{E}_{coop}|I_2\} = \mathbb{E}_{\gamma_{sd}}\left[\frac{1}{2}\mathrm{erfc}\left(\sqrt{\gamma_{sd}+\gamma_{rd}}\right)\right].$$

Since this expression is the same as (3.11) with γ_{rd} and γ_{sd} exchanged, $\mathbb{P}\{\mathcal{E}_{coop}|I_2\}$ is given by

$$\begin{aligned}\mathbb{P}\{\mathcal{E}_{coop}|I_2\}=\mathbb{P}\{\mathcal{E}_{coop}|\gamma_{rd},\bar{\gamma}_{sd}\} &= \mathbb{E}_{\gamma_{sd}}\left[\frac{1}{2}\mathrm{erfc}\left(\sqrt{\gamma_{sd}+\gamma_{rd}}\right)\right]\\ &=e^{\gamma_{rd}/\bar{\gamma}_{sd}}\,h(\gamma_{rd},\bar{\gamma}_{sd}). \qquad (3.15)\end{aligned}$$

If the relay utilizes only $I_1 = \{\gamma_{sr}, \bar{\gamma}_{rd}, \bar{\gamma}_{sd}\}$ to make decisions, then the probability of cooperative error is equal to the BER of a 2-branch MRC receiver in Rayleigh fading, which is given as [10, pp. 846-847]

$$\mathbb{P}\{\mathcal{E}_{coop}|I_1\}=\mathbb{P}\{\mathcal{E}_{coop}|\bar{\gamma}_{rd},\bar{\gamma}_{sd}\} = \mathbb{E}_{\gamma_{sd},\gamma_{rd}}\left[\frac{1}{2}\mathrm{erfc}\left(\sqrt{\gamma_{sd}+\gamma_{rd}}\right)\right] \tag{3.16}$$

$$=\begin{cases}\frac{1}{2}\left(1-\sqrt{\frac{\bar{\gamma}_{rd}}{1+\bar{\gamma}_{rd}}}\right)^2\left(1+\frac{1}{2}\sqrt{\frac{\bar{\gamma}_{rd}}{1+\bar{\gamma}_{rd}}}\right), & \bar{\gamma}_{rd}=\bar{\gamma}_{sd};\\ \frac{1}{2}\left[1-\frac{1}{\bar{\gamma}_{sd}-\bar{\gamma}_{rd}}\left(\bar{\gamma}_{sd}\sqrt{\frac{\bar{\gamma}_{sd}}{1+\bar{\gamma}_{sd}}}-\bar{\gamma}_{rd}\sqrt{\frac{\bar{\gamma}_{rd}}{1+\bar{\gamma}_{rd}}}\right)\right], & \bar{\gamma}_{rd}\neq\bar{\gamma}_{sd}.\end{cases} \tag{3.17}$$

3.2.2 Approximate Expressions for the Probability of Error Propagation

Without loss of generality, we assume that the source sends the symbol $x_s = +1$ and the relay sends the symbol $x_r = -1$. The error occurs if the destination decides that -1 was sent by the source. The decision variable after the destination combines the received signals (given in (3.1) and (3.2)) using MRC is given by:

$$\begin{aligned} y=&\frac{\alpha_{sd}^*\sqrt{E_{b,s}}}{N_0}y_{sd}+\frac{\alpha_{rd}^*\sqrt{E_{b,r}}}{N_0}y_{rd} \\ =&\left(\frac{|\alpha_{sd}|^2E_{b,s}}{N_0}-\frac{|\alpha_{rd}|^2E_{b,r}}{N_0}\right)+\frac{\alpha_{sd}^*\sqrt{E_{b,s}}}{N_0}n_{sd}+\frac{\alpha_{rd}^*\sqrt{E_{b,r}}}{N_0}n_{rd} \\ =&(\gamma_{sd}-\gamma_{rd})+\tilde{n}, \end{aligned} \tag{3.18}$$

where $\tilde{n}$ is the effective noise. The mean and the variance of $\tilde{n}$ are equal to $\mathbb{E}[\tilde{n}]=0$ and $\mathbb{E}[|\tilde{n}|^2]=\frac{1}{2}(\gamma_{sd}+\gamma_{rd})$. The decision rule at the destination is to declare +1 if $y \geq 0$. Then, the probability of error propagation under $I_4=\{\gamma_{sr},\gamma_{rd},\gamma_{sd}\}$ is equal to

$$\begin{aligned} \mathbb{P}\{\mathcal{E}_{prop}|I_4\}=&\mathbb{P}\{\mathcal{E}_{prop}|\gamma_{rd},\gamma_{sd}\}=\mathbb{P}\{y<0|\gamma_{rd},\gamma_{sd}\}=\mathbb{P}\{\tilde{n}>(\gamma_{sd}-\gamma_{rd})|\gamma_{rd},\gamma_{sd}\} \\ =&\frac{1}{2}\text{erfc}\left(\frac{\gamma_{sd}-\gamma_{rd}}{\sqrt{\gamma_{sd}+\gamma_{rd}}}\right). \end{aligned} \tag{3.19}$$

The probability of error propagation under $I_3=\{\gamma_{sr},\bar{\gamma}_{rd},\gamma_{sd}\}$ can be found by averaging (3.19) with respect to γ_{rd}

$$\begin{aligned} \mathbb{P}\{\mathcal{E}_{prop}|I_3\}=&\mathbb{P}\{\mathcal{E}_{prop}|\bar{\gamma}_{rd},\gamma_{sd}\}=\mathbb{E}_{\gamma_{rd}}\left[\mathbb{P}\{\mathcal{E}_{prop}|\gamma_{sd},\gamma_{rd}\}\right] \\ =&\int_0^\infty \text{erfc}\left(\frac{\gamma_{sd}-\gamma_{rd}}{\sqrt{\gamma_{sd}+\gamma_{rd}}}\right)\frac{1}{2\bar{\gamma}_{rd}}e^{-\gamma_{rd}/\bar{\gamma}_{rd}}\mathrm{d}\gamma_{rd}. \end{aligned} \tag{3.20}$$

Similarly,

$$\mathbb{P}\{\mathcal{E}_{prop}|I_2\}=\mathbb{P}\{\mathcal{E}_{prop}|\gamma_{rd},\bar{\gamma}_{sd}\}=\int_0^\infty \text{erfc}\left(\frac{\gamma_{sd}-\gamma_{rd}}{\sqrt{\gamma_{sd}+\gamma_{rd}}}\right)\frac{1}{2\bar{\gamma}_{sd}}e^{-\gamma_{sd}/\bar{\gamma}_{sd}}\mathrm{d}\gamma_{sd}, \tag{3.21}$$

and

$$\begin{aligned} \mathbb{P}\{\mathcal{E}_{prop}|I_1\}=&\mathbb{P}\{\mathcal{E}_{prop}|\bar{\gamma}_{rd},\bar{\gamma}_{sd}\} \\ =&\int_0^\infty\int_0^\infty \text{erfc}\left(\frac{\gamma_{sd}-\gamma_{rd}}{\sqrt{\gamma_{sd}+\gamma_{rd}}}\right)\frac{1}{2\bar{\gamma}_{sd}\bar{\gamma}_{rd}}e^{-\gamma_{sd}/\bar{\gamma}_{sd}}e^{-\gamma_{rd}/\bar{\gamma}_{rd}}\mathrm{d}\gamma_{sd}\mathrm{d}\gamma_{rd}. \end{aligned} \tag{3.22}$$

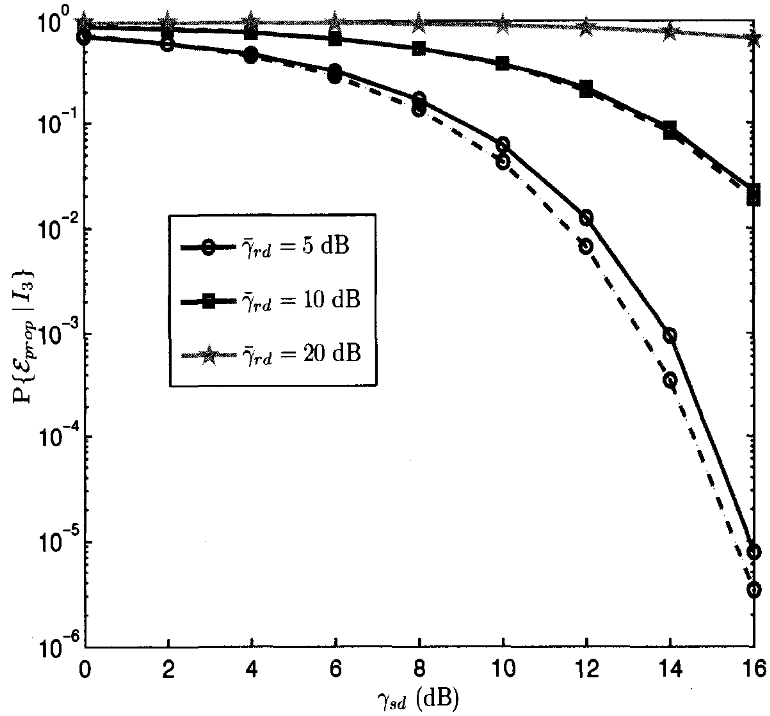

Figure 3.2: Comparison of $\mathbb{P}\{\mathcal{E}_{prop}|I_3\}$ values obtained from the approximation in (3.23) and from the numerical integration of (3.20) as a function of γ_{sd} for different $\bar{\gamma}_{rd}$ values. The exact values are plotted in solid lines and the approximate values are plotted in dashed lines.

Due to the complexity of the exact expressions given in (3.20)-(3.22), we provide approximate expressions for calculating the probability of error propagation for these models. Equation (3.18) shows that, if relay forwards an incorrect signal, this has a strong impact on the decision variable y. For instance, for $\gamma_{rd} \approx \gamma_{sd}$, the post-combining SNR is close to zero even if both γ_{rd} and γ_{sd} are large. Assuming that the incorrect relay signal - not the noise term - is the dominant factor that causes the decision variable y to be negative, we approximate the probability of error by the probability of $\{\gamma_{sd} - \gamma_{rd} < 0\}$.

For I_3, using the fact that γ_{rd} is an exponential random variable with mean $\bar{\gamma}_{rd}$,

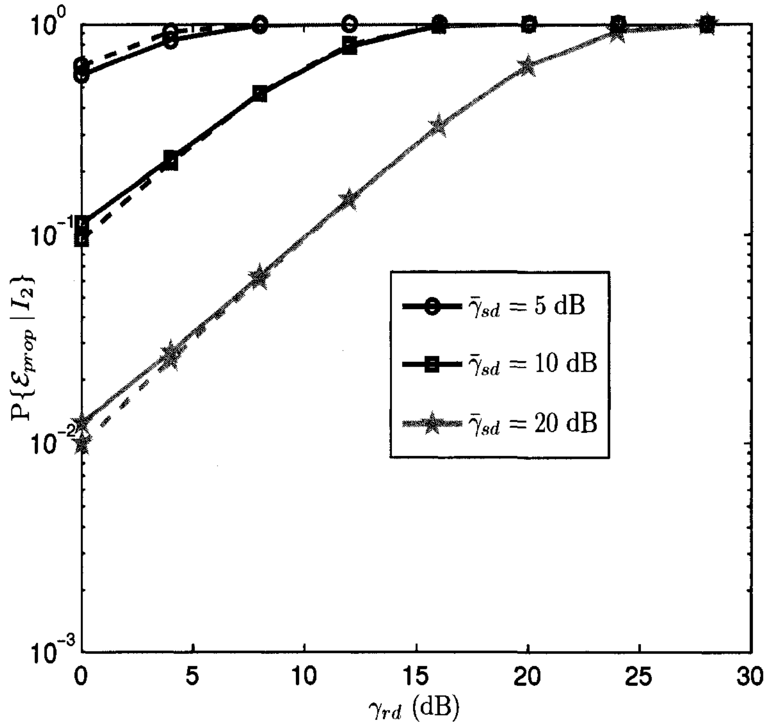

Figure 3.3: Comparison of $\mathbb{P}\{\mathcal{E}_{prop}|I_2\}$ values obtained from the approximation in (3.24) and from the numerical integration of (3.21) as a function of γ_{rd} for different $\bar{\gamma}_{sd}$ values. The exact values are plotted in solid lines and the approximate values are plotted in dashed lines.

we obtain the approximate probability of error as

$$\mathbb{P}\{\mathcal{E}_{prop}|I_3\} \approx \mathbb{P}\{\gamma_{sd} - \gamma_{rd} < 0|\bar{\gamma}_{rd}, \gamma_{sd}\} = \int_{\gamma_{sd}}^{\infty} \frac{1}{\bar{\gamma}_{rd}} e^{-\gamma_{rd}/\bar{\gamma}_{rd}} \,\mathrm{d}\gamma_{rd} = e^{-\gamma_{sd}/\bar{\gamma}_{rd}}. \tag{3.23}$$

Similarly for I_2

$$\mathbb{P}\{\mathcal{E}_{prop}|I_2\} \approx \mathbb{P}\{\gamma_{sd} - \gamma_{rd} < 0|\gamma_{rd}, \bar{\gamma}_{sd}\} = \int_{0}^{\gamma_{rd}} \frac{1}{\bar{\gamma}_{sd}} e^{-\gamma_{sd}/\bar{\gamma}_{sd}} \,\mathrm{d}\gamma_{sd} = 1 - e^{-\gamma_{rd}/\bar{\gamma}_{sd}}. \tag{3.24}$$

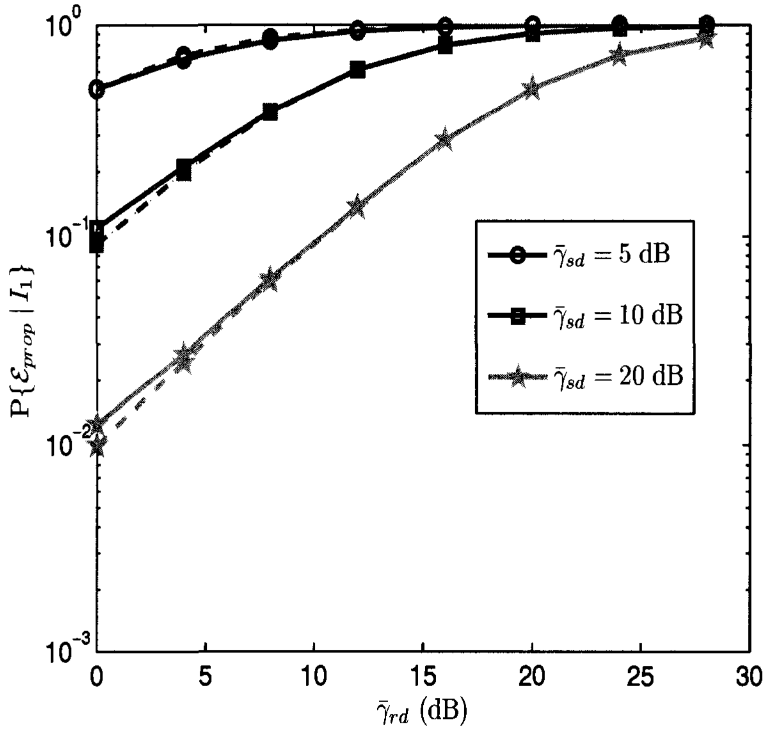

Figure 3.4: Comparison of $\mathbb{P}\{\mathcal{E}_{prop}|I_1\}$ values obtained from the approximation in (3.25) and from the numerical integration of (3.22) as a function of $\bar{\gamma}_{rd}$ for different $\bar{\gamma}_{sd}$ values. The exact values are plotted in solid lines and the approximate values are plotted in dashed lines.

For I_1, since γ_{sd} and γ_{rd} are independent, we obtain

$$\begin{aligned}\mathbb{P}\{\mathcal{E}_{prop}|I_1\} \approx \mathbb{P}\{\gamma_{sd} - \gamma_{rd} < 0|\bar{\gamma}_{rd}, \bar{\gamma}_{sd}\} &= \int_0^{\infty} \int_0^{\gamma_{rd}} \frac{1}{\bar{\gamma}_{sd}\bar{\gamma}_{rd}} e^{-\gamma_{sd}/\bar{\gamma}_{sd}} e^{-\gamma_{rd}/\bar{\gamma}_{rd}} \mathrm{d}\gamma_{sd}\, \mathrm{d}\gamma_{rd} \\ &= \frac{\bar{\gamma}_{rd}}{\bar{\gamma}_{sd} + \bar{\gamma}_{rd}}.\end{aligned} \tag{3.25}$$

To check the accuracy of these approximations at practical SNR values, we compare them with the exact values obtained through the numerical integration of (3.20)-(3.22). Fig.s 3.2-3.4 show that all three approximations are reasonably accurate for a large range of SNR values.

3.2.3 Optimal Threshold Functions and Average e2e BER for Threshold Digital Relaying

In this section, the optimal decision rule given in (3.9) is evaluated for all the models using the probability of error propagation and cooperative error expressions derived in Section 3.2.1 and Section 3.2.2. All the rules simplify to a threshold on the instantaneous SNR of the $S-R$ link.

Relaying based on Model 1

From (3.9) we obtain the relaying policy for Model 1:

$$\mathbb{P}\{\mathcal{E}_{sr}|\gamma_{sr}\} \underset{a_1}{\overset{a_0}{\gtrless}} \delta_1(\bar{\gamma}_{rd}, \bar{\gamma}_{sd}), \tag{3.26}$$

where δ_1 is defined as

$$\begin{aligned}\delta_1(\bar{\gamma}_{rd}, \bar{\gamma}_{sd}) &= \frac{\mathbb{P}\{\mathcal{E}_{sd}|I_1\} - \mathbb{P}\{\mathcal{E}_{coop}|I_1\}}{\mathbb{P}\{\mathcal{E}_{prop}|I_1\} - \mathbb{P}\{\mathcal{E}_{coop}|I_1\}} \\ &\approx \frac{\frac{1}{\bar{\gamma}_{sd}-\bar{\gamma}_{rd}}\left(\bar{\gamma}_{sd}\sqrt{\frac{\bar{\gamma}_{sd}}{1+\bar{\gamma}_{sd}}} - \bar{\gamma}_{rd}\sqrt{\frac{\bar{\gamma}_{rd}}{1+\bar{\gamma}_{rd}}}\right) - \sqrt{\frac{\bar{\gamma}_{sd}}{1+\bar{\gamma}_{sd}}}}{\frac{2\bar{\gamma}_{rd}}{\bar{\gamma}_{rd}+\bar{\gamma}_{sd}} - \left[1 - \frac{1}{\bar{\gamma}_{sd}-\bar{\gamma}_{rd}}\left(\bar{\gamma}_{sd}\sqrt{\frac{\bar{\gamma}_{sd}}{1+\bar{\gamma}_{sd}}} - \bar{\gamma}_{rd}\sqrt{\frac{\bar{\gamma}_{rd}}{1+\bar{\gamma}_{rd}}}\right)\right]}\end{aligned} \tag{3.27}$$

and (3.6), (3.17) and (3.25) have been used to arrive at (3.27). If $\delta_1(\bar{\gamma}_{rd}, \bar{\gamma}_{sd}) > 1/2$, the relay should always transmit since $\mathbb{P}\{\mathcal{E}_{sr}|\gamma_{sr}\}$ is always less than $1/2$. On the other hand, if $\delta_1(\bar{\gamma}_{rd}, \bar{\gamma}_{sd}) \leq 1/2$, the relaying policy can be further simplified to

$$\gamma_{sr} \underset{a_0}{\overset{a_1}{\gtrless}} \gamma_{t1}^*(\bar{\gamma}_{rd}, \bar{\gamma}_{sd}), \tag{3.28}$$

where

$$\gamma_{t1}^*(\bar{\gamma}_{rd}, \bar{\gamma}_{sd}) = \begin{cases} \left(\operatorname{erfc}^{-1}(2\delta_1(\bar{\gamma}_{rd}, \bar{\gamma}_{sd}))\right)^2, & \delta_1(\bar{\gamma}_{rd}, \bar{\gamma}_{sd}) \leq 1/2; \\ 0, & \text{otherwise}, \end{cases} \tag{3.29}$$

and $\operatorname{erfc}^{-1}(z)$ denotes the inverse of the erfc function, which is defined for $0 \leq z \leq 2$.

The average e2e BER of Model 1 for a given threshold γ_{t1} can be expressed using the law of total probability:

$$\begin{aligned}\mathrm{BER}_{e2e}^{(1)}(\bar{\gamma}_{sr},\bar{\gamma}_{rd},\bar{\gamma}_{sd}) = & \mathbb{P}\{\gamma_{sr} > \gamma_{t1}\}\Big[\mathbb{P}\{\mathcal{E}_{sr}|\gamma_{sr} > \gamma_{t1}\}\mathbb{P}\{\mathcal{E}_{prop}\,|\,\bar{\gamma}_{sd},\bar{\gamma}_{rd}\} \\ & + (1 - \mathbb{P}\{\mathcal{E}_{sr}|\gamma_{sr} > \gamma_{t1}\})\mathbb{P}\{\mathcal{E}_{coop}\,|\,\bar{\gamma}_{sd},\bar{\gamma}_{rd}\}\Big] \\ & + \mathbb{P}\{\gamma_{sr} \le \gamma_{t1}\}\mathbb{P}\{\mathcal{E}_{sd}\,|\,\bar{\gamma}_{sd}\}. \end{aligned} \tag{3.30}$$

Since γ_{sr} is an exponential random variable with mean $\bar{\gamma}_{sr}$, the probability that $\{\gamma_{sr} \le \gamma_{t1}\}$ is equal to

$$\mathbb{P}\{\gamma_{sr} \le \gamma_{t1}\} = 1 - \exp(-\gamma_{t1}/\bar{\gamma}_{sr}). \tag{3.31}$$

If $\gamma_{sr} > \gamma_{t1}$, the probability of bit error at the $S - R$ link decreases, but it remains nonzero regardless of the value of γ_{t1}. The probability of bit error at the $S - R$ link given that $\gamma_{sr} > \gamma_{t1}$ is equal to

$$\mathbb{P}\{\mathcal{E}_{sr}|\gamma_{sr} > \gamma_{t1}\} = \frac{1}{2}\left[\mathrm{erfc}(\sqrt{\gamma_{t1}}) - e^{\gamma_{t1}/\bar{\gamma}_{sr}}\sqrt{\frac{\bar{\gamma}_{sr}}{1+\bar{\gamma}_{sr}}}\,\mathrm{erfc}\left(\sqrt{\gamma_{t1}\left(1+\frac{1}{\bar{\gamma}_{sr}}\right)}\right)\right]. \tag{3.32}$$

The derivation of (3.32) is given in Appendix A.2. The average e2e BER for a given threshold value can be calculated analytically by substituting (3.6), (3.17), (3.25), (3.31), and (3.32) into equation (3.30).

Relaying based on Model 2

The optimal decision rule for the case of I_2 is equal to

$$\mathbb{P}\{\mathcal{E}_{sr}|\gamma_{sr}\} \underset{a_1}{\overset{a_0}{\gtrless}} \delta_2(\gamma_{rd},\bar{\gamma}_{sd}), \tag{3.33}$$

where δ_2 is found as

$$\begin{aligned}\delta_2(\gamma_{rd},\bar{\gamma}_{sd}) = & \frac{\mathbb{P}\{\mathcal{E}_{sd}|\bar{\gamma}_{sd}\} - \mathbb{P}\{\mathcal{E}_{coop}|\gamma_{rd},\bar{\gamma}_{sd}\}}{\mathbb{P}\{\mathcal{E}_{prop}|\gamma_{rd},\bar{\gamma}_{sd}\} - \mathbb{P}\{\mathcal{E}_{coop}|\gamma_{rd},\bar{\gamma}_{sd}\}} \\ \approx & \frac{\frac{1}{2}\left(1-\sqrt{\frac{\bar{\gamma}_{sd}}{1+\bar{\gamma}_{sd}}}\right) - e^{\gamma_{rd}/\bar{\gamma}_{sd}}h(\gamma_{rd},\bar{\gamma}_{sd})}{1 - e^{-\gamma_{rd}/\bar{\gamma}_{sd}} - e^{\gamma_{rd}/\bar{\gamma}_{sd}}h(\gamma_{rd},\bar{\gamma}_{sd})}\end{aligned} \tag{3.34}$$

by using (3.15) and (3.24). This rule can be expressed as

$$\gamma_{sr} \underset{a_0}{\overset{a_1}{\gtrless}} \gamma_{t2}^{*}(\gamma_{rd}, \bar{\gamma}_{sd}), \tag{3.35}$$

where

$$\gamma_{t2}^{*}(\gamma_{rd}, \bar{\gamma}_{sd}) = \begin{cases} \left(\operatorname{erfc}^{-1}(2\delta_2(\gamma_{rd}, \bar{\gamma}_{sd}))\right)^2, & \delta_2(\gamma_{rd}, \bar{\gamma}_{sd}) \leq 1/2; \\ 0, & \text{otherwise.} \end{cases} \tag{3.36}$$

The average e2e BER for Model 2 is given by (A.11):

$$\begin{aligned} \mathrm{BER}_{e2e}^{(2)}(\bar{\gamma}_{sr}, \bar{\gamma}_{rd}, \bar{\gamma}_{sd}) \approx \int_0^{\infty} \Bigg[& \frac{1}{2}\left(1 - \sqrt{\frac{\bar{\gamma}_{sd}}{1+\bar{\gamma}_{sd}}}\right)(1 - \exp(-\gamma_{t2}^{*}(\gamma_{rd}, \bar{\gamma}_{sd})/\bar{\gamma}_{sr})) \\ & + \left((1 - e^{-\gamma_{rd}/\bar{\gamma}_{sd}}) - e^{\gamma_{rd}/\bar{\gamma}_{sd}} h(\gamma_{rd}, \bar{\gamma}_{sd})\right) h(\gamma_{t2}^{*}(\gamma_{rd}, \bar{\gamma}_{sd}), \bar{\gamma}_{sr}) \\ & + (1 - e^{-\gamma_{rd}/\bar{\gamma}_{sd}}) \exp(-\gamma_{t2}^{*}(\gamma_{rd}, \bar{\gamma}_{sd})/\bar{\gamma}_{sr}) \Bigg] \frac{1}{\bar{\gamma}_{rd}} e^{\gamma_{rd}/\bar{\gamma}_{rd}} \mathrm{d}\gamma_{rd}. \end{aligned} \tag{3.37}$$

See Appendix A.3 for the derivation of the average e2e BERs of Models 2, 3, and 4. Since the integrals to calculate the average e2e BERs of these models are intractable analytically, we use numerical integration to evaluate them in Section 3.3.

Relaying based on Model 3

For Model 3 the optimal decision rule is given by

$$\mathbb{P}\{\mathcal{E}_{sr}|\gamma_{sr}\} \underset{a_1}{\overset{a_0}{\gtrless}} \delta_3(\bar{\gamma}_{rd}, \gamma_{sd}), \tag{3.38}$$

where δ_3 is given by

$$\begin{aligned} \delta_3(\bar{\gamma}_{rd}, \gamma_{sd}) &= \frac{\mathbb{P}\{\mathcal{E}_{sd}|\gamma_{sd}\} - \mathbb{P}\{\mathcal{E}_{coop}|\bar{\gamma}_{rd}, \gamma_{sd}\}}{\mathbb{P}\{\mathcal{E}_{prop}|\bar{\gamma}_{rd}, \gamma_{sd}\} - \mathbb{P}\{\mathcal{E}_{coop}|\bar{\gamma}_{rd}, \gamma_{sd}\}} \\ &\approx \frac{\frac{1}{2}\operatorname{erfc}(\sqrt{\gamma_{sd}}) - e^{\gamma_{sd}/\bar{\gamma}_{rd}} h(\gamma_{sd}, \bar{\gamma}_{rd})}{e^{-\gamma_{sd}/\bar{\gamma}_{rd}} - e^{\gamma_{sd}/\bar{\gamma}_{rd}} h(\gamma_{sd}, \bar{\gamma}_{rd})}. \end{aligned} \tag{3.39}$$

This rule is equivalent to

$$\gamma_{sr} \underset{a_0}{\overset{a_1}{\gtrless}} \gamma_{t3}^{*}(\bar{\gamma}_{rd}, \gamma_{sd}) \tag{3.40}$$

where

$$\gamma_{t3}^{*}(\bar{\gamma}_{rd},\gamma_{sd}) = \begin{cases} \left(\mathrm{erfc}^{-1}(2\delta_3(\bar{\gamma}_{rd},\gamma_{sd}))\right)^2, & \delta_3(\bar{\gamma}_{rd},\gamma_{sd}) \leq 1/2; \\ 0, & \text{otherwise.} \end{cases} \tag{3.41}$$

The average e2e BER is given by (A.12):

$$\begin{aligned} \mathrm{BER}_{e2e}^{(3)}(\bar{\gamma}_{sr},\bar{\gamma}_{rd},\bar{\gamma}_{sd}) \approx \int_0^\infty \Big[& \frac{1}{2}\mathrm{erfc}(\sqrt{\gamma_{sd}})(1-\exp(-\gamma_{t3}^{*}(\bar{\gamma}_{rd},\gamma_{sd})/\bar{\gamma}_{sr})) \\ & + \left(e^{-\gamma_{sd}/\bar{\gamma}_{rd}} - e^{\gamma_{sd}/\bar{\gamma}_{rd}} h(\gamma_{sd},\bar{\gamma}_{rd})\right) h(\gamma_{t3}^{*}(\bar{\gamma}_{rd},\gamma_{sd}),\bar{\gamma}_{sr}) \\ & + e^{\gamma_{sd}/\bar{\gamma}_{rd}} h(\gamma_{sd},\bar{\gamma}_{rd}) \exp(-\gamma_{t3}^{*}(\bar{\gamma}_{rd},\gamma_{sd})/\bar{\gamma}_{sr}) \Big] \frac{1}{\bar{\gamma}_{sd}} e^{-\gamma_{sd}/\bar{\gamma}_{sd}} \, \mathrm{d}\gamma_{sd}. \end{aligned} \tag{3.42}$$

Relaying based on Model 4

The optimal decision rule in the case of Model 4 is

$$\mathbb{P}\{\mathcal{E}_{sr}|\gamma_{sr}\} \underset{a_1}{\overset{a_0}{\gtrless}} \delta_4(\gamma_{rd},\gamma_{sd}), \tag{3.43}$$

where δ_4 is equal to

$$\begin{aligned} \delta_4(\gamma_{rd},\gamma_{sd}) &= \frac{\mathbb{P}\{\mathcal{E}_{sd}|\gamma_{sd}\} - \mathbb{P}\{\mathcal{E}_{coop}|\gamma_{rd},\gamma_{sd}\}}{\mathbb{P}\{\mathcal{E}_{prop}|\gamma_{rd},\gamma_{sd}\} - \mathbb{P}\{\mathcal{E}_{coop}|\gamma_{rd},\gamma_{sd}\}} \\ &= \frac{\mathrm{erfc}(\sqrt{\gamma_{sd}}) - \mathrm{erfc}\left(\sqrt{\gamma_{sd}+\gamma_{rd}}\right)}{\mathrm{erfc}\left(\frac{\gamma_{sd}-\gamma_{rd}}{\sqrt{\gamma_{sd}+\gamma_{rd}}}\right) - \mathrm{erfc}\left(\sqrt{\gamma_{sd}+\gamma_{rd}}\right)}, \end{aligned} \tag{3.44}$$

and this rule can be expressed as $\gamma_{sr} \underset{a_0}{\overset{a_1}{\gtrless}} \gamma_{t4}^{*}(\gamma_{rd},\gamma_{sd})$, where

$$\gamma_{t4}^{*}(\gamma_{rd},\gamma_{sd}) = \begin{cases} \left(\mathrm{erfc}^{-1}(2\delta_4(\gamma_{rd},\gamma_{sd}))\right)^2, & \delta_4(\gamma_{rd},\gamma_{sd}) \leq 1/2; \\ 0, & \text{otherwise.} \end{cases} \tag{3.45}$$

The average e2e BER is derived in (A.13) and is equal to:

$$\begin{aligned}\mathrm{BER}^{(4)}_{\mathrm{e2e}}(\bar{\gamma}_{sr},\bar{\gamma}_{rd},\bar{\gamma}_{sd})=&\frac{1}{\bar{\gamma}_{sd}\bar{\gamma}_{rd}}\int_0^\infty\int_0^\infty \frac{1}{2}\Bigg[\mathrm{erfc}(\sqrt{\gamma_{sd}})(1-\exp(-\gamma^*_{t4}(\gamma_{rd},\gamma_{sd})/\bar{\gamma}_{sr}))\\ &+\left(\mathrm{erfc}\left(\frac{\gamma_{sd}-\gamma_{rd}}{\sqrt{(\gamma_{sd}+\gamma_{rd})}}\right)-\mathrm{erfc}(\sqrt{\gamma_{rd}+\gamma_{sd}})\right)h(\gamma^*_{t4}(\gamma_{rd},\gamma_{sd}),\bar{\gamma}_{sr})\\ &+\mathrm{erfc}(\sqrt{\gamma_{rd}+\gamma_{sd}})\exp(-\gamma^*_{t4}(\gamma_{rd},\gamma_{sd})/\bar{\gamma}_{sr})\Bigg]e^{-\gamma_{sd}/\bar{\gamma}_{sd}}e^{-\gamma_{rd}/\bar{\gamma}_{rd}}\mathrm{d}\gamma_{rd}\,\mathrm{d}\gamma_{sd}.\end{aligned} \tag{3.46}$$

3.3 Results

In this section, we first describe two benchmark schemes: simple digital relaying and genie-aided digital relaying. We then present numerical examples comparing the e2e BER of threshold digital relaying under the different models presented in this chapter to these benchmark schemes. All the results are obtained from the analytical formulae derived in this chapter. We resort to numerical integration where it is required.

3.3.1 Benchmark Schemes

The descriptions and e2e BERs of the benchmark schemes are given below.

Genie-aided digital relaying

Genie-aided digital relaying is a protocol designed under the hypothetical assumption that the relay has perfect error detection for each symbol. In phase II, the relay retransmits only those symbols received correctly in phase I. Since retransmitting a correctly detected symbol decreases e2e BER while transmitting an incorrectly detected symbol increases it, genie-aided protocol constitutes a performance upper bound for any selective digital relaying scheme. The e2e BER of genie-aided digital relaying is equal to

$$\mathrm{BER}_{e2e}^{genie}(\bar{\gamma}_{sr}, \bar{\gamma}_{rd}, \bar{\gamma}_{sd}) = \mathbb{P}\{\mathcal{E}_{sr}|\bar{\gamma}_{sr}\}\mathbb{P}\{\mathcal{E}_{sd}|\bar{\gamma}_{sd}\} + (1 - \mathbb{P}\{\mathcal{E}_{sr}|\bar{\gamma}_{sr}\})\mathbb{P}\{\mathcal{E}_{coop}|\bar{\gamma}_{rd}, \bar{\gamma}_{sd}\},$$

which can be calculated by using (3.6) and (3.15).

Simple digital relaying

In simple digital relaying, the relay always transmits in phase II. The e2e BER of simple digital relaying is equal to:

$$\mathrm{BER}_{e2e}^{simple}(\bar{\gamma}_{sr}, \bar{\gamma}_{rd}, \bar{\gamma}_{sd}) = \mathbb{P}\{\mathcal{E}_{sr}|\bar{\gamma}_{sr}\}\mathbb{P}\{\mathcal{E}_{prop}|\bar{\gamma}_{rd}, \bar{\gamma}_{sd}\} + (1 - \mathbb{P}\{\mathcal{E}_{sr}|\bar{\gamma}_{sr}\})\mathbb{P}\{\mathcal{E}_{coop}|\bar{\gamma}_{rd}, \bar{\gamma}_{sd}\},$$

which can be calculated by using (3.6), (3.15), and (3.24).

3.3.2 Numerical Results

In Fig. 3.5, we fix $\bar{\gamma}_{rd} = 15$ dB and $\bar{\gamma}_{sd} = 0$ dB and plot the e2e BER as a function of $\bar{\gamma}_{sr}$. In this case, γ_{t1}^* (the optimal threshold for Model 1) remains fixed as seen in (3.29). The threshold is very low ($\gamma_{t1}^* = 0.545$), which can be attributed to the poor quality of the direct link. We observe that when the $S-R$ link is favorable, selective relaying schemes have a small SNR gain (only 1 to 2 dB) compared to simple relaying.

Fig. 3.6(a) shows the BER performance at $\bar{\gamma}_{sr} = 15$ dB and $\bar{\gamma}_{sd} = 5$ dB as a function of $\bar{\gamma}_{rd}$. For simple digital relaying as $\bar{\gamma}_{rd}$ increases, on one hand the probability of error propagation increases, on the other hand the probability of cooperative error decreases. In Fig. 3.6(a), the decrease in the probability of cooperative error is the dominant factor. In Fig. 3.7(a), we plot the e2e BER at $\bar{\gamma}_{sr} = 15$ dB and $\bar{\gamma}_{sd} = 15$ dB as a function of $\bar{\gamma}_{rd}$. We observe that in Fig. 3.7(a) the e2e BER of simple digital relaying increases as the $R-D$ channel becomes stronger. This is because in this case the increase in error propagation dominates over the decrease in

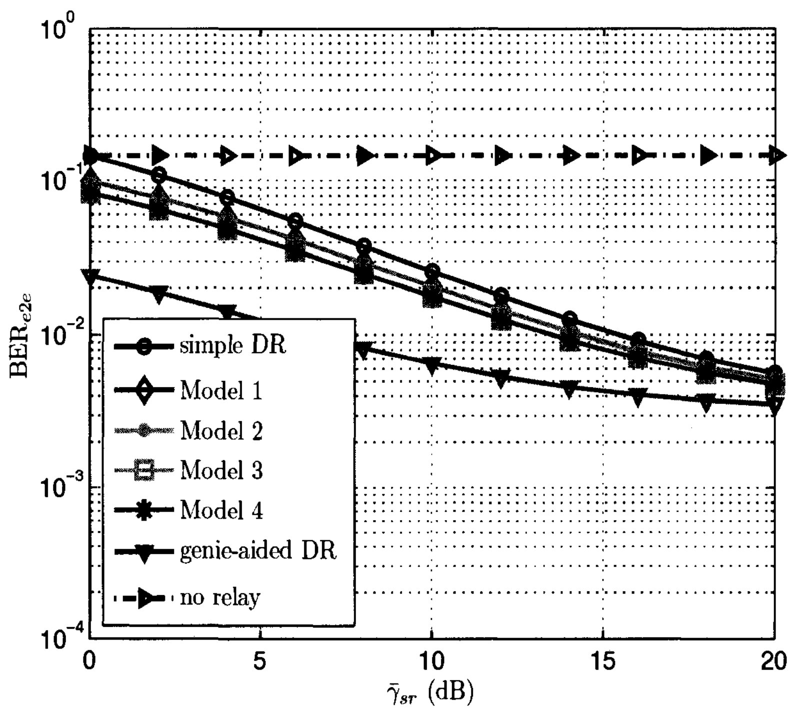

Figure 3.5: The e2e BER for different relaying schemes as a function of $\bar{\gamma}_{sr}$ for $\bar{\gamma}_{rd} = 15$ dB, $\bar{\gamma}_{sd} = 0$ dB.

the cooperative error. In Fig.s 3.6(a) and 3.7(a) for large $\bar{\gamma}_{rd}$, $\mathbb{P}\{\mathcal{E}_{prop}|\bar{\gamma}_{rd}, \bar{\gamma}_{sd}\} \approx 1$ and $\mathbb{P}\{\mathcal{E}_{coop}|\bar{\gamma}_{rd}, \bar{\gamma}_{sd}\} \approx 0$. Thus, the performance of simple digital relaying is limited by the $S-R$ link and can be approximated as $\mathrm{BER}_{e2e}^{(simple)} \approx \bar{P}_b(\bar{\gamma}_{sr})$ for large $\bar{\gamma}_{rd}$. Similarly, $\mathrm{BER}_{e2e}^{(genie)} \approx \bar{P}_b(\bar{\gamma}_{sr}) \times \bar{P}_b(\bar{\gamma}_{sd})$ for large $\bar{\gamma}_{rd}$.

Model 1 has a significant performance gain over simple digital relaying in both Fig. 3.6(a) and Fig. 3.7(a), since, as shown in Fig. 3.6(b) and Fig. 3.7(b), it adaptively increases threshold γ_{t1}^* as $\bar{\gamma}_{rd}$ increases.

Finally, we study a scenario where all the average link SNRs are varied simultaneously. In this scenario, the $S-R$ and $R-D$ links have the same average SNR, while the $S-D$ link has a lower average SNR, which is a typical scenario when R is located around the midpoint of S and D. Specifically, we assume $\bar{\gamma}_{sr} = \bar{\gamma}_{rd} = \bar{\gamma}$

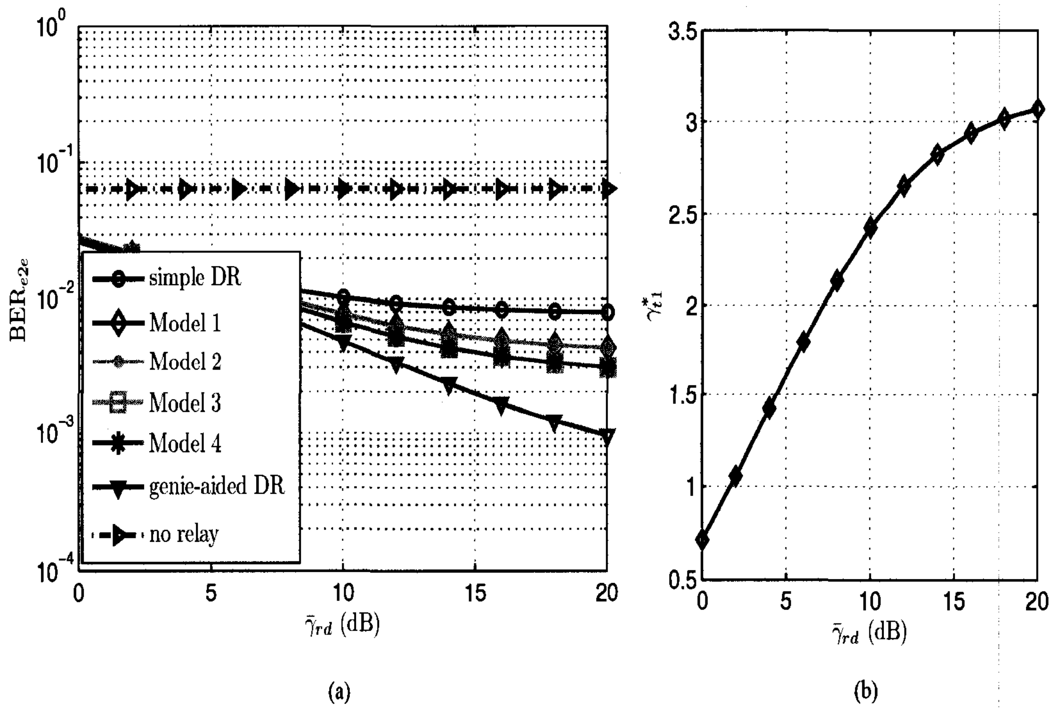

Figure 3.6: The e2e BER for different relaying schemes and the threshold for Model 1 (obtained from (3.29)) as a function of $\bar{\gamma}_{rd}$ for $\bar{\gamma}_{sr} = 15$ dB, $\bar{\gamma}_{sd} = 5$ dB.

dB, $\bar{\gamma}_{sd} = \bar{\gamma} - 12$ dB. In Fig. 3.8(a), we plot e2e BER as a function of $\bar{\gamma}$. It is observed that simple digital relaying and direct transmission (i.e., no relay) have the same slope that is equal to 1, while the rest of relaying schemes have a common slope larger than 1, indicating cooperative diversity gains. The asymptotic diversity gains achieved by SNR-based selective relaying is studied in Chapter 4. Fig. 3.8(b) depicts the behavior of the optimal threshold for Model 1. It is observed that the threshold must be increased as the link SNRs increases.

In all the numerical results, we observe that the performance of SNR-based selective relaying under Model 2 is very close to Model 1 and the performance under Model 4 is very close to Model 3. These observations show that the benefit from exploiting γ_{rd} at the relay is marginal. However, there is a gain both from Model 1 to

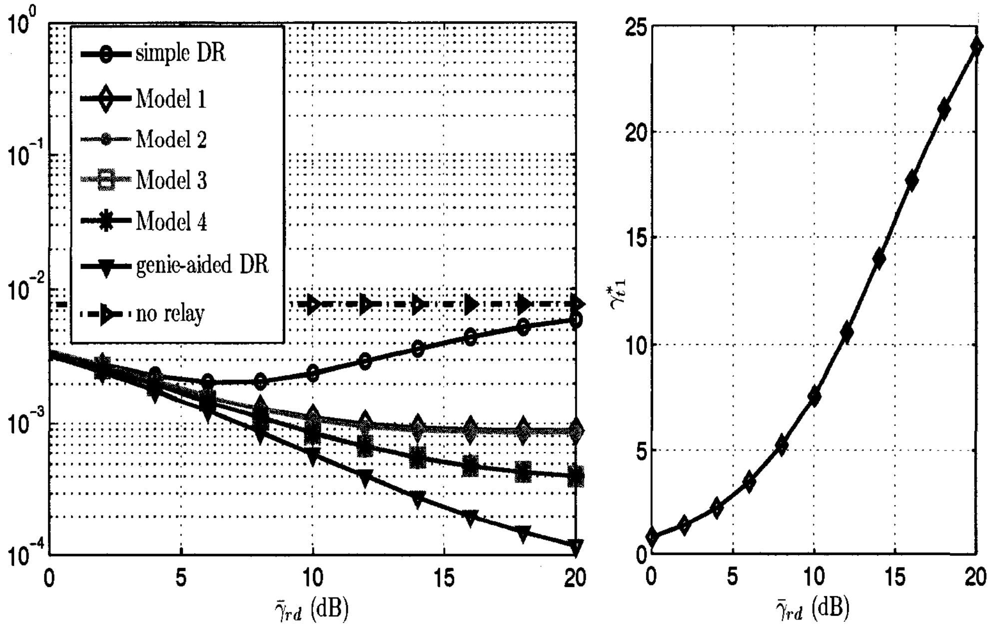

(a) (b)

Figure 3.7: The e2e BER for different relaying schemes and the threshold value for Model 1 (obtained from (3.29)) as a function of $\bar{\gamma}_{rd}$ for $\bar{\gamma}_{sr} = 15$ dB, $\bar{\gamma}_{sd} = 15$ dB.

Model 3 and from Model 2 to Model 4. Hence, it is useful to consider γ_{sd} in relaying decisions. The gain from adapting according to γ_{sd} increases as the average SNR $\bar{\gamma}_{sd}$ increases.

Although SNR-based selection relaying improves the e2e BER compared to simple digital relaying, it still has a significant performance gap compared to genie-aided digital relaying. Therefore, there might be room for improvement through hybrid methods combining SNR-based selection relaying with other methods proposed in the literature such as power control at the relay and better detection methods at the destination [29,30].

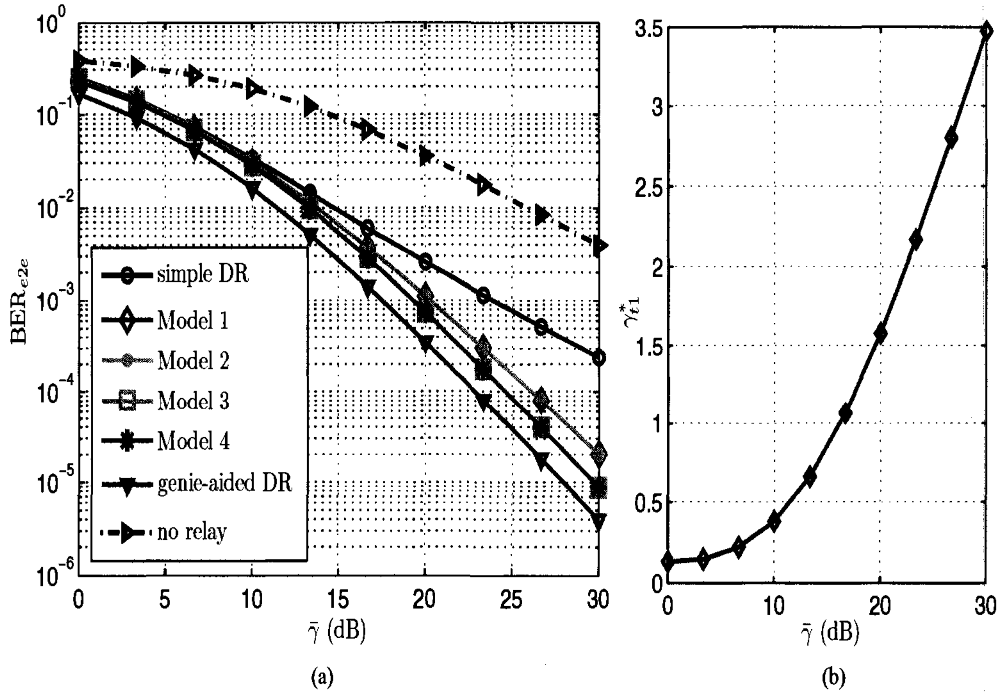

Figure 3.8: The e2e BER for different relaying schemes and the threshold value for Model 1 (obtained from (3.29)) as a function of $\bar{\gamma}$, where $\bar{\gamma}_{sr} = \bar{\gamma}_{rd} = \bar{\gamma}$ dB and $\bar{\gamma}_{sd} = \bar{\gamma} - 12$ dB.

3.4 Conclusions

In this chapter, we proposed and analyzed SNR-based selective relaying schemes to minimize the end-to-end bit error rate in digital diversity relaying systems. These schemes resulted in threshold rules for the source-relay link SNR. We considered various models for the knowledge of the relay on the link SNRs in the network. For all the models considered, although the e2e BERs depend on the average SNR of all three links, the optimal threshold values that minimize the e2e BER are functions of the relay-destination and source-destination link SNRs only. For all the models, it has been shown that using the derived threshold values results in significant improvement of the e2e BER compared to simple digital relaying. By analyzing the performance under four different models, we observed that having the instantaneous source-destination SNR information for relaying decisions reduces the e2e BER. The gain from this information is higher when the source-destination link is stronger. However, the gain from instantaneous relay-destination SNR is negligible in most cases. We realized that threshold digital relaying using the optimal threshold value can also provide diversity gain under all models. In Chapter 4, we will formally analyze the diversity order achieved with threshold digital relaying under Model 1, which has the lowest complexity and overhead.

Chapter 4

Asymptotic BER Analysis of Threshold Digital Relaying

In Chapter 3, we showed that threshold digital relaying is an effective technique to achieve cooperative diversity in uncoded cooperative wireless networks, which suffer from error propagation due to detection errors at the relays. We analytically derived the optimal threshold functions that minimize e2e BER of TDR. In the present chapter, we study the asymptotic e2e BER of the TDR in relation to the optimal threshold. In particular, we consider TDR under Model 1 of Chapter 3, which requires the minimum SNR information at the relay.

We analyze asymptotic BER of TDR when all average link SNRs are changed simultaneously, as the scaled versions of a reference SNR value, which is denoted by SNR. We first show that as this reference value SNR is increased, the optimal threshold that minimizes the e2e BER increases as $\log(\mathsf{SNR})$. The resulting e2e BER decreases as $\log(\mathsf{SNR})/\mathsf{SNR}^2$ and hence the optimal TDR achieves dual diversity. We also prove that, any threshold of the form $\log(c\,\mathsf{SNR})$, where c is a positive constant, achieves the same order of e2e BER as the one achieved by the optimal threshold and provides dual diversity. Based on this result, we derive an approximate threshold that is asymptotically optimal and that results in a BER very close to the BER of the optimal threshold.

Next, we review the relevant work in the literature on the asymptotic BER performance of digital diversity relaying schemes. Some of the references mentioned in Chapter 3 considered the diversity order of their schemes as well. For instance, in [31] Wang et al. analyze the diversity order of their Link Adaptive Relaying (LAR) scheme. They show that the continuous version of LAR achieves full diversity while the on-off version of LAR has no diversity gain. In this chapter we prove that this result is not due to the limitation of on-off power adaptation, but due to the specific threshold used in [31]. An optimal choice of threshold still achieves diversity order 2. In [29] Chen and Laneman also analyze the asymptotic performance of the ML receiver they propose. They show that the diversity of order achieved by this ML receiver is bounded by $M_r/2+1 \leq d \leq M_r/2+3/2$ for M_r odd and is equal to $d=(M_r+2)/2$ for M_r even, where M_r is the number of relays. They prove that for a single relay network ($M_r = 1$), the e2e BER of their system decreases as $\log(\mathsf{SNR})/\mathsf{SNR}^2$ and hence achieves full diversity. The C-MRC of [30], however, is shown to achieve full diversity for any number of relays. In [55] Ponnaluri and Wilson consider only the asymptotic performance of threshold relaying. They study a system with two parallel relays and equal gain combining at the destination. They show that a threshold of the form $c\mathsf{SNR}^{\epsilon/2}$ achieves diversity order of $d=3-\epsilon$. With this threshold, despite the asymptotic diversity gain, the e2e BER performance does not improve significantly in the practical ranges of link SNRs, especially for low ϵ values.

The rest of this chapter is organized as follows: We describe the system model in Section 4.1. Section 4.2 is dedicated to the analysis of the asymptotic BER of the optimal TDR in the high SNR regime. In this section we prove that the e2e BER of the optimal TDR decreases as $\log(\mathsf{SNR})/\mathsf{SNR}^2$. Hence, the diversity order of the optimal TDR is 2. Then, in Section 4.3, we show that any threshold that is in the form of $\gamma_t = \log(c\,\mathsf{SNR})$ can also achieve the same asymptotic performance as the optimal TDR. We also propose a value of c that results in a BER very close to the BER of the optimal threshold. In Section 4.4, we verify our results and compare the performance of the optimal TDR to several similar schemes proposed in the literature. Finally, Section 4.5 summarizes the findings of this chapter.

4.1 System Model

The system model described in Chapter 3 is assumed. We only consider Model 1 of Chapter 3, where the relay has $I_1 = \{\gamma_{sr}, \bar{\gamma}_{rd}, \bar{\gamma}_{sd}\}$ available in order to make relaying decisions. Thus, we drop the model index. The threshold is denoted by γ_t and the optimal threshold that minimizes e2e BER is denoted by γ_t^*. We refer to the TDR using γ_t^* as the optimal TDR. We note that the analysis in this chapter can be extended to the other models (I_2, I_3, and I_4), where the relay can have the instantaneous $R-D$ and $S-D$ SNRs, γ_{rd}, γ_{sd}. The additional instantaneous SNR information can improve e2e BER as shown in Chapter 3. However, the diversity order cannot be improved any further as TDR achieves full diversity under Model 1.

As in Chapter 3, for simplicity, we assume that all the links use BPSK modulation. All the links experience independent Rayleigh fading. The instantaneous received SNR per bit for a link from node i to node j is denoted by γ_{ij} and is given by

$$\gamma_{ij} = X_{ij}^2\,\bar{\gamma}_{ij},$$

where X_{ij}^2 is an exponential random variable with unit mean and $\bar{\gamma}_{ij}$ is the average SNR. Link SNRs vary in time following independent block fading: γ_{ij} is assumed to be constant for two blocks, precluding retransmit diversity. The scalars X_{ij}, and thus γ_{ij}, are independent from link to link.

Notation and Definitions

We represent the average SNR as

$$\bar{\gamma}_{ij} = \kappa_{ij}\,\mathsf{SNR},$$

where SNR is a reference signal-to-noise ratio, and κ_{ij} is a scaling factor with respect to the reference SNR representing non-identical distance dependent loss and shadowing for different links. We adopt the same notation as in Chapter 3 for different error events, e.g. $\mathcal{E}_{ij}$, $\mathcal{E}_{prop}$, and $\mathcal{E}_{coop}$, but we drop I_i from the notation.

In order to study the high SNR behavior of BER, following an approach similar to the one in [22], we fix the parameters κ_{sr}, κ_{rd}, and κ_{sd}, and analyze the e2e BER as $\mathsf{SNR} \to \infty$. Diversity order is a useful measure in quantifying the diversity benefit of any scheme in high SNR regime [22]. Throughout this thesis we adopt the following definition of diversity order given in [22][1]:

$$d = -\lim_{\mathsf{SNR}\to\infty} \left(\log(\mathrm{BER})/\log(\mathsf{SNR})\right). \tag{4.1}$$

Definition 4.1. Let f and g be two positive functions defined on the real numbers. We say $f = O(g)$, if $\limsup_{x\to\infty} \frac{f(x)}{g(x)} < \infty$.

Definition 4.2. Two functions f and g are called asymptotically equivalent, written $f \sim g$, if $\lim_{x\to\infty} \frac{f(x)}{g(x)} = 1$.

4.2 Asymptotic Performance of Optimal TDR

In Chapter 3 the average e2e BER of TDR for a given threshold value has been derived as

$$\begin{aligned}\mathrm{BER}_{e2e}^{TDR}(\gamma_t) =& \mathbb{P}\{\gamma_{sr} > \gamma_t\}\Big[\mathbb{P}\{\mathcal{E}_{sr}|\gamma_{sr} > \gamma_t\}\mathbb{P}\{\mathcal{E}_{prop}\} + (1 - \mathbb{P}\{\mathcal{E}_{sr}|\gamma_{sr} > \gamma_t\})\mathbb{P}\{\mathcal{E}_{coop}\}\Big] \\ &+ \mathbb{P}\{\gamma_{sr} \le \gamma_t\}\mathbb{P}\{\mathcal{E}_{sd}\}.\end{aligned} \tag{4.2}$$

[1] All the logarithms are in the natural base unless indicated otherwise.

and the threshold value that minimizes this BER has been found as

$$\gamma_t^* = \begin{cases} \left(\mathrm{erfc}^{-1}(2\delta)\right)^2, & \delta < 0.5; \\ 0, & \text{otherwise}, \end{cases} \tag{4.3}$$

where δ is equal to

$$\delta = \frac{\mathbb{P}\{\mathcal{E}_{sd}\} - \mathbb{P}\{\mathcal{E}_{coop}\}}{\mathbb{P}\{\mathcal{E}_{prop}\} - \mathbb{P}\{\mathcal{E}_{coop}\}}. \tag{4.4}$$

In the rest of this section, we first show that the optimal threshold function γ_t^* given in (4.3) increases logarithmically with SNR (Lemma 4.1). Then, using this result, we prove that if the relay sets its threshold to γ_t^*, the probability that it remains silent decreases as $\log(\mathsf{SNR})/\mathsf{SNR}$ and the probability that the relay has a detection error decreases at least as fast as $1/\mathsf{SNR}^2$ (Lemmas 4.2 and 4.3). Finally, we use all these results to show that the asymptotic e2e BER of the optimal TDR decreases as $\log(\mathsf{SNR})/\mathsf{SNR}^2$ and the optimal TDR achieves diversity order 2 (Proposition 4.1).

We note that the BER of TDR is greater by a factor of $\log(\mathsf{SNR})$ than the BER of a traditional diversity system, where BER decreases as $1/\mathsf{SNR}^2$ at large SNR. Since the diversity order represents the relation of the BER and SNR up to an exponential factor, the diversity order of TDR is still 2. Hence, we conclude that it is possible to achieve maximum diversity order in a single relay network using threshold relaying with the optimal threshold selection.

4.2.1 Asymptotic Behavior of γ_t^*, $\mathbb{P}\{\gamma_{sr} \leq \gamma_t^*\}$, and $\mathbb{P}\{\mathcal{E}_{sr}|\gamma_{sr} > \gamma_t^*\}$

The results on the asymptotic behavior of γ_t^*, $\mathbb{P}\{\gamma_{sr} \leq \gamma_t^*\}$, and $\mathbb{P}\{\mathcal{E}_{sr}|\gamma_{sr} > \gamma_t^*\}$ are given in Lemmas 4.1, 4.2, and 4.3, respectively. See Appendix B for the proofs.

Lemma 4.1 (Asymptotic behavior of γ_t^*). *The optimal threshold γ_t^*, given in (4.3), is upper and lower-bounded by two log functions for sufficiently large SNR. That is, there exist $c_1, c_2 > 0$ such that*

$$c_1 \log(\mathsf{SNR}) < \gamma_t^*(\mathsf{SNR}) < c_2 \log(\mathsf{SNR}), \quad \text{as } \mathsf{SNR} \to \infty. \tag{4.5}$$

Lemma 4.2 (Asymptotic behavior of $\mathbb{P}\{\gamma_{sr} \leq \gamma_t^*\}$). *For sufficiently large SNR, $\mathbb{P}\{\gamma_{sr} \leq \gamma_t^*\}$ can be upper and lower bounded as follows. There exists $c_1', c_2' > 0$ such that*

$$c_1' \frac{\log(\mathsf{SNR})}{\mathsf{SNR}} < \mathbb{P}\{\gamma_{sr} < \gamma_t^*\} < c_2' \frac{\log(\mathsf{SNR})}{\mathsf{SNR}}, \quad \text{as } \mathsf{SNR} \to \infty. \tag{4.6}$$

Lemma 4.3 (Asymptotic behavior of $\mathbb{P}\{\mathcal{E}_{sr}|\gamma_{sr} > \gamma_t^*\}$). *If the relay uses the optimal threshold γ_t^*, then $\mathbb{P}\{\mathcal{E}_{sr}|\gamma_{sr} > \gamma_t^*\}$ can be upper bounded as follows. There exists a $c > 0$ such that*

$$\mathbb{P}\{\mathcal{E}_{sr}|\gamma_{sr} > \gamma_t^*\} < c\frac{1}{\mathsf{SNR}^2}, \quad \text{as } \mathsf{SNR} \to \infty. \tag{4.7}$$

4.2.2 Asymptotic e2e BER and Diversity Order of the Optimal TDR

Proposition 4.1. *The e2e BER of TDR, given in (4.2), using the threshold γ_t^*, given in (4.3), satisfies $BER_{e2e}^{TDR}(\gamma_t^*) = O(\log(\mathsf{SNR})/\mathsf{SNR}^2)$ and hence achieves the maximum diversity order of 2.*

Proof. Let us denote the first term of (3.30) as P_r and the second term as P_{nr}. Note that P_r is equal to the probability of error when the relay transmits and P_{nr} is equal to the probability of error when the relay does not transmit.

$$P_r = \mathbb{P}\{\gamma_{sr} > \gamma_t^*\}\Big[\mathbb{P}\{\mathcal{E}_{sr}|\gamma_{sr} > \gamma_t^*\}\,\mathbb{P}\{\mathcal{E}_{prop}\} + \mathbb{P}\{\mathcal{E}_{coop}\} - \mathbb{P}\{\mathcal{E}_{sr}|\gamma_{sr} > \gamma_t^*\}\,\mathbb{P}\{\mathcal{E}_{coop}\}\Big]$$
$$P_{nr} = \mathbb{P}\{\gamma_{sr} \leq \gamma_t^*\}\,\mathbb{P}\{\mathcal{E}_{sd}\}.$$

In P_r, the term $\mathbb{P}\{\gamma_{sr} > \gamma_t^*\} = \exp(-\gamma_t/(\kappa_{sr}\mathsf{SNR}))$ goes to 1 as $\mathsf{SNR} \to \infty$. Since $\mathbb{P}\{\mathcal{E}_{prop}\} \sim \frac{\kappa_{rd}}{\kappa_{sd}+\kappa_{rd}}$ (see Appendix B.1 for the proof) and $\mathbb{P}\{\mathcal{E}_{coop}\} \sim \frac{3}{16\kappa_{rd}\kappa_{sd}}\frac{1}{\mathsf{SNR}^2}$, the decay rate of P_r is equal to the minimum of the rates of $\mathbb{P}\{\mathcal{E}_{sr}|\gamma_{sr} > \gamma_t^*\}$ and $\mathbb{P}\{\mathcal{E}_{coop}\}$. From Lemma 4.3, $\mathbb{P}\{\mathcal{E}_{sr}|\gamma_{sr} > \gamma_t^*\} = O(1/\mathsf{SNR}^2)$. Hence, $P_r = O(1/\mathsf{SNR}^2)$.

Since $\mathbb{P}\{\mathcal{E}_{sd}\} \sim \frac{1}{4\kappa_{sd}}\frac{1}{\mathsf{SNR}}$ and $\mathbb{P}\{\gamma_{sr} \leq \gamma_t^*\} = O(\log(\mathsf{SNR})/\mathsf{SNR})$ (from Lemma 4.2), $P_{nr} = O(\log(\mathsf{SNR})/\mathsf{SNR}^2)$. The e2e BER of the optimal TDR satisfies

$$\mathrm{BER}_{e2e}^{TDR}(\gamma_t^*) = P_r + P_{nr} = O(1/\mathsf{SNR}^2) + O(\log(\mathsf{SNR})/\mathsf{SNR}^2) = O(\log(\mathsf{SNR})/\mathsf{SNR}^2).$$

Thus, $\mathrm{BER}_{e2e}^{TDR}(\gamma_t^*)$ is limited by the second term P_{nr}, which corresponds to the event that the SNR of the $S - R$ link is below threshold.

The diversity order of the optimal TDR is equal to

$$\begin{aligned} d^{TDR} &= -\lim_{\mathsf{SNR}\to\infty} \frac{\log(\log(\mathsf{SNR})/\mathsf{SNR}^2)}{\log(\mathsf{SNR})} \\ &= -\lim_{\mathsf{SNR}\to\infty} \frac{\log(\log(\mathsf{SNR}))}{\log(\mathsf{SNR}^2)} + \lim_{\mathsf{SNR}\to\infty} \frac{\log(\mathsf{SNR}^2)}{\log(\mathsf{SNR})} = 2, \end{aligned}$$

since the term $\frac{\log(\log(\mathsf{SNR}))}{\log(\mathsf{SNR})} \to 0$ as $\mathsf{SNR} \to \infty$. □

We note that the non-selective cooperative relaying protocol of [29] also achieves BER of $\log(\mathsf{SNR})/\mathsf{SNR}^2$ using a piece-wise linear detector at the destination and assuming non-coherent demodulation at the relay and the destination.

4.3 An Approximation to the Optimal Threshold

The result given in Lemma 4.1 suggests that the threshold must increase logarithmically with SNR. In this section, we first prove that thresholds of the form $\gamma_t = \log(c\,\mathsf{SNR})$, achieves full diversity. Then, we propose a value for the constant c based on the derivations in Section 4.2.

Proposition 4.2. *The e2e BER of TDR, given in (3.30), using a threshold* $\gamma_t = \log(c\mathsf{SNR})$ *satisfies* $BER_{e2e}^{TDR}(\gamma_t) = O(\log(\mathsf{SNR})/\mathsf{SNR}^2)$ *and achieves the maximum diversity order of* 2 *for any real constant* $c > 0$.

Proof. Substituting $\gamma_t = c\log(\mathsf{SNR})$ and $\bar{\gamma}_{sr} = \kappa_{sr}\mathsf{SNR}$ in (3.31), we obtain

$$\mathbb{P}\{\gamma_{sr} \leq \gamma_t\}=1 - \exp(-(\log(c\mathsf{SNR}))/\kappa_{sr}\mathsf{SNR}) = 1 - \left(\frac{1}{c\mathsf{SNR}}\right)^{\frac{1}{\kappa_{sr}\mathsf{SNR}}}$$
$$\sim\frac{1}{\kappa_{sr}}\frac{\log(\mathsf{SNR})}{\mathsf{SNR}}, \tag{4.8}$$

where (4.8) is obtained from (B.22) given in Appendix B.3. Hence, the second term in (3.30), $P_{nr} = \mathbb{P}\{\gamma_{sr} \leq \gamma_t\}\,\mathbb{P}\{\mathcal{E}_{sd}\} = O(\log(\mathsf{SNR})/\mathsf{SNR}^2)$. As in the proof of Proposition 1, the order of the first term P_r is determined by the term $\mathbb{P}\{\mathcal{E}_{sr}|\gamma_{sr} > \gamma_t\}$, i.e. $O(P_r) = O(\mathbb{P}\{\mathcal{E}_{sr}|\gamma_{sr} > \gamma_t\})$. From (B.26) in the Appendix B.4, for any threshold we have

$$\mathbb{P}\{\mathcal{E}_{sr}|\gamma_{sr} > \gamma_t\}<\frac{1}{2\kappa_{sr}\mathsf{SNR}}\mathrm{erfc}(\sqrt{\gamma_t}) < \frac{1}{2\kappa_{sr}\mathsf{SNR}}e^{-\gamma_t}, \tag{4.9}$$

where the last inequality follows from the following well-known upper bound for erfc [56][2]:

$$\mathrm{erfc}(z) < e^{-z^2}. \tag{4.10}$$

By substituting $\gamma_t = \log(c\mathsf{SNR})$, we obtain

$$\mathbb{P}\{\mathcal{E}_{sr}|\gamma_{sr} > \gamma_t\} < \frac{1}{2\kappa_{sr}c}\frac{1}{\mathsf{SNR}^2}. \tag{4.11}$$

Hence, $\mathbb{P}\{\mathcal{E}_{sr}|\gamma_{sr} > \gamma_t\} = O(1/\mathsf{SNR}^2)$ and $P_r = O(1/\mathsf{SNR}^2)$. Then, $\mathrm{BER}_{e2e}^{TDR}(\log(c\mathsf{SNR})) = P_r + P_{nr} = O(\log(\mathsf{SNR})/\mathsf{SNR}^2)$ and the diversity order of TDR with $\gamma_t = \log(c\,\mathsf{SNR})$ is equal to 2. □

[2]There are tighter upper bounds for erfc, but this bound is sufficient for our purpose.

In order to obtain an approximation for γ_t^*, which is denoted by $\gamma_t^{*,approx}$, we use the upper bound given in (4.10) and the asymptotic expression given in (B.17) in Appendix B.2 as approximations for erfc and δ, respectively:

$$\mathrm{erfc}(z) \approx e^{-z^2} \quad \text{and} \quad \delta \approx \frac{1}{4}\frac{1}{\mathsf{SNR}}\frac{\kappa_{rd}\kappa_{sd}}{\kappa_{rd}+\kappa_{sd}} = \frac{1}{4}\frac{\bar{\gamma}_{rd}\bar{\gamma}_{sd}}{\bar{\gamma}_{rd}+\bar{\gamma}_{sd}}.$$

Then, $\gamma_t^{*,approx}$ is given by

$$\gamma_t^{*,approx} = \begin{cases} -\log\left(\frac{1}{2}\left(\frac{1}{\bar{\gamma}_{rd}}+\frac{1}{\bar{\gamma}_{sd}}\right)\right), & \frac{1}{2}\left(\frac{1}{\bar{\gamma}_{rd}}+\frac{1}{\bar{\gamma}_{sd}}\right) < 1; \\ 0, & \text{otherwise.} \end{cases} \tag{4.12}$$

We note that for sufficiently large SNR, the condition $\frac{1}{2}\left(\frac{1}{\bar{\gamma}_{rd}}+\frac{1}{\bar{\gamma}_{sd}}\right) < 1$ is satisfied and $\gamma_t^{*,approx}$ is equal to

$$\gamma_t^{*,approx} = -\log\left(\frac{1}{2}\left(\frac{1}{\bar{\gamma}_{rd}}+\frac{1}{\bar{\gamma}_{sd}}\right)\right) = \log\left(2\left(\frac{1}{\kappa_{rd}}+\frac{1}{\kappa_{sd}}\right)^{-1}\mathsf{SNR}\right). \tag{4.13}$$

We observe that $\gamma_t^{*,approx} = \log(c\,\mathsf{SNR})$, where $c = 2\left(\frac{1}{\kappa_{rd}}+\frac{1}{\kappa_{sd}}\right)^{-1}$ is greater than zero. Hence, invoking Proposition 2, we conclude that with $\gamma_t^{*,approx}$, $\mathrm{BER}_{e2e}^{TDR}(\gamma_t^{*,approx}) = O(\log(\mathsf{SNR})/\mathsf{SNR}^2)$ and the diversity order is equal to 2. In (4.13), we note that $\gamma_t^{*,approx}$ is equal to the logarithm of the harmonic mean of $\bar{\gamma}_{sd}$ and $\bar{\gamma}_{rd}$.

4.4 Results

In this section, we compare the average BER of the optimal TDR to several schemes. These include the benchmark schemes introduced in Section 3.3.1 of Chapter 3 (simple digital relaying, genie-aided relaying) and the Link Adaptive Relaying (LAR) introduced in [31].

As the two schemes that are simpler than TDR, we consider direct transmission and simple digital relaying. From the average e2e BER expression for this scheme,

$$\mathrm{BER}_{e2e}^{simple} = \underbrace{\mathbb{P}\{\mathcal{E}_{sr}\}}_{O(1/\mathsf{SNR})}\underbrace{\mathbb{P}\{\mathcal{E}_{prop}\}}_{O(1)} + \underbrace{(1-\mathbb{P}\{\mathcal{E}_{sr}\})}_{O(1)}\underbrace{\mathbb{P}\{\mathcal{E}_{coop}\}}_{O(1/\mathsf{SNR}^2)}, \tag{4.14}$$

we observe that the e2e BER performance is limited by the first term and the e2e BER decays as $1/\mathsf{SNR}$. Hence, the diversity order of simple digital relaying is 1.

Genie-aided digital relaying and receive diversity schemes are also considered as performance upper bounds. In the genie-aided relaying, which assumes perfect error detection for each symbol, the relay transmits only those symbols received correctly in the first phase. The e2e BER of the genie-aided digital relaying is equal to

$$\mathrm{BER}_{e2e}^{genie} = \underbrace{\mathbb{P}\{\mathcal{E}_{sr}\}}_{O(1/\mathsf{SNR})}\ \underbrace{\mathbb{P}\{\mathcal{E}_{sd}\}}_{O(1/\mathsf{SNR})} + \underbrace{(1-\mathbb{P}\{\mathcal{E}_{sr}\})}_{O(1)}\underbrace{\mathbb{P}\{\mathcal{E}_{coop}\}}_{O(1/\mathsf{SNR}^2)}, \tag{4.15}$$

As seen from the orders of its terms, genie-aided digital relaying achieves diversity order of 2. The second upper bound, receive diversity, is obtained by assuming that the $S-R$ link is error-free, i.e., $\mathrm{BER}_{e2e}^{Rx2} = \mathbb{P}\{\mathcal{E}_{coop}\}$, where $\mathbb{P}\{\mathcal{E}_{coop}\}$ is given in (3.17).

The Link Adaptive Relaying (LAR) aims to reduce error propagation by adapting the relay transmit power to the link SNRs rather than transmitting with full power P_{full} all the time. If the relay is able to adapt its transmit power continuously, [31] proposes a scheme where the relay transmits with power $\alpha \times P_{full}$, where the scaling factor is equal to $\alpha = \frac{\min(\gamma_{sr},\bar{\gamma}_{rd})}{\bar{\gamma}_{rd}}$. We call this scheme as *LAR-cont*. If the relay can perform only on-off power adaptation, then it can be seen that LAR simplifies to TDR with threshold function $\gamma_{t,LAR} = \bar{\gamma}_{rd}$. We call this scheme as *LAR-on/off*. For all threshold based relaying schemes, the e2e BER can be calculated analytically by plugging in the appropriate threshold value as γ_t in (3.30). We resort to Monte Carlo simulations to obtain the e2e BER of *LAR-cont* only.

In Fig. 4.1 we plot the average BER as a function of SNR in a symmetric network where $\kappa_{sr} = \kappa_{sd} = \kappa_{rd} = 0$ dB. The on-off version of LAR has poor performance; its BER is larger than even the BER of the simple relaying. Since $\gamma_{t,LAR}$ increases linearly with SNR, from (B.21) we observe that $\mathbb{P}\{\gamma_{sr} \leq \gamma_{t,LAR}\}$ will be a constant independent of SNR. Then, in the e2e BER expression given in (3.30) the second term, $\mathbb{P}\{\gamma_{sr} \leq \gamma_{t,LAR}\} \times \mathbb{P}\{\mathcal{E}_{sd}\}$, decreases only as fast as the BER of the $S-D$ link.

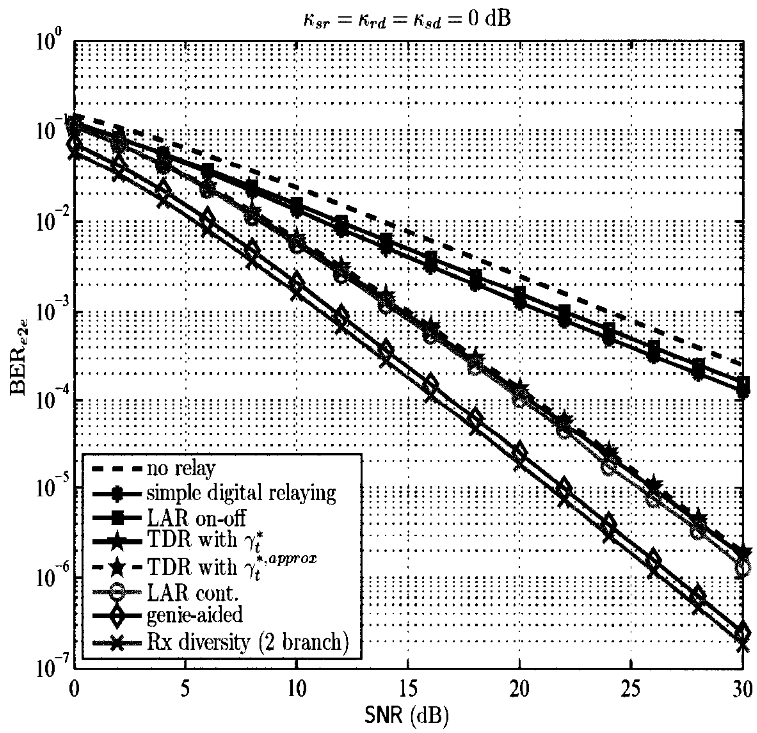

Figure 4.1: The e2e BERs for different schemes as a function of SNR in a symmetric network, where $\kappa_{sr} = \kappa_{rd} = \kappa_{sd} = 0$ dB.

Hence, the diversity order of on-off LAR is 1, which has also been reported in [31]. This argument applies to any TDR scheme that uses a threshold increasing linearly with the SNR. The continuous version of LAR, which is shown to achieve full diversity in [31], performs better than all TDR schemes including the optimal TDR. However, the gap with the optimal TDR is very small. Fig. 4.2 shows the BER of all the schemes for an asymmetric network, where the direct link is weaker than the $S-R$ and $R-D$ links, a typical scenario where R is located on the line segment between S and D. Relative link SNRs are selected as $\kappa_{sr} = \kappa_{rd} = 0$ dB and $\kappa_{sd} = -12$ dB. Unlike the symmetric case, here the optimal TDR outperforms continuous LAR by a very small margin. We note that the α value used in [31] for the continuous LAR is not optimized. Otherwise, it would always outperform the optimal TDR.

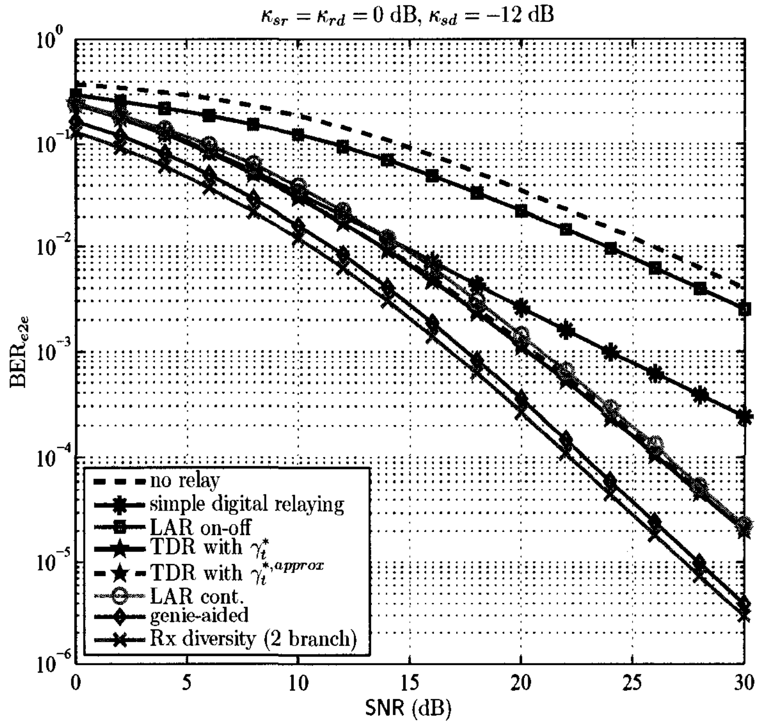

Figure 4.2: The threshold values and the e2e BERs for different schemes as a function of SNR in a nonsymmetric network, where $\kappa_{sr} = \kappa_{rd} = 0$ dB and $\kappa_{sd} = -12$ dB.

Fig. 4.3 and Fig. 4.4 show the variation of the optimal threshold and its approximation as a function of SNR, for the two sets of κ values used in Fig. 4.1 and Fig. 4.2. Although there is an offset between the optimal threshold and the approximation, the two curves are almost parallel to each other. As seen in Fig. 4.1 and Fig. 4.2, the BER of the approximate threshold $\gamma_t^{*,approx}$ is very close to the BER of the optimal threshold.

4.5 Conclusions

In this chapter, we studied the asymptotic BER of threshold based digital diversity relaying. We showed that in a network with a single relay and independent Rayleigh

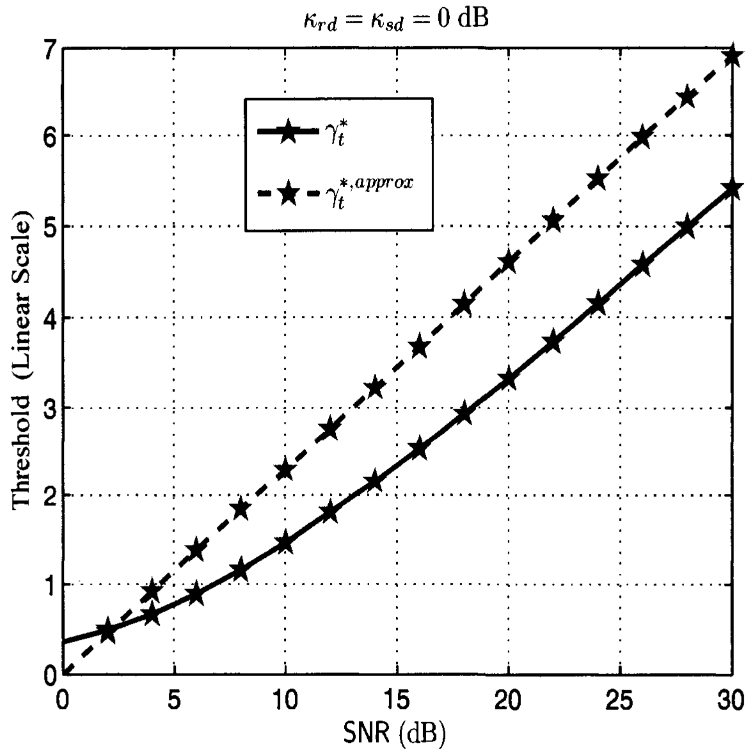

Figure 4.3: The threshold values as a function of SNR with $\kappa_{rd} = \kappa_{sd} = 0$ dB.

fading links, in order to minimize e2e BER, the threshold used by the relay should increase logarithmically with the average link SNR. We proved that this optimal threshold achieves dual diversity. We also showed that any threshold of the form $\log(c\mathsf{SNR})$, where $c > 0$ is a constant, achieves the same diversity order. Moreover, we derived a value for c that results in a BER very close to the BER of the optimal TDR.

In Chapter 5, we propose a threshold based multi-relay protocol to achieve diversity orders higher than 2. In order to limit the bandwidth loss due to multiple relay transmissions, we consider a relay selection protocol, in which at most one relay transmits.

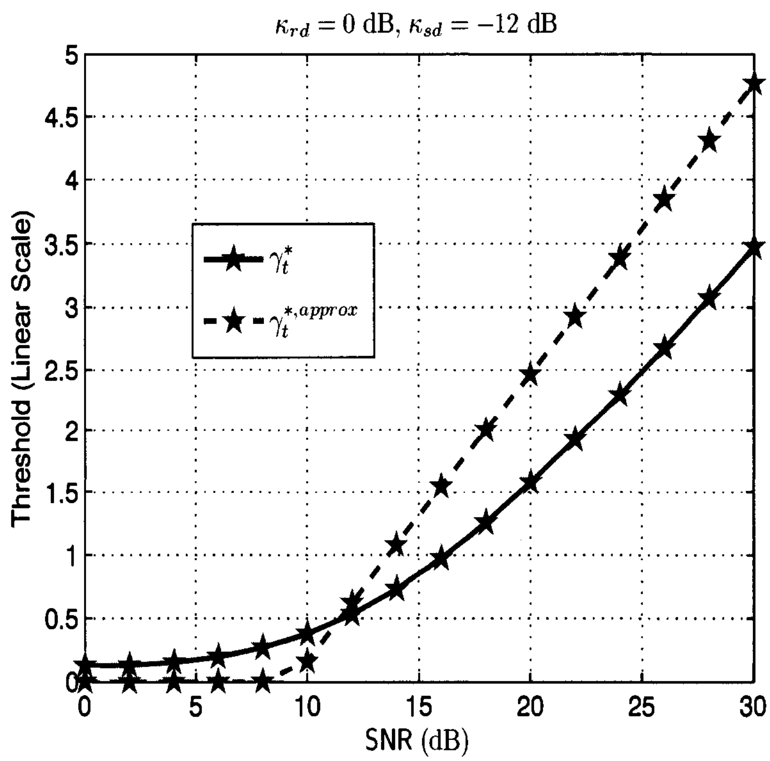

Figure 4.4: The threshold values as a function of SNR in a nonsymmetric network, where $\kappa_{rd} = 0$ dB and $\kappa_{sd} = -12$ dB.

Chapter 5

Threshold Based Relay Selection in Digital Diversity Relaying

In Chapters 3 and 4, we focused on inducing spatial diversity using a single relay. We studied threshold relaying as a method to mitigate error propagation in digital diversity relaying and we showed that optimal threshold relaying can achieve diversity order of 2 in a single relay network. In this chapter, we consider multiple relays to achieve higher orders of diversity at the destination.

Consider a multiple parallel relay configuration as shown in Fig. 5.1. With M_r parallel relays there is a potential to achieve $M_r + 1$ orders of diversity by combining signals from the source and the relays. For instance, following the source transmission, the relays can retransmit one-by-one, spanning $M_r + 1$ time slots. Then, the destination can combine $(M_r + 1)$ signals using the C-MRC scheme of [30]. Alternatively, the relays can use the LAR protocol of [31] and the destination can combine the signals using MRC. Either of these protocols can achieve diversity order of $(M_r + 1)$. However, retransmission of the data by all M_r relays causes a large increase in radio resources, especially for large M_r.

As a remedy to this problem, Laneman and Wornell proposed distributed space-time coding for decode-and-forward relays [35]. In [57], it has been shown that diversity-multiplexing trade-off of distributed space-time coding can be achieved by a relay selection protocol. In this protocol a single, "best" relay is selected to serve for each source-destination pair. Among the relays that receive the data from the source without any errors, the one with the highest instantaneous SNR to the destination is selected as the "best" relay. Both [35] and [57] assume ideal channel coding, in which error propagation does not occur as long as the received SNR at the relays is higher than a rate dependent target SNR value. In this chapter, our goal is to achieve similar diversity orders without relying on channel coding.

We propose Threshold based Relay Selection (TRS) protocol, which generalizes threshold digital relaying to multiple relays. In this protocol only the relays whose received SNRs are larger than a threshold, which we call *reliable relays*, are allowed to retransmit. Our protocol employs selection combining at the destination based only on the relay-destination and source-destination link SNRs. In bandwidth limited scenarios, with channel estimation of these links and feedback from the destination, selection can be done prior to the relay transmissions as performed in [57] and [38]. Then, only the selected relay, the one with the largest SNR to the destination, retransmits, thereby reducing the bandwidth expansion. In the absence of such feedback, all the reliable relays can retransmit sequentially and the same BER performance is achieved.

We note that in C-MRC of [30] the destination needs the exact source-relay SNR for every relay, whereas in the LAR protocol of [31] the power scaling factor used by each relay, which depends on the instantaneous first hop SNR, has to be conveyed to the destination. In the ML detector of [29], the destination requires the knowledge of the average SNRs of every source-relay link. Conveying the average link SNRs is less costly than conveying the exact SNR. However, this protocol cannot achieve full diversity for more than one relay. The TRS protocol proposed in this chapter requires minimal information on the first hop and still achieves full diversity.

A related protocol has been proposed in [58]. In this protocol, the relay selection is performed based on the equivalent e2e BER of each relay channel. This protocol can be viewed as a selection version of C-MRC of [30]. As in C-MRC, it requires the destination to obtain the channel coefficients of the first and second hops, or their product in the case of a simpler scheme, to perform relay selection. However, in TRS, the information passed from the relay to the destination regarding the first hop is limited to whether the relays is a reliable relay or not, which can be represented by a single bit.

The rest of this chapter is organized as follows. In Section 5.1, we describe the system model and the TRS protocol. In Section 5.2, we derive the e2e BER for multiple relays and the optimal threshold for a single relay. In Section 5.3 we show that the protocol achieves full diversity for any number of relays using a threshold function we propose. We present some numerical results in Section 5.4 and conclude with a summary of our findings.

5.1 System Model

A network as shown in Fig. 5.1 is considered in which a source node S communicates with a destination node D with the assistance of M_r relays denoted by $R_1, R_2, \ldots R_{M_r}$. The SNRs of the $S-D$, $S-R_i$ and R_i-D links are denoted by γ_{sd}, $\gamma_{sr,i}$, and $\gamma_{rd,i}$, respectively. To simplify the analysis, we assume that all the relays have the same average SNRs to the source and to the destination, i.e., $\bar{\gamma}_{sr,i} = \bar{\gamma}_{sr}$ and $\bar{\gamma}_{rd,i} = \bar{\gamma}_{rd}$ for $i = 1, 2, \ldots, M_r$. Hence, the link SNRs are characterized by $\bar{\gamma}_{sd}$, $\bar{\gamma}_{sr}$, and $\bar{\gamma}_{rd}$. All links experience independent Rayleigh fading. We assume a general modulation scheme for which the bit error probability can be expressed as $P_b(\gamma) \approx \beta_m \operatorname{erfc}(\sqrt{\alpha_m \gamma})$, where $\alpha_m, \beta_m > 0$. We recall that typically α_m depends on the minimum distance in the constellation and β_m depends on the number of neighbors with minimum distance;

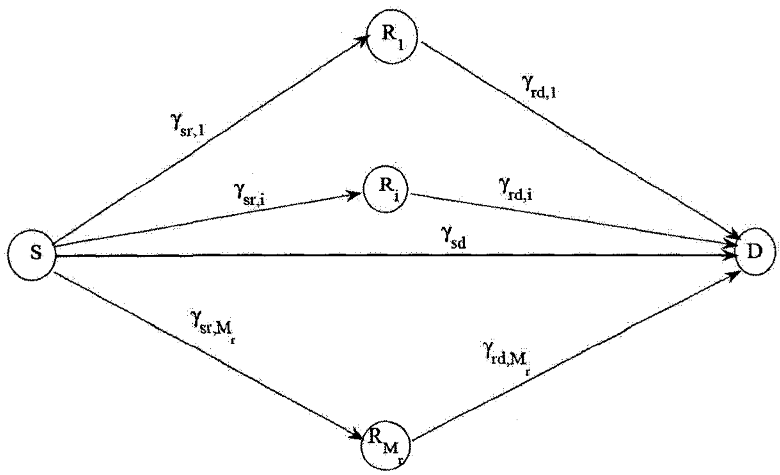

Figure 5.1: The parallel relay configuration with M_r relays.

the bit error probability of most practical modulation schemes can be approximated by selecting (β_m, α_m). The average bit error probability under Rayleigh fading based on this general P_b expression is given in (3.4) as

$$\bar{P}_b(\bar{\gamma}) = \mathbb{E}_\gamma[\beta_m \operatorname{erfc}(\sqrt{\alpha_m \gamma})] = \beta_m \left[1 - \sqrt{\frac{\alpha_m \bar{\gamma}}{1 + \alpha_m \bar{\gamma}}}\right]. \tag{5.1}$$

Some of our derivations are even more general; they are given in terms of P_b and $\bar{P}_b$, and can be evaluated for any modulation scheme.

We consider a two-phase protocol. In the first phase the source transmits while all the relays and the destination listen. Then each relay R_i decides independently whether its detection is sufficiently reliable by comparing its received SNR $\gamma_{sr,i}$ to a threshold value. The SNR information available at the relays is as in I_1 case of Chapter 3; the relays have access to the average link SNRs of the relay-destination and source-destination links but they do not know the instantaneous SNRs of these links.

Those relays whose received SNRs are larger than the threshold are called *reliable relays*. Each reliable relay informs the destination by sending a short message. Let

N_r denote the number of reliable relays. The destination, then, makes a decision based on the SNRs of the reliable relays and the source to the destination[1], i.e., γ_{sd} and $\gamma_{rd,1}, \ldots, \gamma_{rd,N_r}$. Among $N_r + 1$ branches D selects the one with the largest SNR. If the branch from the source is selected, the relays do not transmit and the source transmits the next data. Otherwise, the selected reliable relay transmits and D performs detection based on the selected branch only. We call this protocol the *Threshold based Relay Selection* (TRS) protocol.

In this protocol the information passed from the relay to the destination regarding the first hop is limited to whether the relay is a reliable relay or not, which can be represented by a single bit. We assume that each reliable relay sends a short packet while the other relays remain silent. The destination can also estimate the values of $\gamma_{rd,i}$ for all the reliable relays from these transmissions.

5.2 End-to-end (e2e) BER of the TRS

In this section, we derive the e2e BER of the TRS protocol. Since all the relays are assumed to be identical in their average SNR to the relay and to the destination, the optimal value of their thresholds must be the same. Hence, we derive the e2e BER of the system for a given common threshold γ_t for all relays. Then the e2e BER is given by

$$\text{BER}_{e2e} = \sum_{i=0}^{M_r} \mathbb{P}\{N_r = i\}\mathbb{P}\{\mathcal{E}_{e2e}|N_r = i\}, \tag{5.2}$$

where

$$\mathbb{P}\{N_r = i\} = \binom{M_r}{i} \left(e^{-\gamma_t/\bar{\gamma}_{sr}}\right)^i \left(1 - e^{-\gamma_t/\bar{\gamma}_{sr}}\right)^{M_r - i}.$$

For $N_r = 0$, the destination detects based on the direct link only and, thus, $\mathbb{P}\{\mathcal{E}_{e2e}|N_r = 0\} = \bar{P}_b(\bar{\gamma}_{sd})$. For $N_r \geq 1$, let $\mathcal{A}_s$ denote the event that the destination

[1]We re-index the reliable relays to simplify the notation.

selects the signal received from the source and $\mathcal{A}_{r,k}$ denote the event that the destination selects the signal from the k-th reliable relay ($k \in \{1, \ldots, N_r\}$), respectively:

$$\mathcal{A}_s = \{\gamma_{sd} > \gamma_{rd,j}, \forall j \in \{1, \ldots, N_r\}\}, \text{ and}$$
$$\mathcal{A}_{r,k} = \{\gamma_{rd,k} > \gamma_{sd}, \gamma_{rd,k} > \gamma_{rd,j}, \forall j \in \{1, \ldots, N_r\}, j \neq k\}.$$

Then, the e2e BER conditioned on the number of reliable relays is equal to

$$\begin{aligned}\mathbb{P}\{\mathcal{E}_{e2e}|N_r = i\} =& \mathbb{P}\{\mathcal{E}_{e2e}|\mathcal{A}_s, N_r = i\}\mathbb{P}\{\mathcal{A}_s|N_r = i\} \\ &+ \sum_{k=1}^{i} \mathbb{P}\{\mathcal{E}_{e2e}|\mathcal{A}_{r,k}, N_r = i\}\mathbb{P}\{\mathcal{A}_{r,k}|N_r = i\}.\end{aligned} \tag{5.3}$$

Since all relays are assumed to be identical in their average SNRs to the source and to the destination, the terms included in $\mathcal{A}_{r,k}$ are the same for all k and the index k can be dropped. When the destination selects the source signal, its bit error rate only depends on the $S - D$ link. However, if the destination selects reliable relay j, it will have a bit error if either the $S - R_j$ link or the $R_j - D$ link has a bit error:

$$\mathbb{P}\{\mathcal{E}_{e2e}|\mathcal{A}_s, N_r = i\} = \mathbb{P}\{\mathcal{E}_{sd}|\mathcal{A}_s, N_r = i\} \tag{5.4}$$

and

$$\begin{aligned}\mathbb{P}\{\mathcal{E}_{e2e}|\mathcal{A}_r, N_r = i\} =& \mathbb{P}\{\mathcal{E}_{rd}|\mathcal{A}_r, N_r = i\}(1 - \mathbb{P}\{\mathcal{E}_{sr}|\gamma_{sr} > \gamma_t\}) \\ &+ (1 - \mathbb{P}\{\mathcal{E}_{rd}|\mathcal{A}_r, N_r = i\})\mathbb{P}\{\mathcal{E}_{sr}|\gamma_{sr} > \gamma_t\}.\end{aligned} \tag{5.5}$$

Substituting (5.4) and (5.5) into (5.3), we obtain the e2e BER conditioned on N_r as

$$\begin{aligned}\mathbb{P}\{\mathcal{E}_{e2e}|N_r = i\} =& \mathbb{P}\{\mathcal{E}_{sd}, \mathcal{A}_s|N_r = i\} + i\Big(\mathbb{P}\{\mathcal{E}_{rd}, \mathcal{A}_r|N_r = i\} \\ &+ \mathbb{P}\{\mathcal{E}_{rd}, \mathcal{A}_r|N_r = i\}(1 - 2\mathbb{P}\{\mathcal{E}_{sr}|\gamma_{sr} > \gamma_t\}) \\ &+ \mathbb{P}\{\mathcal{A}_r|N_r = i\}\mathbb{P}\{\mathcal{E}_{sr}|\gamma_{sr} > \gamma_t\}\Big).\end{aligned} \tag{5.6}$$

The probability of bit error at a reliable relay is derived in Appendix A.2 and is equal to

$$\mathbb{P}\{\mathcal{E}_{sr}|\gamma_{sr} > \gamma_t\}=\beta_m\left[\operatorname{erfc}(\sqrt{\alpha_m\gamma_t}) - e^{\gamma_t/\bar{\gamma}_{sr}}\sqrt{\frac{\alpha_m\bar{\gamma}_{sr}}{1+\alpha_m\bar{\gamma}_{sr}}}\right.$$
$$\left.\times\operatorname{erfc}\left(\sqrt{\gamma_t\left(\alpha_m+\frac{1}{\bar{\gamma}_{sr}}\right)}\right)\right]. \tag{5.7}$$

The probability that a particular reliable relay is selected by the destination is equal to

$$\mathbb{P}\{\mathcal{A}_r|N_r = i\}=\frac{1}{i}\left(1-\sum_{j=0}^{i}\binom{i}{j}(-1)^j\frac{1}{1+j(\bar{\gamma}_{sd}/\bar{\gamma}_{rd})}\right). \tag{5.8}$$

The terms $\mathbb{P}\{\mathcal{E}_{sd}, \mathcal{A}_s|N_r = i\}$ and $\mathbb{P}\{\mathcal{E}_{rd}, \mathcal{A}_r|N_r = i\}$ are given by

$$\mathbb{P}\{\mathcal{E}_{sd}, \mathcal{A}_s|N_r = i\} = \sum_{j=0}^{i}\left\{\binom{i}{j}(-1)^j\frac{\bar{\gamma}_{rd}}{j\bar{\gamma}_{sd}+\bar{\gamma}_{rd}}\bar{P}_b\left(\frac{\bar{\gamma}_{sd}\bar{\gamma}_{rd}}{j\bar{\gamma}_{sd}+\bar{\gamma}_{rd}}\right)\right\}, \tag{5.9}$$

and

$$\mathbb{P}\{\mathcal{E}_{rd}, \mathcal{A}_r|N_r = i\}=\sum_{j=0}^{i-1}\left\{\binom{i-1}{j}(-1)^j\left[\frac{1}{j+1}\bar{P}_b\left(\frac{\bar{\gamma}_{rd}}{j+1}\right)\right.\right.$$
$$\left.\left.-\frac{\bar{\gamma}_{sd}}{\bar{\gamma}_{sd}(j+1)+\bar{\gamma}_{rd}}\bar{P}_b\left(\frac{\bar{\gamma}_{sd}\bar{\gamma}_{rd}}{\bar{\gamma}_{sd}(j+1)+\bar{\gamma}_{rd}}\right)\right]\right\}. \tag{5.10}$$

See Appendix C.1 for the derivations of (5.8)-(5.10). By substituting (5.7)-(5.10) into (5.6), and then substituting (5.3), (5.6) into (5.2), we obtain an exact expression for the e2e BER of the threshold based relay selection protocol described in Section 5.1.

Optimal Threshold of TRS for $M_r = 1$

For networks with a single relay, we can derive the threshold that minimizes e2e BER by formulating a simple decision problem as we did in Section 3.2.3 of Chapter 3.

Proposition 5.1. *The threshold that minimizes the e2e BER of the system described in Section 5.1 with a single relay, under Rayleigh fading and a modulation scheme* *that has a bit error probability of $P_b(\gamma)$ and an average bit error probability of $\bar{P}_b(\bar{\gamma})$, is given by*

$$\gamma_t^* = P_b^{-1}(\delta(\bar{\gamma}_{sd}, \bar{\gamma}_{rd})), \tag{5.11}$$

where

$$\delta(\bar{\gamma}_{sd}, \bar{\gamma}_{rd}) = \frac{\frac{\bar{\gamma}_{rd}+\bar{\gamma}_{sd}}{\bar{\gamma}_{rd}}\left(\bar{P}_b\left(\frac{\bar{\gamma}_{rd}\bar{\gamma}_{sd}}{\bar{\gamma}_{rd}+\bar{\gamma}_{sd}}\right) - \bar{P}_b(\bar{\gamma}_{rd})\right)}{1 - 2\frac{\bar{\gamma}_{rd}+\bar{\gamma}_{sd}}{\bar{\gamma}_{rd}}\bar{P}_b(\bar{\gamma}_{rd}) + 2\frac{\bar{\gamma}_{sd}}{\bar{\gamma}_{rd}}\bar{P}_b\left(\frac{\bar{\gamma}_{rd}\bar{\gamma}_{sd}}{\bar{\gamma}_{rd}+\bar{\gamma}_{sd}}\right)}. \tag{5.12}$$

Proof. Let a_0 and a_1 denote the two actions the relay can take: to remain silent or to forward the detected symbols, respectively. Then, the optimal threshold can be obtained by simplifying the following decision rule solved at the relay:

$$\mathbb{P}\{\mathcal{E}_{e2e}|N_r = 1, \gamma_{sr}\} \underset{a_0}{\overset{a_1}{\gtrless}} \mathbb{P}\{\mathcal{E}_{e2e}|N_r = 0, \gamma_{sr}\}. \tag{5.13}$$

Clearly, if the relay remains silent

$$\mathbb{P}\{\mathcal{E}_{e2e}|N_r = 0, \gamma_{sr}\} = \bar{P}_b(\bar{\gamma}_{sd}).$$

If the relay forwards the data the average e2e BER is equal to

$$\begin{aligned}\mathbb{P}\{\mathcal{E}_{e2e}|N_r = 1, \gamma_{sr}\} =& \mathbb{P}\{\mathcal{E}_{e2e}|N_r = 1, \mathcal{A}_s, \gamma_{sr}\}\mathbb{P}\{\mathcal{A}_s|N_r = 1\} \\ &+ \mathbb{P}\{\mathcal{E}_{e2e}|N_r = 1, \mathcal{A}_r, \gamma_{sr}\}\mathbb{P}\{\mathcal{A}_r|N_r = 1\}.\end{aligned}$$

Following the same steps as in Section 5.2, we obtain

$$\begin{aligned}\mathbb{P}\{\mathcal{E}_{e2e}|N_r = 1, \gamma_{sr}\} =& \mathbb{P}\{\mathcal{E}_{sd}, \mathcal{A}_s|N_r = 1\} + \mathbb{P}\{\mathcal{E}_{rd}, \mathcal{A}_r|N_r = 1\} \\ &+ \mathbb{P}\{\mathcal{E}_{rd}, \mathcal{A}_r|N_r = 1\}(1 - 2P_b(\gamma_{sr})) \\ &+ \mathbb{P}\{\mathcal{A}_r|N_r = 1\}P_b(\gamma_{sr}).\end{aligned} \tag{5.14}$$

Note that, (5.14) is the same as (5.6) except that $\mathbb{P}\{\mathcal{E}_{sr}|\gamma_{sr} > \gamma_t\}$ is replaced with $\mathbb{P}\{\mathcal{E}_{sr}|\gamma_{sr}\} = P_b(\gamma_{sr})$, since γ_{sr} is available at the relay.

For $N_r = 1$, (5.8), (5.9), and (5.10) simplify to

$$\mathbb{P}\{\mathcal{E}_{sd}, \mathcal{A}_s | N_r = 1\} = \bar{P}_b(\bar{\gamma}_{sd}) - \frac{\bar{\gamma}_{rd}}{\bar{\gamma}_{sd} + \bar{\gamma}_{rd}} \bar{P}_b\left(\frac{\bar{\gamma}_{sd}\bar{\gamma}_{rd}}{\bar{\gamma}_{sd} + \bar{\gamma}_{rd}}\right),$$
$$\mathbb{P}\{\mathcal{E}_{rd}, \mathcal{A}_r | N_r = 1\} = \bar{P}_b(\bar{\gamma}_{rd}) - \frac{\bar{\gamma}_{sd}}{\bar{\gamma}_{sd} + \bar{\gamma}_{rd}} \bar{P}_b\left(\frac{\bar{\gamma}_{sd}\bar{\gamma}_{rd}}{\bar{\gamma}_{sd} + \bar{\gamma}_{rd}}\right)$$

and

$$\mathbb{P}\{\mathcal{A}_r | N_r = 1\} = \frac{\bar{\gamma}_{rd}}{\bar{\gamma}_{rd} + \bar{\gamma}_{sd}}.$$

We note that for $M_r = 1$ relay, $\mathbb{P}\{\mathcal{E}_{sd}, \mathcal{A}_s | N_r = 1\}$ and $\mathbb{P}\{\mathcal{E}_{rd}, \mathcal{A}_r | N_r = 1\}$ expressions are symmetric with respect to $\bar{\gamma}_{sd}$ and $\bar{\gamma}_{rd}$. After substituting all the terms into (5.13), we obtain the following rule

$$\begin{aligned} P_b(\gamma_{sr}) &\underset{a_0}{\overset{a_1}{\gtrless}} \delta(\bar{\gamma}_{rd}, \bar{\gamma}_{sd}) \\ \gamma_{sr} &\underset{a_0}{\overset{a_1}{\gtrless}} P_b^{-1}(\delta(\bar{\gamma}_{rd}, \bar{\gamma}_{sd})), \end{aligned} \tag{5.15}$$

where $\delta(.,.)$ is given by (5.12). Hence, the threshold that minimizes the e2e BER is equal to $\gamma_t^* = P_b^{-1}(\delta(\bar{\gamma}_{rd}, \bar{\gamma}_{sd}))$. □

5.3 Diversity Order of TRS

In this section, as in Chapter 4, we express all the average link SNRs as $\bar{\gamma}_{ij} = \kappa_{ij}\mathsf{SNR}$ and study the behavior of the e2e BER as $\mathsf{SNR} \to \infty$. Let us first take a close look at the e2e BER minimizing threshold derived in Proposition 5.1, for a network with $M_r = 1$ relay. If $P_b(\gamma) = \beta_m \operatorname{erfc}(\sqrt{\alpha_m \gamma})$, the average error probability given in (3.4) is asymptotically equal to

$$\bar{P}_b(\kappa, \mathsf{SNR}) = \beta_m \left[1 - \sqrt{\frac{\alpha_m \kappa \mathsf{SNR}}{1 + \alpha_m \kappa \mathsf{SNR}}}\right] \sim \frac{\beta_m}{2\alpha_m \kappa} \frac{1}{\mathsf{SNR}}.$$

Substituting this asymptotic expression in (5.12), we observe that,

$$\delta(\kappa_{sd}, \kappa_{rd}, \mathsf{SNR}) \sim \frac{\beta_m}{2\alpha_m} \frac{\kappa_{sd} + \kappa_{rd}}{\kappa_{sd}\kappa_{rd}} \frac{1}{\mathsf{SNR}}. \tag{5.16}$$

By approximating $\operatorname{erfc}(z) \approx e^{-z^2}$, and $\delta \approx \frac{\beta_m}{2\alpha_m} \frac{\kappa_{sd}+\kappa_{rd}}{\kappa_{sd}\kappa_{rd}} \frac{1}{\mathsf{SNR}}$, we obtain

$$\begin{aligned}\gamma_t^* = P_b^{-1}(\delta) &= \frac{1}{\alpha_m} \left(\operatorname{erfc}^{-1}(\delta/\beta_m)\right)^2 \approx \frac{1}{\alpha_m} \log\left(\frac{\beta_m}{\delta}\right) \\ &\approx \frac{1}{\alpha_m} \log\left(2\alpha_m \frac{\kappa_{sd}\kappa_{rd}}{\kappa_{sd} + \kappa_{rd}} \mathsf{SNR}\right)\end{aligned}$$

This approximate expression is the same as the approximate threshold derived in Section 4.3 in Chapter 4 (eqn. 4.13) for a single relay network using BPSK modulation in all the links ($\alpha_m = 1$) and MRC combining at the destination.

Based on the insight from the e2e BER minimizing threshold for $M_r = 1$, for a network with $M_r > 1$ relays we propose a threshold function in the form of $\log(c_1 \mathsf{SNR}^{M_r/\alpha_m})$, where c_1 is a positive constant. Next, we show that TRS can achieve full diversity with the proposed threshold function.

Lemma 5.1 (Asymptotic behavior of $\mathbb{P}\{\mathcal{E}_{e2e}|N_r = i\}$). *With the proposed threshold $\gamma_t^* = \log(c_1 \mathsf{SNR}^{M_r/\alpha_m})$, as $\mathsf{SNR} \to \infty$ the e2e bit error probability conditioned on the number reliable relays $N_r = i$ decays as $\mathbb{P}\{\mathcal{E}_{e2e}|N_r = i\} = O(1/\mathsf{SNR}^{i+1})$.*

See Appendix C.2 for the proof.

Proposition 5.2. *The diversity order of the TRS protocol having M_r relays and employing a modulation scheme that has a BER of $P_b(\gamma) = \beta_m \operatorname{erfc}(\sqrt{\alpha_m \gamma})$, achieves diversity order of $M_r + 1$ using a threshold of $\gamma_t^* = \log(c_1\, \mathsf{SNR}^{M_r/\alpha_m})$, where $c_1 > 0$ is a constant independent of SNR.*

Proof. The e2e BER of TRS is given in (5.2). The first term of (5.2) is equal to

$$\mathbb{P}\{N_r = i\} = \binom{M_r}{i} \left(e^{-\gamma_t/\bar{\gamma}_{sr}}\right)^i \left(1 - e^{-\gamma_t/\bar{\gamma}_{sr}}\right)^{M_r - i}.$$

With the proposed threshold, as $\mathsf{SNR} \to \infty$ we obtain

$$e^{-\gamma_t/\bar{\gamma}_{sr}} = e^{-\log(c_1 \mathsf{SNR}^{M_r/\alpha_m})/(\kappa_{sr}\mathsf{SNR})} \sim 1, \text{ and}$$

$$\begin{aligned}(1 - e^{-\gamma_t/\bar{\gamma}_{sr}}) &= 1 - e^{-\log(c_1 \mathsf{SNR}^{M_r/\alpha_m})/(\kappa_{sr}\mathsf{SNR})} \\ &\sim \frac{\log(c_1 \mathsf{SNR}^{M_r/\alpha_m})}{\kappa_{sr}\mathsf{SNR}}.\end{aligned}$$

Thus, $\mathbb{P}\{N_r = i\}$ is of order

$$\mathbb{P}\{N_r = i\} = O(\log(\mathsf{SNR}^{M_r/\alpha_m})^{M_r-i}/\mathsf{SNR}^{M_r-i}). \tag{5.17}$$

Next, we study how fast the term $\mathbb{P}\{\mathcal{E}_{e2e}|N_r = i\}$ (given in (5.6)) decays with increasing SNR.

Combining the result of Lemma 5.1 with (5.17), we observe that in (5.2) the term with index i, i.e., $\mathbb{P}\{N_r = i\}\mathbb{P}\{\mathcal{E}_{e2e}|N_r = i\}$ decreases as $O(\log(\mathsf{SNR}^{M_r/\alpha_m})^{M_r-i}/\mathsf{SNR}^{M_r+1})$. The order of the sum of these $M_r + 1$ terms is determined by the term that has the slowest decay, which is the term with index $i = 0$. Hence,

$$\mathrm{BER}_{e2e} = O(\log(\mathsf{SNR}^{M_r/\alpha_m})^{M_r}/\mathsf{SNR}^{M_r+1}). \tag{5.18}$$

We observe that while the $M_r + 1$ order diversity achieved by conventional diversity combining schemes will decrease as $1/\mathsf{SNR}^{M_r+1}$, the cooperative diversity achieved by the TRS protocol has a decay of $O(\log(\mathsf{SNR}^{M_r/\alpha_m})^{M_r}/\mathsf{SNR}^{M_r+1})$. However, at large SNR the log term becomes insignificant and the diversity order is equal to

$$d = -\lim_{\mathsf{SNR}\to\infty} \frac{\log(\mathrm{BER}_{e2e})}{\log(\mathsf{SNR})} = M_r + 1. \tag{5.19}$$

□

5.4 Results

5.4.1 Benchmark Protocols

In this section we describe two Relay Selection (RS) protocols to which we compare TRS protocol in terms of e2e BER performance.

Relay Selection with the Instantaneous SNR of the $S-R$ Links (RS-inst)

In RS-inst the relay is selected based on the instantaneous $S-R$ and $R-D$ links. The equivalent BER of the branch through relay k is given by

$$\begin{aligned}P_k^{inst}=&P_b(\gamma_{sr,k})(1-P_b(\gamma_{rd,k}))\\&+P_b(\gamma_{rd,k})(1-P_b(\gamma_{sr,k})),\ k=1,\ldots,M_r.\end{aligned}$$

The direct branch from the source to the destination has an equivalent BER of $P_0^{inst}=P_b(\gamma_{sd})$. The destination selects the branch with the minimum equivalent BER. Then, conditioned on the SNR values, the e2e BER is given by

$$\mathbb{P}\{\mathcal{E}_{e2e}^{(RS-inst)}|\gamma_{sr,1},\ldots,\gamma_{sr,M_r},\gamma_{rd,1},\ldots,\gamma_{rd,M_r},\gamma_{sd}\}=\min_{k\in\{0,1,\ldots,M_r\}}\{P_k^{inst}\} \quad (5.20)$$

and the average e2e BER of this protocol is given by

$$\mathrm{BER}_{e2e}^{(RS-inst)}=\mathbb{E}_{\gamma_{sr,1},\ldots,\gamma_{sr,M_r},\gamma_{rd,1},\ldots,\gamma_{rd,M_r},\gamma_{sd}}\left[\min_{k\in\{0,1,\ldots,M_r\}}\{P_k^{inst}\}\right]. \quad (5.21)$$

The RS-inst is very similar to the C-MRC with relay selection introduced in [58]. The only difference is that the scheme in [58] combines the direct signal from the source with one of the relay signals, whereas RS-inst selects either one of the relay signals or the direct signal.

Relay Selection with Average SNR of the $S-R$ Links (RS-avr)

In RC-avr the destination has no knowledge of $\gamma_{sr,i}$ values and the relay selection is based on the average $S-R$ and the instantaneous $R-D$ SNRs. In this case the equivalent BER of the branch through relay k is given by

$$\begin{aligned} P_k^{avr} = & \bar{P}_b(\bar{\gamma}_{sr,k})(1 - P_b(\gamma_{rd,k})) \\ & + P_b(\gamma_{rd,k})(1 - \bar{P}_b(\bar{\gamma}_{sr,k})), \ k = 1, \ldots, M_r \end{aligned}$$

and $P_0^{avr} = P_b(\gamma_{sd})$. Conditioned on the SNR values the e2e BER of RS-avr is equal to

$$\mathbb{P}\{\mathcal{E}_{e2e}^{(RS-avr)} | \gamma_{rd,1}, \ldots, \gamma_{rd,M_r}, \gamma_{sd}\} = \min_{k \in \{0,1,\ldots,M_r\}} \{P_k^{avr}\} \tag{5.22}$$

and the average e2e BER of RS-avr is given by

$$\mathrm{BER}_{e2e}^{(RS-avr)} = \mathbb{E}_{\gamma_{rd,1},\ldots,\gamma_{rd,M_r},\gamma_{sd}} \left[\min_{k \in \{0,1,\ldots,M_r\}} \{P_k^{avr}\} \right]. \tag{5.23}$$

In these two protocols the relay selection is done by the destination only, whereas in threshold based relay selection both relay and the destination contribute to the decision. While RS-inst is the selection version of the C-MRC of [30], RS-avr can be viewed as the selection version of the ML receiver of [29].

5.4.2 Numerical Results

We consider two scenarios for numerical results: symmetric network scenario and linear network scenario. In the symmetric network, all average link SNRs are the same: $\kappa_{sr} = \kappa_{rd} = \kappa_{sd} = 0$ dB. The linear network is based on a group of relays at the mid-point between the source and the destination. In particular, we assume $\kappa_{sr} = \kappa_{rd} = 0$ dB and $\kappa_{sd} = -12$ dB. The e2e BER of TRS is computed from the analytical expression of Section 5.2 and the threshold values for $M_r > 1$ are determined from the numerical minimization of this expression. Fig. 5.2 shows the e2e BER of different protocols in the symmetric network scenario as a function of SNR for $M_r = 1$ relay. For reference, we also plot the BER in the absence of errors in the $S - R$ links. In this figure, TRS and RS-avr perform similarly, while RS-inst

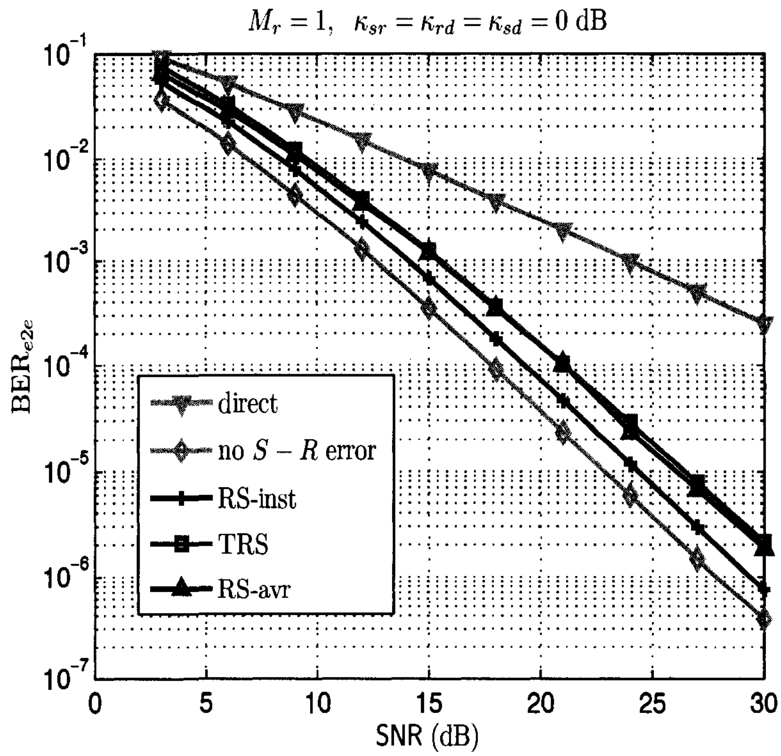

Figure 5.2: The e2e BER for all relaying protocols for $M_r = 1$ relay as a function of SNR in a symmetric network ($\kappa_{sr} = \kappa_{rd} = \kappa_{sd} = 0$ dB). The BER of direct transmission and the BER in the absence of errors in the $S - R_i$ links are also shown as reference curves.

performs slightly better than these two protocols. For $M_r = 1$, all protocols achieve full diversity gain as observed from the slopes of the BER curves.

However, as we increase the number of relays to $M_r = 2$, RS-avr cannot deliver full diversity. In fact, by analyzing RS-avr for M_r values greater than 2, we observed that the diversity order of RS-avr is limited to 2. The TRS achieves full diversity for 2 relays as well, in accordance with our claims in Section 5.3. We conclude that TRS constitutes a good tradeoff between performance and signaling overhead since it performs close to RS-inst with less complexity.

In Fig. 5.4, we show the threshold values used by TRS to minimize the e2e BER in the symmetric network scenario. It is seen that the optimal threshold increases with

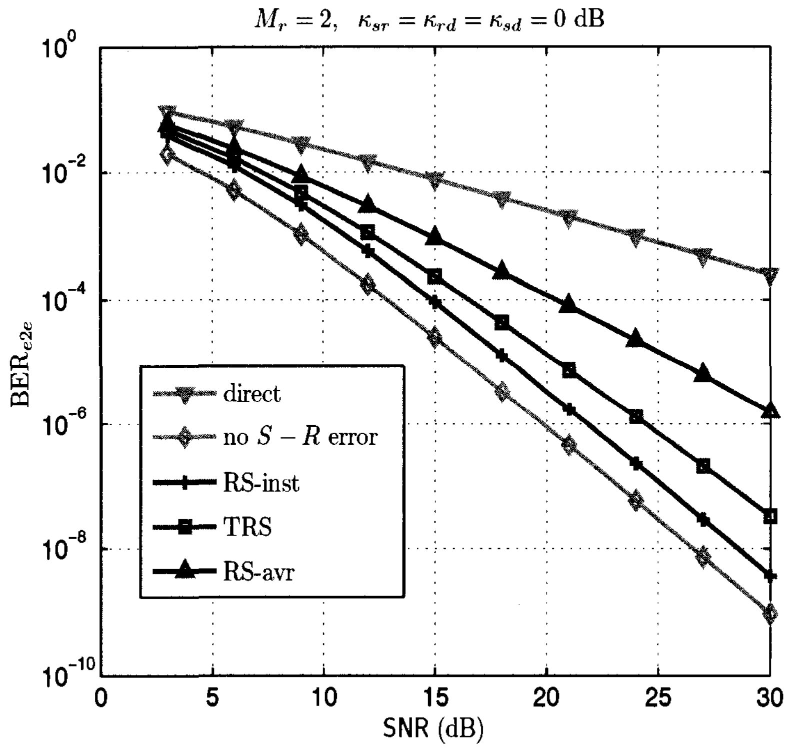

Figure 5.3: The e2e BER for all relaying protocols for $M_r = 2$ relays as a function of SNR in a symmetric network ($\kappa_{sr} = \kappa_{rd} = \kappa_{sd} = 0$ dB).

increasing number of relays. As a function of average SNR, the optimal threshold increases logarithmically. Figs. 5.5 and 5.6 depict the e2e BER for different protocols and the optimal threshold for TRS for the linear network scenario. We see that the conclusions for symmetric scenario are valid for linear scenario as well.

5.5 Conclusions

In this chapter, we have proposed a threshold based relay selection protocol for two hop, multi-relay communication. This protocol requires minimal information about the quality of the source-relay links. We have proposed a threshold function that increases logarithmically with the link SNRs and linearly with the number of relays

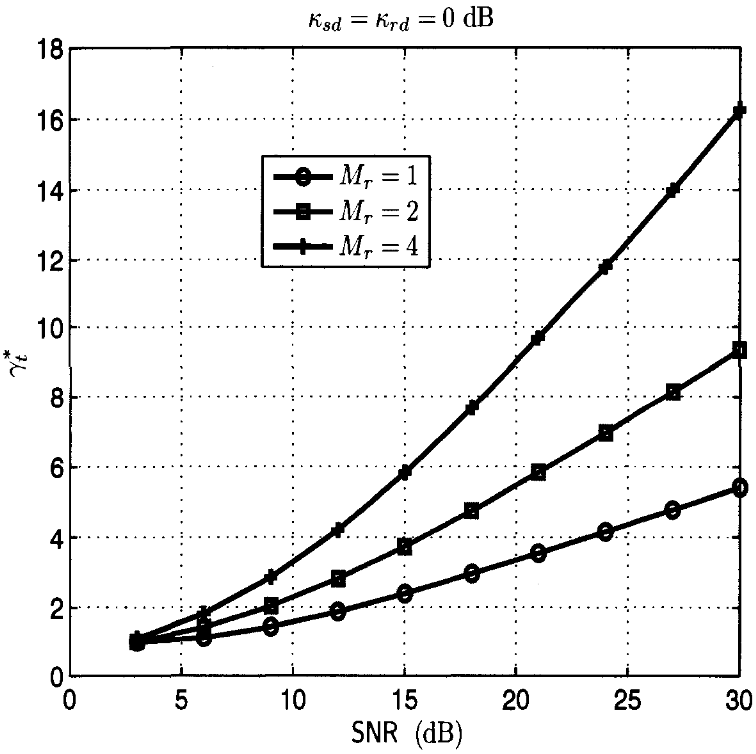

Figure 5.4: The threshold values that minimize the e2e BER of TRS in symmetric networks with different number of relays M_r.

and we have shown that, with a threshold of this form, our protocol achieves full diversity. We have also presented performance results in which the thresholds are determined through numerical optimization and have compared the BER of our protocol to similar protocols found in the literature. We conclude that threshold based relay selection offers an attractive trade-off between performance and signaling overhead as it achieves full diversity without instantaneous $S-R$ SNR knowledge at the destination. Finding optimal thresholds analytically remains as a challenging problem for future work.

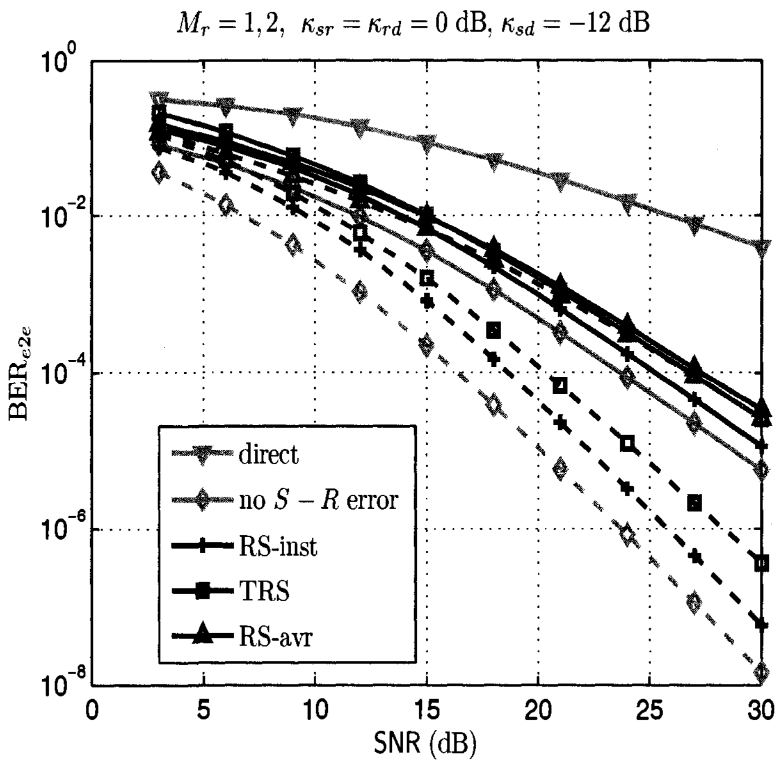

Figure 5.5: The e2e BER for all the protocols with $M_r = 1$ and $M_r = 2$ in a linear network, where $\kappa_{sr} = \kappa_{rd} = 0$ dB, $\kappa_{sd} = -12$ dB. Solid line: $M_r = 1$, dashed line: $M_r = 2$.

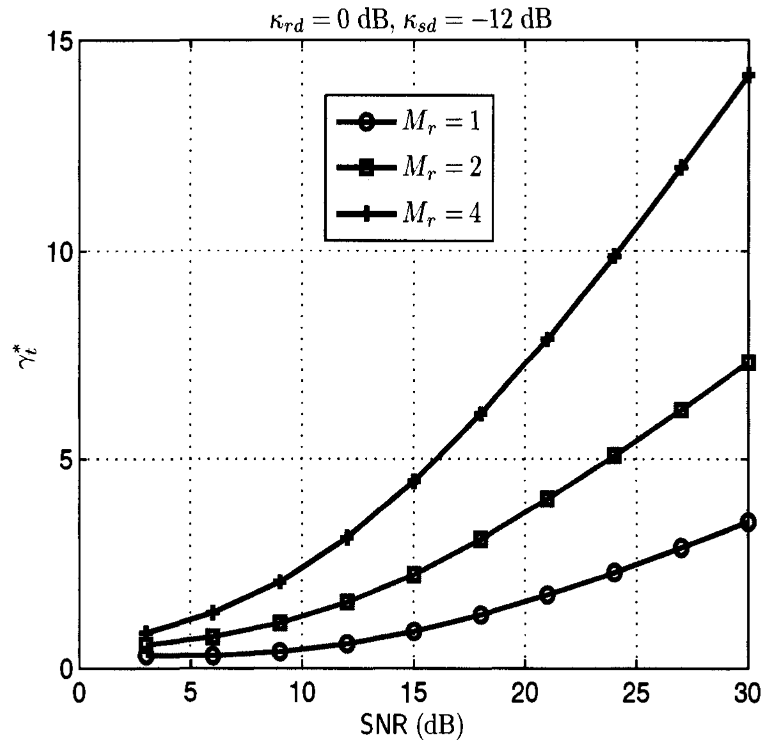

Figure 5.6: The threshold values that minimize the e2e BER in a linear network ($\kappa_{sr} = \kappa_{rd} = 0$ dB, $\kappa_{sd} = -12$ dB) as function of SNR with different number of relays M_r.

Chapter 6

Cooperative Digital Relaying in Wireless Ad-hoc Networks

In the previous chapters, we considered simple and fixed network scenarios, in which average link SNRs are deterministic parameters. These studies conducted for deterministic topologies provide useful understanding of different aspects of diversity relaying. However, in wireless ad hoc networks, the network topology is often random and time-varying. While for some source-destination pairs there might be many relays at favorable locations, there might also exist pairs which can find no relays at all. Thus, the performance obtained in deterministic topologies is not necessarily a good indicator of the network-wide gain from diversity relaying in wireless networks. In this chapter, we incorporate the randomness in node positions into the problem formulation.

Often the ultimate goal in an ad-hoc network is to guarantee connectivity, i.e., maintaining the ability to send a data packet from any source node to any destination node, even when certain links undergo deep fading. Ideally, routing in such a network requires complete knowledge of the state of the network. However, in practice, even medium size networks do not have sufficient resources to discover all possible paths in a time-varying environment in presence of mobility induced fading. Hence, we focus on a more modest two-hop relaying protocol.

We note that diversity relaying in random topologies is closely related with the relay selection problem considered in Chapter 5. In a random topology, in most cases, there will be multiple relays in the vicinity of a source-destination pair. Although the reliability can be increased by using all of these relays, bandwidth and delay constraints limit the number of time slots allocated for retransmissions.

In this chapter, we propose a practical two-hop diversity relaying protocol that can be implemented as an "add-on diversity relaying feature" along with an existing routing protocol in order to improve the performance of each hop. For instance, the source and destination defined in the protocol could constitute one hop of a longer route, which has been determined by a higher layer protocol. Our protocol aims to take advantage of other nodes in the vicinity in an opportunistic fashion.

We assume that the maximum number of relays that can be used for each packet is limited by M_r, which represents bandwidth and delay constraints. Unlike in Chapters 3-5, in this chapter, to simplify the problem, we consider ideal coding. Hence, the nodes that receive the packet with an SNR higher than a minimum value can decode it correctly. Such nodes are called reliable relays. Due to ideal channel coding assumption, error propagation does not occur. First the source transmits a packet, and then selects M_r reliable relays. In general, the relay selection can be done based on the instantaneous or average SNRs of the relays to the destination. In order to limit the feedback from the destination, in this problem we assume relay selection based on average SNR to the destination. Hence, our protocol only requires that each node in the vicinity of the source knows its average SNR to the destination.

Assuming that the relay nodes are distributed according to 2-dimensional Poisson point process, we analytically study the performance of the protocol as a function of node density, fading parameters and node transmit powers. We consider both maximal ratio combining and selection combining at the destination. Our performance metric is e2e outage probability for a given target SNR. In the relaying protocols studied in the rest of this thesis, the second phase takes place even if the destination receives the transmission in the first phase correctly. A widely known technique to improve the packet delivery ratio of data networks with little bandwidth expansion is "automatic repeat request" (ARQ). Several variations of the basic concept have been proposed and their performance has been studied [59–61]. However, ARQ is not very helpful when the fading is slow. When this is the case, applying both ARQ and cooperative diversity could be very effective. In this chapter, we also propose and analyze an ARQ-augmented version of the basic protocol, which we call Relay-Assisted ARQ (RARQ) protocol.

In the literature, few studies consider multihop relaying in random networks [62–64]. In [62] Zorzi and Rao analyze a greedy geographic forwarding algorithm for a multihop network, where a relay for the next hop is chosen "post transmission" among the nodes that receive the data packet correctly. Their criterion for selecting the next relay is having the shortest distance to the destination. The proposed scheme assumes that each node knows its own location and the location of the destination is included in the "header" of the packet. In [65] the same authors describe several possible avoidance/contention resolution schemes by which nodes acknowledge reception, and a single node, the one closest to the destination, is chosen to serve as the next relay. The authors derive upper and lower bounds on the average number of hops the protocol requires when the destination is at a distance D from the source. However, Zorzi and Rao do not consider fading and diversity.

In [63] Khandani et al. derive the routing metric that minimizes end-to-end outage in a multihop network in the presence of Rayleigh fading. This approach requires that the source knows the location of all the nodes in the network. The path is chosen as the best on average based on the node locations. The same work also considers diversity enabled routing under the same assumptions.

In [64] Biswas and Morris propose a protocol called opportunistic multihop routing protocol. This protocol takes advantage of the broadcast nature of wireless transmissions by selecting the "best" relay among the nodes that receive the data packet correctly. The selection criteria is the cost of delivering the packet from each node to the destination rather than the geographical distance. As the cost metric they use the number of hops from the node to the destination along the best route in traditional routing, where the packets are sent along pre-computed routes that are selected to minimize the estimated number of transmissions.

Most published work on diversity relaying, including the rest of the chapters of this thesis, consider optimistic scenarios, where, for example, all the relays are in the midpoint between the source and the destination. Some of the exceptions are [66], [67] and [68]. In [66] Zhao and Valenti propose a multihop protocol they call Hybrid ARq-Based Intra-cluster GEographically-informed Relaying (HARBINGER), which combines Hybrid ARQ and cooperative diversity. As a packet propagates in the network, each transmitting node uses an independent code to encode the packet. Since multiple independently coded replicas of the source data are received, mutual information rather than signal power is accumulated. A node becomes a reliable relay for the packet as soon as it accumulates sufficient mutual information to decode the packet reliably.

In [67] Song and Hatzinakos propose a cooperative relaying protocol called Cooperative Transmission Protocol for Sensor Networks (CTP-SN). They analyze the performance of the protocol in a network where nodes are distributed in two dimensional space according to homogeneous Poisson point process. Unlike our protocol, CTP-SN does not use Channel State Information (CSI) at the transmitting nodes. In CTP-SN an arbitrary region is chosen, and all the nodes in the region that received the packet from the source retransmit to the destination using a space-time code. The authors show that the outage probability decreases exponentially with the node density. Our protocol does not limit the relay locations; any node that receives the source packet successfully can possibly serve as a relay. The authors also describe a variant of the CTP-SN protocol, which includes feedback from the destination. However, this variant requires that all relays can hear the destination, an assumption that is hard to guarantee in practice. The CTP-SN protocol further assumes that every reliable relay knows the relay region associated with each possible pair of source and destination in its neighborhood. This is a more demanding requirement than knowing the (local) mean channel gain to any neighboring node, which is what we assume in this chapter.

Bletsas et al. studied path selection in two hop relaying [68]. They assume that the instantaneous CSI of all source-relay and relay-destination links are available at the source and show that the path selection can achieve the same asymptotic performance (diversity multiplexing trade-off) as the distributed space time coding of [35] with reduced complexity at the destination. They also design a protocol to implement path selection with reduced overhead. Another related work on relay selection is in the context of coded cooperation [69]. In this paper, Lin et al. assume that there exists a "partner" for each source node, which is a pre-selected node that serves as relay for a particular destination. The paper derives the criteria for choosing a particular node as a partner over other existing nodes. End-to-end performance between the source and destination depends consequently on the reliability of the channel between the source and its partner. Our approach differs from this work since we select a relay from those nodes that have actually received correctly. Therefore, different packets may be relayed by different nodes and diversity transmission may take place as long as at least one other node has received the source transmission correctly.

The rest of this chapter is organized as follows. The system model and the relaying protocols are described in Section 6.1 and Section 6.2, respectively. Outage probabilities of the direct transmission and the basic relaying protocol are derived in Section 6.3. In Section 6.4 we discuss some enhancements to the basic relaying protocol including ARQ. Numerical results are presented in Section 6.5. Findings of the chapter are summarized in Section 6.6.

6.1 System Model

A system as shown in Fig. 6.1 is considered. A source node S communicates with a destination node D, and the nodes in the vicinity of S and D can serve as relays.

6.1.1 Node Location Model

We assume a very general node location model. Nodes are distributed in two dimensional space according to homogeneous Poisson point process. A homogeneous Poisson point process is fully described by its density, λ (nodes/area). Some important properties of this process are as follows:

- The number of nodes in a region $\mathcal{A}$ is Poisson distributed random variable with mean $\lambda \times \text{area}(\mathcal{A})$, i.e., $N(\mathcal{A}) \sim Poiss(\lambda \times \text{area}(\mathcal{A}))$. That is,

$$\mathbb{P}\{N(\mathcal{A}) = k\} = e^{-\lambda \times \text{area}(\mathcal{A})} \frac{(\lambda \times \text{area}(\mathcal{A}))^k}{k!}.$$

- The number of nodes in two disjoint regions are independent.
- Given the number of nodes in a region $\mathcal{A}$ the location of each node follows a uniform probability distribution in $\mathcal{A}$.

6.1.2 Propagation Model

Our propagation model includes three components: distance related loss, lognormal shadowing and Rayleigh fading. The SNR at node j due to a transmission from node

i, which is located d_{ij} units away, is given by

$$\gamma_{ij} = \frac{K_c \mathcal{P}_T}{d_{ij}^v \mathcal{P}_N} 10^{Z_{ij}/10} X_{ij}^2, \tag{6.1}$$

where K_c represents all the constant gains such as antenna gains, $\mathcal{P}_T$ is the transmit power, $\mathcal{P}_N$ is the noise power and v is the path loss exponent. We assume that the antennas are omnidirectional and K_c and $\mathcal{P}_N$ are common for all nodes.

Fading components of all the channel gains, i.e., X_{ij} and Z_{ij} terms are independent and identically distributed from link to link. The shadowing component Z_{ij} is a Gaussian random variable with zero mean and variance equal to σ^2, and the Rayleigh fading component X_{ij}^2 is an exponential random variable with unit mean. We assume that the channel coherence time is sufficiently long, such that the channel does not change during the delivery time of a packet, which is at most two time slots.

We assume that all the transmissions are at a fixed rate R (in bits per transmission per Hertz) and all the nodes use an ideal channel coding which is designed for rate R and achieves the Shannon capacity. The codeword length L is assumed to be large enough so that a decoding error occurs if and only if $\log_2(1+\gamma_{ij}) < R$. That is, the transmission by node i is successfully decoded by node j, if and only if the received SNR γ_{ij} is larger than a given target value γ_{tr}, which is equal to $\gamma_{tr} = 2^R - 1$. We define $r_N(\mathcal{P}_T)$ as the transmission range of a node transmitting with power $\mathcal{P}_T$ in the absence of fading:

$$r_N(\mathcal{P}_T) = \left(K_c \frac{\mathcal{P}_T}{\mathcal{P}_N \gamma_{tr}} \right)^{1/v},$$

Then, the event of successful transmission, i.e., $\{\gamma_{ij} > \gamma_{tr}\}$, is equivalent to the event that

$$\{d_{ij} < r_N(\mathcal{P}_T) X_{ij}^{2/v} e^{hZ_{ij}/v}\}, \tag{6.2}$$

where $h = \ln(10)/10$.

The transmit power of the source and the relays are denoted by $\mathcal{P}_s$ and $\mathcal{P}_r$, respectively. Corresponding transmission ranges in the absence of fading are denoted by

r_{Ns} and r_{Nr}, i.e., $r_{Ns} = r_N(\mathcal{P}_s)$ and $r_{Nr} = r_N(\mathcal{P}_r)$. The expectation of γ_{ij} is denoted by $\bar{\gamma}_{ij}$. $\bar{\gamma}_{ij}$ normalized by the target SNR γ_{tr} is denoted by g_{ij}, which is equal to

$$g_{ij} = \frac{\bar{\gamma}_{ij}}{\gamma_{tr}} = \left(\frac{r_N(\mathcal{P}_T)}{d_{ij}}\right)^v \mathbb{E}[X_{ij}^2] = \begin{cases} \left(\frac{r_{Ns}}{d_{ij}}\right)^v, \text{ if node } i \text{ is a source node;} \\ \left(\frac{r_{Nr}}{d_{ij}}\right)^v, \text{ if node } i \text{ is a relay node.} \end{cases} \tag{6.3}$$

6.2 Description of the Basic Relaying Protocol

The protocol has two phases. Fig. 6.1 illustrates the phases of the relaying protocol. In phase I, S transmits a packet with transmit power $\mathcal{P}_s$, specifying the intended destination. We identify useful relays based on the following criterion: to be able to act as relay, a node must decode the transmission of S correctly based on the criterion given in (6.2). Hence, our protocol falls in the class of selective relaying protocols [4]. The nodes that satisfy this constraint are called *reliable relays*. Each reliable relay sends a short acknowledgement message (ACK) to S, which also includes additional information related to the propagation channel between the relay and D. Based on all the information collected from the reliable relays, S decides which relays should relay the packet.

In scenarios where each relay is able to maintain the instantaneous gain of the channel between itself and D, S can pick the relay with the largest gain as in [57]. However, in the present work we assume that nodes can provide only local average SNRs, which do reflect the distance dependent loss and shadowing, but cannot track Rayleigh fading which changes at a faster rate. We do not require that every node in the neighborhood of S to readily provide the instantaneous channel gain to any possible destination that other nodes in its neighborhood might wish to send packets to. This feature allows the protocol to perform also in mobile scenarios.

The source node S can select the relays to participate based on the information

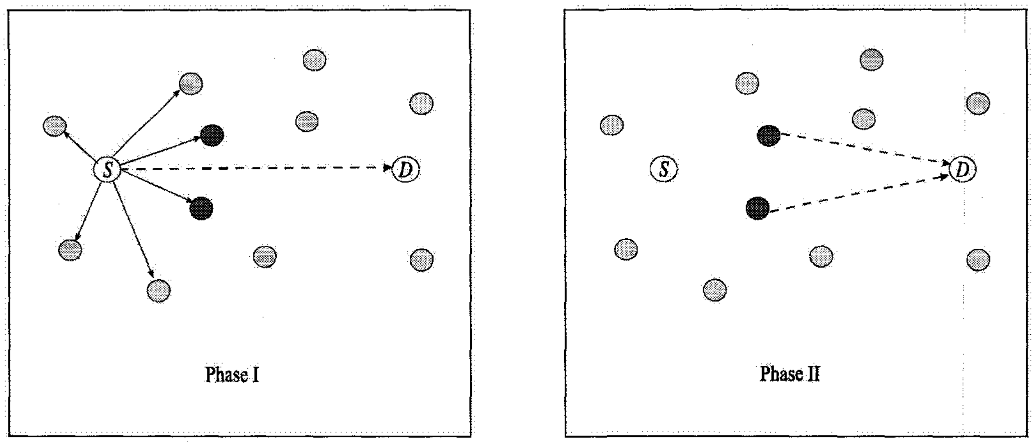

Figure 6.1: The two phases of the relaying protocol for $M_r = 2$. In phase I, the successful transmissions are shown by solid lines. The transmissions that are combined by D are shown by dotted lines.

provided to S, the direct channel between S and D, and, possibly on resource conservation considerations that we do not discuss here. In this chapter, we assume that among all reliable relays with respect to S those with the best average channel gains to D are selected as relays. The maximum number of relays to be selected is limited by M_r. In phase II the selected relays are informed of the decision of S and they transmit to D one by one, in different time slots each using transmit power $\mathcal{P}_r$. Then, D combines all the received signals using either SC or MRC.

6.3 Outage Probability Analysis

6.3.1 Outage Probability of the Direct Transmission

We denote the outage probability of the direct transmission as $P_{o,1}$. The probability that the single hop transmission is not successful conditioned on the average SNR is equal to

$$\mathbb{P}\{\gamma_{sd} < \gamma_{tr} | \bar{\gamma}_{sd}\} = 1 - \exp\left(-\gamma_{tr}/\bar{\gamma}_{sd}\right) = 1 - \exp(-1/g_{sd}). \tag{6.4}$$

Let the distance between S and D be denoted by d_{sd}. Then, the normalized received SNR at D is given by

$$g_{sd} = \left(\frac{r_{Ns}}{d_{sd}}\right)^{\upsilon} e^{hZ_{sd}}. \tag{6.5}$$

Averaging over g_{sd} we obtain

$$\begin{aligned} P_{o,1} &= \mathbb{P}\{\gamma_{sd} < \gamma_{tr}\} = \mathbb{E}_{Z_{sd}}\left[1 - \exp\left(-1/\left((r_{Ns}/d_{sd})^{\upsilon} e^{hZ_{sd}}\right)\right)\right] \\ &= 1 - \int_{-\infty}^{\infty} \frac{1}{\sqrt{2\pi\sigma^2}} e^{-z^2/(2\sigma^2)} \exp(-e^{-hz}(r_{Ns}/d_{sd})^{-\upsilon}) \mathrm{d}z. \end{aligned} \tag{6.6}$$

6.3.2 Outage Probability of the Basic Relaying Protocol

In this section we analyze the outage performance of the relaying protocol described in Section 6.2 for given r_{Ns}, r_{Nr}, M_r, λ and propagation parameters σ and υ. The protocol allows up to M_r relays participate when possible. If the number of available relays N_r is smaller than M_r, then only N_r relays retransmit. In the rest of this section, we first the distribution of various random variables that will be required to derive the outage probability of the basic relaying protocol.

Number of Reliable Relays

To find the probability mass function (PMF) of the number of reliable relays, we make use of a well-known result on Poisson processes [70], which is also used in [71].

Theorem 6.1. *Let the number of objects N in a given region be a Poisson random variable with mean μ. Let ε_i be the event that object i has a certain property. If all ε_i's are independent events and have the same probability of occurrence $p = \mathbb{P}\{\varepsilon_i | N = n\}$ when conditioned on $\{N = n\}$ for all n, then the number of objects out of N objects having the defined property is also Poisson random variable with mean $p\mu$.*

Let $B(a, b; r)$ denote a disc with radius r centered at point (a, b). Suppose that the objects are the nodes in $B(0, 0; r_0)$ and the desired property is having a reliable link to S at $(0, 0)$. Then the number of reliable relays within r_0 of S are

$$N_r(B(0,0;r_0)) \sim Poiss(\mu_r(r_0)), \tag{6.7}$$

where

$$\mu_r(r_0) = \lambda\pi r_0^2 p_r, \tag{6.8}$$

and p_r is the probability that an arbitrary node in $B(0, 0; r_0)$ is a reliable relay.

All the nodes in $B(0, 0; r_0)$ are randomly and uniformly distributed in the region. Hence, d_{sr}, the distance from an arbitrary node to S at $(0, 0)$ has PDF $p_{d_{sr}}(r) = 2r/r_0^2$, $0 \leq r \leq r_0$. Then, we calculate $r_0^2 p_r$ and take its limit as $r_0 \to \infty$, covering the whole plane.

$$\begin{aligned}
\lim_{r_0^2\to\infty} r_0^2\, p_r =& \lim_{r_0^2\to\infty} r_0^2\, \mathbb{P}\{d_{sr} < r_{Ns} X^{2/v} e^{hZ/v}\} \\
=& \lim_{r_0^2\to\infty} r_0^2 \int_{-\infty}^{\infty} p_Z(z) \int_0^{\infty} p_X(x) \int_0^{\min(r_0, r_{Ns}x^{2/v}e^{hZ/v})} \frac{2r}{r_0^2} \mathrm{d}r\, \mathrm{d}x \mathrm{d}z \\
=& \lim_{r_0^2\to\infty} \int_{-\infty}^{\infty} p_Z(z) \int_0^{\infty} p_X(x) \min(r_0^2, r_{Ns}^2 x^{4/v} e^{2hZ/v}) \mathrm{d}x \mathrm{d}z \\
=& r_{Ns}^2\, \mathbb{E}_X[X^{4/v}]\, \mathbb{E}_Z[e^{2hZ/v}].
\end{aligned} \tag{6.9}$$

As derived in [71], $\mathbb{E}_X[X^{4/v}] = \Gamma(1+2/v)$ for Rayleigh distributed X and $\mathbb{E}_Z[e^{2hZ/v}] = \exp(2\varrho^2)$ for $Z \sim \mathcal{N}(0, \sigma^2)$, where

$$\varrho = \frac{h\sigma}{v},$$

and the gamma function $\Gamma(.)$ is defined as

$$\Gamma(x) = \int_0^{\infty} t^{x-1} e^{-t} \mathrm{d}t.$$

Then, the average number of reliable relays in the entire plane is found by substituting (6.9) into (6.8):

$$\mu_r = \lim_{r_0\to\infty} \mu_r(r_0) = \lambda\pi r_{Ns}^2 \Gamma\left(1 + \frac{2}{v}\right) \exp\left(2\varrho^2\right). \tag{6.10}$$

The pmf of the number of reliable relays of S is

$$N_r \sim Poiss\left(\lambda\pi r_{Ns}^2\Gamma\left(1+2/v\right)\exp\left(2\varrho^2\right)\right). \tag{6.11}$$

Distance of a Reliable Relay to the Source

Let d_{sr} denote the distance of an arbitrary node in $B(0,0;r_0)$ to S and $\mathcal{A}(r_0)$ denote the event that this node has a direct connection with S. In Section 9A of [71], PDF of d_{sr} given $\mathcal{A}(r_0)$ as $r_0 \to \infty$ is calculated (eqn (47)):

$$\begin{aligned} p_{d_{sr}|\mathcal{A}}(r) &= \frac{2r\left\{1-\mathbb{E}_Z\left[F_X\left(\sqrt{e^{-hZ}(r/r_{Ns})^v}\right)\right]\right\}}{[r_{Ns}\exp(\varrho^2)]^2\,\mathbb{E}[X^{4/v}]} \\ &= \frac{2r\,\mathbb{E}_Z[\exp\left(-(r/r_{Ns})^v e^{-hZ}\right)]}{[r_{Ns}\exp(\varrho^2)]^2\,\Gamma(1+2/v)}. \end{aligned} \tag{6.12}$$

Distance of a Reliable Relay to the Destination

Consider an arbitrary reliable relay, node i, which has connection to S. Let $d_{rd,i}$ denote the distance of this node to D at $(d_{sd},0)$. Since the locations of such nodes are i.i.d., so are their distances to D. Hence, we drop the relay index and denote the common PDF of the distances of reliable relays to D as $p_{d_{rd}}(l)$. The CDF of d_{rd} can be calculated from

$$F_{d_{rd}}(l) = \int_0^\infty \mathbb{P}\{d_{rd} \le l \,|\, d_{sr} = r\} p_{d_{sr}|\mathcal{A}}(r)\mathrm{d}r. \tag{6.13}$$

We first calculate the probability that the distance of a reliable relay to D is below l given that its distance from S is equal to r. Since the angular distribution of all reliable relays around S is uniform in $[0,2\pi]$, such nodes are located uniformly on the circle $C(0,0;r)$. If the circle $C(0,0;r)$ and the disk $B(d_{sd},0;l)$ intersect partially, i.e., $|l-d_{sd}| < r < l+d_{sd}$, then the probability that $d_{rd} \le l$ is equal to the fraction of the length of $C(0,0;r)$ arc that is within $B(d_{sd},0;l)$. In the illustration of Fig. 6.2, this

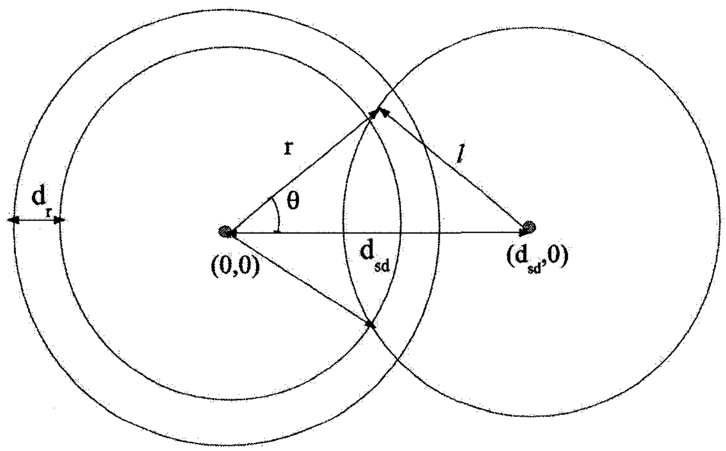

Figure 6.2: Illustration for the calculation of $F_{d_{rd}|d_{sr}}(l|r)$ for $|l - d_{sd}| < r < |l + d_{sd}|$

fraction is equal to θ/π. Using the law of cosines, we can express θ as

$$\theta = \arccos\left(\frac{d_{sd}^2 - l^2 + r^2}{2d_{sd}r}\right).$$

If $l > r + d_{sd}$, then the circle is within the disk and all the points on the circle are within l of the point $(d_{sd}, 0)$. However, if $r > l - d_{sd}$, the disk is inside the circle and none of the nodes on the circle are closer to d_{sd} than l.

Hence, we obtain the conditional CDF $F_{d_{rd}|d_{sr}}(l|r)$ as

$$F_{d_{rd}|d_{sr}}(l|r)=\begin{cases} \frac{1}{\pi}\arccos\left(\frac{d_{sd}^2-l^2+r^2}{2d_{sd}r}\right), & |l - d_{sd}| < r < l + d_{sd}; \\ 1, & 0 < r < l - d_{sd}; \\ 0, & \text{otherwise,} \end{cases}$$

where $l, d_{sd}, r > 0$. Then, averaging over d_{sr}, the CDF of d_{rd} is obtained from

$$\begin{aligned} F_{d_{rd}}(l) =& \int_0^{\infty} F_{d_{rd}|d_{sr}}(l|r) p_{d_{sr}|\mathcal{A}}(r) \mathrm{d}r \\ =& \int_0^{\max\{0, l-d_{sd}\}} p_{d_{sr}|\mathcal{A}}(r) \mathrm{d}r \\ &+ \frac{1}{\pi} \int_{|l-d_{sd}|}^{l+d_{sd}} \arccos\left(\frac{d_{sd}^2 - l^2 + r^2}{2 d_{sd} r}\right) p_{d_{sr}|\mathcal{A}}(r) \mathrm{d}r. \end{aligned} \tag{6.14}$$

We substitute (6.12) in the first integral, use the change of variable $u = r/r_{Ns}$ and obtain

$$\begin{aligned} \int_0^{\max\{0, l-d_{sd}\}} & p_{d_{sr}|\mathcal{A}}(r) \mathrm{d}r = \frac{2}{[\exp(\varrho^2)]^2 \Gamma(1 + 2/v)} \\ \times \int_0^{\max\{0, l-d_{sd}\}} & \frac{r}{r_{Ns}^2} \mathbb{E}_Z \left[\exp\left(-(r/r_{Ns})^v e^{-hZ}\right)\right] \mathrm{d}r \\ = \frac{2}{[\exp(\varrho^2)]^2 \Gamma(1 + 2/v)} & \int_0^{\max\{0, l/r_{Ns} - d_{sd}/r_{Ns}\}} u \mathbb{E}_Z \left[\exp\left(-u^v e^{-hZ}\right)\right] \mathrm{d}u. \end{aligned} \tag{6.15}$$

For the second integral of (6.14), again using $u = r/r_{Ns}$, we can express the integrand in terms of d_{sd}/r_{Ns}, l/r_{Ns} and u:

$$\begin{aligned} \int_{|l-d_{sd}|}^{l+d_{sd}} \arccos\left(\frac{d_{sd}^2 - l^2 + r^2}{2 d_{sd} r}\right) p_{d_{sr}|\mathcal{A}}(r) \mathrm{d}r = \frac{2}{[\exp(\varrho^2)]^2 \Gamma(1 + 2/v)} \\ \times \int_{|l/r_{Ns} - d_{sd}/r_{Ns}|}^{l/r_{Ns} + d_{sd}/r_{Ns}} \left\{ u \mathbb{E}_Z \left[\exp\left(-u^v e^{-hZ}\right)\right] \arccos\left(\frac{(d_{sd}/r_{Ns})^2 - (l/r_{Ns})^2 + u^2}{2 (d_{sd}/r_{Ns}) u}\right) \mathrm{d}u \right\}. \end{aligned} \tag{6.16}$$

Since both (6.15) and (6.16) are functions of l/r_{Ns}, d/r_{Ns}, v and σ only, we denote $F_{d_{rd}}(l)$ as

$$F_{d_{rd}}(l) = h(l/r_{Ns}, d_{sd}/r_{Ns}, v, \sigma). \tag{6.17}$$

Distribution of Average SNR Received at the Destination from an Arbitrary Reliable Relay

Relay selection among the reliable relays is based on the average SNR determined by the distance related loss and the lognormal shadowing. Let $\gamma_{rd,a}$ denote the instantaneous SNR at D as a result of the transmission of an arbitrary reliable relay node.

Normalized by the target SNR, $\gamma_{rd,a}$ is given by

$$\frac{\gamma_{rd,a}}{\gamma_{tr}} = \left(\frac{r_{Nr}}{d_{rd}}\right)^{v} e^{hZ'}(X')^2,$$

where Z' and X' represent the lognormal and Rayleigh fading between the reliable relay node and D. Since $(X')^2$ is exponential distributed with mean equal to 1, locally averaged (over the small scale fading X') and normalized SNR $g_{rd,a}$ is given by

$$g_{rd,a} = \mathbb{E}_{X'}\left[\frac{\gamma}{\gamma_{tr}}\right] = \left(\frac{r_{Nr}}{d_{rd}}\right)^{v} e^{hZ'}.$$

Then the CDF of $g_{rd,a}$ is given by

$$F_{g_{rd,a}}(g) = 1 - \mathbb{E}_{Z'}\left[F_{d_{rd}}\left(r_{Nr}e^{hZ'/v}g^{-1/v}\right)\right] \tag{6.18}$$

$$= 1 - \frac{2}{[\exp(\varrho^2)]^2\,\Gamma(1+2/v)} \int_{-\infty}^{\infty} p_{Z'}(z')\Bigg\{$$

$$\int_0^{\max\{0,(\zeta\exp(hz')/g)^{1/v}-\tilde{d}_{sd}\}} u\mathbb{E}_Z\left[\exp\left(-u^v e^{-hZ}\right)\right] du$$

$$+ \int_{|(\zeta\exp(hz')/g)^{1/v}-\tilde{d}_{sd}|}^{(\zeta\exp(hz')/g)^{1/v}+\tilde{d}_{sd}} \Bigg(u\mathbb{E}_Z\left[\exp\left(-u^v e^{-hZ}\right)\right]$$

$$\times\frac{1}{\pi}\arccos\left(\frac{\tilde{d}_{sd}^2 - (\zeta\exp(hz')/g)^{2/v} + u^2}{2\tilde{d}_{sd}u}\right) du\Bigg)\Bigg\}dz'$$

$$= 1 - \frac{2}{[\exp(\varrho^2)]^2\,\Gamma(1+2/v)} \int_{-\infty}^{\infty}\int_{-\infty}^{\infty} p_{Z'}(z')p_Z(z)\Bigg\{$$

$$\int_0^{\max\{0,(\zeta\exp(hz')/g)^{1/v}-\tilde{d}_{sd}\}} u\exp\left(-u^v e^{-hz}\right) du$$

$$+ \int_{|(\zeta\exp(hz')/g)^{1/v}-\tilde{d}_{sd}|}^{(\zeta\exp(hz')/g)^{1/v}+\tilde{d}_{sd}} \Bigg(u\exp\left(-u^v e^{-hz}\right)$$

$$\times\frac{1}{\pi}\arccos\left(\frac{\tilde{d}_{sd}^{\,2} - (\zeta\exp(hz')/g)^{2/v} + u^2}{2\tilde{d}_{sd}u}\right) du\Bigg)\Bigg\}dzdz', \tag{6.19}$$

where we defined ζ and $\tilde{d}_{sd}$ as

$$\zeta = (r_{Nr}/r_{Ns})^v \quad \text{and} \quad \tilde{d}_{sd} = d_{sd}/r_{Ns}.$$

In Fig. 6.3, we plot $F_{g_{rd,a}}(g)$ for different d_{sd} values.

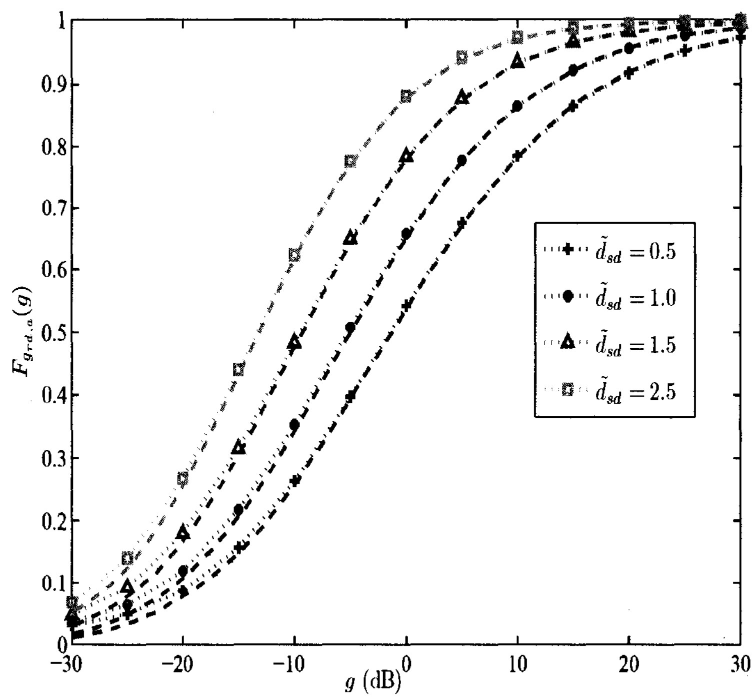

Figure 6.3: The CDF of $g_{rd,a}$ $(F_{g_{rd,a}}(g))$, the average normalized SNR of an arbitrary reliable relay to D. $\upsilon = 4$, $\sigma = 8$, $r_{Ns} = r_{Nr}$ $(\zeta = 1)$. Dotted curves with markers are obtained from (6.19) and dashed curves are obtained through Monte Carlo simulations.

Distribution of the Averaged Normalized SNR of the Best M_r Out of k Reliable Relays

Let us consider the case where we have exactly k reliable relays ($k \geq M_r$) and we choose M_r relays with the largest average SNR. We denote the average SNR of the relays as $\{g_{rd(1)}, g_{rd(2)}, \ldots, g_{rd(M_r)}\}$ where $g_{rd(j)}$ is the j-th largest. The joint PDF of M_r largest of k i.i.d. random variables is given in [72] (equation (9))

$$\begin{aligned} & p^{(k)}_{g_{rd(1)},g_{rd(2)},\ldots,g_{rd(M_r)}}(g_1, g_2, \ldots g_{M_r}) \\ &= \frac{k!}{(k-M_r)!} p_{g_{rd,a}}(g_1) p_{g_{rd,a}}(g_2), \ldots, p_{g_{rd,a}}(g_{M_r}) (F_{g_{rd,a}}(g_{M_r}))^{k-M_r}, \end{aligned} \tag{6.20}$$

where $g_1 > g_2 > \ldots > g_{M_r}$. Note that the above distribution is a function of k.

Average SNR of the Best M_r Reliable Relays Given That $N_r \geq M_r$

The pmf of the number of the reliable relays given there are at least M_r reliable relays is given by:

$$\mathbb{P}\{N_r = k | N_r \geq M_r\} = \frac{\mathbb{P}\{N_r = k, N_r \geq M_r\}}{\mathbb{P}\{N_r \geq M_r\}} = \frac{1}{\mathbb{P}\{N_r \geq M_r\}} \mathbb{P}\{N_r = k\},$$

where $k \geq M_r$.

When we average (6.20) over N_r the number of reliable relays, we obtain:

$$\begin{aligned} p_{g_{rd(1)},g_{rd(2)},\ldots,g_{rd(M_r)}}(g_1, g_2, \ldots g_{M_r}) &= \frac{1}{\mathbb{P}\{N_r \geq M_r\}} \sum_{k=M_r}^{\infty} \Bigg\{ \mathbb{P}\{N_r = k\} \\ & \quad \times p^{(k)}_{g_{rd(1)},g_{rd(2)},\ldots,g_{rd(M_r)}}(g_1, g_2, \ldots g_{M_r}) \Bigg\} \\ &= \frac{1}{\mathbb{P}\{N_r \geq M_r\}} \left\{ \prod_{i=1}^{M_r} p_{g_{rd,a}}(g_i) \right\} \\ & \quad \times \sum_{k=M_r}^{\infty} \exp(-\mu_r) \frac{\mu_r^k}{k!} \frac{k!}{(k-M_r)!} (F_{g_{rd,a}}(g_{M_r}))^{k-M_r} \\ &= \frac{\mu_r^{M_r}}{\mathbb{P}\{N_r \geq M_r\}} \exp\left(-\mu_r(1 - F_{g_{rd,a}}(g_{M_r}))\right) \left\{ \prod_{i=1}^{M_r} p_{g_{rd,a}}(g_i) \right\}, \end{aligned} \tag{6.21}$$

where $F_{g_{rd,a}}(g)$ is given by (6.19).

The derivation of CDF for general M_r seems to be cumbersome, we derive it only for $M_r = 1$ and $M_r = 2$. Substituting $M_r = 1$ in (6.21), we obtain

$$p_{g_{rd(1)}}(g) = \frac{\mu_r}{1 - \exp(-\mu_r)} \exp\left(-\mu_r(1 - F_{g_{rd,a}}(g))\right) p_{g_{rd,a}}(g). \tag{6.22}$$

By integrating the PDF, we obtain the CDF of $g_{rd(1)}$

$$\begin{aligned}
F_{g_{rd(1)}}(g) &= \frac{1}{1 - \exp(-\mu_r)} \int_0^g \mu_r \exp(-\mu_r(1 - F_{g_{rd,a}}(x))) p_{g_{rd,a}}(x) \mathrm{d}x \\
&= \frac{1}{1 - \exp(-\mu_r)} \int_1^{(1 - F_{g_{rd,a}}(g))} -\mu_r \exp(-\mu_r u) \mathrm{d}u \\
&= \frac{1 - \exp(\mu_r F_{g_{rd,a}}(g))}{1 - \exp(\mu_r)},
\end{aligned} \tag{6.23}$$

where we use the change of variables $u = 1 - F_{g_{rd,a}}(x)$ for the integration. Fig. 6.4 shows $F_{g_{rd(1)}}$ for different μ_r values. On the same graph we also plot $F_{g_{rd,a}}$. We observe that as the average number of reliable relays increases, average SNR of the best relay at D improves substantially compared to the average SNR of an arbitrary relay.

For $M_r = 2$ in (6.21), we obtain

$$\begin{aligned}
F_{g_{rd(1)}, g_{rd(2)}}(g_1, g_2) &= \frac{1}{1 - \exp(-\mu_r)(1 + \mu_r)} \\
&\times \int_0^{g_1} \mu_r p_{g_{rd,a}}(t_1) \int_{t_1}^{g_2} \left\{ \mu_r \exp(-\mu_r(1 - F_{g_{rd,a}}(t_2))) p_{g_{rd,a}}(t_2) \mathrm{d}t_2 \, \mathrm{d}t_1 \right\} \\
&= \frac{1 + \exp(\mu_r F_{g_{rd,a}}(g_2)) F_{g_{rd,a}}(g_1) - \exp(\mu_r F_{g_{rd,a}}(g_1))}{\exp(\mu_r) + \mu_r - 1}.
\end{aligned} \tag{6.24}$$

Let $\gamma_{rd(i)}$ denote the instantaneous SNR of the reliable relay that has the i-th highest average value, i.e., $\mathbb{E}_X[\gamma_{(i)}/\gamma_{tr}] \sim g_{rd(i)}$. Note, that $\gamma_{(i)}$ does not necessarily have the i-th highest value among $\gamma_{(j)}$, $j \in \{1, 2, \ldots, k\}$. Let us use $P_{o,2}^{(M_r)}$ to denote the probability of outage of the basic protocol when the maximum number of relays

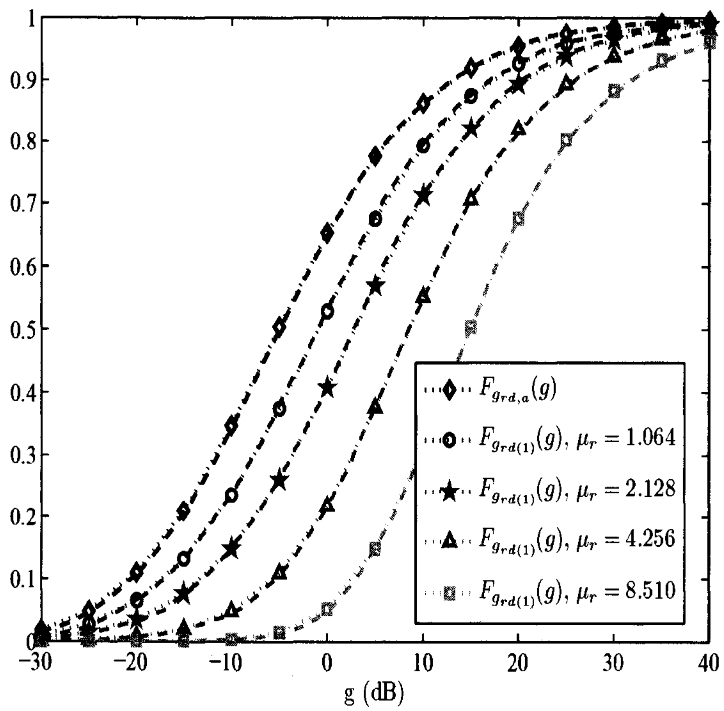

Figure 6.4: The CDF of $g_{rd(1)}$ ($F_{g_{rd(1)}}(g)$), the average SNR of the best reliable relay to D. $\upsilon = 4$, $\sigma = 8$, $\tilde{d}_{sd} = 1$, $\zeta = 1$. Dotted curves with markers are obtained from (6.19) and (6.23) and dashed curves are obtained through Monte Carlo simulations.

is limited to 2. We can express $P_{o,2}^{(M_r)}$ as:

$$\begin{aligned}P_{o,2}^{(M_r)}=&\sum_{k=0}^{M_r-1}\mathbb{P}\{N_r=k\}\mathbb{P}\{\text{outage after signals from}\\&\quad S\text{ and }k\text{ reliable relays are combined}\}\\&+\mathbb{P}\{N_r\geq M_r\}\mathbb{P}\{\text{outage after the signals from}\\&\quad S\text{ and best }M_r\text{ reliable relays are combined}\}.\end{aligned}\tag{6.25}$$

Outage Probability with Maximal Ratio Combining

If D uses MRC, the output SNR after combining is the sum of the SNR values received from S and individual relays [10]. Hence, we can write

$$\begin{aligned}P_{o,2}^{(M_r,MRC)}=&\sum_{k=0}^{M_r-1}\mathbb{P}\{N_r=k\}\mathbb{P}\left\{\left(\frac{\gamma_{sd}}{\gamma_{tr}}+\sum_{i=1}^{k}\frac{\gamma_{rd,i}}{\gamma_{tr}}\right)<1\right\}\\&+\mathbb{P}\{N_r\geq M_r\}\mathbb{P}\left\{\left(\frac{\gamma_{sd}}{\gamma_{tr}}+\sum_{i=1}^{M_r}\frac{\gamma_{rd(i)}}{\gamma_{tr}}\right)<1\right\}.\end{aligned}\tag{6.26}$$

We define two new random variables $\mathcal{G}_1$ and $\mathcal{G}_2$ to shorten the notation.

$$\mathcal{G}_1=\frac{\gamma_{sd}}{\gamma_{tr}}+\sum_{i=1}^{k}\frac{\gamma_{rd,i}}{\gamma_{tr}},\tag{6.27}$$

$$\mathcal{G}_2=\frac{\gamma_{sd}}{\gamma_{tr}}+\sum_{i=1}^{M_r}\frac{\gamma_{rd(i)}}{\gamma_{tr}}.\tag{6.28}$$

Conditioned on g_{sd} and $g_{rd,i}$ for $i=1,2,\ldots,k$, $\mathcal{G}_1$ is a sum of independent exponential random variables. If the means of exponential components are distinct[1], such random variables are called hypoexponential random variable [73]. The PDF of an hypoexponential random variable $\mathcal{G}$ is given by

$$p_{\mathcal{G}}(g;\mu_1,\mu_2,\ldots,\mu_t)=\sum_{i=1}^{t}c_{i,t}\frac{1}{\mu_i}e^{-g/\mu_i},\qquad g\geq 0,$$

[1]In our problem the means of exponential random variables are continuous valued random variables. Hence, the probability that they do not take distinct values is zero.

where $\mu_1, \mu_2, \ldots, \mu_t$ are the means of individual exponential summands and

$$c_{i,t}= \prod_{j=1, j\neq i}^{t} \frac{\mu_i}{\mu_i - \mu_j}.$$

It is straightforward to find the CDF of $\mathcal{G}$ from its PDF:

$$F_{\mathcal{G}}(g; \mu_1, \mu_2, \ldots, \mu_t) = \sum_{i=1}^{t} c_{i,t} \left(1 - e^{-g/\mu_i}\right), \quad g \geq 0. \tag{6.29}$$

Hence, the conditional PDF of $\mathcal{G}_1$ and $\mathcal{G}_2$ can be written as

$$\mathbb{P}\{\mathcal{G}_1 \leq g | g_{sd}, g_{rd,1}, \ldots, g_{rd,k}\}=F_{\mathcal{G}}(g; g_{sd}, g_{rd,1}, \ldots, g_{rd,k}), \tag{6.30}$$

$$\mathbb{P}\{\mathcal{G}_2 \leq g | g_{sd}, g_{rd(1)}, \ldots, g_{rd(M_r)}\}=F_{\mathcal{G}}(g; g_{sd}, g_{rd(1)}, \ldots, g_{rd(M_r)}). \tag{6.31}$$

Then, we can express the first part of (6.26) as:

$$\begin{aligned}
&\sum_{j=0}^{M_r-1} \mathbb{P}\{N_r = k\}\mathbb{P}\left\{ \left(\frac{\gamma_{sd}}{\gamma_{tr}} + \sum_{i=1}^{k} \frac{\gamma_{rd,i}}{\gamma_{tr}} \right) < 1 \right\} \\
&\quad = \sum_{k=0}^{M_r-1} e^{-\mu_r} \frac{\mu_r^k}{k!} \int_0^{\infty} \cdots \int_0^{\infty} F_{\mathcal{G}}(1; g_{sd}, g_1, \ldots, g_k) \\
&\quad \times p_{g_{sd}}(g_{sd})\, p_{g_{rd,1}}(g_1) \ldots p_{g_{rd,k}}(g_k)\, \mathrm{d}g_{sd}\, \mathrm{d}g_1 \ldots \mathrm{d}g_k.
\end{aligned}$$

The second part of (6.26) can be written as:

$$\begin{aligned}
&\mathbb{P}\{N_r \geq M_r\}\mathbb{P}\left\{ \left(\frac{\gamma_{sd}}{\gamma_{tr}} + \sum_{i=1}^{M_r} \frac{\gamma_{rd(i)}}{\gamma_{tr}} \right) < 1 \right\} \\
&\quad = \left(1 - \sum_{k=0}^{M_r-1} e^{-\mu_r} \frac{\mu_r^k}{k!}\right) \int_0^{\infty} \int_0^{\infty} \int_0^{g_1} \cdots \int_0^{g_{M_r-1}} F_{\mathcal{G}}(1; g_{sd}, g_1, \ldots, g_{M_r}) \\
&\quad \times p_{g_{rd(1)}, \ldots, g_{rd(M_r)}}(g_1, \ldots, g_{M_r}) p_{g_{sd}}(g_{sd})\, \mathrm{d}g_1 \ldots \mathrm{d}g_{M_r} \mathrm{d}g_{sd}.
\end{aligned}$$

For $M_r = 1$, (6.26) simplifies to

$$
\begin{aligned}
P_{o,2}^{(1,MRC)} &= e^{-\mu_r} P_{o,1} + (1 - e^{-\mu_r}) \\
&\times \int_0^\infty \int_0^\infty F_{\mathcal{G}}(1; g_{sd}, g_{rd,1}) p_{g_{sd}}(g_{sd}) p_{g_{rd(1)}}(g_1) \mathrm{d}g_{sd} \mathrm{d}g_1 \\
&= e^{-\mu_r} P_{o,1} + (1 - e^{-\mu_r}) \Big\{ 1 - \\
&\int_0^\infty \int_0^\infty \left(\frac{g_{sd}}{g_{sd} - g_1} e^{-1/g_{sd}} + \frac{g_1}{g_1 - g_{sd}} e^{-1/g_1} \right) \\
&\times p_{g_{sd}}(g_{sd}) p_{g_{rd(1)}}(g_1) \mathrm{d}g_{sd} \, \mathrm{d}g_1 \Big\}.
\end{aligned} \tag{6.32}
$$

Outage Probability with Selection Combining

If D use selection combining to combine all the received signals, then we can express the outage probability as

$$
\begin{aligned}
P_{o,2}^{(M_r,SC)} = \mathbb{P}\left\{\frac{\gamma_{sd}}{\gamma_{tr}} < 1\right\} \Bigg(\sum_{k=0}^{M_r-1} \mathbb{P}\{N_r = k\} \prod_{i=1}^{k} \mathbb{P}\left\{\frac{\gamma_{rd,i}}{\gamma_{tr}} < 1\right\} \\
+ \mathbb{P}\{N_r \geq M_r\} \prod_{i=1}^{M_r} \mathbb{P}\left\{\frac{\gamma_{rd(i)}}{\gamma_{tr}} < 1\right\} \Bigg).
\end{aligned} \tag{6.33}
$$

Due to the complexity of the general expressions, we focus on the simplest case and consider SC with $M_r = 1$:

$$
\begin{aligned}
P_{o,2}^{(1,SC)} &= P_{o,1} \left(\mathbb{P}\{N_r = 0\} + (1 - \mathbb{P}\{N_r = 0\}) \mathbb{P}\left\{\frac{\gamma_{rd(i)}}{\gamma_{tr}} < 1\right\} \right) \\
&= P_{o,1} \left(e^{-\mu_r} + (1 - e^{-\mu_r}) \int_0^\infty (1 - \exp(-1/g_1) p_{g_{rd(1)}}(g_1) \mathrm{d}g_1 \right).
\end{aligned} \tag{6.34}
$$

Using integration by parts, we can express the integral in (6.34) as

$$
\begin{aligned}
\int_0^\infty (1 - e^{-1/g_1}) p_{g_{rd(1)}}(g_1) \mathrm{d}g_1 = \underbrace{F_{g_{rd(1)}}(g_1)(1 - e^{-1/g_1}) \Big]_0^\infty}_{\to 0} \\
+ \int_0^\infty (g_1)^{-2} e^{-1/g_1} F_{g_{rd(1)}}(g_1) \mathrm{d}g_1.
\end{aligned}
$$

Then,

$$
P_{o,2}^{(1,SC)} = P_{o,1} \left(e^{-\mu_r} + (1 - e^{-\mu_r}) \int_0^\infty (g_1)^{-2} e^{-1/g_1} F_{g_{rd(1)}}(g_1) \mathrm{d}g_1 \right). \tag{6.35}
$$

Substituting (6.6) and (6.23) into (6.35), we can evaluate $P_{o,2}^{(1,SC)}$ numerically.

6.4 Enhancements to the Basic Relaying Protocol

In this section we propose two enhancements to the basic protocol and discuss implementation issues related to them. In the basic relaying protocol, as well as the rest of the relaying schemes studied in the rest of this thesis, in the first phase the source transmits a data packet and in the second phase one or more of the relays retransmits the message. This protocol can be improved in terms of bandwidth expansion and error/outage performance in two ways.

- In the basic protocol a second phase takes place even if the transmission in the first phase is successful. Assuming that the destination sends an acknowledgement message (ACK) when the source transmission is successful, the second phase can be avoided.

- The basic protocol always selects one of the reliable relays to retransmit. In certain topologies and channel conditions, however, even the best relay's channel to the destination might not be good enough and a retransmission by the source might be more advantageous than the relay transmission. The second enhancement to the basic protocol allows these two options: source retransmission and relay transmission.

Next we describe a protocol, in which we implement these two enhancements. We call this protocol as Relay-Assisted ARQ (RARQ). We note that the second enhancement can also be applied to the basic protocol without ARQ.

6.4.1 Relay-Assisted ARQ Protocol

The protocol has two phases. In the first phase, S transmits a data packet, specifying the intended destination. If D receives the packet successfully, it sends a short ACK message to S. To account for propagation and processing delays, S uses a time-out counter defining a time window for ACK to arrive from D. In case ACK arrives in time, the protocol cycle is terminated. If S does not receive an ACK from D before its timer expires, it assumes that its transmission is not successful and the second phase starts. In the second phase, S broadcasts a message requesting that all reliable relays identify themselves. Each reliable relay sends a short ACK to S, which also includes its mean channel gain to the destination. For simplicity, we limit the number of relays to transmit in the second phase to one relay. S then either instructs the reliable relay with the highest channel gain to D to retransmit the packet, or retransmits the packet itself, which is also what it does when there are no reliable relays. To complete the second phase, the destination combines the two received signals using Maximum Ratio Combining (MRC).

The above description leaves the following important issues unresolved, and we discuss them now. Consider N_r reliable relays with respect to the given source node with average normalized SNRs received at the destination denoted by $g_{rd,1}, \ldots, g_{rd,N_r}$. As in Section 6.3.2 let us denote their maximum as

$$g_{rd(1)} = \max_{i \in \{1,2,\ldots,N_r\}} g_{rd,i}.$$

Depending on the values of $g_{rd(1)}$ and g_{sd}, S decides to retransmits itself, or instructs the reliable relay with mean channel gain $g_{rd(1)}$ to do that. In Section 6.4.3 we derive a target value, $g_{min}(g_{sd})$ for $g_{rd(1)}$, below which source retransmission should be preferred over relay transmission.

We note that concurrent transmissions of the ACKs from multiple reliable relays can cause collisions if not managed by a separate protocol. A simple protocol for this purpose is given below. The source includes the value of g_{min} in the transmitted packet, then reliable relay i does not respond if $g_{rd,i} < g_{min}$. Each reliable relay whose $g_{rd,i} \geq g_{min}$ is required to wait a certain time interval before responding. This time interval is related to the $g_{rd,i}$ of the relay through a properly chosen monotonically decreasing function $G(g_{sd}, g_{rd,i})$. Let the longest waiting time interval, the one corresponding to g_{min}, be Δt_{max} (See Fig 6.5). Then the reliable relay with the highest channel gain to the destination will transmit the ACK first, and the rest, sensing the transmission of the "best" relay, will withdraw. Note that even if some other reliable relays fail to sense the signal of the "best" relay, with high probability no collision will occur, because the ACK messages are short compared to Δt_{max}. S then waits to the end of the Δt_{max} interval (no reliable relay will be on the air beyond this point) and then sends a message to the "best" relay instructing it to transmit to D. The "best" relay then transmits the data packet terminating the cycle. Having to wait for a specific instruction from S prevents the possibility that the "best" relay, not receiving an ACK from D, will transmit even though D may have issued an ACK that was received by S.

6.4.2 Minimum Average SNR for Relay Transmission: g_{min}

If the first transmission by the source fails, there are two possible actions: a_s represents the retransmission by the source and a_r represents the transmission by the best relay. Let P_{s2} and P_{sr} denote the outage probability at the destination if, following a failed transmission, the source chooses a_s and a_r, respectively. Since we only consider the best relay in this analysis, to simplify the notation, we use $\bar{\gamma}_{rd}$ and g_{rd} instead of $\bar{\gamma}_{rd(1)}$ and $g_{rd}(1)$.

Recall that the destination node uses MRC, and therefore the SNR at the MRC

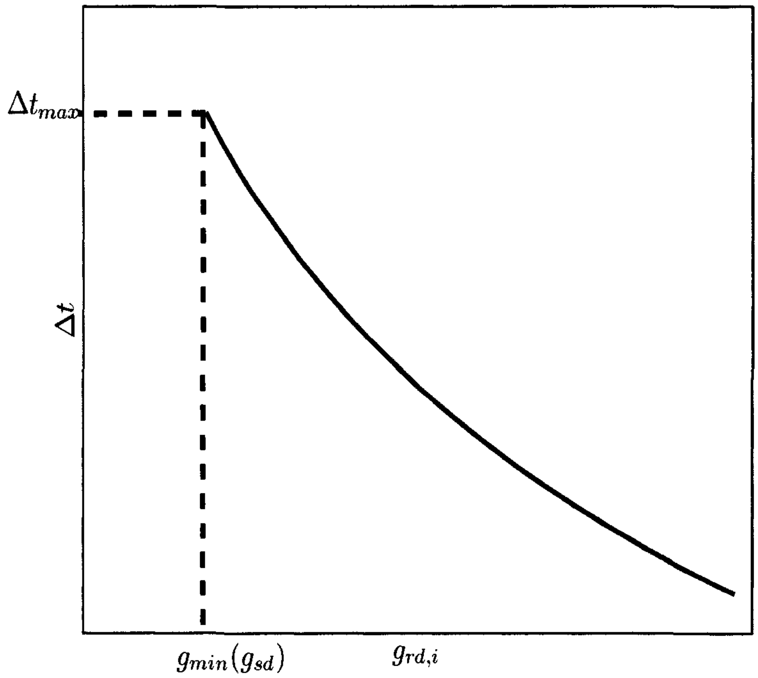

Figure 6.5: $G(g_{sd}, g_{rd,i})$: The waiting time before responding for reliable relay i with $g_{rd,i} \geq g_{min}$.

combiner output is the sum of the SNRs obtained in the two attempts. Hence,

$$\begin{aligned} P_{s2} =& \mathbb{P}\{2\gamma_{sd} < \gamma_t \,|\, \bar{\gamma}_{sd}, \gamma_{sd} < \gamma_t\} = \frac{\mathbb{P}\{\gamma_{sd} < \gamma_t/2 \,|\, \bar{\gamma}_{sd}\}}{\mathbb{P}\{\gamma_{sd} < \gamma_{tr} \,|\, \bar{\gamma}_{sd}\}} \\ =& \frac{1 - \exp\left(-\frac{\gamma_{tr}}{2\bar{\gamma}_{sd}}\right)}{1 - \exp\left(-\frac{\gamma_{tr}}{\bar{\gamma}_{sd}}\right)} = \frac{1 - \exp\left(-\frac{1}{2g_{sd}}\right)}{1 - \exp\left(-\frac{1}{g_{sd}}\right)}, \end{aligned} \tag{6.36}$$

and

$$\begin{aligned}
P_{sr}=&\mathbb{P}\{\gamma_{sd}+\gamma_{rd}<\gamma_t \,|\, \bar{\gamma}_{sd},\bar{\gamma}_{rd},\gamma_{sd}<\gamma_t\} = \frac{\mathbb{P}\{\gamma_{sd}+\gamma_{rd}<\gamma_t,\gamma_{sd}<\gamma_t \,|\, \bar{\gamma}_{sd},\bar{\gamma}_{rd}\}}{\mathbb{P}\{\gamma_{sd}<\gamma_t \,|\, \bar{\gamma}_{sd}\}}\\
=&\frac{1}{1-\exp\left(-\frac{\gamma_t}{\bar{\gamma}_{sd}}\right)}\int_0^{\gamma_{tr}}\int_0^{\gamma_{tr}-\gamma_{sd}}\frac{1}{\bar{\gamma}_{rd}}e^{-\gamma_{rd}/\bar{\gamma}_{rd}}\frac{1}{\bar{\gamma}_{sd}}e^{-\gamma_{sd}/\bar{\gamma}_{sd}}d\gamma_{rd}\,d\gamma_{sd}\\
=&1-\frac{\bar{\gamma}_{rd}}{\bar{\gamma}_{rd}-\bar{\gamma}_{sd}}\frac{\exp\left(-\frac{\gamma_t}{\bar{\gamma}_{rd}}\right)-\exp\left(-\frac{\gamma_t}{\bar{\gamma}_{sd}}\right)}{1-\exp\left(-\frac{\gamma_t}{\bar{\gamma}_{sd}}\right)}\\
=&1-\frac{g_{rd}}{g_{rd}-g_{sd}}\frac{\exp\left(-\frac{1}{g_{rd}}\right)-\exp\left(-\frac{1}{g_{sd}}\right)}{1-\exp\left(-\frac{1}{g_{sd}}\right)}. \qquad (6.37)
\end{aligned}$$

Then, the optimal decision can be found as:

$$P_{sr}\underset{a_r}{\overset{a_s}{\gtrless}}P_{s2} \qquad (6.38)$$

$$1-\frac{g_{rd}}{g_{rd}-g_{sd}}\frac{\exp\left(-\frac{1}{g_{rd}}\right)-\exp\left(-\frac{1}{g_{sd}}\right)}{1-\exp\left(-\frac{1}{g_{sd}}\right)}\underset{a_r}{\overset{a_s}{\gtrless}}\frac{1-\exp\left(-\frac{1}{2g_{sd}}\right)}{1-\exp\left(-\frac{1}{g_{sd}}\right)}. \qquad (6.39)$$

Note that P_{sr} monotonically decreases with g_{rd}. After some arithmetic, (6.39) simplifies to the following form:

$$g_{rd}\underset{a_1}{\overset{a_0}{\gtrless}}g_{min}(g_{sd}),$$

where g_{min} denotes the minimum g_{rd} required for the relay transmission to be advantageous over the source retransmission. The function g_{min} is given by

$$g_{min}(g_{sd})=g_{sd}\left(1-\exp\left(-\frac{1}{2g_{sd}}\right)\right)\left[g_{sd}\left(1-\exp\left(-\frac{1}{2g_{sd}}\right)\right)W(f(g_{sd}))+1\right]^{-1},$$

where we define $f()$ as

$$f(x)=\frac{\exp\left(\frac{1+\exp\left(-\frac{1}{2x}\right)}{2x\left(-1+\exp\left(-\frac{1}{2x}\right)\right)}\right)}{x\left(-1+\exp\left(-\frac{1}{2x}\right)\right)},$$

and W is the Omega function or Lambert's W-function [74]. $W(x)=w$ if x and w satisfy $x=we^w$. Fig. 6.6 shows g_{min} for a wide range of g_{sd} values. We note that

g_{min} has a limit as $g_{sd} \to \infty$:

$$\lim_{g_{sd}\to\infty} g_{min}(g_{sd}) = \frac{1}{W(-2e^{-2})+2} \approx 0.6275.$$

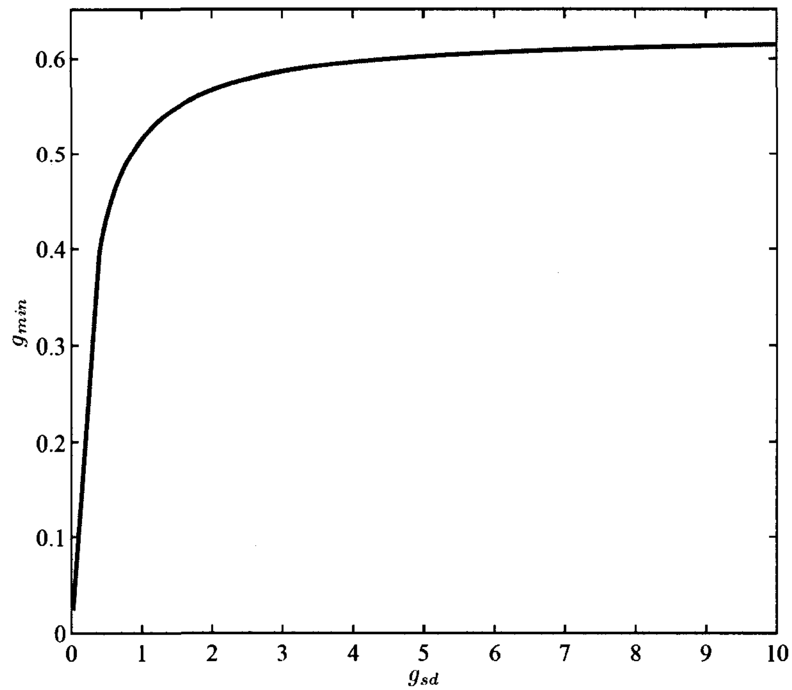

Figure 6.6: Minimum average SNR for relay transmission (g_{min}) as a function of g_{sd}.

6.4.3 Outage Probability of Relay-Assisted ARQ

The outage probability of the relay assisted ARQ protocol can be represented as

$$P_{RARQ} = P_{o,1}P_2, \tag{6.40}$$

where $P_{o,1}$ is probability of outage of the direct transmission and P_2 is the probability that the packet is not received after the second transmission, following a failed first attempt. Let $p_{g_{rd}}$ and $F_{g_{rd}}$ denote the PDF and CDF of g_{rd}, respectively. According to the protocol, the source retransmits if either there is no reliable relay or the g_{rd} is less than $g_{min}(g_{sd})$. For analytical convenience, instead of treating the case of no reliable relays separately, we modify g_{rd} as follows: If there is no reliable relay, we say g_{rd} is equal to zero. We can express P_2 as

$$\begin{aligned} P_2 =& \int_0^{\infty}\int_0^{\infty} \min\{P_{s2}(g_{sd}), P_{sr}(x, g_{sd})\} p_{g_{rd}}(g_{rd}) p_{g_{sd}}(g_{sd}) \mathrm{d}g_{rd}\, \mathrm{d}g_{sd} \\ =& \int_0^{\infty}\int_0^{g_{min}(g_{sd})} P_{s2}(g_{sd}) p_{g_{rd}}(g_{rd}) p_{g_{sd}}(g_{sd}) \mathrm{d}g_{rd}\, \mathrm{d}g_{sd} \\ &+ \int_0^{\infty}\int_{g_{min}(g_{sd})}^{\infty} P_{sr}(x, g_{sd}) p_{g_{rd}}(g_{rd}) p_{g_{sd}}(g_{sd}) \mathrm{d}g_{rd}\, \mathrm{d}g_{sd}. \end{aligned}$$

Due to the complexity of computing this expression numerically, we resort to Monte Carlo simulations to evaluate the performance of RARQ protocol.

6.5 Results

In this section we validate some of the analytical results of this chapter with simulations. In our simulation study, for each data point shown in the graphs a large number of topologies are generated where S is placed at position $(-d_{sd}/2, 0)$ and the destination is placed at position $(+d_{sd}/2, 0)$ on a $K \times K$ square, where K is chosen depending on the node density λ. $N = 600$ other nodes are placed randomly and uniformly on the region. The source and relays are assumed to have identical transmission ranges ($r_{Nr} = r_{Ns}$, $\zeta = 1$). The distance dependent loss exponent v is 4. The log-normal and Rayleigh fading are generated i.i.d. across all the links with $\sigma = 8$ for the log-normal fading.

In Fig. 6.7 we plot the outage probability for single hop transmission and the basic relaying protocol. The curves of $P_{o,2}^{(1,SC)}$ from the simulations and the analysis agree completely, which validates both our analysis and simulation setup. We observe

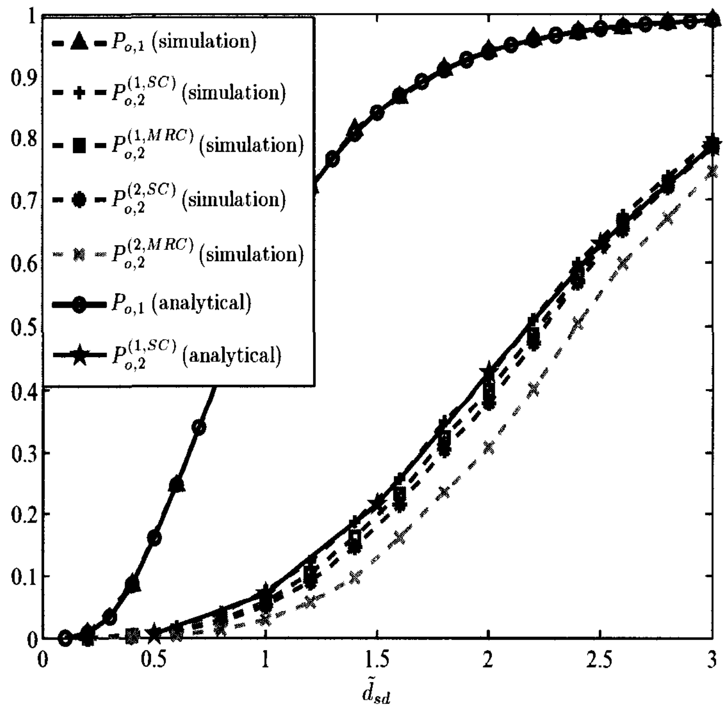

Figure 6.7: Performance comparison of the basic relaying protocol with MRC and SC using $M_r = 1$ and $M_r = 2$ relays at maximum, $\sigma = 8$, $\upsilon = 4$, $\lambda r_{Ns}^2 = 2$ ($\mu_r = 8.51$). Analytical results are obtained from (6.6) and (6.35).

that the basic relaying protocol can decrease the outage probability significantly even if only one relay is allowed and selection combining is performed at D.

We perform simulations to observe the effect of the relay selection criterion on the outage probability. The relaying protocol analyzed in this chapter selects the reliable relay(s) with largest average SNR to D, i.e., the selection criterion is maximum g_{rd}. We compare this protocol to the protocols in which the relay selection is done based on minimum distance to D (d_{rd}) and the instantaneous SNR to D (γ_{rd}). The latter criterion has also been used in Chapter 5 for fixed number of relays and relay locations. We also consider random relay selection, in which one of the reliable relays is selected at random. In Fig. 6.8, we plot the outage probability for different relay selection

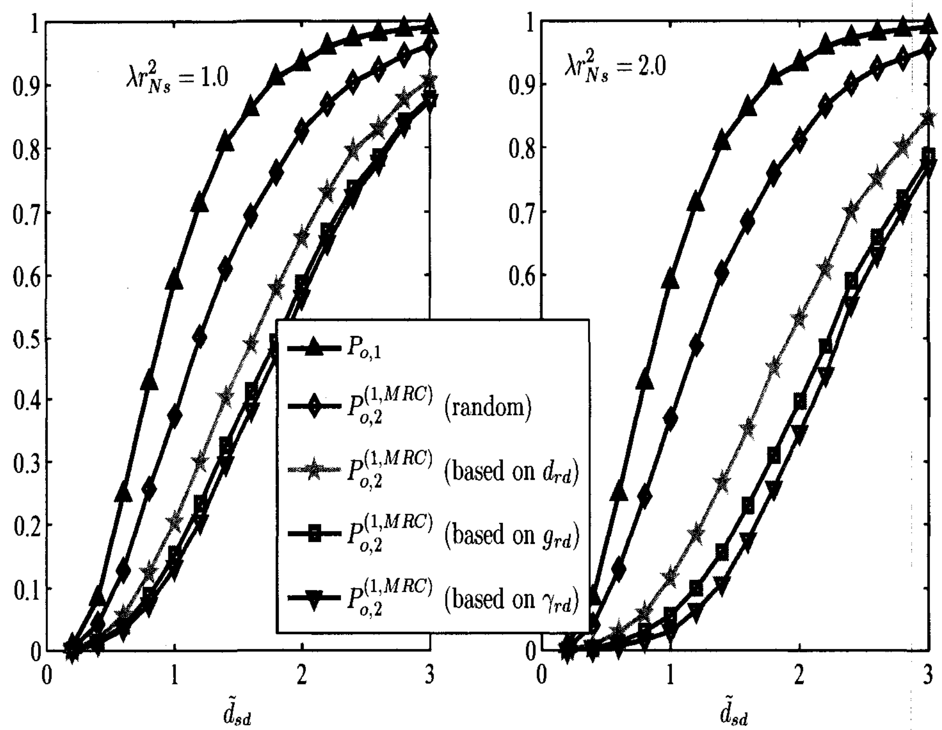

Figure 6.8: Outage probability of the basic relaying protocol with MRC and $M_r = 1$ relay at maximum using different relay selection criteria (distance, average SNR, and instantaneous SNR) as a function of $\tilde{d}_{sd}$. $\sigma = 8$, $\upsilon = 4$. Two relay densities are considered: $\lambda r_{Ns}^2 = 1.0$ ($\mu_r = 4.255$) and $\lambda r_{Ns}^2 = 2.0$ ($\mu_r = 8.51$).

criteria. All the relay selection methods perform significantly better than random relay selection as expected. Surprisingly, the performance of the average SNR based selection is close to the performance of the instantaneous SNR based selection even when the expected number of reliable relays is quite large ($\mu_r = 8.55$). Since the average SNR is also easier to measure compared to the internode distance and easier to keep track compared to the instantaneous SNR, it is a good relay selection criterion.

To examine the effect of relay density on the outage probability, we vary the number of nodes in the area and in Fig. 6.9, we plot the outage probability of the

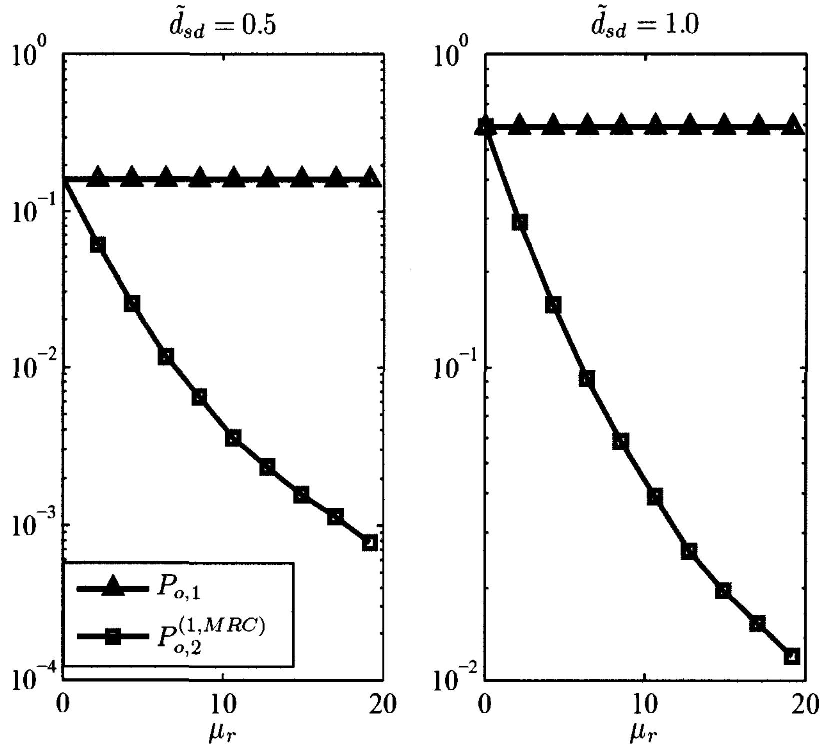

Figure 6.9: Outage probability of the basic relaying protocol with MRC and $M_r = 1$ relay at maximum as a function of μ_r. $\sigma = 8$, $\upsilon = 4$. μ_r is varied by varying λ. Two $\tilde{d}_{sd}$ values are considered: $\tilde{d}_{sd} = 0.5$ and $\tilde{d}_{sd} = 1.0$

basic relay protocol for two different $\tilde{d}_{sd}$ values as a function of μ_r. It is seen that as μ_r increases, the outage probability decreases rapidly from the outage probability of the direct transmission. We also observe that the logarithm of the outage probability decreases linearly with μ_r, which supports the findings of Song and Hatzinakos in [67] that the outage probability decreases exponentially with the relay density in a similar protocol.

In order to study the effect of lognormal shadowing to the outage performance, in Fig. 6.10 we plot the probability of outage as a function of the shadowing parameter σ for two $S - D$ distance values ($\tilde{d}_{sd} = (0.25, 1.0)$) and a fixed value of node density ($\lambda r_{Ns}^2 = 1.0$). We note that the outage probability of direct transmission can increase or decrease with σ depending on the internode distance. For instance in Fig. 6.10 at $\tilde{d}_{sd} = 0.25$, $P_{o,1}$ increases with σ. However, at $\tilde{d}_{sd} = 1.0$, $P_{o,1}$ decreases with σ. A similar effect is expected for the single input multiple output (SIMO) channel formed by the relaying protocol using the selected relay. On the other hand, as seen from (6.10) the average number of reliable relays μ_r increases with σ. The dependence of μ_r to σ is shown in Fig. 6.11. An increase in μ_r is expected to improve outage, as it makes the selected relay to be located closer to the destination. For $\tilde{d}_{sd} = 1.0$, we observe that the overall performance of the relaying protocol improves with increasing σ. For $\tilde{d}_{sd} = 0.25$ for smaller values of σ, the negative effect of lognormal shadowing on the direct and the SIMO channel dominates and the outage probability of the relaying protocol increases with σ. As σ becomes larger, the positive effect of σ on the number of reliable relays dominates and the outage probability of the relaying protocol decreases with increasing σ.

In Fig. 6.12, we compare the outage probability of RARQ protocol to the the outage probability of the basic relaying protocol with a single relay and MRC. For reference we also plot the outage probability of ARQ protocol, in which S retransmits whenever the the direct transmission fails. We observe that RARQ combines the advantages of ARQ and the basic relaying protocol by selecting the best option for any given topology and channel conditions. The gain of RARQ over the basic relaying protocol in terms of outage probability is negligible at larger relay densities. However, the main advantage of RARQ is its reduced bandwidth expansion when the direct link is favorable. Fig 6.13 depicts the average number of transmissions used per packet for different protocols. We note that the basic relaying protocol (with $M_r = 1$) uses two transmissions per packet whenever there is at least one reliable relay. The ARQ and RARQ use the same number of transmissions per packet. Hence, the figure only shows the curve for RARQ.

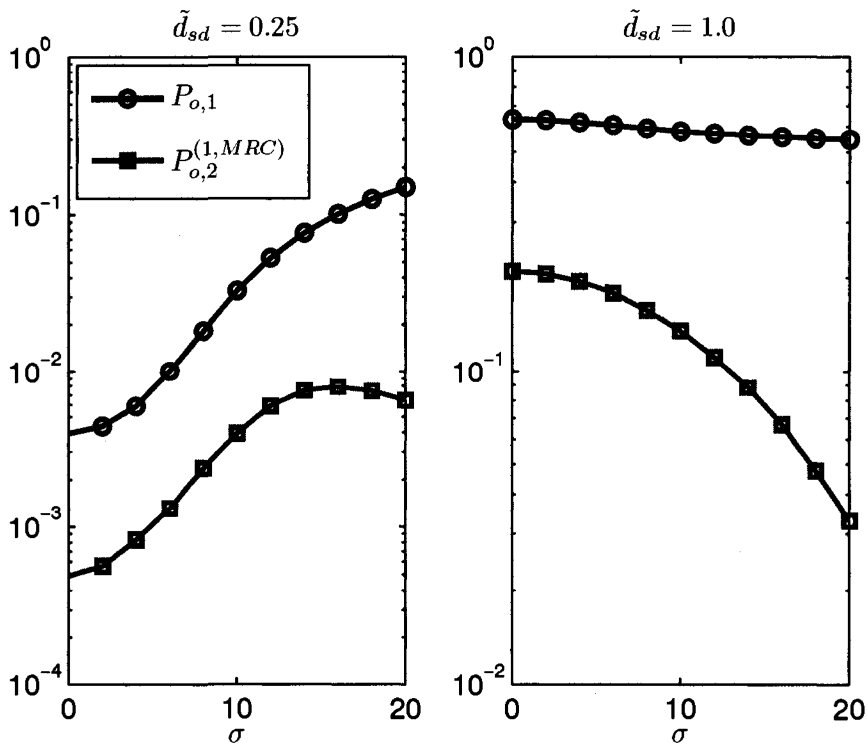

Figure 6.10: Outage probability of the basic relaying protocol with MRC and M_r = 1 relay at maximum as a function of σ. $\upsilon = 4$ and $\lambda r_{Ns}^2 = 1.0$. Two $\tilde{d}_{sd}$ values are considered: $\tilde{d}_{sd} = 0.25$ and $\tilde{d}_{sd} = 1.0$

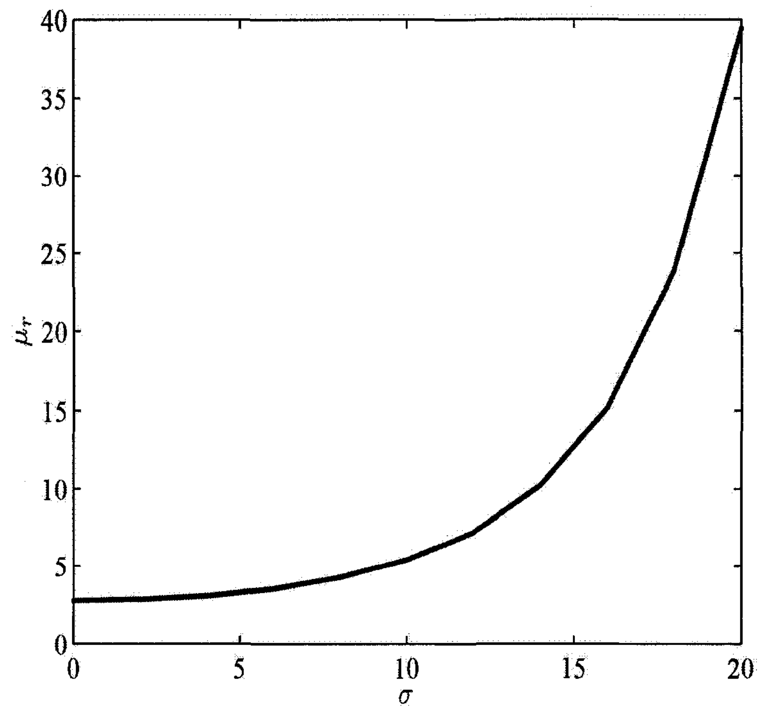

Figure 6.11: Average number of reliable relays as a function of σ. $\upsilon = 4$ and $\lambda r_{Ns}^2 = 1.0$.

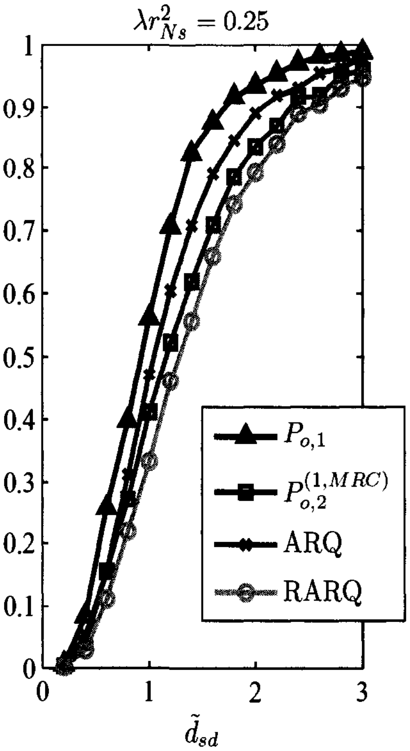

Figure 6.12: Outage probability of the RARQ, ARQ, and the basic relaying protocol (with MRC, $M_r = 1$) as a function of $\tilde{d}_{sd}$. $\sigma = 8$, $\upsilon = 4$. Two relay densities are considered: $\lambda r_{Ns}^2 = 0.25$ ($\mu_r = 1.064$) and $\lambda r_{Ns}^2 = 1.0$ ($\mu_r = 4.255$).

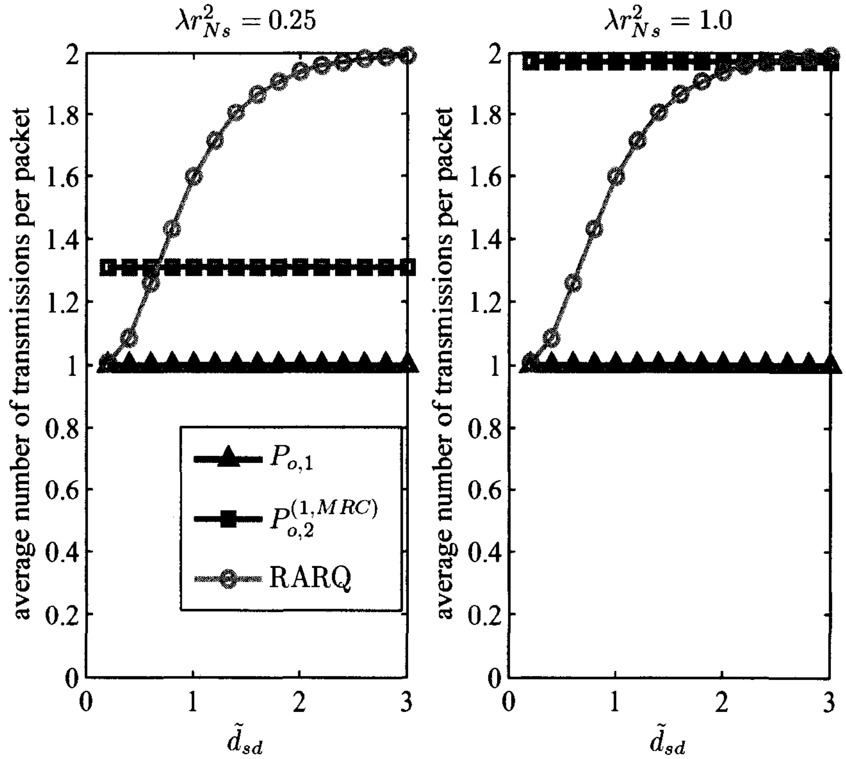

Figure 6.13: Average number of transmissions per packet for the RARQ and the basic relaying protocol (with MRC, $M_r = 1$) as a function of $\tilde{d}_{sd}$. $\sigma = 8$, $\upsilon = 4$. The average number of transmissions per packet of ARQ is the same as that of RARQ and is not shown in the figure. Two relay densities are considered: $\lambda r_{Ns}^2 = 0.25$ ($\mu_r = 1.064$) and $\lambda r_{Ns}^2 = 1.0$ ($\mu_r = 4.255$).

6.6 Conclusions

In this chapter we studied the network-wide benefits of two-hop diversity relaying in wireless ad hoc networks, where the node locations follow a homogeneous Poisson point process on a plane. We have defined a communications protocol where the source chooses nodes to serve as relays out of those that have actually received correctly the data packet transmitted by the source. The source makes this choice based on feedback from each such node, which includes the node's estimate of its average channel gain to the destination node. We derived the CDF of this quantity analytically through numerical integration. We have studied analytically and presented simulation results for the outage probability of the protocol, when the destination node employs selection combining and maximal ratio combining. We showed that two-hop cooperative diversity can be extremely beneficial in random multihop networks.

We have compared the performance of different relay selection criterion and observe that as a relay selection criterion average SNR to the destination constitutes a good trade-off in terms of end-to-end outage performance and the signaling required for the relay selection. We have shown graphically how increasing the intensity of the nodes reduces the outage probability, or to put it differently, allows a further destination to be reached with acceptable packet delivery ratio. We also proposed enhancements to the relaying protocol including an adaptive ARQ scheme assisted by the relays. We have shown the benefits of this protocol in terms of bandwidth expansion and outage performance.

Chapter 7

Cooperative Diversity and Distributed Spatial Multiplexing in Wireless Fixed Relay Networks

In this chapter, we consider diversity relaying opportunities in infrastructure based wireless networks in the presence of fixed relays that are deployed as a part of the infrastructure. Conventional cellular architecture limits the user to base station and base station to user communication to a single hop. However, allowing multi-hop communication can reduce coverage holes within the cell due to unfavorable propagation conditions and also extend cell coverage. Multihop communication is especially critical for the performance observed by the cell edge users, which is one of the main issues for data communication in future wireless networks.

In the previous chapters we considered cooperative diversity relaying among the nodes with similar features. There are two options for relaying in infrastructure based architectures. The relays can be either users assisting each other by forwarding each others' packets or they can be fixed nodes dedicated for relaying. If the users are utilized as relays, cooperation puts a burden on them in terms of power. Fixed relays can take the burden of cooperation from users. They are provisioned to have direct access to the power line. Hence their operation is not limited by battery lifetime [5]. Due to their physical stability and less strict power constraints, deploying fixed relays can also mitigate the security problems of multihop wireless networks by using more powerful key management and encryption schemes.

Fixed relays are also expected to have less severe constraints for cost and size compared to user terminals. While mounting multiple antennas at user terminals might be impractical due to such constraints, fixed relays can easily accommodate multiple antennas. Nodes with multiple-antennas introduce new possibilities in the network.

In point-to-point links, multiple antennas, either on the transmitter or the receiver side, can improve link reliability through receive diversity, transmit beamforming or space-time coding. This feature can be easily transferred to the simple networks that we studied in Chapters 3-5.

Consider a network in which one or more multi-antenna relays assist to a source-destination pair. In this context deploying relays with multi-antennas has many advantages. For instance, in [44] the authors utilize multiple relay antennas to increase the reliability of the source-relay channel. They show that having multiple receive antennas at the relays mitigates error propagation in digital relaying without relying on decoding and error detection at the relay. Relay antennas can also be leveraged to increase the reliability of the relay-destination links through space-time coding or distributed beamforming. In [45], Fan et al. consider the same scenario. They propose to employ MRC at the source-relay links and transmit beamforming at the relay-destination links. In particular, they study the effect of antenna distribution among the relay nodes on the capacity. Given a fixed total number of relay antennas, they show that the capacity is maximum when all the antennas are located at a single relay. In [75] diversity order achievable in general network configurations is studied. The study includes networks with multiantenna nodes and analytically derives the maximum diversity order achievable in such networks.

It is well-known that by deploying multiple antennas at both transmitter and receiver sides, a significant increase in the capacity of wireless channels is possible in rich scattering environments [76], [77]. There is also a rich literature on the capacity of multiuser aspects of MIMO systems [78]. The main focus the research in this area is the so called MIMO broadcast problem, where multi-antenna base station transmits to multiple users simultaneously and applies interference cancelation before the transmission so that users with few antennas can decode their own information reliably. The capacity of two-hop networks including multi-antenna nodes have been studied in [79] and [80]. The asymptotic behavior of the end-to-end achievable capacity of a network with a multi-antenna source and destination, and a large number of relays is studied in [79]. In [80], in a similar setting, the authors analyze end-to-end capacity achievable using different signaling and relay selection techniques. In [81] the same authors consider the outage capacities for these signaling and relay selection techniques.

In point-to-point links, even practical MIMO architectures with certain constraints brings much higher spectral efficiencies than the conventional techniques. For instance, in V-BLAST the data stream is multiplexed into K substreams, where K is the number of transmit antennas, and these substreams are transmitted simultaneously through K antennas [82]. This technique is called spatial multiplexing. At the receiver side different techniques can be used to separate the substreams. The simplicity of spatial multiplexing allows it to be implemented in a distributed fashion on the transmitter side. Individual user antennas can be viewed as different substreams and can transmit simultaneously forming a *distributed spatial multiplexing* system. As the user antennas are not collocated, spatial diversity through space-time coding requires additional communication among the users and thus, is not practical in this scenario. Introducing a multiantenna relay to a distributed spatial multiplexing system, as shown Fig. 7.1, and combining the signals arriving directly from the users and through the relays improves the end-to-end reliability of this system.

This chapter is an initial study that explores the potential benefits of multi-antenna relays for spatial multiplexing of different users sending data to a common multi-antenna destination such as a base station or an access point. Neither of the aforementioned papers included the direct link from source to destination in their analysis. Combining source and relay signals, where both signals are spatially multiplexed and possibly have different average SNRs, is a new problem that appears only in multi-stream diversity relaying.

In our study, we consider zero forcing decision feedback detector (ZF-DF) type MIMO receivers and study their outage performance under various (non-selective and selective) digital relaying protocols. For diversity relaying protocol, we propose two schemes, *Joint ZF-DF* and *Parallel ZF-DF*, for joint processing (combining and decoding) of the direct user signals and the signal from the relay. We show that with the proposed selective diversity relaying protocols and joint ZF-DF processing, the outage probability of the system can be decreased significantly.

We note that when the destination has multiple antennas a straightforward way of increasing diversity is to reduce the number of simultaneously transmitting users in order to have extra degrees of freedom at the receiver. For instance, in a point-to-point V-BLAST system, each extra receive antenna will increase the diversity order of all users by one. This will, of course, require more bandwidth, since reducing the number of simultaneously transmitting users decreases the effective rate. We also compare the performance of relaying protocols to a time sharing protocol using the same bandwidth and energy.

Three multi-stream digital relaying protocols for the spatial multiplexing of M_s

users are considered. Conventional Digital Relaying (CDR) is digital relaying without diversity combining at the destination. Non-selective Digital Relaying (NDR) and Selective Digital Relaying (SDR) are extensions of well-known digital relaying protocols [4] to spatially multiplexed signals. In NDR, the relay retransmits, regardless of the quality of user-relay channels. In SDR, the relay is allowed to transmit only when it can decode all the user streams without error. We analyze the impact of these strategies on the outage performance of the system. The NDR and SDR can be viewed as the multi-stream versions of the simple digital relaying and the genie-aided digital relaying introduced in Chapter 3 as benchmarks.

Based on the SDR protocol described in this chapter, Khuong and Le-Ngoc propose a more flexible protocol called cooperative re-transmission of trustable (CRT) users [83]. In CRT the relay sends a short feedback message to the users indicating which user streams have been received reliably at the relay. Then, the relay transmits only the reliable user streams while the rest of the users retransmit their own data streams synchronously. They study the optimal relay location for CRT and SDR, and show that the flexibility of CRT can provide SNR gain over SDR. In [84] and [85] the same authors study another protocol similar to SDR and CRT. In this protocol, unlike ours, the relays transmit one by one, which provides higher reliability in the user-relay communication, but also increases the bandwidth expansion. They include code combining as opposed to diversity combining by jointly encoding the user streams at the relay and jointly decoding the relayed signal and direct signals at the destination. In [84] space time block coding in relay-destination link is also considered.

We first investigate ways of combining the direct signal and the relay signal using a V-BLAST receiver. We define two methods based on Zero Forcing with Decision Feedback Detection (ZF-DF). In *Joint ZF-DF*, two output signals are stacked and ZF-DF is applied to this equivalent system. In the second method, which we call

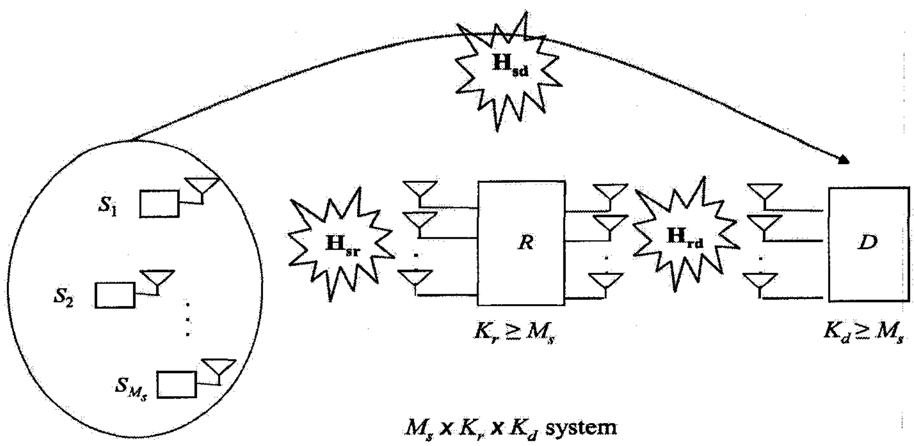

Figure 7.1: An $M_s \times K_r \times K_d$ system: M_s single antenna source nodes, a relay with K_r antennas and a destination with K_d antennas.

Parallel ZF-DF, the data of a user is estimated independently from the direct and relay output signals. These two estimates are combined to detect and decode the stream.

In accordance with the results for single-stream relaying [4], selective diversity relaying, if used with joint ZF-DF detection at the destination, can improve the outage performance significantly, even if the direct signals have lower average SNRs than the relayed signal.

7.1 System Model

We consider a system with M_s source nodes, each with a single antenna and a destination with K_d antennas ($K_d \geq M_s$). In the context of uplink communication in a cell, these source nodes are users selected by a higher layer protocol to be served in the next time slots and the destination is the basestation. We note that there might be more than M_s users within the coverage of the basestation. In our system the source nodes represent the users selected by the basestation to be served in the next time slots. The problem of scheduling of the users in the cell is beyond the scope of our work.

A fixed relay with K_r antennas ($K_r \geq M_s$) assists the communication between the users and the destination. We call such a system as an $M_s \times K_r \times K_d$ system. All channels, Source-Relay channel ($\mathbf{H_{sr}}$), Source-Destination channel ($\mathbf{H_{sd}}$), and Relay-Destination channel ($\mathbf{H_{rd}}$), are assumed to experience independent Rayleigh fading. We also assume slow block fading, which implies that all channels stay unchanged for two block durations, where each block duration is equal to L symbol periods. The channel state information is available only at the receiver side for all three links.

As the performance metric, the probability of *system outage* event is used, which is defined as the union of individual user outages. We assume that user i has a fixed target rate R_i and encodes its data independently using a single input single output (SISO) encoder whose rate depends on R_i but its codeword length is fixed and equal to L. The block length L is assumed to be large enough so that a decoding error occurs if and only if $\log_2(1+\beta_{i,r}) < \mathrm{R}_i$, where $\beta_{i,r}$ is the post-processing SNR of user i at the relay.

Source nodes transmit synchronously but without any cooperation. Both the relay and the destination use ZF-DF receivers. In the absence of errors in the source-relay link, the system is equivalent to a horizontally coded layered space-time architecture, which is usually referred to as H-BLAST [86]. To simplify the analysis, we assume that the order of decoding is the same at the relay and the destination and it is independent of the channel realizations.

It is also possible to increase relay-destination channel reliability through space-time coding. The focus of this chapter is "multi-stream" relaying, where more than one user streams are relayed simultaneously by forming MIMO channels between the source(s), the relay and the destination.

Notation

Superscripts T and H are used for transpose and Hermitian conjugate of matrices, respectively. $diag\{x_1, x_2, \ldots, x_n\}$ stands for an $n \times n$ diagonal matrix with given elements on its diagonal. $\mathbf{I}_n$ and $\mathbf{0}_{m,n}$ denote the $n \times n$ identity matrix and $m \times n$ zero matrix, respectively. $\mathbf{A}(i_1 : i_2, j_1 : j_2)$, with $i_1 \leq i_2$ and $j_1 \leq j_2$, represents the submatrix of $\mathbf{A}$ composed of rows $i = i_1, i_1+1, \ldots, i_2$ and columns $j = j_1, j_1+1, \ldots, j_2$. $\mathbf{A}(i, j)$ denotes the element at the i-th row and the j-th column of $\mathbf{A}$.

A real Gaussian vector with zero mean and identity covariance matrix is called a standard real Gaussian random vector. A circularly symmetric complex Gaussian vector with zero mean and identity covariance matrix is called standard Gaussian random vector and is denoted by $\mathcal{CN}(\mathbf{0}, \mathbf{I})$. A central chi-square random variable with n degrees of freedom is denoted by $\chi^2(n)$.

The system outage probability of the MIMO channel between the users and the destination is denoted by $P_o^{s \to d}$. Similarly, the system outage probabilities of the user-relay channel and relay-destination MIMO channels are denoted by $P_o^{s \to r}$ and $P_o^{r \to d}$, respectively. $P_o^{s,r \to d}$ represents the system outage probability after combining at the destination, given that the relay decoded all the streams correctly.

7.1.1 Multi-stream Relaying Protocols

We consider three digital relaying protocols: The conventional Digital Relaying (CDR), Non-selective Digital Relaying (NDR), and Selective Digital Relaying (SDR). In all protocols, transmission takes place in two equal time slots, each having L symbol periods. During the first time slot, M_s active users transmit simultaneously in a synchronous manner. Then, in the second slot, the relay transmits using at most M_s antennas.

In all protocols, relay decodes the signals from the users, and then reencodes its estimates and retransmits the resulting block $\hat{\mathbf{C}}$ in the second slot. It uses the same SISO encoder as user i for regenerating this user's signal. The streams of different users are spatially multiplexed and transmitted from randomly assigned antennas.

- **Conventional Digital Relaying (CDR):** In CDR, the relay retransmits regardless of the outcome of the transmission in the first time slot and the destination decodes based on the relay signal only.

- **Non-Selective Digital Relaying (NDR):** In NDR, the relay retransmits regardless of the outcome of the transmission in the first time slot and the destination decodes based on the direct and the relayed signals.

- **Selective Digital Relaying (SDR):** The relay transmits only if it can decode all M_s streams reliably. Otherwise, it remains silent. The destination decodes based on both the direct and the relayed signals when the relay retransmits.

7.2 Outage Analysis of Direct Transmission and Multistream Relaying Protocols

First, we review the outage probability of the direct transmission from sources to the destination, which uses ZF-DF.

7.2.1 Outage Probability of Direct Transmission

The system is described by

$$\mathbf{Y_d} = \mathbf{H_{sd}} \mathbf{W_d} \mathbf{C} + \mathbf{N}, \tag{7.1}$$

where $\mathbf{C} \in \mathbb{C}^{M_s \times L}$ is the transmit signal block of M_s sources, $\mathbf{Y_d} \in \mathbb{C}^{K_d \times L}$ is the received block. $\mathbf{H_{sd}}$ is the channel matrix with independent, circularly symmetric complex gaussian elements representing i.i.d. Rayleigh fading, $\mathcal{CN}(\mathbf{0}, \mathbf{I})$. $\mathbf{N} \in \mathbb{C}^{K_d \times L}$ is Gaussian noise with temporally and spatially independent elements having distribution $\mathbf{N}(i,j) \sim \mathcal{CN}(0,1)$. $\mathbf{W_d} = diag\{\sqrt{\bar{\gamma}_{1,d}}, \ldots, \sqrt{\bar{\gamma}_{M_s,d}}\}$ and $\bar{\gamma}_{i,d}$ is the average SNR of source i's direct signal at the destination.

We assume that the source streams are decoded according to their indices. Each time, the total received signal is projected onto a subspace orthogonal to the streams that are yet to be detected. From [87], the resulting output SNR for the i-th source detected can be obtained as

$$\beta_{\mathbf{i,d}} = \frac{1}{2} \bar{\gamma}_{i,d}\, z(2(K_d - M_s + i)), \tag{7.2}$$

where $\mathbf{z}(m)$ represents a chi-square random variable with m degrees of freedom. After all the data block is projected, source i is decoded. Then, the codeword of source i is regenerated and its effect is canceled from the total signal. It is well known that this procedure is equivalent to Gram-Schmidt orthogonalization of the channel matrix [88]. Assuming that $\mathbf{H_{sd}}$ has linearly independent columns, which happens with very high probability, it can be uniquely decomposed as [89]

$$\mathbf{H_{sd}} = \mathbf{Q_{sd}} \mathbf{R_{sd}},$$

where $\mathbf{Q_{sd}} \in \mathbb{C}^{M_s \times M_s}$ is unitary, satisfying $\mathbf{Q_{sd}^H} \mathbf{Q_{sd}} = \mathbf{I}_{M_s}$ and $\mathbf{R_{sd}} \in \mathbb{C}^{M_s \times K_d}$ is an upper triangular matrix whose diagonal elements are positive. Then, $\mathbf{R_{sd}}(M_s, M_s)\mathbf{W}(M_s, M_s)$ corresponds to the output SNR of the first stream decoded.[1]

[1]In this representation decoding order is decreasing source index, source M_s is decoded first.

Moreover, the output SNRs obtained by this procedure are independent, given that the decoding order is independent of matrix $\mathbf{H_{sd}}$ [90, pp. 100-101].

Source i is in outage whenever $\log_2(1+\beta_{i,d}) < \mathbf{R}_i$, where R_i is the target rate of source i. Hence, the outage probability for source i is equal to

$$P_o^{s_i \to d}(M_s, K_d, \bar{\gamma}_{i,d}) = \mathbb{P}\{\log_2(1+\beta_{i,d}) < \mathrm{R}_i\} = \mathbb{P}\{\beta_{i,d} < \gamma_{tr,i}\} \tag{7.3}$$

$$= F_{\chi 2\,,\,2(K_d - M_s + i)}(2\gamma_{tr,i}/\bar{\gamma}_{i,d}), \tag{7.4}$$

where $\gamma_{tr,i} = 2^{\mathrm{R}_i} - 1$ and $F_{\chi 2\,,\,k}(.)$ denotes the CDF of the chi-square distribution with k degrees of freedom. Since the output SNRs for different sources are independent, the system outage probability can be expressed as

$$P_o^{s \to d}(M_s, K_d, \mathbf{W_d}) = 1 - \prod_{i=1}^{M_s} \mathbb{P}\{\beta_{i,d} > \mathrm{R}_i\}$$

$$= 1 - \prod_{i=1}^{M_s} \left[1 - F_{\chi 2\,,\,2(K_d - M_s + i)}(2\gamma_{tr,i}/\bar{\gamma}_{i,d})\right]. \tag{7.5}$$

7.2.2 Outage Probability of the Time-Division Direct Transmission (TDDT)

Having noted that all the relay protocols use twice the bandwidth used by direct transmission, we define the following protocol to enable a fair comparison between relaying and direct transmission: In Time-Division Direct Transmission (TDDT), sources are divided into two sets of equal size. Assuming M_s is even, each set has $M_s/2$ sources. In the first time slot, the first set of streams are transmitted from their assigned antennas and the second set follows in the second slot. The system outage of this protocol is given by

$$P_o^{TDDT} = 1 - \Big(\left(1 - P_o^{s \to d}(M_s/2, K_d, \mathbf{W_{d1}})\right) \times \left(1 - P_o^{s \to d}(M_s/2, K_d, \mathbf{W_{d2}})\right) \Big), \tag{7.6}$$

where $\mathbf{W_{d1}}$ and $\mathbf{W_{d2}}$ are the $M_s/2 \times M_s/2$ weight matrices for the two groups.

7.2.3 Outage Probability of Relaying Protocols

Let $\mathbf{Y_{d1}}$ and $\mathbf{Y_{d2}}$ be the received signals at the destination in the first and second time slots, respectively. These received signals can be represented as

$$\mathbf{Y_{d1}}{=}\mathbf{H_{sd}}\mathbf{W_d}\mathbf{C}+\mathbf{N_{d1}} \tag{7.7}$$

$$\mathbf{Y_{d2}}{=}\mathbf{H_{rd}}\mathbf{W_r}\hat{\mathbf{C}}+\mathbf{N_{d2}}, \tag{7.8}$$

where $\mathbf{W_r}$ is a diagonal matrix whose entries depend on the average SNR at the destination due to the relay transmission. We assume that the relay allocates the power uniformly for all active antennas. Hence, $\mathbf{W_r}$ is given by $\mathbf{W_r}=\sqrt{\gamma_r}\mathbf{I}_{M_s}$. Similarly, we represent the source-relay channel as:

$$\mathbf{Y_r}=\mathbf{H_{sr}}\mathbf{W_{sr}}\mathbf{C}+\mathbf{N_r}, \tag{7.9}$$

where $\mathbf{W_{sr}}$ depends on the average received SNRs.

If the source-relay channel is in outage, i.e., at least one of the sources is in outage in this channel ($\hat{\mathbf{C}} \neq \mathbf{C}$), we assume that data of some sources will be decoded incorrectly at the destination, causing a system outage.

The outage probability of the three protocols are equal to

$$P_o^{CDR}{=}P_o^{s\to r}+(1-P_o^{s\to r})\,P_o^{r\to d}, \tag{7.10}$$

$$P_o^{NDR}{=}P_o^{s\to r}+(1-P_o^{s\to r})P_o^{s,r\to d}, \tag{7.11}$$

$$P_o^{SDR}{=}P_o^{s\to r}P_o^{s\to d}+(1-P_o^{s\to r})P_o^{s,r\to d}, \tag{7.12}$$

where all the arguments are dropped to simplify notation. The outage probabilities $P_o^{s\to r}(M_s,K_r,\mathbf{W_{sr}})$ and $P_o^{r\to d}((M_s,K_d,\mathbf{W_r}))$ can be computed as in (7.5). The term $P_o^{s,r\to d}$ depends on the combining method used at the destination.

7.3 Combining Methods for Diversity Relaying Protocols

In this section we investigate the outage at the destination, given that the relay decodes all the sources correctly. We propose two methods for detecting $\mathbf{C}$ based on $\mathbf{Y_{d1}}$ and $\mathbf{Y_{d2}}$: *Joint ZF-DF (JZF-DF)* and *Parallel ZF-DF (PZF-DF)*.

7.3.1 Joint ZF-DF (JZF-DF)

Assuming correct decoding of all M_s streams at the relay, the equivalent system is given by

$$\mathbf{Y_e} = \mathbf{H_e C} + \mathbf{N_e}, \tag{7.13}$$

where

$$\mathbf{H_e} = \begin{bmatrix} \mathbf{H_{sd} W_d} \\ \\ \mathbf{H_{rd} W_r} \end{bmatrix}, \tag{7.14}$$

and $\mathbf{Y_e} = [\mathbf{Y_{d1}}^T \ \mathbf{Y_{d2}}^T]^T$, $\mathbf{N_e} = [\mathbf{N_{d1}}^T \ \mathbf{N_{d2}}^T]^T$. Then, the destination decodes the equivalent $M_s \times 2K_d$ system based on (7.13).

7.3.2 Parallel ZF-DF (PZF-DF)

This detection method is based on parallel zero forcing and per stream combining. Let i be the index of the stream to be detected. First, the outputs $\mathbf{Y_{d1}}$ and $\mathbf{Y_{d2}}$ are filtered independently to nullify the interference of the streams yet to be detected. Next, the filtered signals are combined using maximal ratio combining. After the stream is detected and decoded based on the combined output, the contribution of stream i is subtracted both from $\mathbf{Y_{d1}}$ and $\mathbf{Y_{d2}}$.

This procedure can be mathematically represented as follows. After the QR decomposition, we have

$$\mathbf{H_{sd}} = \mathbf{Q_{sd}}\mathbf{R_{sd}} \text{ and } \quad \mathbf{H_{rd}} = \mathbf{Q_{rd}}\mathbf{R_{rd}},$$

where $\mathbf{Q_{sd}}, \mathbf{Q_{rd}} \in \mathbb{C}^{M_s,M_s}$ are unitary matrices satisfying $\mathbf{Q_{sd}^H}\mathbf{Q_{sd}} = \mathbf{Q_{rd}^H}\mathbf{Q_{rd}} = \mathbf{I}_{M_s}$ and $\mathbf{R_{sd}}, \mathbf{R_{rd}} \in \mathbb{C}^{M_s,K_d}$ are upper triangular matrices whose diagonal elements are positive. Then, we can write

$$\tilde{\mathbf{Y}}_\mathbf{1} = \mathbf{R_{sd}}\mathbf{W_d}\mathbf{C} + \tilde{\mathbf{N}}_\mathbf{1} \tag{7.15}$$

$$\tilde{\mathbf{Y}}_\mathbf{2} = \mathbf{R_{rd}}\mathbf{W_r}\mathbf{C} + \tilde{\mathbf{N}}_\mathbf{2}, \tag{7.16}$$

where $\tilde{\mathbf{Y}}_\mathbf{1} = \mathbf{Q_{sd}^H}\mathbf{Y_{d1}}$, $\tilde{\mathbf{Y}}_\mathbf{2} = \mathbf{Q_{rd}^H}\mathbf{Y_{d2}}$ and $\tilde{\mathbf{N}}_\mathbf{1}, \tilde{\mathbf{N}}_\mathbf{2}$ are statistically equivalent to $\mathbf{N_{d1}}$ and $\mathbf{N_{d2}}$. In this notation, decoding order is in terms of decreasing source index. ZF-DF decoding corresponds to decoding the last stream first and cancelling the effect of this codeword from all upper streams. To decode source j, destination combines j-th row of $\tilde{\mathbf{Y}}_\mathbf{1}$ and $\tilde{\mathbf{Y}}_\mathbf{2}$ using maximal ratio combining:

$$\mathbf{Y_c}(j,:) = \mathbf{R_{sd}}(j,j)\mathbf{W_d}(j,j)\mathbf{Y_{d1}}(j,:) + \mathbf{R_{rd}}(j,j)\mathbf{W_r}(j,j)\mathbf{Y_{d2}}(j,:). \tag{7.17}$$

Then, stream j is decoded based on $\mathbf{Y_c}(j,:)$ and its effect on $\tilde{\mathbf{Y}}_\mathbf{1}(1:j-1,:)$ and $\tilde{\mathbf{Y}}_\mathbf{2}(1:j-1,:)$ are cancelled. By continuing this process for all the streams, output SNR for source j, which is decoded as the i-th stream ($j = M_s - i + 1$) is given by

$$\beta_{\mathbf{i,d}} = \frac{1}{2}\left(\bar{\gamma}_{j,d}z^{(1)}(2(K_d - M_s + i)) + \bar{\gamma}_r z^{(2)}(2(K_d - M_s + i))\right), \tag{7.18}$$

where $z^{(1)}(m)$ and $z^{(2)}(m)$ are i.i.d. with $\chi^2(m)$ distribution.

7.3.3 $P_o^{s,r\to d}$ with JZF-DF and PZF-DF

Here, we analyze the performances of JZF-DF and PZF-DF under the assumption that the relay decoded all the sources correctly. We introduce two special topologies

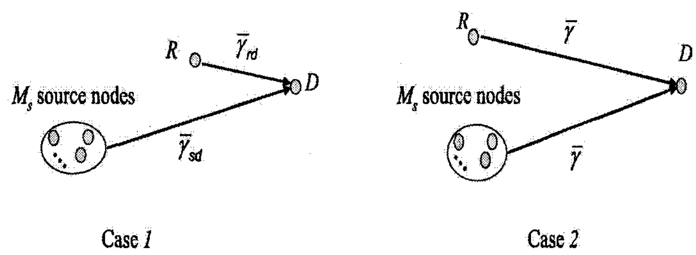

Figure 7.2: Illustration of *case 1* and *case 2*. In *case 1*, $\bar{\gamma}_{i,d} = \bar{\gamma}_{sd}$ for all $i = 1, 2, \ldots, M_s$. In *case 2*, in addition to this condition, $\bar{\gamma}_{rd} = \bar{\gamma}_{sd}$. However, in both cases, the sources can have arbitrary distances to the relay.

for which the performance comparison of JZF-DF and PZF-DF is easier. In *case 1*, it is assumed that all the sources have the same average SNR to the destination. Hence, $\mathbf{W_r} = \sqrt{\bar{\gamma}_r}\,\mathbf{I}_{M_s}$ and $\mathbf{W_d} = \sqrt{\bar{\gamma}_d}\,\mathbf{I}_{M_s}$. In *case 2*, which is a special case of *case 1*, the relay signal and the direct channel have the same average SNR, $\mathbf{W_r} = \mathbf{W_d} = \sqrt{\bar{\gamma}}\,\mathbf{I}_{M_s}$. Fig. 7.2 illustrates these special topologies.

$P_o^{s,r\to d}$ with JZF-DF

We note that, unlike individual channel matrices $\mathbf{H_{sd}}$ and $\mathbf{H_{rd}}$, for general diagonal $\mathbf{W_d}$ and $\mathbf{W_r}$, $\mathbf{H_e}$ is not a normal data matrix[2]. Thus, many useful results on normal data matrices do not apply to this problem.

Hence, for JZF-DF, only two special cases introduced above will be considered. Clearly, in *case 2*, JZF-DF is equivalent to direct transmission with $2K_d$ receive antennas instead of K_d. Hence, output SNR for the ith stream is chi-square distributed with $2(2K_d - M_s + i)$ degrees of freedom and diversity order is increased by K_d for all streams compared to the direct transmission.

[2]A random matrix is a normal data matrix if all of its row vectors are i.i.d. complex normal random vectors with arbitrary covariance matrix. Each column vector, however, must have identity covariance matrix [91].

In *case 1*, we can represent the equivalent channel as a Rayleigh channel with receive correlation [92] [93]:

$$\mathbf{H_e} = \mathbf{H_r H_w}, \tag{7.19}$$

where

$$\mathbf{H_r} = \begin{bmatrix} \sqrt{\bar{\gamma}_d}\,\mathbf{I}_{K_d} & \mathbf{0} \\ \mathbf{0} & \sqrt{\bar{\gamma}_r}\,\mathbf{I}_{K_d} \end{bmatrix}, \tag{7.20}$$

and $\mathbf{H_w} \in \mathbb{C}^{2K_d \times M_s}$ is a Rayleigh channel, whose elements are i.i.d. and distributed as $\mathbf{H_w}(i,j) \sim \mathcal{CN}(0,1)$. Exact CDF of output SNR for ZF receiver in a correlated Rayleigh MIMO channel is given in [94][3].

$P_o^{s,r\to d}$ with PZF-DF

In *case 2*, (7.18) simplifies to

$$\beta_{i,d} = \frac{1}{2}\bar{\gamma}\, z\left(4(K_d - M_s + i)\right), \tag{7.21}$$

where $z(m) \sim \chi^2(m)$. Hence, it is clear that, PZF-DF combining at the destination doubles the diversity order at each stage and the diversity order for the i-th source is $2(K_d - M_s + i)$, which is smaller than or equal to the one achieved by JZF-DF $(2K_d - M_s + i)$, for all $i = 1, 2, \ldots, M_s$ for any $M_s \geq 2$.

From (7.18), we observe that output SNR is a weighted sum of two chi-square random variables with even degrees of freedom. Theorem 2.4 of [95] provides a closed-form expression for the exact CDF of the weighted sum of an arbitrary number of chi-square random variables in terms of a finite sum of chi-square CDFs[4]. For completeness this theorem is given below.

[3] The derivation in [94] assumes that $\mathbf{R_{RX}} = \mathbf{H_r H_r}^H$ has distinct eigenvalues and its final results do not apply to our problem. Hence, for the numerical results we present in this chapter, we derived the CDF of output SNRs for a system with channel matrix given in (7.19) and (7.20).

[4] A less general form of this result later published in [96].

Theorem 7.1 (Theorem 2.4 of [95]). *The exact distribution of* $X = \sum_{j=1}^{r} \lambda_j \chi^2(\nu_j)$, *where the* $\nu_j = 2g_j$ *are even integers, is a weighted finite sum of* χ^2 *distributions,*

$$\mathbb{P}\{X > X_0\} = \sum_{j=1}^{r} \sum_{s=1}^{s_j} \alpha_{js} \mathbb{P}\{\chi^2(2s) > X_0/\lambda_j\},$$

and α_{js} *is a constant involving only the* λ*'s and is given by*

$$\alpha_{js} = f_j^{(g_j - s)}(0)/(g_j - s)!$$

where $f_j^{(h)}(0)$ *is obtained by differentiating* $f_j(y)$ h *times with respect to* y *and then putting* $y = 0$ *and*

$$f_j(y) = \prod_{i \neq j}^{r} \left[\frac{\lambda_j - \lambda_i}{\lambda_j} + y \frac{\lambda_i}{\lambda_j} \right]^{-\nu_i/2}.$$

Applying this theorem to our case, we obtain:

$$\mathbb{P}\{\beta_{i,d} > x\} = 1 - \sum_{j=1}^{2} \sum_{s=1}^{g_i} \alpha_{js} \mathbb{P}\left\{ \chi^2(2s) > \frac{x}{\lambda_j} \right\}, \tag{7.22}$$

where

$$\alpha_{1s} = f(g_i, s) \left(\frac{\lambda_2}{\lambda_1} \right)^{g_i - s} \left(\frac{\lambda_1 - \lambda_2}{\lambda_1} \right)^{-2g_i + s} \tag{7.23}$$

$$\alpha_{2s} = f(g_i, s) \left(\frac{\lambda_1}{\lambda_2} \right)^{g_i - s} \left(\frac{\lambda_2 - \lambda_1}{\lambda_2} \right)^{-2g_i + s}, \tag{7.24}$$

$$f(g_i, s) = (-1)^{g_i - s} \frac{(2g_i - s - 1)!}{(g_i - s)!(g_i - 1)!}, \tag{7.25}$$

$g_i = K_d - M_s + i$, $\lambda_1 = \bar{\gamma}_d/2$ and $\lambda_2 = \bar{\gamma}_r/2$. Note that (7.22) gives the exact outage probability for the i-th source with PZF-DF for general $\mathbf{W_r}$ and $\mathbf{W_d}$.

7.4 Results

We compare the system outage probability of all protocols and combining methods. All terminals transmit with the same power per antenna in each protocol. We consider two scenarios for the average link SNRs: linear network and symmetric network. In the linear network, the relay is located at the midpoint between the source nodes and the destination. That is, $\bar{\gamma}_{i,d} = \bar{\gamma}_{i,r}$. In particular, we assume that $\bar{\gamma}_{sd}$ is 12 dB lower than $\bar{\gamma}_{sr}$ and $\bar{\gamma}_{rd}$. This network is an example of *case 1*. In the symmetric network, all the links between all the antennas have the same average SNR, i.e., $\bar{\gamma}_{i,d} = \bar{\gamma}_{i,r} = \bar{\gamma}_{rd}$. Symmetric network is an example of *case 2*. The x-axis shows the SNR of the source-destination channel for direct transmission. For other protocols we plot the outage for the same total energy as the direct transmission. Target SNR $\gamma_{tr,i}$ is taken as 10 dB for all sources.

In Fig. 7.3, we plot the system outage probability of all protocols using both analytical results and Monte Carlo simulations for the linear network. Analytical curves are obtained from (7.5), (7.6), (7.10)-(7.12), and the derivations in Section 7.3.3. In simulations, output SNRs and outage rates are calculated based on a large number of randomly generated channel matrices. Having validated our analytical expressions for *case 1* in Fig. 7.3, in Fig. 7.4 we plot (analytical) system outage probability for a $2 \times 3 \times 2$ system for the linear network. As expected, conventional relaying provides only a constant SNR gain over direct transmission. In Fig. 7.3, we observe that the performance of NDR is limited by the source-relay channel, regardless of the combining method used at the destination. The NDR is also outperformed by TDDT at high average SNRs. For this configuration, we can conclude that the relaying protocol (NDR vs. SDR) is the dominant factor that determines the outage performance. In Fig. 7.4, however, we see that NDR and SDR have almost identical outage performances and the outage probability is mostly determined by the combining scheme.

In Fig.s 7.5 and 7.6 we plot the performance of $2 \times 2 \times 2$, and $2 \times 3 \times 2$ systems in the symmetric network. The observations for the linear network are valid for the symmetric network with the same configuration. The main difference is that in the symmetric network relaying protocols do not have any gain against the path loss and

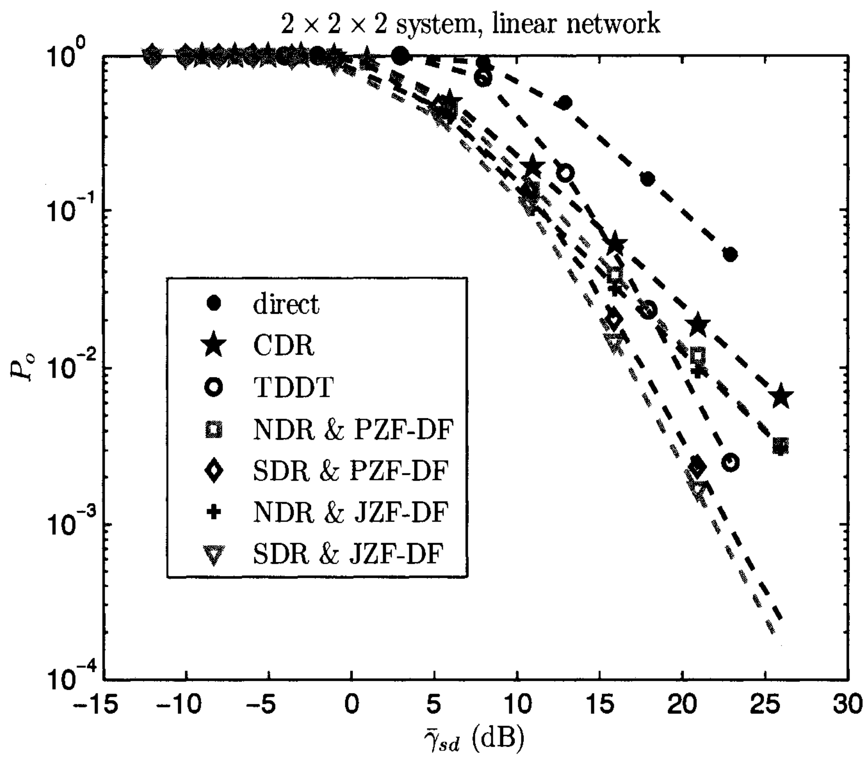

Figure 7.3: System outage probability of $2 \times 2 \times 2$ system in linear network case as a function of the average link SNR. Markers show simulation results and dashed lines show analytical results.

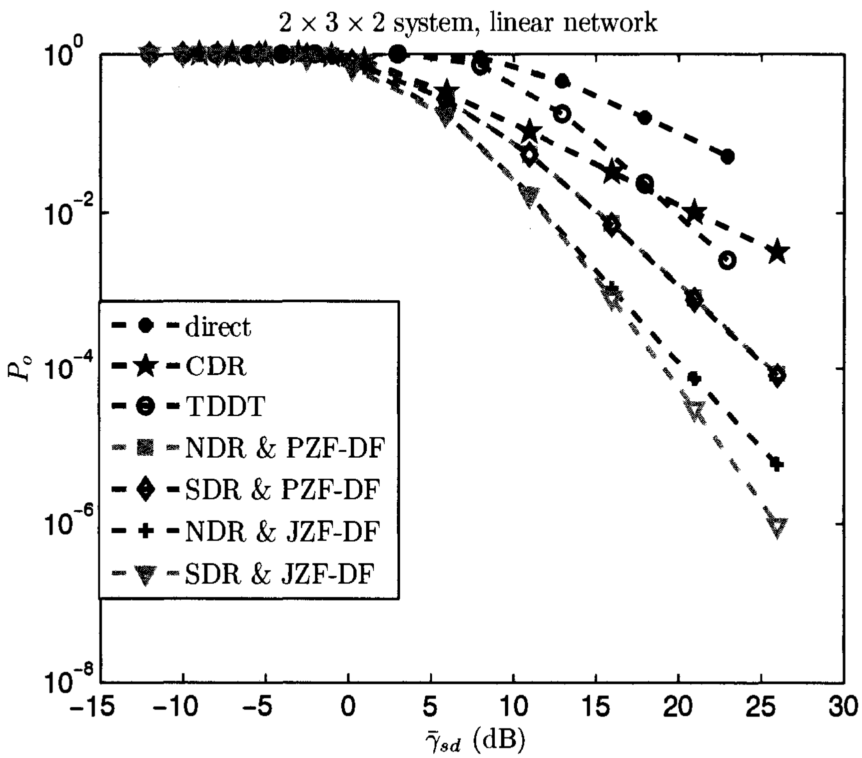

Figure 7.4: System outage probability of $2 \times 3 \times 2$ system in linear network case as a function of average link SNR.

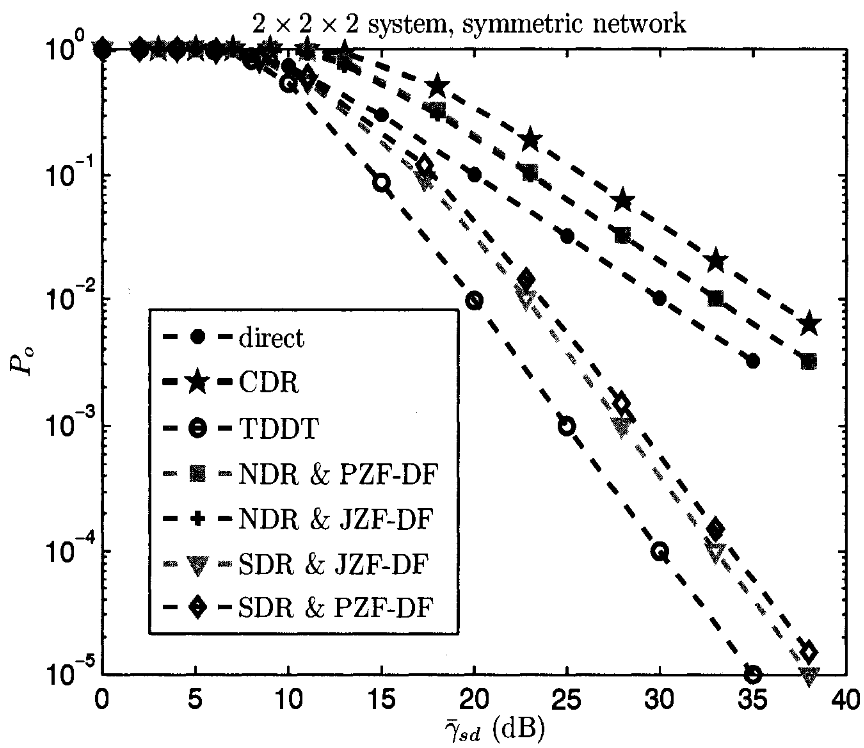

Figure 7.5: System outage probability of $2 \times 2 \times 2$ system in symmetric network case as a function of average link SNR.

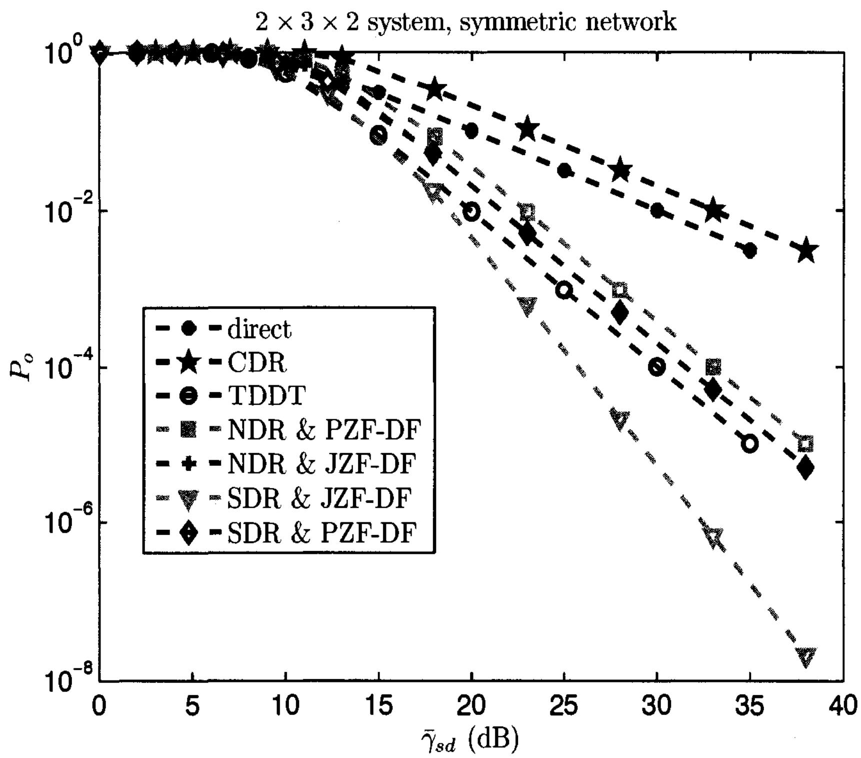

Figure 7.6: System outage probability of $2 \times 3 \times 2$ system in symmetric network case as a function of average link SNR.

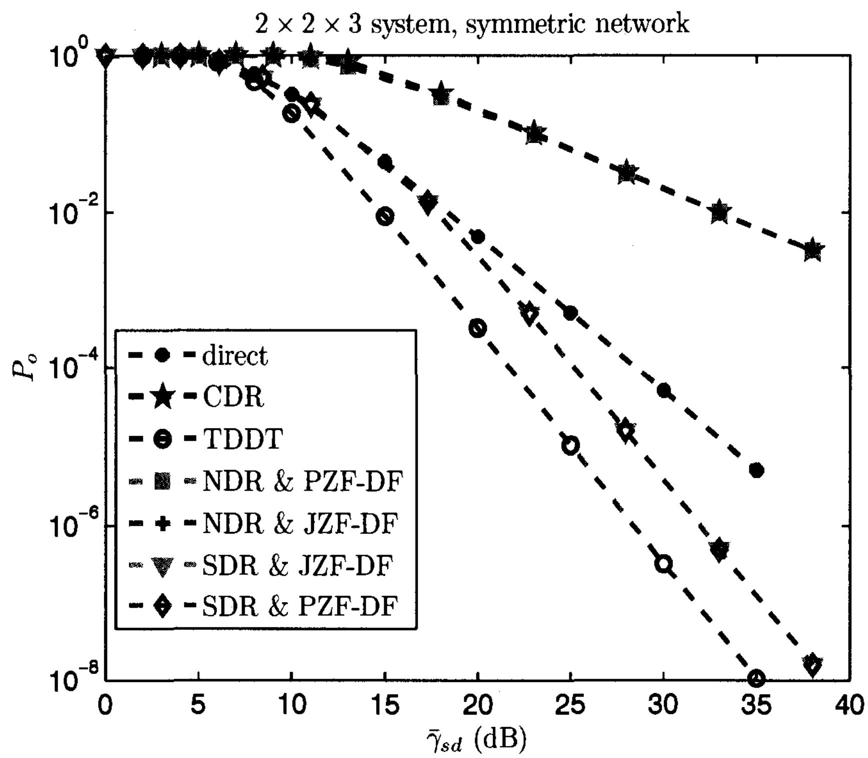

Figure 7.7: System outage probability of $2 \times 2 \times 3$ system in symmetric network case as a function of average link SNR.

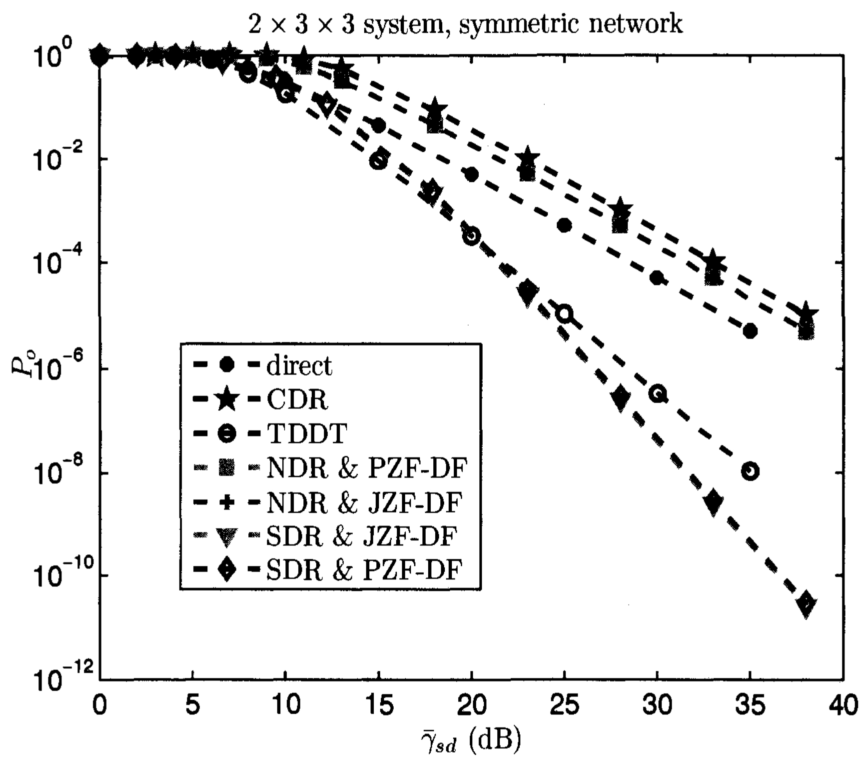

Figure 7.8: System outage probability of $2 \times 3 \times 3$ system in symmetric network case as a function of average link SNR.

hence they have less gain against direct transmission and TDDT.

In Figs. 7.7 and 7.8, we plot the system outage for $2 \times 2 \times 3$ and $2 \times 3 \times 3$ systems, respectively, again for the symmetric network case. In $2 \times 2 \times 3$ system, the TDDT protocol performs better than all the relaying protocol. This is due to the small number of antennas at the relay (K_r) compared to the number of antennas at the destination. As soon as we increase K_r to 3, as shown in Fig. 7.8, the SDR with either PZF-DF or JZF-DF outperforms TDDT.

7.5 Conclusions

This chapter discusses the potential benefits of using a multi-antenna relay in the spatial multiplexing of independent single antenna users communicating with a common multi-antenna destination. Digital relaying protocols of fixed vs. selective and conventional vs. diversity kind were considered. For diversity relaying, which has not been tackled so far in the context of multiple users/streams, we proposed two ZF-DF type combiners/decoders (JZF-DF and PZF-DF) to be used at the destination. We derived outage expressions, in closed-form for some special cases, and evaluated the performance for selective and non-selective relaying protocols.

Our study indicates that, as in single user case, significant gains can be obtained if spatially multiplexed data streams are relayed using diversity relaying instead of conventional relaying. Selective diversity relaying is crucial when the user-relay channel has lower diversity than the cooperative channel from the users and the relay to the destination, which is expected in most practical configurations. When user-relay channel is sufficiently reliable, which, for example, happens if the relay has a large number of antennas, diversity protocols are the most advantageous compared to conventional relaying. In this case, the performances of NDR and SDR for the same combining method are very close. Then, the outage probability is determined by the combining method used by the destination rather than the protocol used by the relay and JZF-DF has a considerably better performance than PZF-DF.

Chapter 8

Conclusions and Future Work Directions

Multihop communication presents many challenges as well as opportunities in wireless networks. In this thesis, we focused on cooperative diversity, which is one of the opportunities presented by multihop communication. We considered two-hop digital relaying in different scenarios and studied relaying strategies and combining schemes to induce end-to-end diversity. It is well-known that fixed relaying and combining strategies, in which relays forward the received data blindly and the destination combines the received signals independent of channel qualities, result in poor end-to-end performance. In this thesis, we concentrated on selective relaying strategies to achieve the diversity potential of cooperative diversity relaying.

The main conclusions and suggested future work for each part are summarized below.

1. Threshold based cooperative digital relaying as a method to mitigate error propagation without relying on channel coding has been studied.

    - A set of optimal threshold values that minimize the e2e BER in a single relay network under different CSI assumptions at the relay have been derived analytically. The BER performance of these thresholds have been evaluated and it has been shown that the optimal threshold selection can improve BER significantly.

- The asymptotic BER performance of threshold relaying has been analyzed. It has been observed that the optimal threshold increases logarithmically with the average link SNRs. It has been proven that the threshold relaying with the optimal threshold achieves full diversity. In addition, any threshold that increases logarithmically with the average link SNRs achieves the same diversity order as the optimal threshold.

- Threshold relaying for multiple parallel relays has been studied in the context of relay selection. A simple threshold based relay selection protocol has been proposed and its e2e error performance has been analyzed. Threshold values for the relays have been proposed and it has been shown that with the proposed threshold values the threshold based relay selection protocol achieves full diversity.

- Possible future work items for this topic are as follows:

  - Threshold based relaying policies in the presence of feedback from the destination to the source and the relays can be investigated. The objective is to obtain diversity with very infrequent retransmissions as in ARQ protocols. Our preliminary study shows that a single bit feedback from the destination based on received SNR of the direct link can achieve full diversity order with negligible multiplexing loss.

  - The analysis of optimal thresholds and their performance can be extended to networks which allow more than two hops.

  - The exact threshold expressions derived in this thesis are based on BPSK modulation. Extension of these expressions to more general modulation schemes, such as M-QAM can be another topic for future studies.

2. A selective cooperative relaying protocol for wireless ad hoc networks has been proposed and its network-wide benefit in random network topologies has been evaluated.

   - A simple two-hop relaying protocol has been designed for random and dynamic environments. This protocol selects different relays for different data packets opportunistically based on the outcome, i.e., success or failure, of the source-relay transmission and the local mean SNR of the relay-destination channels.

   - The outage probability of the relaying protocol has been evaluated analytically assuming that the relay nodes are distributed according to a two-dimensional Poisson point process with a given density. It has been shown that cooperative relaying can increase the average performance of the network significantly in such random topologies.

   - The performances of several relay selection criteria, such as distance from the relay to the destination and instantaneous SNR from the relay to the destination, have been studied. The average SNR to the destination has been identified as a good trade-off in terms of end-to-end outage performance and the signaling required for the relay selection.

   - Future studies on this topic may target the investigation of the gain of multi-hop cooperative relaying in terms of end-to-end throughput in random topologies.

3. The potential of multiple-antenna relays has been analyzed in the context of uplink in the form of distributed spatial multiplexing of multiple users.

   - To be employed in decode-and-forward diversity relaying of multiple data streams simultaneously, two different methods have been proposed to combine the direct user signals and the relayed signal. These methods, called Parallel ZF-DF and Joint ZF-DF, are both based on ZF-DF type MIMO receivers. The end-to-end outage performance has been derived analytically with these two combining schemes assuming i.i.d. Rayleigh fading.

- It is shown that using the proposed combining schemes in conjunction with selective decode-and-forward diversity relaying, the outage performance can be improved compared to the performance of direct transmission schemes.
- Possible future work on this topic includes:
  - designing transmit antenna selection and precoding strategies at the relay based on all the link quality information available for different channels.
  - analyzing the end-to-end diversity achieved by different relaying and combining schemes.
  - scheduling algorithms for selecting the set of users to be served based on the end-to-end performance.

List of References

[1] B. H. Walke, S. Mangold, and L. Berlemann, *IEEE 802 Wireless Systems: Protocols, Multi-hop Mesh/Relaying, Performance and Spectrum Coexistence.* Wiley & Sons, 2006.

[2] IEEE 802.16m System Requirements Document, available at http://wirelessman.org/tgm/docs/80216m-07_002r6.pdf.

[3] A. Sendonaris, E. Erkip, and B. Aazhang, "User cooperation diversity– Part I: System description," *IEEE Transactions on Communications*, vol. 51, pp. 1927–1938, Nov. 2003.

[4] N. Laneman, D. Tse, and G. Wornell, "Cooperative diversity in wireless networks: Efficient protocols and outage behavior," *IEEE Transactions on Information Theory*, vol. 50, pp. 3062–3080, Dec. 2004.

[5] R. Pabst, B. H. Walke, D. C. Schultz, P. Herhold, H. Yanikomeroglu, S. Mukherjee, H. Viswanathan, M. Lott, W. Zirwas, M. Dohler, H. Aghvami, D. D. Falconer, and G. P. Fettweis, "Relay-based deployment concepts for wireless and mobile broadband cellular radio," *IEEE Communications Magazine*, vol. 42, pp. 80–89, Sept. 2004.

[6] H. Takagi and L. Kleinrock, "Optimal transmission ranges for randomly distributed packet radio terminals," *IEEE Transactions on Communications*, vol. 32, pp. 246–257, Mar. 1984.

[7] L. Kleinrock and J. Silvester, "Spatial reuse in multihop packet radio networks," *Proc. of IEEE*, vol. 75, pp. 156–167, Jan. 1987.

[8] F. A. Tobagi, "Modeling and performance analysis of multihop packet radio networks," *Proc. of IEEE*, vol. 75, pp. 135–155, Jan. 1987.

[9] J. G. Andrews, A. Ghosh, and R. Muhamed, *Fundamentals of WiMAX: Understanding Broadband Wireless Networking.* Prentice Hall, 2007.

[10] J. G. Proakis, *Digital Communications.* McGraw-Hill, 2000.

[11] M. O. Hasna and M.-S. Alouini, "Harmonic mean and end-to-end performance of transmission systems with relays," *IEEE Transactions on Wireless Communications*, vol. 52, pp. 130–135, Jan. 2004.

[12] M. O. Hasna and M.-S. Alouini, "Outage probability of multihop transmission over Nakagami fading channels," *IEEE Communications Letters*, vol. 7, pp. 216 – 218, May 2003.

[13] A. Florea and H. Yanikomeroglu, "On the optimal number of hops in infrastructure-based fixed relay networks," in *Proc. of IEEE Globecom Conference*, Nov. 2005.

[14] Ö. Oyman, J. N. Laneman, and S. Sandhu, "Multihop relaying for broadband wireless mesh networks: From theory to practice," *IEEE Communications Magazine*, vol. 45, pp. 116–122, Nov. 2007.

[15] E. M. Royer and C.-K. Toh, "A review of current routing protocols for ad hoc mobile wireless networks," *IEEE Personal Communications*, vol. 6, pp. 46–55, Apr. 1999.

[16] R. Rajaraman, "Topology control and routing in ad hoc networks: A survey," *ACM SIGACT News*, vol. 33, pp. 60 – 73, June 2002.

[17] T. ElBatt and A. Ephremides, "Joint scheduling and power control for wireless ad hoc networks," *IEEE Transactions on Wireless Communications*, vol. 3, pp. 74–85, Jan. 2004.

[18] R. Ramanathan, J. Redi, C. Santivanez, D. Wiggins, and S. Polit, "Ad hoc networking with directional antennas: a complete system solution," *IEEE Journal on Selected Areas in Communications*, vol. 23, pp. 496– 506, Mar. 2005.

[19] M. Takai, J. Martin, and R. Bagrodia, "Effects of wireless physical layer modeling in mobile ad hoc networks," in *Proc. of ACM MobiHoc Conference*, Oct. 2001.

[20] V. Tarokh, H. Jafarkhani, and A. R. Calderbank, "Space-time block coding for wireless communications: Performance results," *IEEE Journal on Selected Areas in Communications*, vol. 17, pp. 451–460, Mar. 1999.

[21] D. Tse and P. Viswanath, *Fundamentals of Wireless Communication.* Cambridge University Press, 2005.

[22] L. Zheng and D. Tse, "Diversity and multiplexing: A fundamental trade-off in multiple antenna channels," *IEEE Trans. Information Theory*, vol. 49, pp. 1073– 1096, May 2003.

[23] T. M. Cover and A. E. Gamal, "Capacity theorems for the relay channel," *IEEE Transactions on Information Theory*, vol. 25, pp. 572–584, Sep. 1979.

[24] E. C. van der Meulen, "Three-terminal communication channels," *Advances in Applied Probability*, vol. 3, pp. 120–154, Spring 1971.

[25] A. Host-Madsen and J. Zhang, "Capacity bounds and power allocation for wireless relay channels," *IEEE Transactions on Information Theory*, vol. 51, pp. 2020–2040, June 2005.

[26] G. Kramer, M. Gastpar, and P. Gupta, "Cooperative Strategies and Capacity Theorems for Relay Networks," *IEEE Transactions on Information Theory*, vol. 51, pp. 3037–3063, Sept. 2005.

[27] J. Boyer, D. D. Falconer, and H. Yanikomeroglu, "Multihop diversity in wireless relaying channels," *IEEE Transactions on Communications*, vol. 52, pp. 1820–1830, Oct. 2004.

[28] A. Ribeiro, X. Cai, and G. B. Giannakis, "Symbol error probabilities for general cooperative links," *IEEE Transactions on Wireless Communications*, vol. 4, pp. 1264–1273, May 2005.

[29] D. Chen and J. Laneman, "Modulation and demodulation for cooperative diversity in wireless systems," *IEEE Transactions on Wireless Communications*, vol. 5, pp. 1785–1794, July 2006.

[30] T. Wang, A. Cano, G. B. Giannakis, and J. N. Laneman, "High-performance cooperative demodulation with decode-and-forward relays," vol. 55, pp. 1427–1438, July 2007.

[31] T. Wang, R. Wang, and G. Giannakis, "Smart regenerative relays for link-adaptive cooperative communications," in *Proc. of 40-th Annual Conference on Information Sciences and Systems (CISS)*, Mar. 2006.

[32] J. Boyer, D. D. Falconer, and H. Yanikomeroglu, "Cooperative connectivity models for wireless relay networks," *IEEE Transactions on Wireless Communications*, vol. 6, pp. 1992–2000, June 2007.

[33] A. Stefanov and E. Erkip, "Cooperative coding for wireless networks," *IEEE Transactions on Communications*, vol. 52, pp. 1470–1476, Sept. 2004.

[34] T. E. Hunter and A. Nosratinia, "Diversity through coded cooperation," *IEEE Transactions on Wireless Communications*, vol. 5, pp. 283–289, Feb. 2006.

[35] J. N. Laneman and G. W. Wornell, "Distributed space-time-coded protocols for exploiting cooperative diversity in wireless networks," *IEEE Transactions on Information Theory*, vol. 49, pp. 2415–2425, Oct. 2003.

[36] Y. Jing and B. Hassibi, "Distributed space-time coding in wireless relay networks," *IEEE Transactions on Wireless Communications*, vol. 5, pp. 3524–3536, Dec. 2006.

[37] P. Anghel, G. Leus, and M. Kaveh, "Multi-user space-time coding in cooperative networks," in *Proc. of International Conference on Acoustics, Speech, and Signal Processing*, Apr. 2003.

[38] E. Beres and R. Adve, "Selection cooperation in multi-source cooperative networks," *IEEE Transactions on Wireless Communications*, vol. 7, pp. 118–127, Jan. 2008.

[39] A. Bletsas, A. Khisti, and M. Win, "Opportunistic cooperative diversity with feedback and cheap radios," *IEEE Transactions on Wireless Communications*, vol. 7, pp. 1823–1827, May 2008.

[40] A. Adinoyi, Y. Fan, H. Yanikomeroglu, and V. Poor, "On the performance of selective relaying," in *Proc. IEEE Vehicular Technology Conference (VTC) Fall*, Sept. 2008.

[41] K. Azarian, H. Gamal, and P. Schniter, "On the achievable diversity-multiplexing tradeoff in half-duplex cooperative channels," *IEEE Transactions on Information Theory*, vol. 51, pp. 4152–4172, Dec. 2005.

[42] P. Mitran, H. Ochiai, and V. Tarokh, "Space-time diversity enhancements using collaborative communications," *IEEE Transactions on Information Theory*, vol. 51, pp. 2041–2057, June 2005.

[43] H. Ochiai, P. Mitran, and V. Tarokh, "Variable-Rate Two-Phase Collaborative Communication Protocols for Wireless Networks," *IEEE Transactions on Information Theory*, vol. 52, pp. 4299–4313, Sept. 2006.

[44] A. Adinoyi and H. Yanikomeroglu, "Cooperative relaying in multi-antenna fixed relay networks," *IEEE Transactions on Wireless Communications*, vol. 6, pp. 533–544, Feb. 2007.

[45] Y. Fan, A. Adinoyi, J. Thompson, and H. Yanikomeroglu, "Antenna combining for multi-antenna multi-relay channels," *European Transactions on Telecommunications*, vol. 18, pp. 617–626, Oct. 2007.

[46] S. Valentin, T. Volkhausen, F. A. Onat, H. Yanikomeroglu, and H. Karl, "Enabling partial forwarding by decoding-based one and two-stage selective cooperation," in *Proc. of IEEE Cognitive and Cooperative Wireless Networks (CoCoNET) Workshop collocated with IEEE ICC*, May 2008.

[47] Texas Instruments, CC2420 data sheet. 2.4 GHz IEEE 802.15.4 / ZigBee-Ready RF Transceiver. Available at: http://focus.ti.com/lit/ds/symlink/cc2420.pdf.

[48] I. F. Akyildiz, W. Su, Y. Sankarasubramaniam, and E. Cayirci, "A survey on sensor networks," *IEEE Communications Magazine*, vol. 40, pp. 102–114, Aug. 2002.

[49] M. Zorzi and R. R. Rao, "Coding tradeoffs for reduced energy consumption in sensor networks," in *Proc. of IEEE Personal, Indoor and Mobile Radio Communications (PIMRC)*, Sept. 2004.

[50] P. Herhold, E. Zimmermann, and G. Fettweis, "A simple cooperative extension to wireless relaying," in *Proc. of International Zurich Seminar on Communications*, 2004. Long version, available at http://wwwmns.ifn.et.tu-dresden.de/publications/2004/Herhold_P_IZS_04.pdf.

[51] A. Adinoyi and H. Yanikomeroglu, "Multi-antenna aspects of parallel fixed wireless relays," in *Proc. of IEEE Wireless Communications and Networking Conference (WCNC)*, Apr. 2006.

[52] W. P. Siriwongpairat, T. Himsoon, W. Su, and K. J. R. Liu, "Optimum threshold-selection relaying for decode-and-forward cooperation protocol," in *Proc. of IEEE Wireless Communications and Networking Conference (WCNC)*, Apr. 2006.

[53] T. Wang, A. Cano, and G. Giannakis, "Link-adaptive cooperative communications without channel state information," in *Proc. of Military Communications Conference (MILCOM)*, Oct. 2006.

[54] A. Goldsmith, *Wireless Communications.* Cambridge University Press, 2005.

[55] S. P. Ponnaluri and S. G. Wilson, "On diversity of cooperative relaying protocols," in *Proc. of IEEE International Conference on Communications and Networking (ChinaCom)*, Aug. 2007.

[56] J. M. Wozencraft and I. M. Jacobs, *Principles of Communication Engineering.* Waveland Press, 1965.

[57] A. Bletsas, H. Shin, and M. Z. Win, "Outage-optimal cooperative communications with regenerative relays," in *Proc. of 40-th Annual Conference on Information Sciences and Systems (CISS), Princeton, NJ*, Mar. 2006.

[58] Z. Yi and I.-M. Kim, "Decode-and-forward cooperative networks with relay selection," in *Proc. of Vehicular Technology Conference (VTC) Fall*, Oct. 2007.

[59] J. Metzner and D. Chang, "Efficient selective repeat ARQ strategies for very noisy and fluctuating channels," *IEEE Transactions on Communications*, vol. 33, pp. 409–416, May 1985.

[60] S. Kallel and D. Haccoun, "Generalized type II hybrid ARQ scheme using punctured convolutional coding," *IEEE Transactions on Communications*, vol. 38, pp. 1938–1946, Nov. 1990.

[61] Y. Guan-Ding, Z. Zhao-Yang, and Q. Pei-Liang, "Space-time code ARQ protocol for wireless networks," in *Proc. of International Conference on Wireless Communications, Networking and Mobile Computing*, Sep. 2005.

[62] M. Zorzi and R. R. Rao, "Geographic random forwarding (GeRaF) for ad hoc and sensor networks: Multihop performance," *IEEE Transactions on Mobile Computing*, vol. 2, pp. 337–348, Dec. 2003.

[63] E. Khandani, E. Modiano, J. Abounadi, and L. Zheng, "Reliability and route discovery in wireless networks," in *Proc. of Conference on Information Sciences and Systems (CISS)*, Mar. 2005.

[64] S. Biswas and R. Morris, "ExOR: Opportunistic multi-hop routing for wireless networks," in *Proc. of SIGCOMM Conference on Applications, Technologies, Architectures, and Protocols for Computer Communications*, Oct. 2005.

[65] M. Zorzi and R. R. Rao, "Geographic random forwarding (GeRaF) for ad-hoc and sensor networks: energy and latency performance," *IEEE Transactions on Mobile Computing*, vol. 2, pp. 349–365, Oct. 2003.

[66] B. Zhao and M. C. Valenti, "Practical relay networks: a generalization of hybrid-ARQ," *IEEE Journal on Selected Areas in Communications*, vol. 23, pp. 7–18, Jan. 2005.

[67] L. Song and D. Hatzinakos, "Cooperative transmission in poisson distributed wireless sensor networks: protocol and outage probability," *IEEE Transactions on Wireless Communications*, vol. 5, pp. 2834– 2843, Oct. 2006.

[68] A. Bletsas, A. Khisti, D. Reed, and A. Lippman, "A simple cooperative diversity method based on network path selection," *IEEE Journal on Selected Areas in Communications*, vol. 24, pp. 659–672, Mar. 2006.

[69] Z. Lin, E. Erkip, and A. Stefanov, "Cooperative regions and partner choice in coded cooperative systems," *IEEE Transactions on Communications*, vol. 54, pp. 1323–1334, July 2006.

[70] J. F. C. Kingman, *Poisson Processes.* Oxford University Press, 1993.

[71] S. Mukherjee and D. Avidor, "Outage probabilities in poisson and clumped poisson-distributed hybrid ad-hoc networks," in *Proc. of IEEE Conference on Sensor and Ad-hoc Networks (SECON)*, Sep. 2005.

[72] N. Kong, T. Eng, and L. Milstein, "A selection combining scheme for rake receivers," in *Proc. of IEEE International Conference on Universal Personal Communications (ICUPC)*, Nov. 1995.

[73] S. M. Ross, *An Introduction to Probability Models.* Harcourt Academic Press, 2000.

[74] E. W. Weisstein, "Lambert W-function." From MathWorld–A Wolfram Web Resource (http://mathworld.wolfram.com/LambertW-Function.html).

[75] J. Boyer, D. D. Falconer, and H. Yanikomeroglu, "Diversity order bounds for wireless relay networks," in *Proc. of IEEE Wireless Communications and Networking Conference (WCNC)*, Mar. 2007.

[76] E. Telatar, "Capacity of multi-antenna gaussian channels," *European Transactions on Telecommunications*, vol. 10, pp. 585–595, Nov. 1999.

[77] G. J. Foschini and M. J. Gans, "On limits of wireless communications in a fading environment when using multiple antennas," *Wireless Personal Communications*, vol. 6, pp. 311–335, Mar. 1998.

[78] A. Goldsmith, S. Jafar, N. Jindal, and S. Vishwanath, "Capacity limits of MIMO channels," *IEEE Journal on Selected Areas in Communications*, vol. 21, pp. 684–702, June 2003.

[79] H. Bölcskei, R. U. Nabar, Ö. Oyman, and A. J. Paulraj, "Capacity scaling laws in MIMO relay networks," *IEEE Transactions on Wireless Communications*, vol. 5, pp. 1433–1444, June 2006.

[80] Y. Fan and J. Thompson, "MIMO configurations for relay channels: Theory and practice," *IEEE Transactions on Wireless Communications*, vol. 6, pp. 1774–1786, May 2007.

[81] Y. Fan and J. Thompson, "On the outage capacity of MIMO multihop networks," in *Proc. of IEEE Globecom Conference*, Nov. 2005.

[82] P. Wolniansky, G. Foschini, G. Golden, and R. Valenzuela, "V-BLAST: An architecture for realizing very high data rates overthe rich-scattering wireless channel," in *Proc. of URSI International Symposium on Signals, Systems, and Electronics*, Oct. 1998.

[83] H.-V. Khuong and T. Le-Ngoc, "A bandwidth-efficient cooperative relaying scheme with limited feedback information," in *Proc. of 24-th Queen's Biennial Symposium on Communications*, June 2008.

[84] H.-V. Khuong and T. Le-Ngoc, "A bandwidth-efficient cooperative relaying scheme with space-time block coding and iterative decoding," in *Proc. of International Conference on Communications and Electronics (ICCE)*, June 2008.

[85] H.-V. Khuong and T. Le-Ngoc, "Bandwidth-efficient cooperative relaying schemes with multiantenna relay." *EURASIP Journal on Advances in Signal Processing*, Article ID 683105, 11 pages, 2008. doi:10.1155/2008/683105.

[86] G. Foschini, D. Chizhik, M. Gans, C. Papadias, and R. Valenzuela, "Analysis and performance of some basic space-time architectures," *IEEE Journal on Selected Areas in Communications*, vol. 21, pp. 303– 320, Apr. 2003.

[87] J. H. Winters, J. Salz, and R. D. Gitlin, "The impact of antenna diversity on the capacity of wireless communication systems," *IEEE Transactions on Communications*, vol. 42, pp. 1740 –1751, 1994.

[88] T. Guess, H. Zhang, and T. Kotchiev, "The outage capacity of BLAST for MIMO channels," in *Proc. of IEEE International Conference on Communications (ICC'03)*, May 2003.

[89] R. Horn and C. Johnson, *Matrix Analysis.* Cambridge University Press, 1990.

[90] R. J. Muirhead, *Aspects of Multivariate Statistical Theory.* Wiley & Sons, 1982.

[91] K. V. Mardia, J. T. Kent, and J. M. Bibby, *Multivariate Analysis.* Academic Press, 1979.

[92] M. Kiessling and J. Speidel, "Asymptotically tight bound on SER of MIMO zero-forcing receivers with correlated fading," in *Proc. of International Symposium on Information Theory (ISIT)*, 2004.

[93] H. Shin and J. H. Lee, "Capacity of multiple-antenna fading channels: Spatial fading correlation, double scattering, and keyhole," *IEEE Transactions on Information Theory*, vol. 49, 2003.

[94] M. Kiessling, "MIMO zero-forcing receivers Part I: Multivariate statistical analysis." submitted for publication, available at http://www.inue.uni-stuttgart.de/publications/pub_2005/kiessling_ZF_performance.pdf.

[95] G. E. P. Box, "Some theorems on quadratic forms applied in the study of analysis of variance problems, I. Effect of inequality of variance in the one-way classification," *The Annals of Mathematical Statistics*, vol. 25, pp. 484–498, 1954.

[96] N. C. Beaulieu and J. Hu, "A closed-form expression for the outage probability of decode-and-forward relaying in dissimilar rayleigh fading channels," *IEEE Communications Letters*, vol. 10, pp. 813–815, Dec. 2006.

[97] M. K. Simon and M.-S. Alouini, *Digital Communication over Fading Channels: A Unified Approach to Performance Analysis.* Wiley & Sons, 2000.

[98] M. K. Simon, S. M. Hinedi, and W. C. Lindsey, *Digital Communication Techniques: Signal Design and Detection.* Prentice Hall, 1995.

[99] F. A. Onat, A. Adinoyi, Y. Fan, H. Yanikomeroglu, and J. S. Thompson, "Optimum threshold for SNR-based selective digital relaying schemes in cooperative wireless networks," in *Proc. of IEEE Wireless Communications and Networking Conference (WCNC)*, Mar. 2007.

[100] D. V. Widder, *Advanced Calculus.* Eaglewood Cliffs, 1961.

[101] J. W. Craig, "A new, simple, and exact result for calculating the probability of error for two-dimensional signal constellations," in *Proc. of IEEE Military Communications Conference (MILCOM)*, Oct. 1991.

Appendix A

Derivations for Chapter 3

A.1 Derivation of $h(x, y)$ Given in (3.14)

We first introduce two integrals, which we derive using integration by parts.

$$J_1(a,b,c;x_0,x_1) = \int_{x_0}^{x_1} \mathrm{erfc}\left(\sqrt{ax+b}\right) e^{-cx} \mathrm{d}x$$
$$= \left\{ -\frac{1}{c}\mathrm{erfc}(\sqrt{ax+b})e^{-cx} - \frac{1}{c}\sqrt{\frac{a}{a+c}}\left(1 - \mathrm{erfc}\left(\sqrt{(a+c)/a}\,\sqrt{ax+b}\right)\right) e^{bc/a} \right\} \Bigg]_{x_0}^{x_1}, \tag{A.1}$$

where $x_0, x_1, c \geq 0$, $(a+c)/a \geq 0$, and

$$J_2(a,b,c;x_0,x_1) = \int_{x_0}^{x_1} \mathrm{erfc}\left(a\sqrt{x}+b\right) e^{-cx} \mathrm{d}x = \left\{ -\frac{1}{c}\mathrm{erfc}(a\sqrt{x}+b)e^{-cx} \right.$$
$$\left. - \frac{a}{c\sqrt{a^2+c}}\left(1 - \mathrm{erfc}\left(\sqrt{a^2+c}\,\sqrt{x} + ab/\sqrt{a^2+c}\right)\right) \exp(-b^2 + a^2b^2/(a^2+c)) \right\} \Bigg]_{x_0}^{x_1}, \tag{A.2}$$

where $x_0, x_1, c \geq 0$.

The function $h(x, y)$, which is defined as $h(x,y) = \int_x^\infty \frac{1}{2y} e^{-t/y} \mathrm{erfc}(\sqrt{t})\mathrm{d}t$, can be expressed as

$$h(x,y) = \frac{1}{2y} J_1(1, 0, 1/y; x, \infty)$$
$$= \frac{1}{2}\mathrm{erfc}(\sqrt{x})e^{-x/y} - \sqrt{\frac{y}{1+y}}\frac{1}{2}\mathrm{erfc}\left(\sqrt{x\left(1+\frac{1}{y}\right)}\right), \tag{A.3}$$

which is the same as the expression given in (3.14). In [50], the authors used a similar derivation to obtain Eqn. (15) of their paper.

A.2 Derivation of $\mathbb{P}\{\mathcal{E}_{sr}|\gamma_{sr} > \gamma_t\}$

Consider a general modulation scheme that has a probability of bit error rate of $P_b(\gamma) = \beta_m \mathrm{erfc}(\sqrt{\alpha_m \gamma})$. The probability of bit error at the $S - R$ link given that $\gamma_{sr} > \gamma_t$ is equal to

$$\mathbb{P}\{\mathcal{E}_{sr}|\gamma_{sr} > \gamma_t\} = \int \beta_m \,\mathrm{erfc}(\sqrt{\alpha_m \gamma_{sr}})\, p_{\gamma_{sr}|\gamma_{sr}>\gamma_{t1}}(\gamma_{sr})\mathrm{d}\gamma_{sr}, \tag{A.4}$$

$$\mathbb{P}\{\mathcal{E}_{sr}|\gamma_{sr} > \gamma_{t1}\}=\frac{\exp(\gamma_{t1}/\bar{\gamma}_{sr})}{\bar{\gamma}_{sr}} \int_{\gamma_{t1}}^{\infty} \beta_m \mathrm{erfc}(\sqrt{\alpha_m \gamma_{sr}})\, \exp(-\gamma_{sr}/\bar{\gamma}_{sr})\, \mathrm{d}\gamma_{sr} \tag{A.5}$$

$$= \exp(\gamma_{t1}/\bar{\gamma}_{sr})\frac{\beta_m}{\bar{\gamma}_{sr}} J_1(\alpha_m, 0, 1/\bar{\gamma}_{sr}; \gamma_t, \infty) \tag{A.6}$$

$$= \beta_m \left[\mathrm{erfc}(\sqrt{\alpha_m \gamma_{t1}}) - e^{\gamma_{t1}/\bar{\gamma}_{sr}} \sqrt{\frac{\alpha_m \bar{\gamma}_{sr}}{1+\alpha_m \bar{\gamma}_{sr}}}\, \mathrm{erfc}\left(\sqrt{\gamma_{t1}\left(\alpha_m + \frac{1}{\bar{\gamma}_{sr}}\right)}\right)\right] \tag{A.7}$$

where we substituted the function J_1 given by (B.8) to obtain (A.7) from (A.6).

A.3 Average BER Calculation for Models 2, 3, and 4

For Model 2 the e2e BER conditioned on γ_{sr} and γ_{rd} is equal to

$$\mathrm{BER}_{e2e}^{(2)}(\gamma_{sr}, \gamma_{rd}, \bar{\gamma}_{sd}) = \begin{cases} \mathbb{P}\{\mathcal{E}_{sd}|\bar{\gamma}_{sd}\}, & \gamma_{sr} < \gamma_{t2}^{*}(\gamma_{rd}, \bar{\gamma}_{sd}); \\ \mathbb{P}\{\mathcal{E}_{sr}|\gamma_{sr}\} \left(\mathbb{P}\{\mathcal{E}_{prop}|\gamma_{rd}, \bar{\gamma}_{sd}\} - \mathbb{P}\{\mathcal{E}_{coop}|\gamma_{rd}, \bar{\gamma}_{sd}\}\right) & \\ +\mathbb{P}\{\mathcal{E}_{coop}|\gamma_{rd}, \bar{\gamma}_{sd}\}, & \text{otherwise.} \end{cases}$$

The average e2e BER can be obtained by averaging $\mathrm{BER}^{(2)}_{e2e}(\gamma_{sr}, \gamma_{rd}, \bar{\gamma}_{sd})$ over γ_{sr} and γ_{rd}:

$$\begin{aligned}\mathrm{BER}^{(2)}_{e2e}(\bar{\gamma}_{sr}, \bar{\gamma}_{rd}, \bar{\gamma}_{sd}) &= \mathbb{E}_{\gamma_{sr},\gamma_{rd}}\left[\mathrm{BER}^{(2)}_{e2e}(\gamma_{sr}, \gamma_{rd}, \bar{\gamma}_{sd})\right] \\ &= \mathbb{E}_{\gamma_{rd}}\left[\mathbb{E}_{\gamma_{sr}}\left[\mathrm{BER}^{(2)}_{e2e}(\gamma_{sr}, \gamma_{rd}, \bar{\gamma}_{sd})\right]\right]. \end{aligned} \tag{A.8}$$

The first expectation is equal to

$$\begin{aligned}\mathbb{E}_{\gamma_{sr}}\left[\mathrm{BER}^{(2)}_{e2e}(\gamma_{sr}, \gamma_{rd}, \bar{\gamma}_{sd})\right] &= \int_0^{\gamma^*_{t2}(\gamma_{rd},\bar{\gamma}_{sd})} \mathbb{P}\{\mathcal{E}_{sd}|\bar{\gamma}_{sd}\} p_{\gamma_{sr}} \mathrm{d}\gamma_{sr} \\ &= \int_{\gamma^*_{t2}(\gamma_{rd},\bar{\gamma}_{sd})}^{\infty} \mathbb{P}\{\mathcal{E}_{sr}|\gamma_{sr}\}\left(\mathbb{P}\{\mathcal{E}_{prop}|\gamma_{rd}, \bar{\gamma}_{sd}\} - \mathbb{P}\{\mathcal{E}_{coop}|\gamma_{rd}, \bar{\gamma}_{sd}\}\right) p_{\gamma_{sr}} \mathrm{d}\gamma_{sr} \\ &+ \int_{\gamma^*_{t2}(\gamma_{rd},\bar{\gamma}_{sd})}^{\infty} \mathbb{P}\{\mathcal{E}_{coop}|\gamma_{rd}, \bar{\gamma}_{sd}\} p_{\gamma_{sr}} \mathrm{d}\gamma_{sr} \\ &= \mathbb{P}\{\mathcal{E}_{sd}|\bar{\gamma}_{sd}\}(1 - \exp(-\gamma^*_{t2}(\gamma_{rd}, \bar{\gamma}_{sd})/\bar{\gamma}_{sr})) \\ &+ \left(\mathbb{P}\{\mathcal{E}_{prop}|\gamma_{rd}, \bar{\gamma}_{sd}\} - \mathbb{P}\{\mathcal{E}_{coop}|\gamma_{rd}, \bar{\gamma}_{sd}\}\right) h(\gamma^*_{t2}(\gamma_{rd}, \bar{\gamma}_{sd}), \bar{\gamma}_{sr}) \\ &+ \mathbb{P}\{\mathcal{E}_{coop}|\gamma_{rd}, \bar{\gamma}_{sd}\} \exp(-\gamma^*_{t2}(\gamma_{rd}, \bar{\gamma}_{sd})/\bar{\gamma}_{sr}) \end{aligned} \tag{A.9}$$

By taking the expectation of (A.9) over γ_{rd} we obtain

$$\begin{aligned}\mathrm{BER}^{(2)}_{e2e}(\bar{\gamma}_{sr}, \bar{\gamma}_{rd}, \bar{\gamma}_{sd}) = \mathbb{E}_{\gamma_{rd}}\Big[&\mathbb{P}\{\mathcal{E}_{sd}|\bar{\gamma}_{sd}\}(1 - \exp(-\gamma^*_{t2}(\gamma_{rd}, \bar{\gamma}_{sd})/\bar{\gamma}_{sr})) \\ &+ \left(\mathbb{P}\{\mathcal{E}_{prop}|\gamma_{rd}, \bar{\gamma}_{sd}\} - \mathbb{P}\{\mathcal{E}_{coop}|\gamma_{rd}, \bar{\gamma}_{sd}\}\right) h(\gamma^*_{t2}(\gamma_{rd}, \bar{\gamma}_{sd}), \bar{\gamma}_{sr}) \\ &+ \mathbb{P}\{\mathcal{E}_{coop}|\gamma_{rd}, \bar{\gamma}_{sd}\} \exp(-\gamma^*_{t2}(\gamma_{rd}, \bar{\gamma}_{sd})/\bar{\gamma}_{sr})\Big]. \end{aligned} \tag{A.10}$$

After substituting (3.6), (3.15), and (3.24) into (A.10) the average BER of Model 2 is found as

$$\begin{aligned}\mathrm{BER}^{(2)}_{e2e}(\bar{\gamma}_{sr}, \bar{\gamma}_{rd}, \bar{\gamma}_{sd}) \approx \int_0^{\infty} \Bigg[&\frac{1}{2}\left(1 - \sqrt{\frac{\bar{\gamma}_{sd}}{1+\bar{\gamma}_{sd}}}\right)(1 - \exp(-\gamma^*_{t2}(\gamma_{rd}, \bar{\gamma}_{sd})/\bar{\gamma}_{sr})) \\ &+ \left((1 - e^{-\gamma_{rd}/\bar{\gamma}_{sd}}) - e^{\gamma_{rd}/\bar{\gamma}_{sd}} h(\gamma_{rd}, \bar{\gamma}_{sd})\right) h(\gamma^*_{t2}(\gamma_{rd}, \bar{\gamma}_{sd}), \bar{\gamma}_{sr}) \\ &+ (1 - e^{-\gamma_{rd}/\bar{\gamma}_{sd}}) \exp(-\gamma^*_{t2}(\gamma_{rd}, \bar{\gamma}_{sd})/\bar{\gamma}_{sr})\Bigg] \frac{1}{\bar{\gamma}_{rd}} e^{\gamma_{rd}/\bar{\gamma}_{rd}} \mathrm{d}\gamma_{rd}. \end{aligned} \tag{A.11}$$

In a similar manner, the e2e BER for Model 3 and Model 4 are calculated as

$$\begin{aligned}\mathrm{BER}_{e2e}^{(3)}(\bar{\gamma}_{sr},\bar{\gamma}_{rd},\bar{\gamma}_{sd})\approx\int_0^{\infty}\Big[&\frac{1}{2}\mathrm{erfc}(\sqrt{\gamma_{sd}})(1-\exp(-\gamma_{t3}^{*}(\bar{\gamma}_{rd},\gamma_{sd})/\bar{\gamma}_{sr}))\\&+\big(e^{-\gamma_{sd}/\bar{\gamma}_{rd}}-e^{\gamma_{sd}/\bar{\gamma}_{rd}}h(\gamma_{sd},\bar{\gamma}_{rd})\big)\,h(\gamma_{t3}^{*}(\bar{\gamma}_{rd},\gamma_{sd}),\bar{\gamma}_{sr})\\&+e^{\gamma_{sd}/\bar{\gamma}_{rd}}h(\gamma_{sd},\bar{\gamma}_{rd})\exp(-\gamma_{t3}^{*}(\bar{\gamma}_{rd},\gamma_{sd})/\bar{\gamma}_{sr})\Big]\frac{1}{\bar{\gamma}_{sd}}e^{-\gamma_{sd}/\bar{\gamma}_{sd}}\,\mathrm{d}\gamma_{sd},\end{aligned} \tag{A.12}$$

and

$$\begin{aligned}\mathrm{BER}_{e2e}^{(4)}(\bar{\gamma}_{sr},\bar{\gamma}_{rd},\bar{\gamma}_{sd})=\frac{1}{\bar{\gamma}_{sd}\bar{\gamma}_{rd}}\int_0^{\infty}\int_0^{\infty}\frac{1}{2}\Bigg[&\mathrm{erfc}(\sqrt{\gamma_{sd}})(1-\exp(-\gamma_{t4}^{*}(\gamma_{rd},\gamma_{sd})/\bar{\gamma}_{sr}))\\&+\left(\mathrm{erfc}\left(\frac{\gamma_{sd}-\gamma_{rd}}{\sqrt{(\gamma_{sd}+\gamma_{rd})}}\right)-\mathrm{erfc}(\sqrt{\gamma_{rd}+\gamma_{sd}})\right)h(\gamma_{t4}^{*}(\gamma_{rd},\gamma_{sd}),\bar{\gamma}_{sr})\\&+\mathrm{erfc}(\sqrt{\gamma_{rd}+\gamma_{sd}})\exp(-\gamma_{t4}^{*}(\gamma_{rd},\gamma_{sd})/\bar{\gamma}_{sr})\Bigg]e^{-\gamma_{sd}/\bar{\gamma}_{sd}}e^{-\gamma_{rd}/\bar{\gamma}_{rd}}\mathrm{d}\gamma_{rd}\,\mathrm{d}\gamma_{sd}.\end{aligned} \tag{A.13}$$

A.4 The Threshold that Minimizes Symbol Error Rate for MPSK Modulation

Consider the case where the source and the relay modulate their signals using MPSK. Let the symbols be denoted by $x_0,\ldots,x_{M-1}$, where $x_i=e^{j2\pi i/M}$. The symbol sent by the source and the relay are denoted by x_s and x_r, respectively. The received signals are given by $y_{sr}=\alpha_{sr}\sqrt{E_{s,s}}x_s+n_{sr}$, $y_{sd}=\alpha_{sd}\sqrt{E_{s,s}}x_s+n_{sd}$, and $y_{rd}=\alpha_{rd}\sqrt{E_{s,r}}x_r+n_{rd}$, where $E_{s,s}$ is the energy per symbol spent by the source and $E_{s,r}$ is the energy per symbol spent by the relay. Let γ_{ij} and $\bar{\gamma}_{ij}$ denote the instantaneous and average SNR per symbol.

Consider Model 1, where the relay makes decisions based on $I_1=\{\gamma_{sr},\bar{\gamma}_{rd},\bar{\gamma}_{sd}\}$. The decision rule to minimize e2e symbol error rate (SER) is $\mathbb{P}\{\mathcal{E}_{e2e}|I_1,a_0\}\underset{a_0}{\overset{a_1}{\gtrless}}\mathbb{P}\{\mathcal{E}_{e2e}|I_1,a_1\}$, where $\mathcal{E}_{e2e}$ represents the e2e symbol error event.

$\mathbb{P}\{\mathcal{E}_{e2e}|I_1, a_0\} = \mathbb{P}\{\mathcal{E}_{sd}|\bar{\gamma}_{sd}\}$ and is given in [97, Eqn. (8.112)]. Without loss of generality, let us assume that the source transmits x_0. Then the term $\mathbb{P}\{\mathcal{E}_{e2e}|I_1, a_1\}$ can be decomposed as

$$\begin{aligned}\mathbb{P}\{\mathcal{E}_{e2e}|I_1, a_1\} = &\sum_{i=1}^{M-1} \mathbb{P}\{x_r = x_i|x_s = x_0\}\mathbb{P}\{\mathcal{E}_{prop}|x_s = x_0, x_r = x_i, \bar{\gamma}_{rd}, \bar{\gamma}_{sd}\} \\ &+ \mathbb{P}\{x_r = x_0|x_s = x_0\}\mathbb{P}\{\mathcal{E}_{coop}|\bar{\gamma}_{rd}, \bar{\gamma}_{sd}\}.\end{aligned} \tag{A.14}$$

The term $\mathbb{P}\{\mathcal{E}_{coop}|\bar{\gamma}_{rd}, \bar{\gamma}_{sd}\}$ is given in [97, Eqn. (9.14)]. The term $\mathbb{P}\{x_r = x_i|x_s = x_0\}$ is obtained in integral form in [98, Eqn. (4.198.b)], and [97, Eqn. (8.29)]. We observe that in M-ary modulation, unlike in BPSK, there are $M-1$ ways of making an incorrect decision and their impacts on detection at the destination are not necessarily the same. After MRC the decision variable is given by $y = \gamma_{sd} + \gamma_{rd}e^{j2\pi i/M} + \tilde{n}$ (derivation is given in Section 3.2.2). As in Section 3.2.2, we assume that an incorrectly detected symbol sent by the relay constitutes the dominant cause of detection errors at the destination. That is, the term $\mathbb{P}\{\mathcal{E}_{prop}|x_s = x_0, x_r = x_i, \bar{\gamma}_{rd}, \bar{\gamma}_{sd}\}$ can be approximated by the probability that $\gamma_{sd} + \gamma_{rd}e^{j2\pi i/M}$ falls in the decision region of symbol x_i, denoted as $\mathcal{R}_i$. Exploiting the geometry of the MPSK constellation, one can easily derive that $\gamma_{sd} + \gamma_{rd}e^{j2\pi i/M} \in \mathcal{R}_i$ if and only if $\gamma_{sd} - c_{i,M}\,\gamma_{rd} < 0$, where

$$c_{i,M} \triangleq \begin{cases} \frac{\sin(\pi(2i-1)/M)}{\sin(\pi/M)}, & i = 1, 2, \ldots, \lfloor M/2 \rfloor; \\ -\frac{\sin(\pi(2i+1)/M)}{\sin(\pi/M)}, & i = \lfloor M/2 \rfloor + 1, \ldots, M-1. \end{cases} \tag{A.15}$$

Then, as in (3.25), we can calculate an approximate expression for $\mathbb{P}\{\mathcal{E}_{prop}|x_0, x_i, \bar{\gamma}_{rd}, \bar{\gamma}_{sd}\}$:

$$\begin{aligned}\mathbb{P}\{\mathcal{E}_{prop}|x_0, x_i, \bar{\gamma}_{rd}, \bar{\gamma}_{sd}\} \approx &\,\mathbb{P}\{\gamma_{sd} - c_{i,M}\,\gamma_{rd} < 0|\bar{\gamma}_{rd}, \bar{\gamma}_{sd}\} \\ &= \int_0^\infty \int_0^{c_{i,M}\gamma_{rd}} \frac{1}{\bar{\gamma}_{sd}\bar{\gamma}_{rd}} e^{-\gamma_{sd}/\bar{\gamma}_{sd}} e^{-\gamma_{rd}/\bar{\gamma}_{rd}} \mathrm{d}\gamma_{sd}\, \mathrm{d}\gamma_{rd} \\ &= \frac{\bar{\gamma}_{rd}c_{i,M}}{\bar{\gamma}_{sd} + \bar{\gamma}_{rd}c_{i,M}}.\end{aligned} \tag{A.16}$$

By substituting (A.16) and the other terms into (A.14), the decision rule can be determined. Since $\mathbb{P}\{\mathcal{E}_{e2e}|I_1, a_1\}$ decreases with γ_{sr}, the decision rule is a threshold rule on γ_{sr}, where the optimal threshold is a function of $\bar{\gamma}_{rd}$ and $\bar{\gamma}_{sd}$. Obtaining a closed-form expression for the optimal threshold is quite difficult. However, bounds such as union bound, can be used to derive approximations for $\mathbb{P}\{\mathcal{E}_{e2e}|I_1, a_1\}$, thereby leading to approximate closed-form expressions for the optimal threshold.

Appendix B

Derivations for Chapter 4

B.1 Asymptotic Behavior of the Probability of Error Propagation

In this section we derive upper and lower bounds for $\mathbb{P}\{\mathcal{E}_{prop}\}$ and, invoking the Pinching Theorem, we prove that $\lim_{\mathsf{SNR}\to\infty} \mathbb{P}\{\mathcal{E}_{prop}\} = \kappa_{rd}/(\kappa_{rd}+\kappa_{sd})$. The probability of error propagation is given by [99]

$$\begin{aligned}\mathbb{P}\{\mathcal{E}_{prop}\} &= \frac{1}{2}\mathbb{E}_{\gamma_{rd},\gamma_{sd}}\left[\operatorname{erfc}\left(g(\gamma_{sd},\gamma_{rd})\right)\right] = \frac{1}{2}\mathbb{E}_{\gamma_{rd}}\left[\mathbb{E}_{\gamma_{sd}|\gamma_{rd}}\left[\operatorname{erfc}\left(g(\gamma_{sd},\gamma_{rd})\right)\right]\right]\\ &= \frac{1}{2}\int_0^\infty \frac{1}{\bar{\gamma}_{rd}}e^{-\gamma_{rd}/\bar{\gamma}_{rd}}\int_0^\infty \operatorname{erfc}\left(g(\gamma_{sd},\gamma_{rd})\right)\frac{1}{\bar{\gamma}_{sd}}e^{-\gamma_{sd}/\bar{\gamma}_{sd}}\mathrm{d}\gamma_{sd}\,\mathrm{d}\gamma_{rd}, \quad \text{(B.1)}\end{aligned}$$

where

$$g(\gamma_{sd},\gamma_{rd}) = \frac{\gamma_{sd}-\gamma_{rd}}{\sqrt{\gamma_{sd}+\gamma_{rd}}}.$$

Let us denote the upper and lower bounds for $\mathbb{P}\{\mathcal{E}_{prop}\}$, as p_l and p_u, and the upper and lower bounds for the inner integral in (B.1), i.e. $\mathbb{E}_{\gamma_{sd}|\gamma_{rd}}\left[\operatorname{erfc}\left(g(\gamma_{sd},\gamma_{rd})\right)\right]$, as f_l and f_u. Let μ_g and μ_h be the geometric and harmonic means of two positive numbers, where $\mu_g(x,y)=\sqrt{xy}$ and $\mu_h(x,y)=2xy/(x+y)$. The square of $g(\gamma_{sd},\gamma_{rd})$ can be expressed as

$$g^2(\gamma_{sd},\gamma_{rd}) = \gamma_{sd}+\gamma_{rd}-2\mu_h(\gamma_{sd},\gamma_{rd}).$$

When $g(\gamma_{sd}, \gamma_{rd}) \geq 0$, i.e., $\gamma_{sd} \geq \gamma_{rd}$, making use of the fact that $\mu_h(x, y) \leq \mu_g(x, y)$ we reach the following inequality

$$\begin{aligned} g^2(\gamma_{sd}, \gamma_{rd}) &\geq \gamma_{sd} + \gamma_{rd} - 2\sqrt{\gamma_{sd}\gamma_{rd}} = (\sqrt{\gamma_{sd}} - \sqrt{\gamma_{rd}})^2 \\ &\Rightarrow g(\gamma_{sd}, \gamma_{rd}) \geq \sqrt{\gamma_{sd}} - \sqrt{\gamma_{rd}}, \qquad \gamma_{sd} \geq \gamma_{rd}. \end{aligned} \tag{B.2}$$

For the region where $g(\gamma_{sd}, \gamma_{rd}) < 0$, i.e., $\gamma_{sd} < \gamma_{rd}$, due to the fact that $m_h(x, y) \geq \min(x, y)$, we have

$$g^2(\gamma_{sd}, \gamma_{rd}) \leq \gamma_{sd} + \gamma_{rd} - 2\min(\gamma_{sd}, \gamma_{rd}) \;\Rightarrow\; g(\gamma_{sd}, \gamma_{rd}) \geq -\sqrt{\gamma_{rd} - \gamma_{sd}}, \qquad \gamma_{sd} < \gamma_{rd}. \tag{B.3}$$

From (B.2) and (B.3), $\mathbb{E}_{\gamma_{sd}|\gamma_{rd}}\left[\operatorname{erfc}\left(g(\gamma_{sd}, \gamma_{rd})\right)\right]$ can be bounded as follows:

$$\mathbb{E}_{\gamma_{sd}|\gamma_{rd}}\left[\operatorname{erfc}\left(g(\gamma_{sd}, \gamma_{rd})\right)\right] = \int_0^\infty \operatorname{erfc}(g(\gamma_{sd}, \gamma_{rd})) \frac{1}{\bar{\gamma}_{sd}} e^{-\gamma_{sd}/\bar{\gamma}_{sd}} \mathrm{d}\gamma_{sd} \leq f_u(\gamma_{rd}, \bar{\gamma}_{sd}),$$

where

$$\begin{aligned} f_u(\gamma_{rd}, \bar{\gamma}_{sd}) &\triangleq \int_0^{\gamma_{rd}} \operatorname{erfc}\left(-\sqrt{\gamma_{rd} - \gamma_{sd}}\right) \frac{1}{\bar{\gamma}_{sd}} e^{-\gamma_{sd}/\bar{\gamma}_{sd}} \mathrm{d}\gamma_{sd} \\ &+ \int_{\gamma_{rd}}^\infty \operatorname{erfc}\left(\sqrt{\gamma_{sd}} - \sqrt{\gamma_{rd}}\right) \frac{1}{\bar{\gamma}_{sd}} e^{-\gamma_{sd}/\bar{\gamma}_{sd}} \mathrm{d}\gamma_{sd} \end{aligned} \tag{B.4}$$

Following a similar approach, we also derive a lower bound for $\mathbb{E}_{\gamma_{sd}|\gamma_{rd}}\left[\operatorname{erfc}\left(g(\gamma_{sd}, \gamma_{rd})\right)\right]$. It can be easily verified that

$$g(\gamma_{sd}, \gamma_{rd}) \leq \sqrt{\gamma_{sd}} - \sqrt{\gamma_{rd}}, \qquad \gamma_{sd} \leq \gamma_{rd}, \qquad \text{and} \tag{B.5}$$

$$g(\gamma_{sd}, \gamma_{rd}) \leq \sqrt{\gamma_{sd} - \gamma_{rd}}, \qquad \gamma_{sd} > \gamma_{rd}. \tag{B.6}$$

Thus, $f_l(\gamma_{rd}, \bar{\gamma}_{sd}) \leq \mathbb{E}_{\gamma_{sd}|\gamma_{rd}}\left[\operatorname{erfc}\left(g(\gamma_{sd}, \gamma_{rd})\right)\right]$, where

$$\begin{aligned} f_l(\gamma_{rd}, \bar{\gamma}_{sd}) &\triangleq \int_0^{\gamma_{rd}} \operatorname{erfc}\left(\sqrt{\gamma_{sd}} - \sqrt{\gamma_{rd}}\right) \frac{1}{\bar{\gamma}_{sd}} e^{-\gamma_{sd}/\bar{\gamma}_{sd}} \mathrm{d}\gamma_{sd} \\ &+ \int_{\gamma_{rd}}^\infty \operatorname{erfc}\left(\sqrt{\gamma_{sd} - \gamma_{rd}}\right) \frac{1}{\bar{\gamma}_{sd}} e^{-\gamma_{sd}/\bar{\gamma}_{sd}} \mathrm{d}\gamma_{sd}. \end{aligned} \tag{B.7}$$

Next, we introduce two integrals, which we derive using integration by parts, to be used to calculate f_u and f_l.

$$J_1(a,b,c;x_0,x_1) = \int_{x_0}^{x_1} \mathrm{erfc}\left(\sqrt{ax+b}\right) e^{-cx} \mathrm{d}x$$
$$= \left\{-\frac{1}{c}\mathrm{erfc}(\sqrt{ax+b})e^{-cx} - \frac{1}{c}\sqrt{\frac{a}{a+c}}\left(1-\mathrm{erfc}\left(\sqrt{(a+c)/a}\,\sqrt{ax+b}\right)\right)e^{bc/a}\right\}\Bigg]_{x_0}^{x_1}, \tag{B.8}$$

where $x_0, x_1, c \geq 0$, $(a+c)/a \geq 0$, and

$$J_2(a,b,c;x_0,x_1) = \int_{x_0}^{x_1} \mathrm{erfc}\left(a\sqrt{x}+b\right) e^{-cx} \mathrm{d}x = \left\{-\frac{1}{c}\mathrm{erfc}(a\sqrt{x}+b)e^{-cx}\right.$$
$$\left.-\frac{a}{c\sqrt{a^2+c}}\left(1-\mathrm{erfc}\left(\sqrt{a^2+c}\,\sqrt{x}+ab/\sqrt{a^2+c}\right)\right)\exp(-b^2+a^2b^2/(a^2+c))\right\}\Bigg]_{x_0}^{x_1}, \tag{B.9}$$

where $x_0, x_1, c \geq 0$. Using $\mathrm{erfc}(-x) = 2 - \mathrm{erfc}(x)$, (B.4) is expressed in terms of J_1 and J_2. Then, by substituting (B.8) and (B.9) for J_1 and J_2, we obtain[1]

$$\begin{aligned} f_u(\gamma_{rd}, \bar{\gamma}_{sd}) =& 2\left(1-e^{-\gamma_{rd}/\bar{\gamma}_{sd}}\right) - (1/\bar{\gamma}_{sd})J_1(-1,\gamma_{rd},1/\bar{\gamma}_{sd},0,\gamma_{rd}) \\ &+(1/\bar{\gamma}_{sd})J_2(1,-\sqrt{\gamma_{rd}},1/\bar{\gamma}_{sd},\gamma_{rd},\infty) \\ =&\mathrm{erfc}\left(-\sqrt{\gamma_{rd}}\right) - \frac{1}{\sqrt{1-1/\bar{\gamma}_{sd}}}\left(1-\mathrm{erfc}\left(\sqrt{\gamma_{rd}}\sqrt{(1-1/\bar{\gamma}_{sd})}\right)\right)e^{-\gamma_{rd}/\bar{\gamma}_{sd}} \\ &-\frac{1}{\sqrt{1+1/\bar{\gamma}_{sd}}}\mathrm{erfc}\left(\sqrt{\gamma_{rd}}\frac{1/\bar{\gamma}_{sd}}{\sqrt{1+1/\bar{\gamma}_{sd}}}\right)\exp\left(-\gamma_{rd}/(1+\bar{\gamma}_{sd})\right). \end{aligned} \tag{B.10}$$

Similarly,

$$\begin{aligned} &f_l(\gamma_{rd}, \bar{\gamma}_{sd}) \\ &= \frac{1}{\sqrt{1+1/\bar{\gamma}_{sd}}}\Bigg[-e^{-\gamma_{rd}/\bar{\gamma}_{sd}} - e^{-\gamma_{rd}/(1+\bar{\gamma}_{sd})}\left(1-\mathrm{erfc}\left(\sqrt{\gamma_{rd}}/\left(\bar{\gamma}_{sd}\sqrt{1+1/\bar{\gamma}_{sd}}\right)\right)\right) \\ &+(2-\mathrm{erfc}(\sqrt{\gamma_{rd}}))\sqrt{1+1/\bar{\gamma}_{sd}} - e^{-\gamma_{rd}/(1+\bar{\gamma}_{sd})}\left(1-\mathrm{erfc}\left(\sqrt{\gamma_{rd}}/\sqrt{1+1/\bar{\gamma}_{sd}}\right)\right)\Bigg]. \end{aligned} \tag{B.11}$$

[1]It is assumed that $\bar{\gamma}_{sd} \geq 1$, which is satisfied when SNR is sufficiently large.

Upper and lower bounds for $\mathbb{P}\{\mathcal{E}_{prop}\}$ are found by using (B.1) and taking the expectation of f_u and f_l w.r.t. γ_{rd}:

$$f_l(\gamma_{rd}, \bar{\gamma}_{sd}) \leq \mathbb{E}_{\gamma_{sd}|\gamma_{rd}} \left[\operatorname{erfc}\left(g(\gamma_{sd}, \gamma_{rd})\right)\right] \leq f_u(\gamma_{rd}, \bar{\gamma}_{sd}) \Rightarrow \tag{B.12}$$

$$\underbrace{\frac{1}{2}\mathbb{E}_{\gamma_{rd}}[f_l(\gamma_{rd}, \bar{\gamma}_{sd})]}_{p_l(\bar{\gamma}_{rd}, \bar{\gamma}_{sd})} \leq \mathbb{P}[\mathcal{E}_{prop}] \leq \underbrace{\frac{1}{2}\mathbb{E}_{\gamma_{rd}}[f_u(\gamma_{rd}, \bar{\gamma}_{sd})]}_{p_u(\bar{\gamma}_{rd}, \bar{\gamma}_{sd})}. \tag{B.13}$$

Then we express p_l and p_u in terms of J_2:

$$\begin{aligned} p_u(\bar{\gamma}_{rd}, \bar{\gamma}_{sd}) =& -\underbrace{\frac{\bar{\gamma}_{sd}}{2(\bar{\gamma}_{sd} + \bar{\gamma}_{rd})}\frac{1}{\sqrt{1 - 1/\bar{\gamma}_{sd}}}}_{t_1} + \underbrace{\frac{1}{2\bar{\gamma}_{rd}}J_2(-1, 0, 1/\bar{\gamma}_{rd}, 0, \infty)}_{t_2} \\ &+ \underbrace{\frac{1}{2\bar{\gamma}_{rd}}\frac{1}{\sqrt{1 - 1/\bar{\gamma}_{sd}}}J_2\left(\sqrt{1 - 1/\bar{\gamma}_{sd}}, 0, (\bar{\gamma}_{rd} + \bar{\gamma}_{sd})/(\bar{\gamma}_{rd}\bar{\gamma}_{sd}), 0, \infty\right)}_{t_3} \\ &- \underbrace{\frac{1}{2\bar{\gamma}_{rd}}\frac{1}{\sqrt{1 + 1/\bar{\gamma}_{sd}}}J_2\left(1/(\bar{\gamma}_{sd}\sqrt{1 + 1/\bar{\gamma}_{sd}}), 0, (1 + \bar{\gamma}_{sd} + \bar{\gamma}_{rd})/(\bar{\gamma}_{rd} + \bar{\gamma}_{rd}\bar{\gamma}_{sd}), 0, \infty\right)}_{t_4}. \end{aligned}$$

We substitute $\bar{\gamma}_{sd} = \kappa_{sd}\mathsf{SNR}$ and $\bar{\gamma}_{rd} = \kappa_{rd}\mathsf{SNR}$ in (B.14), and take its limit as $\mathsf{SNR} \to \infty$. Since $t_1 \to (1/2)\kappa_{sd}/(\kappa_{sd} + \kappa_{rd})$, $t_2 \to 1$, $t_3 \to 0$ and $t_4 \to (1/2)\kappa_{sd}/(\kappa_{sd} + \kappa_{rd})$, we conclude that

$$\lim_{\mathsf{SNR}\to\infty} p_u = \frac{\kappa_{rd}}{\kappa_{rd} + \kappa_{sd}}. \tag{B.14}$$

Following the same approach for p_l, we obtain

$$\begin{aligned} p_l(\gamma_{rd}, \bar{\gamma}_{sd}) =& 1 - \underbrace{\frac{1}{2\sqrt{1 + 1/\bar{\gamma}_{rd}}}\left(\frac{\bar{\gamma}_{sd}}{\bar{\gamma}_{sd} + \bar{\gamma}_{rd}} + \frac{2(1 + \bar{\gamma}_{sd})}{1 + \bar{\gamma}_{sd} + \bar{\gamma}_{rd}}\right)}_{s_1} \\ &+ \underbrace{\frac{1}{\sqrt{1 + 1/\bar{\gamma}_{rd}}}\frac{1}{2\bar{\gamma}_{rd}}J_2\left(1/(\bar{\gamma}_{sd}\sqrt{1 + 1/\bar{\gamma}_{sd}}), 0, (1 + \bar{\gamma}_{sd} + \bar{\gamma}_{rd})/(\bar{\gamma}_{rd} + \bar{\gamma}_{rd}\bar{\gamma}_{sd}), 0, \infty\right)}_{s_2} \\ &- \underbrace{\frac{1}{2\bar{\gamma}_{rd}}J_2(1, 0, 1/\bar{\gamma}_{rd}, 0, \infty)}_{s_3} \\ &+ \underbrace{\frac{1}{\sqrt{1 + 1/\bar{\gamma}_{rd}}}\frac{1}{2\bar{\gamma}_{rd}}J_2\left(1/\sqrt{1 + 1/\bar{\gamma}_{sd}}), 0, (1 + \bar{\gamma}_{sd} + \bar{\gamma}_{rd})/(\bar{\gamma}_{rd} + \bar{\gamma}_{rd}\bar{\gamma}_{sd}), 0, \infty\right)}_{s_4} \end{aligned} \tag{B.15}$$

Since $s_1 \to (3/2)\kappa_{sd}/(\kappa_{sd}+\kappa_{rd})$, $s_2 \to (1/2)\kappa_{sd}/(\kappa_{sd}+\kappa_{rd})$, $s_3 \to 0$, and $s_4 \to 0$ as $\mathsf{SNR} \to \infty$, we conclude that $\lim_{\mathsf{SNR}\to\infty} p_l = \frac{\kappa_{rd}}{\kappa_{rd}+\kappa_{sd}}$. Using this result combined with (B.14), the Pinching Theorem implies that

$$\lim_{\mathsf{SNR}\to\infty} p_l \le \lim_{\mathsf{SNR}\to\infty} P\{\mathcal{E}_{prop}\} \le \lim_{\mathsf{SNR}\to\infty} p_u \Rightarrow \lim_{\mathsf{SNR}\to\infty} P\{\mathcal{E}_{prop}\} = \frac{\kappa_{rd}}{\kappa_{rd}+\kappa_{sd}}. \quad \text{(B.16)}$$

B.2 Proof of Lemma 4.1 – Asymptotic Behavior of γ_t^*

It can be easily verified that $\lim_{\mathsf{SNR}\to\infty} \frac{\delta(\mathsf{SNR})}{1/\mathsf{SNR}} = \frac{1}{4}\frac{\kappa_{sd}+\kappa_{rd}}{\kappa_{sd}\kappa_{rd}}$. Hence, $\delta(\mathsf{SNR})$ is asymptotically equivalent to

$$\delta(\mathsf{SNR}) \sim \frac{1}{4}\frac{\kappa_{sd}+\kappa_{rd}}{\kappa_{sd}\kappa_{rd}}\frac{1}{\mathsf{SNR}}. \quad \text{(B.17)}$$

For large SNR, $\delta(\mathsf{SNR}) < 1/2$. Thus, we ignore the second case in (4.3) and assume that $\gamma_t^*(\mathsf{SNR}) = \left(\mathrm{erfc}^{-1}(2\delta(\mathsf{SNR}))\right)^2$.

We make use of the following inequality given in [100, pp. 371]:

$$\sqrt{1-e^{-z^2}} < |\mathrm{erf}(z)| < \sqrt{1-e^{-2z^2}}.$$

By replacing $\mathrm{erfc}(z) = 1 - \mathrm{erf}(z)$, the threshold value is equal to $\gamma_t^*(\mathsf{SNR}) = \left(\mathrm{erf}^{-1}(1-2\delta(\mathsf{SNR}))\right)^2$. Since $\mathrm{erf}(z) \ge 0$ for all $z \ge 0$, and $\sqrt{\gamma_t^*} \ge 0$, we can write

$$\sqrt{1-e^{-\gamma_t^*}} < \mathrm{erf}(\sqrt{\gamma_t^*}) < \sqrt{1-e^{-2\gamma_t^*}}. \quad \text{(B.18)}$$

Substituting $\mathrm{erf}(\sqrt{\gamma_t^*}) = 1 - 2\delta$ from (4.3), we obtain

$$\frac{1}{2}\log\left(\frac{1}{4\delta(1-\delta)}\right) < \gamma_t^* < \log\left(\frac{1}{4\delta(1-\delta)}\right). \quad \text{(B.19)}$$

It can be easily verified that

$$\lim_{\mathsf{SNR}\to\infty} \log\left(\frac{1}{4\delta(1-\delta)}\right) / \log(\mathsf{SNR}) = 1. \quad \text{(B.20)}$$

Thus, there exists constants $b_1, b_2 > 0$ such that

$$b_1 \log(\mathsf{SNR}) < \log\left(\frac{1}{4\delta(1-\delta)}\right) < b_2 \log(\mathsf{SNR}),$$

and (4.5) holds for $c_1 = b_1/2$ and $c_2 = b_2$, which concludes the proof. $\square$

B.3 Proof of Lemma 4.2 – Asymptotic Behavior of $\mathbb{P}\{\gamma_{sr} \leq \gamma_t^*\}$

Since γ_{sr} has mean $\bar{\gamma}_{sr} = \kappa_{sr}\mathsf{SNR}$, the probability that $\gamma_{sr} \leq \gamma_t$, and hence relay remains silent, is equal to

$$\mathbb{P}\{\gamma_{sr} \leq \gamma_t\} = 1 - \exp\left(-\frac{1}{\kappa_{sr}}\frac{\gamma_t(\mathsf{SNR})}{\mathsf{SNR}}\right) = 1 - (\exp(-\gamma_t(\mathsf{SNR})))^{\frac{1}{\kappa_{sr}\mathsf{SNR}}}. \quad \text{(B.21)}$$

By substituting the bounds derived in Lemma 4.1 into (B.21), we obtain

$$1 - (\exp(-c_2\log(\mathsf{SNR})))^{\frac{1}{\kappa_{sr}\mathsf{SNR}}} < \mathbb{P}\{\gamma_{sr} \leq \gamma_t^*\} < 1 - (\exp(-c_1\log(\mathsf{SNR})))^{\frac{1}{\kappa_{sr}\mathsf{SNR}}} \Rightarrow$$
$$1 - \left(\frac{1}{\mathsf{SNR}}\right)^{\frac{c_2}{\kappa_{sr}\mathsf{SNR}}} < \mathbb{P}\{\gamma_{sr} \leq \gamma_t^*\} < 1 - \left(\frac{1}{\mathsf{SNR}}\right)^{\frac{c_1}{\kappa_{sr}\mathsf{SNR}}}.$$

We note that

$$\lim_{\mathsf{SNR}\to\infty} \frac{1 - \left(\frac{1}{\mathsf{SNR}}\right)^{\frac{c}{\kappa_{sr}\mathsf{SNR}}}}{\log(\mathsf{SNR})/\mathsf{SNR}} = \frac{c}{\kappa_{sr}},$$

and hence,

$$1 - \left(\frac{1}{\mathsf{SNR}}\right)^{\frac{c}{\kappa_{sr}\mathsf{SNR}}} \sim \frac{c}{\kappa_{sr}}\frac{\log(\mathsf{SNR})}{\mathsf{SNR}}. \quad \text{(B.22)}$$

Then, there exist positive constants b_1' and b_2' such that

$$\frac{b_1' c_1}{\kappa_{sr}}\frac{\log(\mathsf{SNR})}{\mathsf{SNR}} < \mathbb{P}\{\gamma_{sr} \leq \gamma_t^*\} < \frac{b_2' c_2}{\kappa_{sr}}\frac{\log(\mathsf{SNR})}{\mathsf{SNR}},$$

and (4.6) is satisfied for $c_1' = \frac{b_1' c_1}{\kappa_{sr}}$ and $c_2' = \frac{b_2' c_2}{\kappa_{sr}}$. $\square$

B.4 Proof of Lemma 4.3 – Asymptotic Behavior of $\mathbb{P}\{\mathcal{E}_{sr}|\gamma_{sr} > \gamma_t^*\}$

Using Craig's formula given in [101], erfc can be represented as

$$\mathrm{erfc}(z) = \frac{2}{\pi}\int_0^{\pi/2} \exp(-z^2/\sin^2(\theta))\mathrm{d}\theta.$$

Substituting this alternate representation in (A.6) results in

$$\mathbb{P}\{\mathcal{E}_{sr}|\gamma_{sr} > \gamma_t\} = \frac{\exp(\gamma_t/\bar{\gamma}_{sr})}{2\bar{\gamma}_{sr}}\int_{\gamma_t}^{\infty} \mathrm{erfc}(\sqrt{\gamma_{sr}})\exp(-\gamma_{sr}/\bar{\gamma}_{sr})\,\mathrm{d}\gamma_{sr} \tag{B.23}$$

$$= \frac{\exp(\gamma_t/\bar{\gamma}_{sr})}{\pi\bar{\gamma}_{sr}}\int_{\gamma_t}^{\infty} \exp\left(-\frac{\gamma_{sr}}{\bar{\gamma}_{sr}}\right)\int_0^{\pi/2} \exp\left(-\frac{\gamma_{sr}}{\sin^2\theta}\right)\mathrm{d}\theta\,\mathrm{d}\gamma_{sr} \tag{B.24}$$

$$= \frac{\exp(\gamma_t/\bar{\gamma}_{sr})}{\pi\bar{\gamma}_{sr}}\int_0^{\pi/2}\int_{\gamma_t}^{\infty} \exp\left(-\gamma_{sr}\left(\frac{1}{\sin^2\theta} + \frac{1}{\bar{\gamma}_{sr}}\right)\right)\mathrm{d}\gamma_{sr}\,\mathrm{d}\theta$$

$$= \frac{1}{\pi}\int_0^{\pi/2} \frac{\sin^2\theta}{\bar{\gamma}_{sr} + \sin^2\theta}\exp(-\gamma_t/\sin^2\theta)\mathrm{d}\theta. \tag{B.25}$$

Since $\frac{\sin^2(\theta)}{\bar{\gamma}_{sr}+\sin^2(\theta)} < \frac{1}{\bar{\gamma}_{sr}}$ for any $\bar{\gamma}_{sr} > 0$, $\mathbb{P}\{\mathcal{E}_{sr}|\gamma_{sr} > \gamma_t\}$ is upper bounded by

$$\mathbb{P}\{\mathcal{E}_{sr}|\gamma_{sr} > \gamma_t\} < \frac{1}{\pi}\int_0^{\pi/2} \frac{1}{\bar{\gamma}_{sr}}\exp(-\gamma_t/\sin^2\theta)\mathrm{d}\theta = \frac{1}{2\bar{\gamma}_{sr}}\mathrm{erfc}(\sqrt{\gamma_t}). \tag{B.26}$$

By substituting $\gamma_t = \gamma_t^*$, $\bar{\gamma}_{sr} = \kappa_{sr}\mathsf{SNR}$, and $\mathrm{erfc}(\sqrt{\gamma_t^*}) = 2\delta$ from (4.3), (B.26) is simplified to

$$\mathbb{P}\{\mathcal{E}_{sr}|\gamma_{sr} > \gamma_t^*\} < \frac{1}{\kappa_{sr}}\frac{\delta(\mathsf{SNR})}{\mathsf{SNR}}. \tag{B.27}$$

Since $\delta(\mathsf{SNR}) \sim \frac{1}{4}\frac{\kappa_{sd}+\kappa_{rd}}{\kappa_{sd}\kappa_{rd}}\frac{1}{\mathsf{SNR}}$, there exists a constant $c'' > 0$ such that $\delta(\mathsf{SNR}) < c''/\mathsf{SNR}$ for sufficiently large SNR. Hence, using (B.27) we obtain

$$\mathbb{P}\{\mathcal{E}_{sr}|\gamma_{sr} > \gamma_t\} < \frac{1}{\kappa_{sr}\mathsf{SNR}}\delta(\mathsf{SNR}) < \frac{c''}{\kappa_{sr}}\frac{1}{\mathsf{SNR}^2}, \tag{B.28}$$

and we conclude that (4.7) holds for $c = c''/\kappa_{sr}$. □

Appendix C

Derivations for Chapter 5

C.1 Derivation of Eqn.s (5.8), (5.9), and (5.10)

To shorten the notation in the rest of the derivations we drop the condition $\{N_r = i\}$ in the terms $\mathbb{P}\{\mathcal{E}_{sd}, \mathcal{A}_s | N_r = i\}$, $\mathbb{P}\{\mathcal{E}_{rd}, \mathcal{A}_r | N_r = i\}$, $\mathbb{P}\{\mathcal{A}_s | N_r = i\}$, and $\mathbb{P}\{\mathcal{A}_r | N_r = i\}$ from the notation. Note that these terms are conditioned on $\{N_r = i\}$.

Derivation of Eqn. (5.8)

The probability of $\mathcal{A}_s$ can be expressed as

$$\begin{aligned}
&\mathbb{P}\{\mathcal{A}_s\}=\mathbb{P}\{\gamma_{sd} > \gamma_{rd,1}, \ldots \gamma_{rd,i}\} \\
&= \int_0^\infty p_{\gamma_{sd}}(\gamma_{sd}) \int_0^{\gamma_{sd}} p_{\gamma_{rd,1}}(\gamma_{rd,1}) \ldots \\
&\times \int_0^{\gamma_{sd}} p_{\gamma_{rd,i}}(\gamma_{rd,i}) \mathrm{d}\gamma_{rd,i} \ldots \mathrm{d}\gamma_{rd,1} \mathrm{d}\gamma_{sd} \\
&= \int_0^\infty \frac{1}{\bar{\gamma}_{sd}} e^{\gamma_{sd}/\bar{\gamma}_{sd}} \left(1 - e^{-\bar{\gamma}_{sd}/\bar{\gamma}_{rd}}\right)^i \mathrm{d}\gamma_{sd}
\end{aligned} \tag{C.1}$$

Using the binomial expansion for $(1 - e^{-\gamma_{sd}/\bar{\gamma}_{rd}})^i$ we obtain

$$\mathbb{P}\{\mathcal{A}_s\} = \sum_{j=0}^{i} \left\{ \binom{i}{j} (-1)^j \frac{1}{1 + j(\bar{\gamma}_{sd}/\bar{\gamma}_{rd})} \right.$$

Since the probability of being selected by the destinations is the same for all potential relays and independent of index k, we denote it by $\mathbb{P}\{\mathcal{A}_r\}$ and calculate as $\mathbb{P}\{\mathcal{A}_r\} = \frac{1}{i}(1 - \mathbb{P}\{\mathcal{A}_s\})$. Hence,

$$\mathbb{P}\{\mathcal{A}_{r,k}\} = \frac{1}{i}\left(1 - \sum_{j=0}^{i}\left\{\binom{i}{j}(-1)^j \frac{1}{1 + j(\bar{\gamma}_{sd}/\bar{\gamma}_{rd})}\right)\right..$$

Derivation of Eqn. (5.9)

The term $\mathbb{P}\{\mathcal{E}_{sd}, \mathcal{A}_s\}$ is equal to the following integral

$$\begin{aligned}\mathbb{P}\{\mathcal{E}_{sd}, \mathcal{A}_s\} =& \int_{\mathcal{A}_s} P_b(\gamma_{sd}) p_{\gamma_{rd,1}}(\gamma_{rd,1}) \dots p_{\gamma_{rd,i}}(\gamma_{rd,i}) \\ & \times p_{\gamma_{sd}}(\gamma_{sd}) \mathrm{d}\gamma_{rd,1} \dots \mathrm{d}\gamma_{rd,i} \mathrm{d}\gamma_{sd} \\ =& \int_0^{\infty} P_b(\gamma_{sd})(1 - e^{-\gamma_{sd}/\bar{\gamma}_{rd}})^i \frac{1}{\bar{\gamma}_{sd}} e^{-\gamma_{sd}/\bar{\gamma}_{sd}} \mathrm{d}\gamma_{sd}\end{aligned}$$

Again, using the binomial expansion for $(1 - e^{-\gamma_{sd}/\bar{\gamma}_{rd}})^i$ we obtain

$$\mathbb{P}\{\mathcal{E}_{sd}, \mathcal{A}_s\} = \sum_{j=0}^{i}\left\{\binom{i}{j}(-1)^j \frac{\bar{\gamma}_{rd}}{j\bar{\gamma}_{sd} + \bar{\gamma}_{rd}} \bar{P}_b\left(\frac{\bar{\gamma}_{sd}\bar{\gamma}_{rd}}{j\bar{\gamma}_{sd} + \bar{\gamma}_{rd}}\right)\right\}$$

Derivation of Eqn. (5.10)

Similarly, the error probability given that a particular relay R_k is selected is equal to

$$\begin{aligned}\mathbb{P}\{\mathcal{E}_{rd}, \mathcal{A}_{r,k}\} =& \int_{\mathcal{A}_{r,k}} P_b(\gamma_{rd,k}) p_{\gamma_{rd,1}}(\gamma_{rd,1}) \dots p_{\gamma_{rd,i}}(\gamma_{rd,i}) \\ & \times p_{\gamma_{sd}}(\gamma_{sd}) \mathrm{d}\gamma_{rd,1} \dots \mathrm{d}\gamma_{rd,i} \mathrm{d}\gamma_{sd} \\ =& \int_0^{\infty} P_b(\gamma_{rd,k})(1 - e^{-\gamma_{rd,k}/\bar{\gamma}_{rd}})^{i-1} \\ & \times (1 - e^{-\gamma_{rd,k}/\bar{\gamma}_{sd}}) \frac{1}{\bar{\gamma}_{rd}} e^{-\gamma_{rd,k}/\bar{\gamma}_{rd}} \mathrm{d}\gamma_{rd,k} \\ =& \sum_{j=0}^{i-1}\left\{\binom{i-1}{j}(-1)^j \left[\frac{1}{j+1}\bar{P}_b\left(\frac{\bar{\gamma}_{rd}}{j+1}\right)\right.\right. \\ & \left.\left. - \frac{\bar{\gamma}_{sd}}{\bar{\gamma}_{sd}(j+1) + \bar{\gamma}_{rd}} \bar{P}_b\left(\frac{\bar{\gamma}_{sd}\bar{\gamma}_{rd}}{\bar{\gamma}_{sd}(j+1) + \bar{\gamma}_{rd}}\right)\right]\right\}.\end{aligned}$$

C.2 Proof of Lemma 5.1

We prove this lemma by analyzing the orders of terms in (5.6) as $\mathsf{SNR} \to \infty$.

Part 1: Let us first analyze the asymptotic behavior of $\mathbb{P}\{\mathcal{E}_{sd}, \mathcal{A}_s | N_r = i\}$ and $\mathbb{P}\{\mathcal{E}_{rd}, \mathcal{A}_r | N_r = i\}$. In the absence of errors at the reliable relays the bit error probability at the destination would be equal to the performance of $(i+1)$ branch selection combining (SC), where one of the branches has average SNR of $\bar{\gamma}_{sd}$, and the rest have $\bar{\gamma}_{rd}$. The probability of bit error of SC can be expressed as

$$\bar{P}_b^{SC}(i, \bar{\gamma}_{sd}, \bar{\gamma}_{rd}) = \mathbb{P}\{\mathcal{E}_{sd}, A_s | N_r = i\} + i\mathbb{P}\{\mathcal{E}_{rd}, A_r | N_r = i\}.$$

Hence, $\mathbb{P}\{\mathcal{E}_{sd}, A_s | N_r = i\} \leq \bar{P}_b^{SC}(i, \bar{\gamma}_{sd}, \bar{\gamma}_{rd})$ and $\mathbb{P}\{\mathcal{E}_{rd}, A_r | N_r = i\} \leq \bar{P}_b^{SC}(i, \bar{\gamma}_{sd}, \bar{\gamma}_{rd})$. Since SC is known to achieve diversity order equal to the number of its branches, we conclude that both $\mathbb{P}\{\mathcal{E}_{sd}, \mathcal{A}_s | N_r = i\}$ and $\mathbb{P}\{\mathcal{E}_{rd}, \mathcal{A}_r | N_r = i\}$ decrease at least as fast as $1/\mathsf{SNR}^{i+1}$: $\mathbb{P}\{\mathcal{E}_{sd}, A_s | N_r = i\} = O(1/\mathsf{SNR}^{i+1})$ and $\mathbb{P}\{\mathcal{E}_{rd}, A_r | N_r = i\} = O(1/\mathsf{SNR}^{i+1})$.

Part 2: Now, let us examine the order of the term $\mathbb{P}\{\mathcal{E}_{sr} | \gamma_{sr} > \gamma_t\}$ if $\gamma_t = \log(c_1 \mathsf{SNR}^{M_r/b})$. The analysis closely follows that given in Chapter 4 for $M_r = 1$ relay. In Chapter 4 for BPSK and any threshold γ_t it is shown that $\mathbb{P}\{\mathcal{E}_{sr} | \gamma_{sr} > \gamma_t\} < \frac{1}{2\bar{\gamma}_{sr}} \mathrm{erfc}(\sqrt{\gamma_t})$. In the case of $P_b(\gamma) = \beta_m \mathrm{erfc}(\alpha_m \gamma)$, this bound can easily be generalized to

$$\mathbb{P}\{\mathcal{E}_{sr} | \gamma_{sr} > \gamma_t\} < \frac{1}{\bar{\gamma}_{sr}} b\mathrm{erfc}(\sqrt{\alpha_m \gamma_t}). \tag{C.2}$$

Using the well-known bound $\mathrm{erfc}(z) < e^{-z^2}$, we obtain

$$\mathbb{P}\{\mathcal{E}_{sr} | \gamma_{sr} > \gamma_t\} < \frac{\beta_m}{\bar{\gamma}_{sr}} e^{-\alpha_m \gamma_t}. \tag{C.3}$$

By substituting $\gamma_t = \log(c_1 \mathsf{SNR}^{M_r/\alpha_m})$, we conclude that

$$\mathbb{P}\{\mathcal{E}_{sr} | \gamma_{sr} > \gamma_t\} < \frac{\beta_m}{\bar{\gamma}_{sr}} \frac{1}{c_1^{\alpha_m}} \frac{1}{\mathsf{SNR}^{M_r}} = \frac{\beta_m}{c_1^{\alpha_m} \kappa_{sr}} \frac{1}{\mathsf{SNR}^{M_r+1}}. \tag{C.4}$$

Thus $\mathbb{P}\{\mathcal{E}_{sr}|\gamma_{sr} > \gamma_t\} = O(1/\mathsf{SNR}^{M_r+1})$.

Part 3: As seen in (5.8), $\mathbb{P}\{\mathcal{A}_r|N_r = i\}$ depends on $\bar{\gamma}_{rd}$ and $\bar{\gamma}_{sd}$ only through their ratio. Hence, this quantity is independent of SNR and $\mathbb{P}\{\mathcal{A}_r|N_r = i\} = O(1)$.

Combining Parts 1, 2 and 3, we obtain

$$\begin{aligned}\mathbb{P}\{\mathcal{E}_{e2e}|N_r = i\} = &\underbrace{\mathbb{P}\{\mathcal{E}_{sd}, \mathcal{A}_s|N_r = i\}}_{O(1/\mathsf{SNR}^{i+1})} + i \times \Bigg(\underbrace{\mathbb{P}\{\mathcal{E}_{rd}, \mathcal{A}_r|N_r = i\}}_{O(1/\mathsf{SNR}^{i+1})} \\ &+ \underbrace{\mathbb{P}\{\mathcal{E}_{rd}, \mathcal{A}_r|N_r = i\}}_{O(1/\mathsf{SNR}^{i+1})}\underbrace{(1 - 2\mathbb{P}\{\mathcal{E}_{sr}|\gamma_{sr} > \gamma_t\})}_{O(1)} \\ &+ \underbrace{\mathbb{P}\{\mathcal{A}_r|N_r = i\}}_{O(1)}\underbrace{\mathbb{P}\{\mathcal{E}_{sr}|\gamma_{sr} > \gamma_t\}}_{O(1/\mathsf{SNR}^{M_r+1})}\Bigg). \end{aligned} \tag{C.5}$$

Hence, $\mathbb{P}\{\mathcal{E}_{e2e}|N_r = i\} = O(1/\mathsf{SNR}^{i+1})$.

Appendix D

Work Published, Submitted, and in Preparation

Chapter 3

- **Furuzan Atay Onat**, Abdulkareem Adinoyi, Yijia Fan, Halim Yanikomeroglu, John S. Thompson, and Ian D. Marsland, "Threshold selection for SNR-based selective digital relaying in cooperative wireless networks", *IEEE Transactions on Wireless Communications*, vol. 7, no. 11, pp. 4226-4237, Nov. 2008.

- **Furuzan Atay Onat**, Abdulkareem Adinoyi, Yijia Fan, Halim Yanikomeroglu, and John S. Thompson, "Optimum threshold for SNR-based selective digital relaying schemes in cooperative wireless networks", in *Proc. IEEE Wireless Communication and Networking Conference (WCNC)*, Mar. 2007, Hong Kong.

- Stefan Valentin, Tobias Volkhausen, **Furuzan Atay Onat**, Halim Yanikomeroglu, and Holger Karl, "Decoding-based channel estimation for selective cooperation diversity protocols", in *Proc. IEEE International Symposium on Personal, Indoor and Mobile Radio Communications (PIMRC)*, Sep. 2008, Cannes, France [Collaboration based on Chapter 3].

- Stefan Valentin, Tobias Volkhausen, **Furuzan Atay Onat**, Halim Yanikomeroglu, and Holger Karl, "Enabling partial forwarding by decoding-based one and two-stage selective cooperation", in *Proc. IEEE Cognitive and Cooperative Wireless Networks (CoCoNET) Workshop* collocated with *IEEE ICC*, May 2008, Beijing, China [Collaboration based on Chapter 3].

- Stefan Valentin, Tobias Volkhausen, **Furuzan Atay Onat**, Halim Yanikomeroglu, and Holger Karl, "Decoding-based partial forwarding for selective cooperation", in preparation for *IEEE Transactions on Wireless Communications* [Collaboration based on Chapter 3].

- Stefan Valentin, Tobias Volkhausen, Holger Karl, **Furuzan Atay Onat**, and Halim Yanikomeroglu, "Decoding-based Channel State Estimation for Channel-adaptive Communication (EFEC2)". EU/US Patent proposal 2040 08 EFEC2, submitted by University of Paderborn, 15 Sep. 2008; international filing: in progress.

Chapter 4

- **Furuzan Atay Onat**, Yijia Fan, Halim Yanikomeroglu, and John S. Thompson, "Asymptotic BER analysis of threshold digital relaying in cooperative wireless networks", *IEEE Transactions on Wireless Communications*, vol. 7, no. 12, Dec. 2008.

- **Furuzan Atay Onat**, Yijia Fan, Halim Yanikomeroglu, and John S. Thompson, "Asymptotic BER analysis of threshold digital relaying schemes in cooperative wireless systems", in *Proc. IEEE Wireless Communication and Networking Conference, (WCNC)*, Apr. 2008, Las Vegas, Nevada, USA.

Chapter 5

- **Furuzan Atay Onat**, Yijia Fan, Halim Yanikomeroglu, and H. Vincent Poor, "Threshold based relay selection in cooperative wireless networks", in *Proc. IEEE Globecom Conference*, Dec. 2008, New Orleans, USA.

- Yijia Fan, **Furuzan Atay Onat**, Halim Yanikomeroglu, and H. Vincent Poor, "Threshold Based Distributed Detection That Achieves Full Diversity in Wireless Sensor Networks", in *Proc. Asilomar Conference on Signals, Systems, and Computers*, Oct. 2008, Pacific Grove, California, USA [Extension of Chapter 5].

- **Furuzan Atay Onat**, Yijia Fan, Halim Yanikomeroglu, and H. Vincent Poor, "Threshold based relay selection in cooperative wireless sensor networks", submitted to *IEEE Transactions on Wireless Communications*, Jan. 2009.

Chapter 6

- **Furuzan Atay Onat**, Dan Avidor, and Sayandev Mukherjee, "Two-hop relaying in random networks with limited channel state information", in *Proc. Fourth Annual IEEE Communications Society Conference on Sensor, Mesh and Ad Hoc Communications and Networks (SECON)*, June, 2007, San Diego, California, USA.

- **Furuzan Atay Onat**, Dan Avidor, "Relay-assisted ARQ in wireless ad-hoc networks", in *Proc. IEEE Wireless Communication and Networking Conference, (WCNC)*, Apr. 2008, Las Vegas, Nevada, USA.

- **Furuzan Atay Onat**, Dan Avidor and Halim Yanikomeroglu, "Multihop relaying and relay-assisted ARQ in wireless ad-hoc networks", in preparation for journal submission.

Chapter 7

- **Furuzan Atay Onat**, Halim Yanikomeroglu, and Shalini Periyalwar, "Adaptive multi-stream relaying", in *Proc. IEEE Canadian Conference on Electrical & Computer Engineering (CCECE)*, May 2006, Ottawa, Ontario, Canada.

- **Furuzan Atay Onat**, Halim Yanikomeroglu, and Shalini Periyalwar, "Relay-assisted spatial multiplexing in wireless fixed relay networks", in *Proc. IEEE Globecom Conference*, Nov. 2006, San Francisco, California, USA.

Other Work

- Dan Avidor, Sayandev Mukherjee, and **Furuzan Atay Onat**, "Transmit power distribution of wireless ad-hoc networks with topology control", *IEEE Transactions on Wireless Communications*, vol. 7, pp. 1111 - 1116, Apr. 2008.

- **Furuzan Atay Onat**, Ivan Stojmenovic, and Halim Yanikomeroglu, "Generating random graphs for the simulation of wireless ad hoc, actuator, sensor, and internet networks",*Pervasive and Mobile Computing Journal (Elsevier)*, vol. 4, no. 5, pp. 597-615, Oct. 2008.

- **Furuzan Atay Onat** and Ivan Stojmenovic "Generating random graphs for wireless actuator networks", *IEEE International Symposium on a World of Wireless, Mobile and Multimedia Networks (WoWMoM)* (extended paper), Jun. 2007, Helsinki, Finland.

- Başak Can, Halim Yanikomeroglu, **Furuzan Atay Onat**, Hiroyuki Yomo, and Elisabeth De Carvalho, "Link adaptive cooperative diversity schemes for cellular wireless relay networks with fixed relays", submitted to *Springer Wireless Networks Journal*, Oct. 2008.

- Dan Avidor, Sayan Mukherjee, and **Furuzan Atay Onat**, "Transmit power distribution of wireless ad-hoc networks with topology control", 26^{th} *Annual IEEE Conference on Computer Communications (INFOCOM)*, May 2007, Anchorage, Alaska, USA.

- Başak Can, Halim Yanikomeroglu, **Furuzan Atay Onat**, Elisabeth de Carvalho, and Hiroyuki Yomo, "Efficient cooperative diversity schemes and radio resource allocation for IEEE 802.16j", *IEEE Wireless Communication and Networking Conference (WCNC)*, Apr. 2008, Las Vegas, Nevada, USA.